5-2018

Novel Determinants That Influence Azole Susceptibility in Candida glabrata and Candida albicans

Sarah Garland Whaley
University of Tennessee Health Science Center

Novel Determinants That Influence Azole Susceptibility in Candida glabrata and Candida albicans

Document Type
Dissertation

Degree Name
Doctor of Philosophy (PhD)

Program
Pharmaceutical Sciences

Track
Bioanalysis

Research Advisor
P. David Rogers, Pharm.D., Ph.D.

Committee
Damian J. Krysan, M.D., Ph.D. Richard E. Lee, Ph.D. Bernd Meibohm, Ph.D. Frank Park, Ph.D.

ORCID
http://orcid.org/0000-0001-5851-0490

DOI
10.21007/etd.cghs.2018.0447

NOVEL DETERMINANTS THAT INFLUENCE AZOLE SUSCEPTIBILITY IN *CANDIDA GLABRATA* AND *CANDIDA ALBICANS*

A Dissertation
Presented for
The Graduate Studies Council
The University of Tennessee
Health Science Center

In Partial Fulfillment
Of the Requirements for the Degree
Doctor of Philosophy
From The University of Tennessee

By
Sarah Garland Whaley
May 2018

DEDICATION

To my Uncle John who didn't need a degree to be an amazing scientist.

ACKNOWLEDGEMENTS

I would like to start by thanking my advisor who after reading my scientific writing knows for certain that my true talent lies in writing manifestos. Thank you for your patience and for your example. I have learned science, but also much more than that from your leadership.

Second I would also like to thank the members of my committee Damian Krysan, Richard Lee, Bernd Meibohm and Frank Park. Thank you for investing time in my training. I appreciate each of your insight and encouragement throughout this process.

I would not have made it to this point if not for my co-workers and other members of the UT family. Thank you to all of my labmates past and present. Thank you to the members of SCA@M. Thank you to the Department of Clinical Pharmacy and the Department of Pharmaceutical Sciences administration and support staff. Thank you to my classmates Also thank you to all of my friends who have always been supportive and encouraging.

Finally and those of you who know me well know this one is most important to me, my family. My parents who sacrificed to give us every opportunity. The rest of my crew - Dewey, Jenny, David, Jen, Rebecca, Zak, Jordan, Megan, Emily, Matt, Austin, Luke Grace, Dylan, Rhea, Weston, and Kennedy, I could not ask for more supportive, loving family. Thank you all for the constant encouragement to hurry up and finish.

ABSTRACT

Despite the scientific and medical communities' best efforts, the incidence of fungal infections in susceptible populations continues to rise. The most common cause of these opportunistic fungal infections is *Candida*. In fact, *Candida* is the fourth most common pathogen associated with nosocomial blood stream infections. Reported mortality rates for patients with candidemia vary, but have not decreased in the past fifteen years and are reported to be as high as 50%. *Candida glabrata*, second only to *Candida albicans* among *Candida* infections, expresses high rates of resistance to treatment with arguably the best class of currently available antifungals - the azoles. Other available antifungals have associated toxicities, are not available as oral dosage forms or are cost prohibitive. As multidrug resistant *C. glabrata* have been reported, the need to find ways to overcome resistance to azoles is more pressing than ever. The work described here highlights our efforts to develop a better understanding of azole resistance in *Candida*, with a focus on *C. glabrata*, which can then be utilized to inform better strategies for decreasing or preventing resistance.

In *C. glabrata* clinical azole resistance is mediated almost exclusively by activating mutations in the zinc cluster transcription factor Pdr1, which controls the genes encoding the multidrug resistance transporters Cdr1, Pdh1, and Snq2. However, the specific relative contribution of these transporters to resistance is not known. In order to determine this, the *SAT1* flipper method was used to delete *CDR1*, *PDH1*, and *SNQ2* in a strain of *C. glabrata* engineered to carry a clinically relevant activating mutation in *PDR1*. Susceptibility testing was performed according to the CLSI guidelines with minor modifications and confirmed with Etest strips. Of the single transporter deletion strains, only *CDR1* deletion resulted in decreased azole MIC. Deletion of *PDH1* in combination with *CDR1* resulted in a moderate decrease in MIC from that observed with deletion of *CDR1* alone. *SNQ2* deletion only decreased the MIC in the triple deletion strain in the absence of both *CDR1* and *PDH1*. Deletion of all three transporters in combination decreased the MIC to the level observed in the *PDR1* deletion strains for some, but not all of the azoles tested, which indicates additional Pdr1 targets likely play a minor role in this process. These results demonstrate that Cdr1 is the most important Pdr1-mediated multidrug resistance transporter for azole resistance in *C. glabrata*, suggesting that targeting this transporter alone might be sufficient to overcome this clinical problem.

Upc2 and Ecm22 in *S. cerevisiae* and Upc2 in *C. albicans* are the transcriptional regulators of *ERG11*, the gene encoding the target of azoles in the ergosterol biosynthesis pathway. Recently two homologs for these transcription factors, *UPC2A* and *UPC2B*, were identified in *C. glabrata*. One of these, *UPC2A*, was shown to influence azole susceptibility. We hypothesized that due to the global role for Upc2 in sterol biosynthesis in *S. cerevisiae* and *C. albicans*, disruption of *UPC2A* would enhance the activity of fluconazole in both azole-susceptible-dose dependent (SDD) and -resistant *C. glabrata* clinical isolates. To test this hypothesis, we constructed mutants disrupted for *UPC2A* and *UPC2B* alone and in combination in a matched pair of clinical azole-SDD and -resistant isolates. Disruption of *UPC2A* in both the SDD and resistant isolates resulted in

increased susceptibility to sterol biosynthesis inhibitors, including a reduction in fluconazole minimum inhibitory concentration and minimum fungicidal concentration, enhanced azole activity by time-kill analysis, a decrease in ergosterol content, and downregulation of baseline and inducible expression of several sterol biosynthesis genes. Our results indicate that Upc2A is a key regulator of ergosterol biosynthesis and is essential for resistance to sterol biosynthesis inhibitors in *C. glabrata*. As such, the *UPC2A* pathway may represent a potential co-therapeutic target for enhancing azole activity against this organism.

The importance of Pdr1 in azole resistance in *C. glabrata* is well established. Our understanding of how Pdr1 is being regulated, however, is predominantly informed by regulation of similar systems in other organisms. In order to identify genes that interact with the Pdr1 transcriptional pathway, and influence the susceptibility of *C. glabrata* to fluconazole, we screened a collection of deletion mutants for those exhibiting increased resistance to fluconazole. Deletion of the gene coding for a protein homologous to the *S. cerevisiae* J protein Jjj1 resulted in decreased fluconazole susceptibility. We used the *SAT1* flipper method to generate independent deletion mutants for *JJJ1* in a SDD clinical isolate. Expression of both *CDR1* and *PDR1* was increased in the absence of *JJJ1*. In the absence of *CDR1* or *PDR1*, deletion of *JJJ1* had only a modest effect on fluconazole susceptibility. Transcriptional profiling using RNA-Seq revealed up-regulation of genes of the Pdr1 regulon in the absence of *JJJ1*. Jjj1 appears to be a negative regulator of fluconazole resistance in *C. glabrata* and acts primarily through up-regulation of the ABC transporter gene *CDR1* via activation of the Pdr1 transcriptional pathway.

Unlike *C. glabrata* which has essentially one mechanism of resistance, in *C. albicans* clinical azole resistance can be attributed to multiple mechanisms, often in combination. The *RTA3* gene, coding for a member of the Rta1p-like lipid-translocating exporter family, is coordinately upregulated with the ABC transporter genes *CDR1* and *CDR2* in azole-resistant clinical isolates of *C. albicans* that carry activating mutations in the transcription factor Tac1p. We show here that deleting *RTA3* in an azole-resistant clinical isolate carrying a Tac1p activating mutation lowered fluconazole resistance by two-fold, while overexpressing *RTA3* in an azole-susceptible clinical isolate resulted in enhanced fluconazole tolerance associated with trailing growth in a liquid microtiter plate assay. We also demonstrate that an Rta3p-GFP fusion protein localizes predominantly to the plasma membrane, consistent with a putative function for Rta3p as a lipid translocase.

PREFACE

The overarching theme of my graduate research has been development of a deeper understanding of azole resistance in *Candida*. The impetus for this being the currently limited antifungal treatment options and the paucity of new drugs in later stages of development. The azoles are the most widely used antifungal therapy due to their favorable side effect profile, dosage form options and low cost. However, the incidence of resistance to the azoles continues to increase, so much so, that the azoles are no longer recommended as first line therapy for candidiasis. In order to develop strategies for overcoming resistance and reestablishing the utility of the azole class of antifungals, we need to better understand the mechanisms of resistance to azoles in *Candida*.

My dissertation will begin with a general review of azole resistance in *Candida* with a focus on the differences between clinically relevant non-*albicans* species. The second chapter is a more comprehensive review of *Candida glabrata*, as that is the subject of the bulk of the research included here. This will be followed by chapters three to five, which detail three distinct projects related to *C. glabrata* azole resistance. The last chapter summarizes the findings from my graduate work and details my thoughts on possible future directions for these projects. My work in *C. albicans* is included in Appendix A.

In chapter three I investigated the hypothesis that each of the ABC transporters known to be involved in azole resistance in *C. glabrata* do not contribute equally. I show here that *CDR1* codes for the transporter with the largest impact, while the transporters coded for by *PDH1* and *SNQ2* play a much-reduced role in azole resistance.

In chapter four I investigated the hypothesis that the transcription factor coded for by *UPC2A* influences azole susceptibility in a resistant clinical isolate, in addition to a susceptible dose dependent isolate. Prior to the work described here Upc2A had been shown to regulate key genes in the ergosterol biosynthesis pathway including the target for the azoles and deletion of *UPC2A* lead to increased azole susceptibility. We were able to show that deletion of *UPC2A* in a clinical isolate with a gain of function mutation in the transcription factor *PDR1* that results in upregulation of the ABC transporters responsible for effluxing the azoles also lead to increased azole susceptibility.

In chapter five I investigated the hypothesis that the transcription factor Pdr1 is negatively regulated by the J protein coded for by *JJJ1*. Deletion of *JJJ1* resulted in moderate increased expression of *PDR1* and marked increased expression of *CDR1*. Additional ABC transporters do not appear to play a role.

My work in *C. glabrata* reiterates the importance of the transcription factor Pdr1 in azole resistance. Activating mutations in *PDR1* leading to increased efflux of azoles are essentially the only mechanism of resistance found in resistant clinical isolates. My work explores regulation of Pdr1 by Jjj1 and the relative importance of the downstream effectors of Pdr1 – the ABC transporters that efflux azoles from the cell. In addition, the

seemingly unrelated ergosterol biosynthesis pathway, which is controlled by the transcription factor Upc2A is also linked to Pdr1. Treatment with fluconazole in a strain lacking *UPC2A* does not result in upregulation of *PDR1*, *CDR1*, *SNQ2* and *PDH1* to the same extent as drug treatment in the presence of *UPC2A*.

Finally, in Appendix A I investigated the hypothesis that the putative lipid translocase, Rta3*,* contributes to the azole-resistant phenotype in *C. albicans*. Tac1 is a transcription factor that has a function in *C. albicans* similar to that of Pdr1 in *C. glabrata*. Activation of Tac1 leads to increased expression of the genes encoding the ABC transporters *CDR1* and *CDR2*, as well as *RTA3*. Overexpression of *RTA3* in a wild type strain increased tolerance to azoles and deletion of *RTA3* in a resistant strain increased susceptibility to fluconazole.

In my exploration of azole resistance in both *Candida albicans* and *Candida glabrata* the theme has been transcriptional regulation. All three of the transcription factors discussed here are activated by treatment with fluconazole and regulate in the case of Upc2A key genes in the ergosterol biosynthesis pathway and in the case of Tac1 and Pdr1 ABC transporters, as well as other genes that play lesser roles in azole resistance. These transcriptional pathways are imperative for *Candida* to become resistant to the azoles class of antifungals and could potentially be targeted for development of new co-therapeutics that would allow for successful treatment with the azoles.

TABLE OF CONTENTS

LIST OF TABLES

LIST OF FIGURES

CHAPTER 1. AZOLE ANTIFUNGAL RESISTANCE IN *CANDIDA ALBICANS* AND EMERGING NON-*ALBICANS CANDIDA* SPECIES*

INTRODUCTION

Candida albicans and emerging non-*albicans Candida* (NAC) species such as *C. glabrata*, *C. parapsilosis*, *C. tropicalis*, and *C. krusei* can cause superficial infections of the oral and vaginal mucosa as well as disseminated bloodstream and deep-tissue infections. Species involvement varies by infection site and by geography. *Candida* infections are most often caused by *C. albicans* as evidenced by epidemiological studies in the United States (1), Europe (2), and the Middle East (3). Of all the NAC species, *C. glabrata* is the most commonly isolated from patients with candidemia in North America (4-6), and Northern Europe (7, 8), as well as other geographic areas studied with the exception of Latin America (9). *C. glabrata* is also the most common NAC species found to be the causative agent in vulvovaginal candidiasis (VVC) (10-14) and candiduria (15, 16). In some patient populations, for example, candidemia in patients with hematologic malignancy and VVC in diabetic patients, *C. glabrata* is even more common than *C. albicans* (17-19). *C. parapsilosis* is well known for its threat to the pediatric population, as it is responsible for 17–50% of all fungemia in infants and neonates (20, 21). *C. parapsilosis* is also second only to *C. albicans* in incidence as a cause of *Candida* endocarditis with mortality rates between 42 and 65% (22, 23). In the Asia-Pacific region, *C. tropicalis* has been reported to constitute 20–45% of *Candida* isolates (9, 24). *C. tropicalis* infections are commonly associated with malignancy, with some studies reporting higher prevalence among patients with hematologic diseases such as acute myeloid leukemia (25-29). Mortality associated with *C. tropicalis* candidemia in these populations unfortunately remains high, ranging from 30 to 70%, with the highest rates most commonly observed among the elderly (25, 26, 29-31). *C. krusei* is the fourth most common NAC species associated with invasive candidiasis and candidemia, accounting for approximately 2.7% of NAC species isolated across the United States (6). Moreover, the number of *C. krusei* isolates implicated in these types of infections has increased over time (6, 32). In particular, patients with hematologic malignancies and bone marrow transplants have been shown to be at increased risk of *C. krusei* infection (33-35).

AZOLE RESISTANCE IN *CANDIDA* INFECTIONS

There are several classes of compounds that comprise the arsenal used to treat *Candida* infections. The polyenes, azoles, echinocandins, nucleoside analogs, and allylamines are used with varying efficacy depending on the type and site of infection and

---

* Reprinted with permission. **Whaley SG, Berkow EL, Rybak JM, Nishimoto AT, Barker KS, Rogers PD.** 2016. Azole Antifungal Resistance in *Candida albicans* and Emerging Non-albicans *Candida* Species. Front Microbiol **7:**2173. (36)

the sensitivity of the *Candida* species (9, 37-39). The most commonly prescribed antifungal used for most *C. albicans* infections is fluconazole, a member of the azole class of antifungals (9). Azoles inhibit 14-α-sterol demethylase, encoded by the *ERG11* gene, which is an enzyme involved in the biosynthesis of the fungal-specific membrane sterol ergosterol. As some NAC species exhibit intrinsic resistance to azoles, their use is likely a contributing factor to the more frequent incidence of infections caused by these NAC species (40-42). Moreover, many studies have documented the ability of *Candida* to develop high-level resistance to azole antifungals (40, 41). A compilation of fluconazole MIC ranges and epidemiological cutoff values for *Candida* species is presented in **Table 1-1**.

Infections caused by *C. albicans* are associated with varying levels of fluconazole resistance depending on the type of infection. *C. albicans* isolates from candidemic patients have the lowest incidence of azole resistance (0–5%) (43-45). The incidence of fluconazole resistance in *C. albicans* isolates from oropharyngeal candidiasis (OPC) is higher and depends upon previous fluconazole treatment and prior OPC infections (46, 47). *C. glabrata* has the highest incidence of azole resistance among *Candida* clinical isolates and exhibits intrinsic decreased susceptibility to the azole class of antifungals (6, 40), including the newest addition to the class, isavuconazole (48). *C. glabrata* is also able to develop high-level resistance after exposure to azole antifungals (49, 50) and is one of the most frequent species isolated in breakthrough infections from patients receiving azole prophylaxis (19, 51, 52). Of increasing concern are the number of multidrug resistant isolates of *C. glabrata* that are being recovered clinically (53-57). In the Asia-Pacific region, fluconazole resistance in *C. tropicalis* ranges from 0 to as high as 83% (58-60). The worldwide incidence of fluconazole resistance in *C. parapsilosis* disseminated infections ranges between 2 and 5% (44, 61, 62). As *C. krusei* exhibits intrinsic resistance to fluconazole, there is some controversy whether its increased infection rate is related to fluconazole prophylaxis or previous treatment (63-66). Clearly, an understanding of molecular mechanisms driving intrinsic and development of high-level azole resistance is warranted.

AZOLE ANTIFUNGAL RESISTANCE MECHANISMS

Candida albicans

Resistance to azole antifungals in *Candida* (summarized in **Figure 1-1**) has been most extensively studied in *C. albicans*. One mechanism of resistance identified in this species is the presence of point mutations in *ERG11*. Previous studies have identified amino acid substitutions that result in decreased fluconazole susceptibility and have noted that several of these critical allelic variations cluster in three “hot spot” regions within Erg11p (67). Recently, 63 fluconazole-resistant *C. albicans* clinical isolates were examined for mutations within their *ERG11* alleles, and 55 were found to carry at least one mutation that resulted in amino acid substitutions, with nine such predicted amino

Table 1-1. Fluconazole MIC ranges and epidemiological cutoff values for *Candida* species.

***Candida* species (# of isolates tested)**	**MIC range (mode)[1]**	**Percent of resistant isolates**
C. albicans (5265)	0.06 - ≥128 (0.12)	3.5
C. glabrata (7538)	0.12 - ≥128 (4)	7.8
C. krusei (1075)	0.25 - ≥128 (16)	96.6
C. parapsilosis (6023)	0.06 - ≥128 (0.5)	3.4
C. tropicalis (3748)	0.06 - ≥128 (0.25)	2.3

[1]MIC values are in mg/L

Data sources:
CLSI. 2012. Reference Method for Broth Dilution Antifungal Susceptibility Testing of Yeasts; Fourth Informational Supplement, 4th ed. Clinical Laboratory Standards Institute, Wayne, PA.
Espinel-Ingroff A, Pfaller MA, Bustamante B, Canton E, Fothergill A, Fuller J, Gonzalez GM, Lass-Florl C, Lockhart SR, Martin-Mazuelos E, Meis JF, Melhem MS, Ostrosky-Zeichner L, Pelaez T, Szeszs MW, St-Germain G, Bonfietti LX, Guarro J, Turnidge J. 2014. Multilaboratory study of epidemiological cutoff values for detection of resistance in eight Candida species to fluconazole, posaconazole, and voriconazole. Antimicrob Agents Chemother 58:2006-2012.

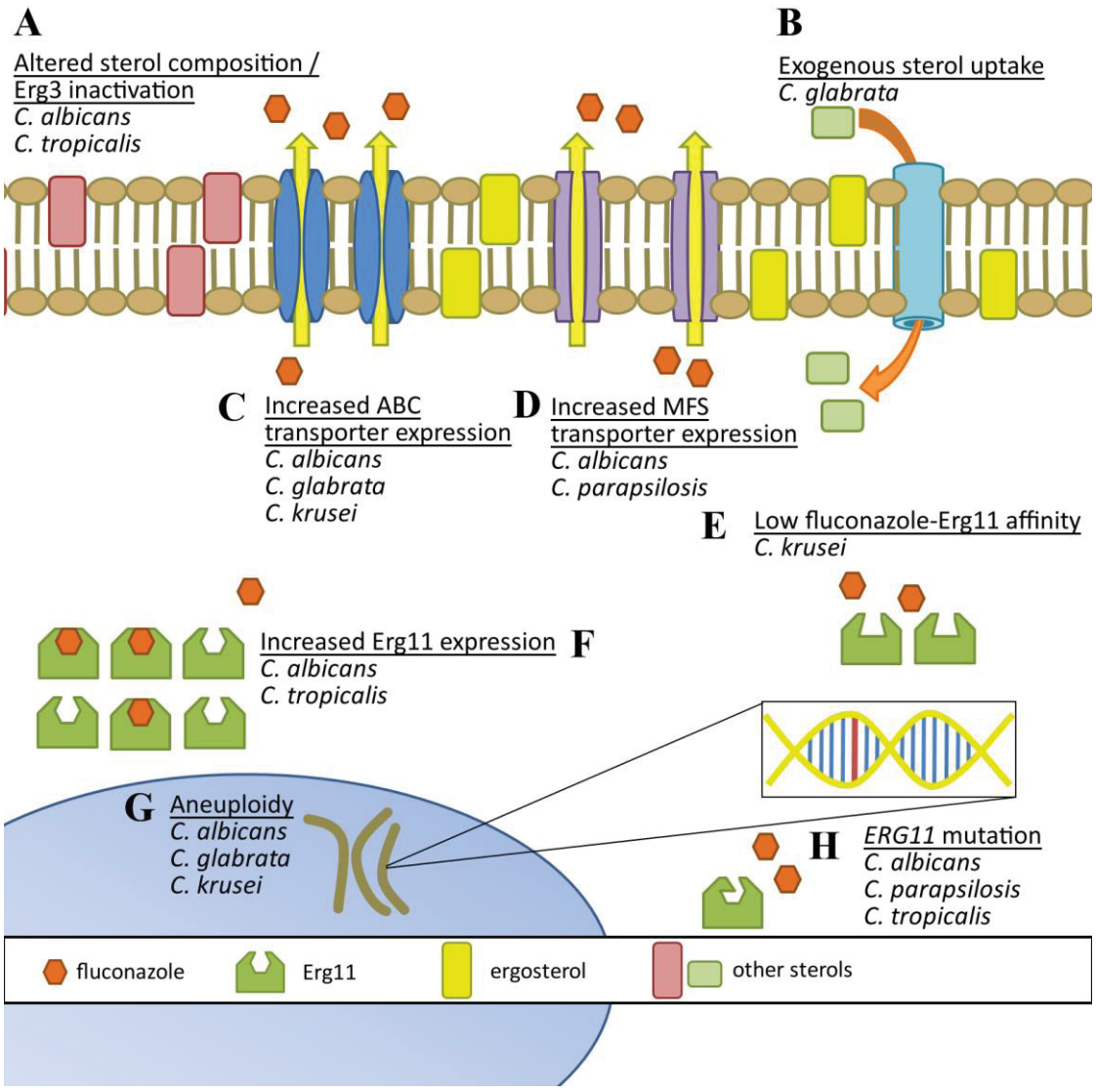

Figure 1-1. Comparison of documented fluconazole resistance mechanisms in *Candida* species.

(A) Erg3 inactivation results in utilization of alternative sterols in the yeast membrane. (B) Uptake of exogenous sterols helps circumvent endogenous sterol production inhibition by fluconazole. Increased production of both (C) ATP-binding cassette efflux pumps and (D) major facilitator superfamily transporters reduces intracellular accumulation of azoles. (E) Inherently low affinity of fluconazole binding to species-specific Erg11 may decrease fluconazole's potential to inhibit the protein. (F) Increased expression of Erg11 protein can help overcome azole activity and (G) aneuploidy may promote genetic adaptation to azole exposure. (H) Mutations in *ERG11* can also result in proteins with reduced affinity for fluconazole binding.

acid substitutions being novel (68). Molecular modeling of the substitutions that resulted in decreased fluconazole susceptibility when expressed in a susceptible background revealed that the mutations clustered in either the predicted catalytic site, the fungus-specific external loop, or on the proximal surface potentially interacting with the loop or near the heme. Additionally, a study involving site-directed mutagenesis of wild-type *ERG11* to introduce mutations identified in 23 *C. albicans* clinical isolates demonstrated nine of these mutations result in increased fluconazole resistance (69). Five of the amino acid substitutions were predicted to be at or near the active site of Erg11p.

Another mechanism of fluconazole resistance in *C. albicans* is the increased expression of *ERG11* due to activating mutations in the gene encoding the zinc-cluster transcriptional regulator Upc2p. *C. albicans* Upc2 is a homolog of the *Saccharomyces cerevisiae ERG* gene regulator pair Upc2/Ecm22. Initially, Upc2 involvement in fluconazole resistance in *C. albicans* was demonstrated when Δ*upc2 C. albicans* strains were shown to be highly susceptible to azoles while those over-expressing Upc2 had increased fluconazole resistance (70). Further studies examining a matched set of fluconazole-susceptible and—resistant *C. albicans* clinical isolates in which fluconazole resistance was not associated with overexpression of drug efflux pumps revealed SNPs in one *UPC2* allele and overexpression of several *ERG* genes and *UPC2* in the resistant isolate (71). Expression of *UPC2* alleles in fluconazole-susceptible strains resulted in increased fluconazole resistance (71-73). Interestingly, three additional matched sets of *ERG11*-overexpressing clinical *C. albicans* isolates have been described which have no sequence differences in *UPC2* between the susceptible and resistant isolates in each pair (72), indicating that other mechanisms of *ERG11* upregulation exist. While these studies were important in establishing Upc2p as a regulator of *ERG11* expression in the context of fluconazole resistance, it was assumed that *UPC2*-mediated fluconazole resistance is a rare occurrence. However, a large study involving 63 fluconazole-resistant *C. albicans* clinical isolates demonstrated 47 of these isolates overexpressed *ERG11* by at least 2-fold (74). Twenty-nine of these *ERG11*-overexpressing isolates contained a missense mutation in *UPC2*, and eight single amino acid substitutions were elucidated from their *UPC2* alleles. Seven of these alleles were found to be associated with increased *ERG11* expression, increased ergosterol production, and decreased fluconazole susceptibility.

Two other mechanisms of fluconazole resistance in *C. albicans* involve the overexpression of drug efflux pumps Mdr1p and Cdr1p/Cdr2p. *TAC1* (transcriptional activator of *CDR* genes) is a zinc-cluster transcription factor whose regulon is hallmarked by the ATP-binding cassette (ABC) transporter-encoding genes *CDR1* and *CDR2* (75). Activation of expression of the *TAC1* regulon is through binding of *TAC1* to the DRE (drug response element) present in the promoters of *TAC1*-regulated genes (75, 76). At least nine hyperactive *TAC1* alleles have been identified (77), and fluconazole minimum inhibitory concentrations (MIC) associated with the isolates from which these alleles have been discovered have revealed that *TAC1* demonstrates codominance resulting in intermediate fluconazole MIC in *TAC1*-heterologous strains and high fluconazole MIC upon loss of heterozygosity (77, 78). Because *TAC1* resides on the left arm of Chr5 with *ERG11*, such loss of heterozygosity in the presence of hyperactive *TAC1* and mutated *ERG11* results in high-level azole resistance (77, 79).

Mdr1p is a major facilitator superfamily (MFS) efflux pump usually expressed at non-detectable levels in wildtype *C. albicans* strains, induced in the presence of benomyl, diamide, and hydrogen peroxide, and constitutively overexpressed in some fluconazole-resistant *C. albicans* isolates (80). *MRR1*, multidrug resistance regulator 1, was identified by comparing the transcriptomes of sets of matched isolates in which the fluconazole-resistant isolates overexpressed *MDR1* (81). Disruption of *MRR1* in these resistant isolates led to a decrease in fluconazole MIC, while introduction of each of the mutant alleles individually into a wildtype fluconazole-susceptible background in the native *MRR1* locus conferred fluconazole resistance to the constructed strain. Another study examined additional *MRR1* allelic variations in *MDR1*-mediated fluconazole resistance (82). In most cases the resistant isolates/strains were homozygous for the *MRR1* allele containing the gain-of-function mutations due to mitotic recombination and chromosome loss.

A less common mechanism of azole resistance in *C. albicans* is inactivation of the *ERG3* gene, which encodes the ergosterol biosynthesis enzyme sterol Δ5,6 desaturase. Erg3p catalyzes one of the final steps in the pathway and also converts nontoxic 14α-methylated sterol intermediates, that accumulate during azole treatment, into the toxic sterol 14α-methylergosta-8,24(28)-dien-3β,6α-diol. Inactivation or deletion of the *ERG3* gene, therefore, prevents such toxic sterols from being synthesized. Only a handful of clinical *C. albicans* isolates have documented azole resistance due to *ERG3* inactivation (83-88).

Aneuploidy plays a role in azole resistance in *C. albicans* as demonstrated by comparative genome hybridization (89). As alluded to earlier, a common aneuploidy found in azole-resistant strains involves Chr5. Similarly, loss of heterozygosity (LOH) has been shown to occur in azole-resistant *C. albicans* (78). Examination of *TAC1* in a matched set of azole-susceptible and -resistant *C. albicans* isolates revealed that the susceptible isolate harbored two wildtype alleles of *TAC1*, while the resistant isolate contained only one of those alleles in which a single nucleotide polymorphism (SNP) translated into an activating amino acid substitution (N977D).

Candida parapsilosis

Because azole resistance has been extensively studied in *C. albicans*, attempts to elucidate mechanisms of azole resistance in *C. parapsilosis* have involved examining orthologous genes and yielded mixed results. A study of a series of six isolates from a single patient found a single SNP in *MRR1* present in the two fluconazole-resistant isolates (90). Nine fluconazole-resistant isolates were obtained from candidemia patients in a Brazilian hospital and examined for *CDR1*, *MDR1*, and *ERG11* overexpression as well as the presence of SNPs in the *ERG11* gene (91). Each of the resistant isolates possessed a single homozygous SNP (A395T) which corresponds to a Y132F amino acid substitution. In addition, while none of the isolates overexpressed *MDR1* as compared to the *C. parapsilosis* reference strain ATCC22019, *CDR1* expression was between 3.3- and 9.2-fold higher in these isolates as compared to the reference strain, and *ERG11* was

overexpressed between 1.5- and 7.4-fold. While this study indicated an association between *CDR1* and *ERG11* and fluconazole resistance in *C. parapsilosis*, a causal link was not definitively proven.

In a larger-scale study, 30 resistant isolates, 37 susceptible-dose-dependent isolates, and 55 susceptible isolates were collected from hospitals in four U.S. cities, and their *ERG11* genes were sequenced (92). Five SNPs were identified in 54 of the isolates; amino acid substitution Y132F, found in 17 resistant isolates, was the only one found exclusively in resistant isolates. Twenty-three isolates harbored SNPs in *MRR1*. Of the nine SNPs identified, only three were found exclusively in resistant isolates. Quantitative PCR measuring relative *MDR1* expression revealed nine isolates (six with a SNP in *MRR1*, three without) with at least 5-fold increase in *MDR1* expression compared to a composite expression level from a subset of susceptible isolates. However, the expression levels were a fraction of the levels achieved by *MDR1*-mediated azole resistance in *C. albicans*. Without definitive experiments in which introduction of a mutated *ERG11* allele confers azole resistance in a susceptible isolate, these results remain suggestive.

In an effort to identify potential mechanisms of azole resistance on a genome-wide scale in *C. parapsilosis*, fluconazole-, voriconazole-, and posaconazole-resistant strains were developed experimentally by serial passage in liquid culture containing either fluconazole, voriconazole, or posaconazole (93). The fluconazole- and voriconazole-resistant strains were cross-resistant to both fluconazole and voriconazole and possessed similar transcriptional profiles as assessed by microarray analysis; however, the posaconazole-resistant strain was not cross-resistant to the other azoles and had a distinct transcriptional profile. Among the genes differentially expressed in fluconazole- and voriconazole-resistant strains were the stress response gene *GRP2*, as well as *MDR1* and *MRR1*. *ERG11* was not differentially expressed in these strains. However, in the posaconazole-resistant strain, the ergosterol biosynthesis genes *ERG11* and *ERG6*, as well as *ERG* gene regulator *UPC2* were among the genes differentially expressed.

In a study using laboratory strains of *C. parapsilosis* in which previously-determined gain-of-function alleles of *CpMRR1* were introduced into the native locus, strains containing Mrr1p with a G583R amino acid substitution from a fluconazole-resistant *C. parapsilosis* isolate led to resistant fluconazole and voriconazole MIC compared to strains harboring the wildtype allele (94). Similarly, strains with single SNP-containing *MRR1* alleles had a ~5-fold increase in *MRR1* gene expression and ~70-fold increase in *MDR1* gene expression.

In another study, 35 unrelated fluconazole-resistant and four unrelated susceptible isolates of *C. parapsilosis* were examined to elucidate mechanisms of fluconazole resistance in *C. parapsilosis* (95). Sixteen resistant isolates overexpressed *CDR1*, three other resistant isolates exhibited *MDR1* overexpression, and eight resistant isolates demonstrated overexpression of *ERG11* as compared to the susceptible isolates. When sequencing orthologues of *UPC2*, *MRR1*, and *TAC1* in order to identify putative gain-of-function mutations that would lead to overexpression of *ERG11*, *MDR1*, and *CDR1*, only

one heterozygous mutation in *UPC2* was recovered from one isolate, suggesting that *ERG11* overexpression in fluconazole-resistant *C. parapsilosis* is not mediated by *UPC2*. *TAC1* mutations that were recovered did not fully correspond with *CDR1* overexpression and those recovered were not analogous to those found in gain-of-function *CaTAC1* alleles. Similarly, *MRR1* mutations recovered did not correspond to any mutations found in gain-of-function alleles of *CaMRR1*. Subsequently, *CDR1* was deleted from three of the *CDR1*-overexpressing isolates which only resulted in a one-dilution decrease in fluconazole MIC. *MDR1* deletion in three *MDR1*-overexpressing isolates revealed a one-dilution decrease in fluconazole MIC in two isolates and no change in fluconazole MIC in the third. To address the role of alterations in the ergosterol biosynthesis pathway in azole resistance in *C. parapsilosis*, *ERG11*, and *ERG3* were sequenced. No *ERG3* mutations were recovered, which was supported by the sterol profiles of the isolates. A single *ERG11* mutation (Y132F) was recovered in one resistant isolate and a combination of Y132F and R398I mutations was found in an additional ten isolates. In nine of these eleven isolates there was a change in the sterol profile indicative of a change in Erg11 functionality. This study indicates that while differential expression of efflux pumps is commonly found in azole-resistant *C. parapsilosis* isolates, the resistant phenotype is not solely due to their overexpression but instead is multifactorial and involves *ERG11* mutation and/or overexpression.

Candida tropicalis

As compared with other species of *Candida*, relatively little is known about the mechanisms of azole resistance in *C. tropicalis*. An analysis of 52 clinical *C. tropicalis* isolates from China found the average *ERG11* expression level more than 4-fold higher among fluconazole-resistant isolates than -susceptible isolates (96). Moreover, *ERG11* expression was even higher among a subset of fluconazole-resistant isolates also resistant to itraconazole and voriconazole. These results were recently echoed by a similar study characterizing 35 *C. tropicalis* isolates from Korean university hospitals, nine of which were fluconazole-non-susceptible (97). While considerable variability in *ERG11* expression (~150-fold) was observed in the highly fluconazole-susceptible group, *ERG11* expression was significantly higher among both less fluconazole-susceptible (MIC 1–2 μg/ml) and fluconazole-non-susceptible (MIC ≥ 4 μg/ml) isolates. This study also sequenced the *C. tropicalis UPC2* gene and found several heterozygous and homozygous mutations. However, many of these mutations have been observed in fluconazole-susceptible isolates not found to overexpress *ERG11*, and further characterization of their impact on the regulatory function of *UPC2* is needed.

Molecular characterization of azole-resistant clinical *C. tropicalis* isolates has also revealed alterations in the ergosterol biosynthetic pathway (96-99). A fluconazole-resistant *C. tropicalis* isolate recovered from a clinical blood specimen from Tunisia was found to have mutations in both *ERG3* and *ERG11* which were individually observed to be detrimental to ergosterol biosynthesis when heterologously expressed in *S. cerevisiae* (99). Notably, the *ERG11* mutation in this isolate consisted of a deletion of 132 nucleotides resulting in a D275V amino acid substitution and the loss of 44 amino acids

near the N-terminus of Erg11p. Homozygous replacement of the wild-type *C. tropicalis ERG11* with the truncated clinical variant, with or without the associated clinical *ERG3* mutation, resulted in high-level fluconazole resistance in a fluconazole-susceptible reference strain of *C. tropicalis*. Additionally, an *ERG11* mutation resulting in decreased fluconazole susceptibility due to the amino acid substitution Y132F, has been well characterized in *C. albicans* and was recently observed in a fluconazole-resistant *C. tropicalis* isolate from a patient with candidemia (100).

One of the first studies to associate the overexpression of efflux pumps with azole resistance in *C. tropicalis* utilized serial passaging of a reference *C. tropicalis* isolate on media containing various concentrations of fluconazole to produce genetically-related isolates with reduced fluconazole susceptibility (101). After passaging, all isolates with reduced susceptibility to fluconazole demonstrated increased expression of both *C. tropicalis MDR1* and a gene with high homology to *C. albicans CDR1*. In both cases, the increased expression was found to then be diminished in fluconazole-susceptible revertants obtained from further passaging on fluconazole-free media. The role of efflux pump overexpression in azole resistance among clinical *C. tropicalis* isolates has been less clearly defined. When the expression of *MDR1* and *CDR1* was examined in the aforementioned 52 clinical *C. tropicalis* isolates from China, no significant difference was observed between fluconazole-susceptible and -resistant isolates (96). In contrast, among the 35 clinical isolates from Korean university hospitals, expression of both *MDR1* and *CDR1* was observed to be significantly higher among both less-fluconazole-susceptible and fluconazole-non-susceptible isolates. However, it is important to note the large degree of variability in the expression of *MDR1* and *CDR1* observed in the highly fluconazole-susceptible control group, ~50-fold and ~30-fold respectively (31). To date, experiments to directly delineate the potential role of these efflux pumps has yet to be performed in *C. tropicalis*, and the homologs of *C. albicans MRR1* and *TAC1* have not been examined.

Candida krusei

C. krusei is intrinsically resistant to fluconazole, though the precise mechanism is not completely understood. Several studies have attributed *C. krusei*'s innate azole resistance to efflux pump activity, namely through the ATP-binding cassette transporter Abc1p, and reduced drug accumulation (102-104) in combination with reduced azole affinity for Erg11p (102, 104-107). Changes in the cell membrane affecting membrane fluidity may be implicated in azole resistance as well since there is evidence to suggest that intracellular azole accumulation occurs through one or possibly both mechanisms of passive and facilitated diffusion (108, 109). Additionally, the discovery of a trisomy in the *ERG11*-containing chromosome in a *C. krusei* strain suggests aneuploidy may not be uncommon in this species, though the effects as it relates to azole resistance are not yet known (104).

Resistance mechanisms against other azoles are also not clearly defined. For example, analysis of itraconazole-resistant *C. krusei* isolates revealed that reduced

intracellular content of the drug and not altered affinity for the drug target likely drives itraconazole resistance (102, 110). However, more recently it has been suggested that overexpression of genes encoding both Erg11p and the efflux pump Abc2p may also play a role with itraconazole resistance (111, 112). Despite its fungicidal activity in *C. krusei* (113) resistance to voriconazole has also emerged, and current research supports a theory where overexpression of the genes encoding the efflux pump Abc2 and Erg11 impart more transient resistance properties, while increased expression of Abc1p and point mutations in *ERG11* predominate as time progresses to yield a stably resistant pathogen in the prolonged presence of voriconazole (114). Erg11p amino acid substitutions have been observed in azole-resistant *C. krusei* and, in the case of Y166S, have been predicted to interfere with Erg11p function (114, 115). While the newer antifungal agents posaconazole and isavuconazole have shown good activity against *C. krusei* (116, 117), reports of resistance against these agents are relatively sparse (44, 118). However, in a recent analysis examining NAC strains in the U.S. by region, *Candida krusei* resistance to posaconazole was highest in the eastern United States, with posaconazole resistance occurring in 13–16.7% of isolates (6). Nevertheless, the mechanisms of resistance in *C. krusei* against these agents remain to be investigated.

Candida glabrata

C. glabrata is unique among the *Candida* species discussed here as it is a haploid yeast more closely related to *S. cerevisiae*. Development of azole resistance in clinical isolates of *C. glabrata* has been almost exclusively linked to the presence of activating mutations in the zinc cluster transcription factor Pdr1 (119) that lead to differential expression of downstream targets. Nearly all clinical isolates have been found to have *PDR1* mutations, with such mutations found in the inhibitory domain, activating domain, middle homology region, and xenobiotic binding region. The rapid acquisition of *PDR1* mutations could be due to the high incidence of mutations in the mismatch repair gene *MSH2*, which results in a hypermutable phenotype (120). The activating mutations exhibit distinct expression patterns of the downstream effector genes, with the exception of increased expression of *CDR1* and *PUP1*, and no correlation has been found between location of the mutation and altered gene expression (121-125). Among the genes whose pleiotropic drug response element (PDRE) is directly bound by Pdr1 (126), only three, the ABC transporters *CDR1* (127), *PDH1* (*CDR2*) (128, 129), and *SNQ2* (130, 131), have been linked directly to azole resistance. Recent work has shown increased expression of four MFS transporters in clotrimazole resistant isolates compared to clotrimazole susceptible clinical isolates. Disruption of one of these, *TPO3*, moderately increased susceptibility to clotrimazole and fluconazole (132). These findings suggest MFS transporters may have a minor role in azole resistance in *C. glabrata*.

Surprisingly, *ERG11* does not appear to play an important role in clinical azole resistance in *C. glabrata* (119, 127, 130). Increased expression of *ERG11* has been observed in only two clinical isolates of *C. glabrata* (133, 134). The upregulation in one isolate was later found to be due to duplication of the entire chromosome containing *ERG11* and the phenotype was lost with subsequent passaging in azole-free media (135).

A single resistant clinical isolate of *C. glabrata* has been shown to have a nonfunctional 14-α-sterol demethylase due to a missense mutation in *ERG11*, which led to the complete absence of ergosterol in the cell membrane (55). No additional clinical isolates have been identified to have resistance mechanisms related to the azole target.

C. glabrata has the ability to grow with altered cell membrane sterols, which allows for evasion of azole treatment. *C. glabrata* is able to take up exogenous sterols (136), both when the ergosterol biosynthesis pathway is blocked and under normal conditions in wild type strains (137, 138). Aus1p has been identified as the sterol transporter responsible for tolerance to azoles in the presence of exogenous sterols (139). *C. albicans* has recently been shown to take up sterols under aerobic conditions; however, *C. glabrata* is more liberal in its ability to take up sterols and does so in both aerobic and anaerobic conditions and, in the presence of serum and fluconazole, enhances uptake under aerobic conditions (140).

Azole resistance in *C. glabrata* has also been attributed to the formation of petite mutants, which are cells that have lost mitochondrial function resulting in respiratory deficiency (141, 142). Petite mutants can be generated in the laboratory by treatment with azoles or ethidium bromide. This mutant phenotype has been recovered clinically (143, 144), but is not common among clinical isolates. Azole resistance in petite mutants has been attributed to upregulation of the ABC transporters *CDR1*, *CDR2*, and *SNQ2* (129, 144), which is dependent on Pdr1 (121). Petite mutants exhibit altered sterol profiles with a disproportionate amount of ergosterol and very little of ergosterol intermediates; however, no changes in the sequence of *ERG11* or its expression have been detected (145).

CONCLUSIONS

Candida species are responsible for a majority of superficial and disseminated fungal infections in humans. While azole antifungals have long provided effective treatment for such infections, recent epidemiological studies indicate that intrinsic azole resistance in some *Candida* species as well as development of high-level azole resistance is a problem of critical importance in the clinical setting. While extensive studies to elucidate molecular mechanisms of high-level azole resistance in *C. albicans* has uncovered the role of ergosterol biosynthesis gene mutation and *ERG* gene and drug efflux pump upregulation as key mediators of azole resistance, there are clearly other factors at play that contribute significantly to such resistance. Similarly, while NAC are closely related to *C. albicans*, that does not necessarily translate to analogous molecular mechanisms of azole resistance.

Of the NAC species highlighted in this review, *C. parapsilosis*, *C. tropicalis*, *C. krusei*, and *C. glabrata* all express ABC transporter and/or MFS genes orthologous to *CaCDR1* and *CaMDR1*. However, as discussed, the altered expression of these genes in azole-resistant NAC appear to contribute differently to resistance in different species. Moreover, the transcriptional regulators and genetic mutations governing azole efflux and

sterol biosynthesis in *C. tropicalis*, *C. parapsilosis*, and *C. krusei* have not been fully examined. Finally, there exist clear differences in the mutations in *ERG11* that are found to influence azole resistance in clinical isolates among these species. As azole resistance continues to emerge in these species, a more complete understanding of the important differences among resistance mechanisms employed by these species will be needed in order to circumvent this important clinical problem.

CHAPTER 2. AZOLE RESISTANCE IN *CANDIDA GLABRATA**

INTRODUCTION

The incidence of fungal infections continues to rise in susceptible populations, which include transplant patients, those with AIDS, patients with malignancy, those on immunosuppressive therapy, patients receiving total parenteral nutrition and premature infants (146). The most common cause of these opportunistic fungal infections is *Candida* (5). Collectively *Candida* species are the fourth most common cause of nosocomial blood stream infections in the United States (147, 148). Reported mortality rates for patients with candidemia vary, but are as high as 40% and have not decreased in the past fifteen years (5, 149-151). *Candida glabrata* is the second most common cause of *Candida* infections in most geographic populations studied (5, 7, 8, 152-158) and in some clinical populations is the most common, surpassing *Candida albicans* among patients with hematologic malignancies (19), diabetics (152, 159), and patients with an abdominal source of infection (152, 159).

Currently there are three classes of antifungals used clinically for the treatment of candidiasis. Amphotericin B, which targets ergosterol, the primary sterol in the fungal cell membrane, has long represented the gold standard for therapy, but is hampered by significant infusion-related adverse events and nephrotoxicity. As such, its use has decreased in recent years. The azole antifungals target lanosterol 14-α-demethylase which represents a key step in the biosynthesis of ergosterol. One member of this class, fluconazole is the most widely prescribed antifungal agent, is inexpensive, and is available for both oral and intravenous administration. While fluconazole is acceptable as first line therapy for invasive candidiasis in patients who are not critically ill and have not had prior azole exposure, its utility has been hindered by the emergence of resistance, particularly in *C. glabrata*. Multiple studies have shown a link between azole prophylaxis and increased rates of infection with *C. glabrata* (19, 52, 160, 161) and in one study azole prophylaxis was only a risk factor for resistant isolates of *C. glabrata* (50). The echinocandins, which target the fungal cell wall, have therefore become first line agents for treatment of this indication (39). However, resistance to this class of antifungal has also begun to emerge. In addition many reports of multidrug resistant isolates of *C. glabrata* have emerged in recent years (54, 55, 57, 162-164). It is therefore imperative to understand the basis of azole antifungal resistance in order to preserve this class of antifungal and overcome this clinical problem. In this review we will provide an overview of the mechanisms of azole antifungal resistance in *C. glabrata* with a focus on recent important discoveries in the field.

---

* Reprinted with permission. **Whaley SG, Rogers PD.** 2016. Azole Resistance in *Candida glabrata*. Curr Infect Dis Rep **18:**41.

MULTIDRUG TRANSPORTERS

Pdh1, which stands for pleomorphic drug resistance homolog (also known as Cdr2 for *Candida* drug resistance), was the first drug transporter identified as participating in azole resistance in *C. glabrata*. This ATP binding cassette (ABC) transporter was discovered independently by two groups. Initially a series of isolates taken from a patient being treated with fluconazole for oral candidiasis was studied. Azole resistance was observed in the later isolates of this series and was associated with a decrease in intracellular fluconazole. There was also a significant increase in the transcript level of a gene with 72.5% identity with the *Saccharomyces cerevisiae* ABC transporter *PDR5* (pleiotropic drug resistance), which was called *PDH1*. Treatment with fluconazole also increased expression of *PDH1* in the susceptible isolate, but did not further increase expression in one of the later resistant isolates from the series (128). The same group continued their work on *PDH1* later demonstrating that deletion of *PDH1* in a mutant *C. glabrata* strain already lacking *CDR1* resulted in an increase in fluconazole susceptibility. When *PDH1* was overexpressed in the *CDR1* deletion strain fluconazole minimum inhibitory concentration (MIC) was restored to that of the wild type (165).

A second group identified the same gene by observing that a strain in which *CDR1* was deleted was still able to become resistant to azoles in vitro. A search for additional transporters potentially responsible for this observation led to the discovery of two such transporters. These were *PDH1* (which these investigators named *CDR2*) and *SNQ2*. *CDR2* exhibited very low levels of expression in azole susceptible strains, but was upregulated as much as 100-fold in resistant strains. Heterologous expression of *CDR2* in *S. cerevisiae* decreased susceptibility to azoles, whereas *SNQ2* was not examined further (129).

A second ABC transporter in *C. glabrata*, named Cdr1, was later found to have a significant role in azole resistance. Initial studies of two sets of matched isolate pairs from patients receiving fluconazole treatment for oral candidiasis revealed that there was a decrease in fluconazole accumulation in the resistant isolates as compared to the susceptible parent isolates. Expression analysis of candidate genes revealed *CDR1* to be the only transporter tested that was upregulated in both resistant isolates. *CDR1* stands for *Candida* drug resistance and was named due to homology with the *C. albicans* gene of the same name. The sequence shares 75% identity with *S. cerevisiae PDR5*, which encodes an ABC transporter well established as a cause of pleiotropic drug resistance in this organism. Deletion of *CDR1* in a resistant isolate reduced susceptibility to azoles and increased fluconazole accumulation as compared to the resistant isolate (127). When *CDR1* and *PDH1* (*CDR2*) were constitutively expressed in *S. cerevisiae*, the level of resistance to azoles was higher in the strain expressing *CDR1*. This implies that *CDR1* is the most important of these transporters in high-level azole resistance in *C. glabrata* (129). Like *PDR5* in *S. cerevisiae* and *PDH1* in *C. glabrata*, expression of *CDR1* has also been shown to increase upon exposure to azole antifungals (119).

The ABC transporter Snq2 (sensitivity to 4-nitroquinoline-n-oxide), named due to its similarity to the *S. cerevisiae* gene with the same name, was initially thought to play a

minor role in azole resistance if any (129). Subsequent analysis of *C. glabrata* isolates from hospital infections over a three-year period solidified the importance of *SNQ2* in azole resistance. In addition to the expected upregulation of *CDR1* and *PDH1* in the resistant isolates, several also exhibited upregulation of *SNQ2* although to a lesser extent. The increased expression was often in combination with upregulation of the other ABC transporters, but was the only ABC transporter with increased expression in two isolates that were resistant to the tested azoles (130). Further analysis of one resistant clinical isolate with basal levels of *CDR1* and *PDH1* and increased expression of *SNQ2* demonstrated the importance of *SNQ2* in azole resistance. Disruption of *SNQ2* in this isolate resulted in an azole susceptible phenotype. Reintroduction of *SNQ2* restored the resistant phenotype (131).

In *C. albicans* the major facilitator superfamily (MFS) transporter Mdr1 also plays a significant role in azole resistance (166, 167). In *C. glabrata* the MFS transporter gene *QDR2* (quinidine resistance) was shown to be upregulated in a resistant strain compared to a susceptible matched isolate by microarray analysis and confirmed by qPCR (168). Later studies showed *QDR2* was upregulated in a second resistant isolate compared to its parent (124). Subsequent investigation of *QDR2* in azole resistance showed a weak link that likely does not have clinical significance for systemic fungal infections. Disruption of *QDR2* increased sensitivity to the imidazoles - ketoconazole, miconazole, and clotrimazole, but had no effect on fluconazole or itraconazole sensitivity. Overexpresssion of *QDR2* decreased sensitivity to ketoconazole, miconazole, and clotrimazole (169).

TRANSCRIPTIONAL REGULATION OF AZOLE RESISTANCE

In *S. cerevisiae* there are two transcription factors that regulate expression of efflux pumps, Pdr1 and Pdr3. In *C. glabrata* after observing that the known efflux transporters at the time were coordinately upregulated with azole treatment the closest homolog for Pdr1 and Pdr3 was identified as Pdr1 (119). In *S. cerevisiae* the *PDR3* promoter contains binding sites for both Pdr1 and Pdr3, which allows for autoregulation. These binding sites are called pleiotropic drug response elements (PDRE). An initial study showed upregulation of *PDR1* in a lab derived resistant strain of *C. glabrata*, but not in the resistant clinical isolates and additional laboratory derived resistant strains (119). Later work showed that the promoter regions of Pdr1, as well as the efflux transporters contain the PDRE (125). Pdr1 was shown to bind directly to the PDRE in the promoters of *CDR1*, *PDH1*, *SNQ2* and *QDR2* as well as additional members of the Pdr1 regulon (126).

The most important mechanism of resistance in *C. glabrata* is the acquisition of activating mutations in the gene encoding the transcription factor Pdr1 that lead to upregulation of ABC transporters. Other than a few rare instances that will be discussed later in this review practically all clinical isolates that have developed high level azole resistance have been found to have Pdr1 activating mutations. Many different *PDR1* mutations that affect azole susceptibility have been identified in every region of the gene.

These mutations result in distinct patterns of altered gene expression among Pdr1 target genes and no correlation between location of the mutation and gene expression has been identified (51, 119, 121-125, 131, 168).

REGULATION OF PDR1

Mediator complex

The mechanism for activation of Pdr1 by fluconazole and other xenobiotics is similar to activation of pregnane X receptor in mammalian systems and Pdr1/Pdr3 in *S. cerevisiae*. Ketoconazole was found to bind directly to Pdr1. Gal11A was identified as a co-activator for drug dependent activation and interacts with Pdr1 through a binding domain that is similar to the KIX domain in humans. Gal11A is a component of the tail portion of the Mediator complex, which interacts with RNA polymerase II to regulate transcription. Infection with strains lacking Pdr1 and strains lacking Gal11A resulted in comparable increased survival with fluconazole treatment compared to wild type in a *Caenorhabditis elegans* model of infection (170). An inhibitor for the interaction between the KIX domain on Gal11A and Pdr1 was identified through a high throughput screen. This compound named iKIX1 prevented ketoconazole-induced upregulation of efflux pumps, as well as upregulation due to activating mutations in Pdr1 (171). This suggests that it may be possible to overcome Pdr1-mediated azole resistance in *C. glabrata* by chemically interfering with Pdr1 activity.

In addition to Gal11A three additional subunits of the Mediator complex have been implicated in azole resistance. Screening a transposon mutagenesis library for genes that when deleted resulted in increased susceptibility to azoles identified *MED2* (mediator complex) and *PGD1* (polyglutamine domain), both genes code for members of the tail portion of the Mediator complex (172). Subsequent deletion of *MED2* predictably also resulted in increased sensitivity to azoles. Similar to results seen for a Gal11A mutant strain described above, deletion of *MED2* prevented fluconazole-induced upregulation of *CDR1*. Med2, as well as two additional components of the Mediator complex, Nut1 (negative regulation of URS2) and Srb8 (suppressor of RNA polymerase B) were required for induced fluconazole resistance due to expression of an ectopic vector expressing *PDR1* with an activating mutation. However, two additional components of the tail portion of Mediator were not required. No direct interaction was observed between Pdr1 and Med2 in co-immunoprecipitation experiments (173).

Negative regulators of azole resistance

One of the homologs for Pdr1 in *S. cerevisiae* forms a heterodimer with the transcription factor Stb5 (Sin3 binding protein) before binding to the promoter of ABC transporters (174). The homolog for Stb5 was identified in *C. glabrata* and further studied for a potential role in azole resistance. Deletion of Stb5 resulted in a minimal

increase in voriconazole MIC, but no difference was observed with fluconazole. Microarray studies revealed of the 68 genes upregulated in a strain with *STB5* deleted 34 were also upregulated in a strain overexpressing *PDR1*. The upregulation of *PDR1*, *CDR1*, and *PDH1* in the Stb5 deletion strain was confirmed by qPCR analysis. These findings indicate a role in for Stb5 as a negative regulator of Pdr1 in *C. glabrata* (175).

Sirtuins, found in all organisms, are regulatory proteins that are dependent on nicotinamide adenine dinucleotide (NAD^+) and function as deacetylases. In *C. glabrata* there are five members of this family. NAD^+ is limited in certain niches in the host, such as the urinary tract and *C. glabrata* is unable to synthesize it. Under these conditions sirtuins are inactivated resulting in derepression of target genes. Previous work has focused on derepression of genes involved in host adaptation, for example adhesins, which are important for virulence. More recently one of the members of the sirtuin class of proteins in *C. glabrata*, Hst1 (homologues of Sir2), has been shown to participate in regulation of Pdr1. An initial microarray study showed increased expression of efflux pumps regulated by Pdr1 in an Hst1 deletion strain (176).

Additional work by a second group further elucidated the importance of the regulation by Hst1. Resistance to fluconazole increased in the presence of nicotinamide (NAM), which is an inhibitor of the sirtuin class of proteins. Deletion of Hst1 resulted in a six-fold increase in fluconazole MIC, while none of the other sirtuin deletion strains shared this phenotype. In Pdr1 and Cdr1 deletion strains, the deletion of Hst1 resulted in a minimal increase in MIC. *PDR1* expression was moderately increased and *CDR1* was increased approximately 20 fold in the Hst1 deletion strain. As in other organisms, Hst1 was found to function in complex with Sum1 (suppressor of mar1-1) and Rfm1 (repression factor of middle sporulation element). Deletion of any member of the complex resulted in the same altered fluconazole susceptibility. These experiments indicate a role for the Hst1-Rfm1-Sum1 complex in the negative regulation of Pdr1 (177).

ALTERATION OF DRUG TARGET

The azole target, lanosterol 14-α-demethylase has been implicated in resistance in other species of *Candida*, both through alteration of the azole binding site and increased expression due to activating mutations in the transcription factor responsible for its regulation. In a comprehensive analysis of 29 resistant *C. glabrata* clinical isolates, none had increased *ERG11* expression and none were found to carry a mutation in *ERG11* suggesting that alterations in this gene are not important for clinical resistance in *C. glabrata* (130). Anecdotal incidents of a role for *ERG11* have been reported. Activity of lanosterol 14-α-demethylase was increased in a resistant clinical isolate (133) and was later attributed to a chromosomal duplication (135). *ERG11* expression was found to be increased in a single azole-resistant oral isolate after recurrent infection in a patient receiving treatment for neck cancer (134). The first clinical isolate possessing a mutation in *ERG11* in *C. glabrata* was reported in 2012 in an isolate recovered from a urine sample. A missense mutation resulted in the glycine at position 315 being replaced with

aspartic acid. *ERG11* in this isolate was nonfunctional as exhibited by its sterol profile which had no detectable ergosterol and >80% lanosterol (55).

STEROL HOMEOSTASIS

The sterol biosynthesis pathway is a focus of antifungal therapy due to its unique components in yeast versus the human host. The sterol composition of the cell is influenced by regulation of the sterol biosynthesis pathway, drug treatment, and exogenous sterol uptake. Altered sterols in the cell membrane can lead to altered membrane fluidity, which affects membrane proteins and can lead to static growth. Expression of the enzymes in the sterol biosynthesis pathway including the azole target Erg11 are regulated by the zinc cluster transcription factor, Upc2A (178). Deletion of *UPC2A* in *C. glabrata* results in decreased expression of ergosterol biosynthesis genes and prevents the induction of ergosterol biosynthesis when treated with inhibitors of the pathway. *UPC2A* also plays a role in azole susceptibility. Disruption of *UPC2A* in both susceptible and resistant isolate decreased fluconazole minimum inhibitory concentration (MIC), minimum fungicidal concentration (MFC), and enhanced fluconazole activity by time-kill analysis. This suggests the Upc2A pathway might represent the key to overcoming azole resistance in this organism (179).

Treatment with the azole class of antifungals inhibits the synthesis of ergosterol resulting in static growth. One potential explanation for *C. glabrata*'s inherent reduced susceptibility to the azole antifungals is the ability to take up exogenous sterols. While the ability to take up sterols had previously been shown in *S. cerevisiae*, the first description of this phenomenon in *C. glabrata* was in Erg9 deletion strains. *ERG9* was placed under the control of a tet promoter, such that upon treatment with doxycycline *ERG9* was depleted. In lab media depletion of *ERG9* resulted in rapid cell death, but in mice *ERG9* depletion had a negligible effect on *C. glabrata* growth. Serum from multiple sources was able to recover the growth defect in vivo and the effect was shown to be attributable to cholesterol (136). Additional studies from a separate group confirmed the ability of *C. glabrata* to take up exogenous sterols in a strain with a transposon inserted into Erg1 (137). Further work on the conditions required for sterol uptake in *C. glabrata* revealed that sterols can be taken up in aerobic conditions in a Upc2A independent manner or anaerobic conditions in a Upc2A dependent manner. In aerobic conditions sterol uptake can also be induced by the presence of bovine serum or fluconazole in a Upc2A dependent manner (140).

The realization that identification of *C. glabrata* as the causative agent in some infections (mainly urinary tract) was missed because the isolates required media containing bile for growth lead to further studies in sterol uptake. Cholesterol was identified as the probable component in bile responsible for growth in these isolates. Bile supplementation was also found to decrease azole susceptibility in clinical isolates not dependent on bile for growth (180). A subsequent study of the same isolates revealed that four of the five were defective in sterol synthesis and the remaining isolate was defective in heme synthesis. These isolates were able to grow in the presence of cholesterol, human

serum or bovine serum. *C. albicans* mutants for similar pathways were unable to grow in the presence of exogenous sterols. Cholesterol was also taken up in an isolate that had no growth defect or deficiency in sterol synthesis (138).

A better understanding of how exogenous sterols are taken up could potentially lead to development of a co-therapeutic that would allow the azoles and other antifungals that act on the ergosterol pathway to be more effective against *C. glabrata*. *AUS1* was identified as the transporter responsible for exogenous sterol uptake due to its similarity to sterol transporters that act in anaerobic conditions in *S. cerevisiae*. Depletion of *AUS1* prevented the recovery of *ERG9* mutants by exogenous sterols (139). *UPC2A* and its homolog *UPC2B* were both shown to be important for *AUS1* expression (178). Recent work also demonstrated a role for iron in the function of *AUS1* sterol transport (181).

VIRULENCE

Increased resistance in microbial pathogens results in decreased fitness and virulence in the majority of cases. In *C. albicans* azole resistance is often associated with a fitness cost in vitro, but in vivo there appear to be compensatory mechanisms that decrease or eliminate the growth defect (182). However, in *C. glabrata* recent work has demonstrated that the most common mechanism for resistance to the azole class of antifungals, activating mutations in *PDR1*, results in increased fitness and virulence both in vivo and in vitro.

Initial in vivo experiments conducted in a murine model of infection demonstrated an increased fungal load in the kidney, liver and spleen for strains altered to possess different GOF mutations in *PDR1* compared to the wild type. These alleles were also associated with reduced survival of the mice tested. When *PDR1* was disrupted there was no difference in fungal load or virulence compared to wild type. This initial study demonstrated that Pdr1 is not required for infection and basal level of virulence, but GOF mutations do offer a competitive advantage (123). *PDR1* activating mutations did not influence replication or survival inside macrophages in culture and were not associated with increased cytokine production. However, strains with activating mutations in *PDR1* displayed greater adhesion to epithelial cells and reduced uptake by macrophages (183). The reduced uptake by macrophages in strains with a *PDR1* activating mutation was dependent on the background strain and the increased adhesion was dependent on the specific activating mutation (184).

Mutations in *PDR1* are known to result in different transcriptional profiles that do not appear to be explained by location of the mutation (122, 124, 185). A large analysis of multiple mutations found from clinical isolates of *C. glabrata* revealed only two genes that were coordinately regulated with all *PDR1* activating mutations – *CDR1* and *PUP1* (Pdr1 upregulated) were both upregulated. Since the increased virulence phenotype is seen with all *PDR1* GOF mutations, these genes were suspected to be involved. Cdr1 is an ABC transporter known to be associated with azole resistance that has been discussed previously in this review. *PUP1* codes for a protein of unknown function. A highly

similar protein in *S. cerevisiae* is thought to be located in the mitochondria, but also has no known function. Deletion of *CDR1* and *PUP1* in an azole-resistant clinical isolate revealed that both genes were required for the increased virulence seen in the strain with a GOF mutation in *PDR1*. In the susceptible clinical isolate with wild type *PDR1* the deletion of *PUP1* resulted in decreased fungal burden in kidney, but no decrease in survival. Similarly, when *CDR1* and *PUP1* were overexpressed in a strain disrupted for *PDR1* there was an increased tissue fungal burden, but no increase in virulence (185).

Adherence is an important virulence factor for *C. glabrata*. Members of the glycosylphosphatidylinositol-dependent class of proteins called adhesins are known to be involved in host interaction. Expression of various adhesins was measured, but only *EPA1* expression correlated with increased adherence of the different activating mutations. *EPA1* has a PDRE in its promotor region, but Pdr1 did not bind by ChIP analysis. Disruption of *EPA1* in a strain expressing an activating mutation in *PDR1* decreased adhesion back to the level of strains with a wild type *PDR1*. In a mouse urinary tract infection model *EPA1* was required for *PDR1* mediated increased fungal burden in the bladder and kidneys (184). Med2 discussed above in relation to potentially regulating Pdr1 has also been implicated in adherence to epithelial cells. Med2 deletion strains display increased adherence to ovary epithelial cells and increased expression of *EPA1* and *EPA7* (173).

GENETIC INSTABILITY

Petite mutants

In *S. cerevisiae*, strains with mitochondrial defects form small, or petite colonies. Such petite mutants exhibit upregulation of the pleiotropic drug response through Pdr3 (186, 187). Petite mutants of *C. glabrata* were first identified after the observation that resistant colonies consistently appeared in the zone of inhibition when assessing azole susceptibility by the disc diffusion method. These colonies were found to be respiratory deficient and lacked mitochondrial DNA. Petite mutants generated by selection on ethidium bromide exhibited resistance to azoles (141). Expression of ABC transporters *CDR1* and *PDH1* were shown to be upregulated in petite mutants generated by ethidium bromide exposure (129) and the azole resistance pattern was dependent on Pdr1 (121). No alteration in *ERG11* expression or sequence have been identified, however petite mutants contain only small amounts of the intermediates from the ergosterol biosynthesis pathway – a disproportionate amount of ergosterol exists (145). Conflicting data exist about whether or not petite mutants have enhanced virulence in animal models (144, 188). Most recently a petite mutant recovered from a patient showed increased virulence, but a petite mutant generated in the laboratory from the same wild type parent isolate using ethidium bromide did not have increased virulence (144). Relative to the number of invasive *C. glabrata* infections a very small number of petite mutants have been recovered clinically (143, 189).

Mutator phenotype

The ability of *C. glabrata* to develop multidrug resistance has been attributed to its haploid phenotype allowing for rapid genetic changes. DNA repair machinery has been implicated in bacteria and in *C. albicans* that possess a hyper mutation phenotype. A recent study evaluated the potential for DNA repair machinery to play a role in *C. glabrata* multidrug resistance. Mutants were made for homologs for genes involved in mismatch repair and double-strand break repair in other organisms. Disruption of the genes themselves did not alter antifungal susceptibility, however alteration in both pathways resulted in generation of more antifungal resistant mutants than wild type. Mutations in *MSH2* (MutS homolog), which is involved in mismatch repair, were found in greater than 50% of clinical *C. glabrata* isolates. The increased mutation rate in these isolates leads to a higher rate of antifungal resistance in vivo and in vitro (120).

Chromosomal changes

Karyotyping of *C. glabrata* clinical isolates has previously revealed genetic rearrangements in sequential isolates taken from the same patient, but the importance of these changes with regards to resistance was not well understood (190, 191). Along with typical rearrangements and duplications, *C. glabrata* has the ability to form new chromosomes. Although previously shown in *C. albicans* (89), subsequent analysis of a group of *C. glabrata* clinical isolates revealed that genes associated with azole resistance were among the regions found to be duplicated. Subsequent growth in vitro in the presence of azole resulted in retention of the extra chromosome, while growth without drug resulted in loss of the chromosome in 70% of daughter cells (192). A second study from the same group confirmed the previous association between chromosomal changes and resistance with a larger collection of isolates (193). The stability of these changes and their true impact on clinical resistance in *C. glabrata* are not well understood at this time.

Heteroresistance

Heteroresistance, which was first described in 1947 has been seen in both gram positive and gram negative bacteria, as well as *Cryptococcus*. The term refers to clonal cell populations that vary in susceptibility to an antibiotic. This phenomena can result in treatment failure and selection for resistant populations due to inappropriate drug therapy from mistaking the entire population as susceptible (194). The ability of *C. glabrata* to develop resistance during azole therapy suggests heteroresistance occurs in this pathogen as well.

Recent analysis of a collection of *C. glabrata* clinical isolates indicates that heteroresistance is indeed widespread among this pathogen. Of the 52 isolates tested for fluconazole susceptibility 30 exhibited heteroresistance. No heteroresistance was observed when testing susceptibility to echinocandins. Activity of ABC transporter activity measured by rhodamine 6G efflux correlated with degree of heteroresistance to

fluconazole. However, none of the strains exhibiting heteroresistance had an activating mutation in *PDR1*. In animal studies persistent infection was more common in mice infected with strains with the heteroresistant phenotype compared to strains with no heteroresistance. This phenotype is still not well understood in *C. glabrata*, but this initial study reveals heteroresistance may be playing an important role in clinical azole resistance (195).

CONCLUSION

While azole resistance in *C. glabrata* remains an important clinical threat, the work described in this review is reason to be optimistic about reclaiming the azoles as an effective treatment option in the future. As the molecular and genetic basis of azole resistance in this fungal pathogen is better understood, it will be possible to design inhibitors of sterol demethylase that circumvent the relevant multidrug transporters and to discover compounds that can serve as co-therapeutic agents to overcome azole resistance.

CHAPTER 3. RELATIVE CONTRIBUTION OF THE ABC TRANSPORTERS CDR1, PDH1, AND SNQ2 TO AZOLE RESISTANCE IN *CANDIDA GLABRATA*

INTRODUCTION

The ATP-binding cassette (ABC) transporters are a large family of clinically relevant proteins found across prokaryotic and eukaryotic organisms. ABC transporters act as drug efflux pumps in *Candida glabrata* as well as in the related yeasts *Saccharomyces cerevisiae* and *Candida albicans*. Additional members of the ABC transporter family play a role in lipid homeostasis, which may also influence antifungal treatment, as the drug targets are influenced by lipid content in the cell (196).

In *C. albicans*, contributions of different mechanisms of resistance to the azole class of antifungals have been well characterized (197). There are two ABC transporters known to contribute to the resistance phenotype in *C. albicans*, Cdr1 and Cdr2. Deletion of each transporter in a clinical isolate with an activating mutation in the gene encoding the transcription factor Tac1, which results in increased expression of *CDR1* and *CDR2*, established Cdr1 as most important in azole resistance (198). In *C. glabrata* resistance in clinical isolates is due primarily to activating mutations in the transcription factor Pdr1 that lead to increased expression of the genes encoding one of three ABC transporters, Cdr1, Pdh1 or Snq2 (127-131, 165). *CDR1* was found to be upregulated in a resistant clinical isolate of *C. glabrata* when compared to the susceptible paired isolate. Deletion of *CDR1* in the resistant isolate resulted in decreased susceptibility to the level of the susceptible matched isolate. Reintegration of *CDR1* into the deletion mutant restored the azole-resistant phenotype (127). *PDH1* was also first implicated when its expression was found to be increased in azole-resistant clinical isolates of *C. glabrata* (128) and then further study showed deletion of *PDH1* results in decreased susceptibility to fluconazole (129). The most recent ABC transporter that has been shown to contribute to azole resistance is Snq2. It was found to have increased expression in two azole-resistant clinical isolates that did not overexpress *CDR1* or *PDH1* (130) and subsequently shown in one of the same isolates to be required for the azole-resistant phenotype (131).

In order to overcome azole resistance in *C. glabrata* it is first important to thoroughly understand the mechanisms by which it develops resistance to the azoles. While it is known that in *C. glabrata* the vast majority of clinical resistance has been attributed to upregulation of ABC transporters, the relative importance of each of these remains unclear. Based on previous work in *C. glabrata* and *C. albicans* we predicted that Cdr1 plays the largest role in azole resistance. In this study we used a strain engineered to carry an activating mutation in *PDR1* from an azole-resistant clinical isolate that results in upregulation of all three ABC transporters that have been shown to influence azole susceptibility in *C. glabrata*. By generating deletion strains of each transporter alone and in combination we were able to characterize their individual contributions to the phenotype.

MATERIALS AND METHODS

Strains and growth media

All strains used in this study are listed in **Table 3-1**. The clinical isolates and the *PDR1* replacement strain have been described previously. (124, 199) All strains were stored as frozen stocks at -80°C with 40% glycerol. Strains were routinely grown in YPD (1% yeast extract, 2% peptone, and 2% dextrose) broth at 30°C in a shaking incubator except as indicated for specific experimental conditions.

PX5-α *Escherichia coli* chemically competent cells (Protein Express, Cincinnati, OH) were used as the host for plasmid construction and propagation. These strains were grown at 37°C in Luria-Bertani (LB) broth or on LB plates supplemented with 100 µg/ml ampicillin (Sigma, St. Louis, MO) or 50 µg/ml kanamycin (Fisher BioReagents, Fair Lawn, NJ).

Plasmid construction

For deletion of *CDR1*, *PDH1* and *SNQ2* we modified plasmid pSFS2. (200) Upstream homology regions approximately 800 - 1000 bp long were amplified using primer pairs CgCDR1A/CgCDR1B, CgPDH1/CgPDH1B or CgSNQ2A/CgSNQ2B and digested with ApaI/XhoI or KpnI/ApaI as indicated for insertion into their respective plasmids. Downstream homology regions approximately 800 - 1000 bp long were amplified using primer pairs CgCDR1C/CgCDR1D, CgPDH1C/CgPDH1D or CgSNQ2C/CgSNQ2D and digested with SacII/SacI or NotI/SacII as indicated for insertion into their respective plasmids. The disruption cassettes consisting of the *SAT1* flipper cassette and upstream and downstream flanking sequences of either *CDR1*, *PDH1* or *SNQ2* were excised from the final plasmids pCgCDR1, pCgPDH1 or pCgSNQ2 and gel purified. Primers used to construct the cassettes are listed in **Table 3-2**.

Strain construction

C. glabrata cells were transformed by the lithium acetate method using approximately 1 µg of DNA. The ApaI/SacI fragments from pCgCDR1 and pCgSNQ2 and the KpnI/SacII fragment from pCgPDH1 were excised and gel purified prior to transformation. The transformed cells were allowed to recover 6 h in YPD at 30ºC before being plated on YPD-agar plates containing 200 µg/ml nourseothricin (Jena Biochemical, Germany) and incubated at 30ºC. Positive transformants were selected within 24 h and successful insertion of the disruption cassette at the target gene locus was confirmed by Southern hybridization using gene specific probes. Subsequently, induction of the flipper recombinase gene in the disruption cassette was performed by overnight growth of the positive transformant clones in YPD at 30ºC with shaking (under no selective pressure). Selection for excision of the *SAT1* flipper cassette was then performed by plating on

Table 3-1. Strains used in the ABC transporter study.

Strain	Parent	Genotype or description	Reference
SM1		Azole-susceptible clinical isolate	(199)
SM3		Azole-resistant clinical isolate	(199)
SM1RPDR1(SM3)	SM1Δ*pdr1*	*pdr1*Δ::*FRT-PDR1*^{SM3}	(124)
S1RPS3CDR1M2A and -B	SM1RPDR1(SM3)	*pdr1*Δ::*FRT-PDR1*^{SM3}/*cdr1*Δ::*FRT*	This study
S1RPS3PDH1M2A and -B	SM1RPDR1(SM3)	*pdr1*Δ::*FRT-PDR1*^{SM3}/*pdh1*Δ::*FRT*	This study
S1RPS3SNQ2M2A and -B	SM1RPDR1(SM3)	*pdr1*Δ::*FRT-PDR1*^{SM3}/*snq2*Δ::*FRT*	This study
S1RPS3CAPDH1M2A	S1RPS3CDR1M2A	*pdr1*Δ::*FRT-PDR1*^{SM3}/*cdr1*Δ::*FRT*/ *pdh1*Δ::*FRT*	This study
S1RPS3CBPDH1M2A	S1RPS3CDR1M2B	*pdr1*Δ::*FRT-PDR1*^{SM3}/*cdr1*Δ::*FRT*/ *pdh1*Δ::*FRT*	This study
S1RPS3CASNQ2M2A	S1RPS3CDR1M2A	*pdr1*Δ::*FRT-PDR1*^{SM3}/*cdr1*Δ::*FRT*/ *snq2*Δ::*FRT*	This study
S1RPS3CBSNQ2M2A	S1RPS3CDR1M2B	*pdr1*Δ::*FRT-PDR1*^{SM3}/*cdr1*Δ::*FRT*/ *snq2*Δ::*FRT*	This study
S1RPS3CAPASNQ2M2A	S1RPS3CAPDH1M2A	*pdr1*Δ::*FRT-PDR1*^{SM3}/*cdr1*Δ::*FRT*/ *pdh1*Δ::*FRT*/*snq2*Δ::*FRT*	This study
S1RPS3CBPASNQ2M2A	S1RPS3CBPDH1M2A	*pdr1*Δ::*FRT-PDR1*^{SM3}/*cdr1*Δ::*FRT*/ *pdh1*Δ::*FRT*/*snq2*Δ::*FRT*	This study

Table 3-2. Primers used in the ABC transporter study.

Primer name	Primer sequence[1]
CgCDR1A	5'- CATAGATCAGGGCCCATTACATTAGCACAG - 3'
CgCDR1B	5'- CTCAGTGTTGCTCGAGATAGGGTTGATAC - 3'
CgCDR1C	5'- GTTCTGTTAGTTCCGCGGACTCTCGTAGAT - 3'
CgCDR1D	5'- GTGAATACAAACAAGAGCTCCACAATAATA - 3'
CgPDH1A	5'- AAACAGTCTATGGTACCACAAGTTTGCACA - 3'
CgPDH1B	5'- CCGTATACGTTTCGGGCCCTTGTCATCAA - 3'
CgPDH1C	5'- ACAGAAGATGCGGCCGCTATGGTATATTTATT - 3'
CgPDH1D	5'- ATTCCTTAATAACCGCGGAAGTTGACTTTA - 3'
CgSNQ2A	5'- TTGAGTATCTTAGGGCCCTTGTTTTCAGTT - 3'
CgSNQ2B	5'- GATAGAATACTCGAGTTGTCGCTGTGCGC - 3'
CgSNQ2C	5'- GCTATTTATTACCGCGGCCATGTCAGAG - 3'
CgSNQ2D	5'- AGACAGATATTGAGCTCCACTACTGCTGAG - 3'

[1]Underlined bases indicate introduction of restriction enzyme cloning sites to allow directional cloning into the *SAT1*-flipper cassette.

YPD-agar plates and incubating for up to 24 h at 30ºC. Clones were selected and confirmed by Southern hybridization using gene specific probes.

Isolation of genomic DNA and Southern hybridization

Genomic DNA from *C. glabrata* was isolated as described previously. (201) For confirmation by Southern hybridization, approximately 10 μg of genomic DNA was digested with the appropriate restriction enzymes, separated on a 1% agarose gel containing ethidium bromide, transferred by vacuum blotting onto a nylon membrane and fixed by UV-crosslinking. Hybridization was performed with the Amersham AlkPhos Direct Labeling and Detection System (GE Healthcare, Pittsburg, PA) as per manufacturer instructions.

Susceptibility testing

Susceptibility testing was performed by microbroth dilution assay and by Epsilometer test strips (Etest). Microbroth dilution was performed according to the CLSI guidelines outlined in M27-A3 with a few modifications. (202) Fluconazole (MP Biomedicals, Salon, OH) stock solution was prepared by reconstitution in water to 5 mg/mL. Colonies grown overnight on Sabouraud dextrose plates were diluted to $2.5x10^3$ cells/ml in RPMI 1640 (Sigma, St. Louis, MO) with 2% glucose, MOPS, pH 7.0. Plates were incubated at 35°C for 48 h. Absorbance at 600 nm was read with a BioTek Synergy 2 microplate reader (BioTek, Winooski, VT); background due to medium was subtracted from all readings. The MIC was defined as the lowest concentration inhibiting growth by at least 50% relative to the drug-free control after incubation with drug for 48 h. Etest (bioMerieux) susceptibility assay was performed per manufacturer instructions with some modifications. Colonies were selected from cultures grown overnight on Sabouraud dextrose plates and diluted in water to 0.5 McFarland standard. Sterile cotton swabs were used to streak plates prior to Etest strip placement. Plates were incubated at 35°C and read at 24 and 48h.

RESULTS

CDR1 deletion alone alters fluconazole susceptibility in a resistant *C. glabrata* strain

The *SAT1* flipper strategy for gene disruption was used to generate deletion strains in *C. glabrata*. Single gene deletion mutants were made for each ABC transporter known to contribute to azole resistance (*CDR1*, *SNQ2*, and *PDH1*). The azole-resistant strain SM1RPDR1(SM3) was used as the parent strain for the mutants. This strain was made in our laboratory previously by replacing the *PDR1* allele in fluconazole susceptible doses dependent clinical isolate SM1 with the *PDR1* allele from azole-resistant isolate SM3, which contains the well characterized L946S activating mutation

(124). Isolate SM1 was recovered from a patient with an abdominal abscess prior to antifungal treatment. SM3 was recovered from an abscess from the same patient 46 days later after a course of fluconazole, followed by caspofungin and then amphotericin B. Pulsed field gel electrophoresis of the two isolates was indistinguishable (199).

Susceptibility testing was performed by broth dilution for a panel of azoles, as well as Etest for fluconazole. Both assays confirmed susceptibility data published previously for SM1, SM3 and SM1RPDR1(SM3). The fluconazole MIC for SM1 is 8 (**Table 3-3** and **Figure 3-1A**), which would be considered susceptible dose dependent according to the most recent breakpoints. The fluconazole MIC for both SM3 and SM1RPDR1(SM3) is 256. Deletion of *CDR1* in strain SM1RPDR1(SM3) resulted in a decreased fluconazole MIC from 256 to 16. However, neither *PDH1* nor *SNQ2* single deletion mutants exhibited a change in fluconazole MIC. Fluconazole Etest susceptibility testing confirmed the results from the broth microdilution assay (**Figure 3-1C**). The same trend was seen with additional azoles tested (**Table 3-3**). Among single ABC transporter deletion mutants *CDR1* alone was able to alter azole susceptibility.

PDH1 and *SNQ2* contribute to fluconazole resistance to a lesser extent than *CDR1*

Previous studies have demonstrated a role for Pdh1 and Snq2 in resistance to azoles. However, we show here that deletion of *PDH1* or *SNQ2* in an azole-resistant strain overexpressing all three transporters resulted in no change in fluconazole susceptibility (**Table 3-3** and **Figure 3-1A**). In order to determine if *PDH1* and *SNQ2* impact fluconazole resistance in the absence of *CDR1*, double and triple deletion strains were made using the *SAT1* flipper method described above.

When *PDH1* and *CDR1* were deleted in combination, the MIC is consistently one-fold lower than the MIC for the strain in which *CDR1* alone is deleted (**Table 3-3** and **Figure 3-1B**). When *SNQ2* and *CDR1* were deleted in combination, the MIC is the same as that observed for the *CDR1* single deletion strain. To investigate the possibility that the presence of *PDH1* is masking the effect of *SNQ2* we constructed a strain with all three transporters deleted. The MIC for the triple deletion strain was consistently one-fold less than that of the *CDR1* and *PDH1* deletion strain. The patterns seen by microbroth dilution were confirmed by Etest susceptibility testing (**Figure 3-1C**).

CDR1, *PDH1*, and *CDR1* mutants exhibit similar susceptibility patterns to other azole antifungals

Of interest is the potential for these transporters to affect members of the azole class of antifungals differently. Newer triazoles in the class have improved spectrum of activity against additional fungal pathogens. The differences in chemical structure could influence the interaction with efflux pumps resulting in different ABC transporters preferentially effluxing different azoles. However, overall the patterns for all azoles tested are similar with few differences (**Table 3-3**). The magnitude of changes in MIC are

Table 3-3. Azole susceptibilities performed by microbroth dilution for selected strains.

	MIC (μg/ml)				
Strain	**FLC[1]**	**ITC**	**KTC**	**MC**	**VRC**
SM1	8	0.5	0.063	0.125	0.125
SM3	256	32	4	1	8
SM1RPDR1(SM3)	256	32	4	1	8
Δ*cdr1*	16	0.5	0.25	0.25	0.25
Δ*pdh1*	256	32	4	1	8
Δ*snq2*	256	32	4	1	8
Δ*cdr1*Δ*pdh1*	8	0.125	≤0.031	0.063	0.063
Δ*cdr1*Δ*snq2*	16	0.5	0.25	0.25	0.25
Δ*pdh1*Δ*snq2*	256	32	4	1	8
Δ*cdr1*Δ*pdh1*Δ*snq2*	2	0.125	≤0.031	≤0.016	0.031

[1]Fluconazole (FLC), Itraconazole (ITC), Voriconazole (VRC), Ketoconazole (KTC), Miconazole (MC)

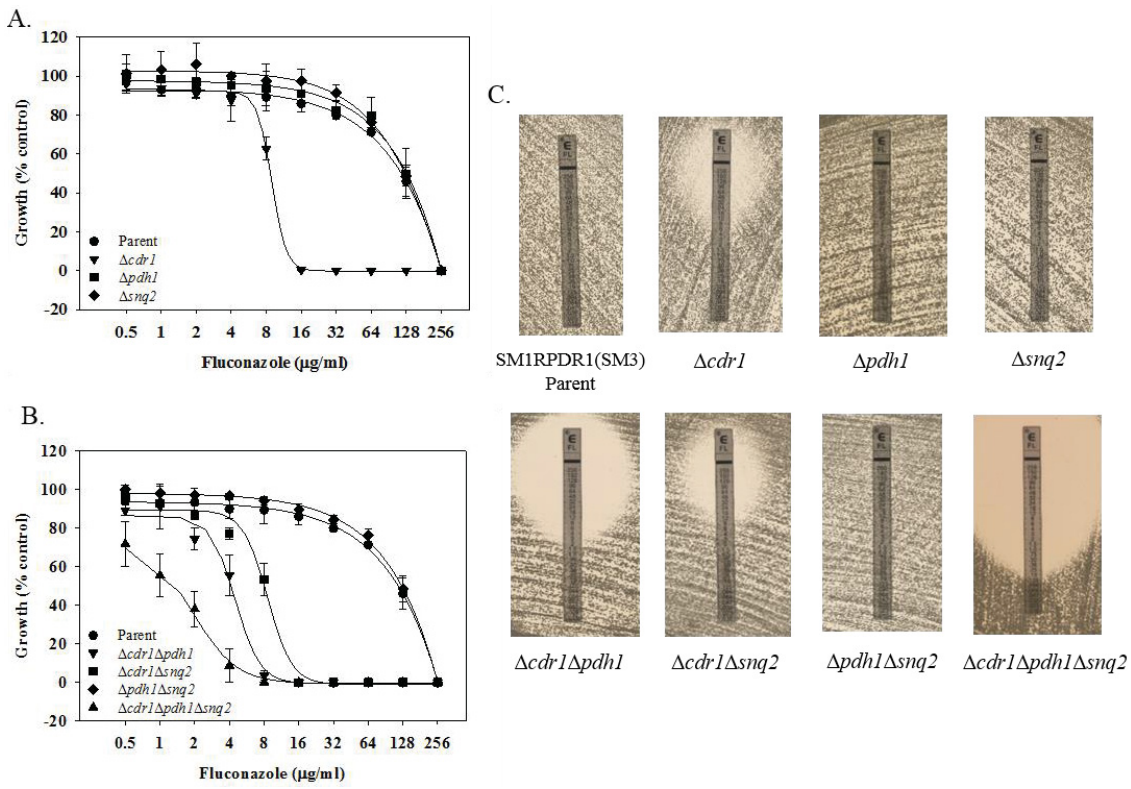

Figure 3-1. Fluconazole susceptibility testing.

Microbroth dilution assays were setup as described above for single deletion strains (A) or double and triple deletion strains (B). Cultures were resuspended at 48h and absorbance at 600nm was measured and background subtracted. Data is represented as percent of no drug treatment control. Etest assays (C) were performed per manufacturer instructions with some modifications as described.

different among the azoles for the different ABC transporters. In general however, the differences from the parent strain and the triple ABC transporter deletion strain were 6 to 8 drug dilutions for all azoles tested. Among the single deletion mutants, Cdr1 was the only transporter able to influence the MIC for all azoles tested. Interestingly, deletion of *SNQ2* had no impact on itraconazole or ketoconazole MIC. No notable differences were observed in susceptibilities to echinocandins and amphotericin B in the mutant strains (data not shown).

CDR1, *PDH1*, and *SNQ2* explain most, but not all of Pdr1's contribution to azole resistance

All three ABC transporters in this study are known targets of Pdr1. All three transporters are upregulated in strains that possess an activating mutation in *PDR1* (123, 124, 131). Pdr1 has also been shown to bind to the promoter regions of each transporter by Chip-Seq (126). In order to determine if these three transporters account for the entirety of Pdr1's importance to azole resistance we compared *PDR1* deletion strains to the triple ABC transporter deletion strain. Both the susceptible dose dependent and resistant clinical isolates lacking *PDR1* have similar growth patterns (**Figure 3-2**). There is a distinctly different growth pattern for the triple deletion mutant, which indicates that there are likely additional genes of the Pdr1 regulon that contribute to azole resistance.

DISCUSSION

Activating mutations in the zinc cluster transcription factor Pdr1 that result in upregulation of ABC transporters are found in the vast majority of azole-resistant clinical isolates of *C. glabrata*. Similarly to the transcription factors Pdr1 and Pdr3 in the closely related yeast *S. cerevisiae* (203), Pdr1 in *C. glabrata* exerts its regulatory effects by binding a pleiotropic drug response element (PDRE) (125, 126). Pdr1 is also auto regulated due to a PDRE in its promotor region (125). Developing a better understanding of this mechanism of azole resistance is important for discovering new treatment strategies. For example, a small molecule that could inhibit efflux by the ABC transporters would allow clinicians to once again successfully treat *C. glabrata* with azoles.

Many different activating mutations have been found throughout the coding sequence for *PDR1* that result in similar decreases in azole susceptibility (121-125, 204). However, there are differences in the gene expression patterns of the Pdr1 regulon for the various mutations. Of particular interest are the patterns of expression of the three ABC transporters known to influence azole susceptibility, which do not appear to correlate with location of the mutation (123).

ABC transporter expression profiles in clinical isolates reveal a wide distribution of expression patterns. *CDR1*, *PDH1* or both *CDR1* and *PDH1* were found to be highly

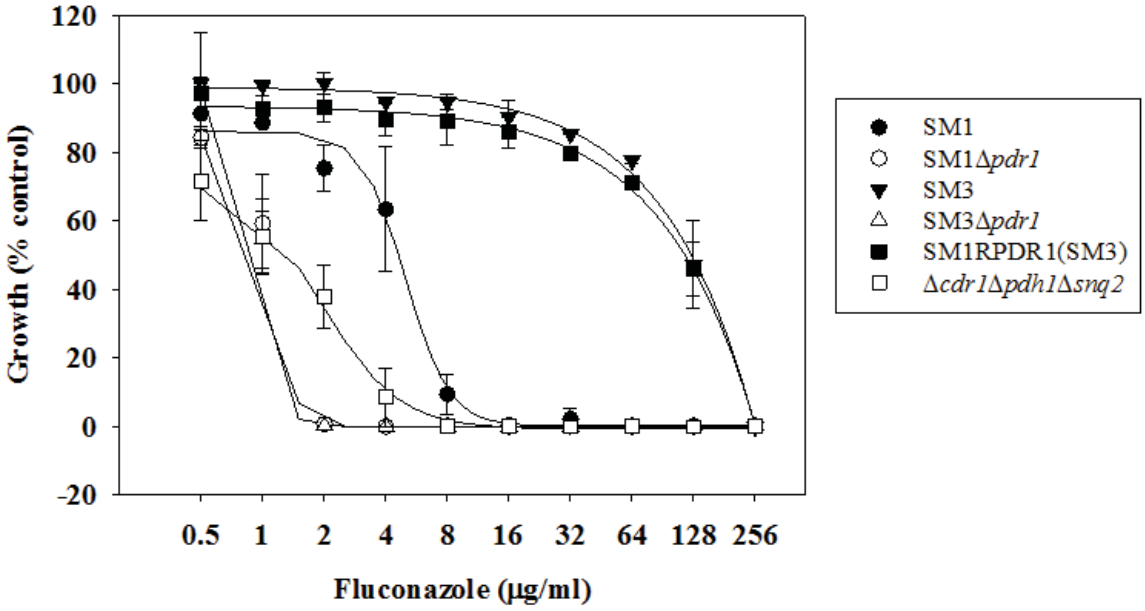

Figure 3-2. Comparison of fluconazole susceptibilities in *PDR1* deletion strains versus the ABC transporter triple deletion strain.

Microbroth dilution assays were setup as described above. Cultures were resuspended at 48h and absorbance at 600nm was measured and background subtracted. Data is represented as percent of no drug treatment control.

expressed in 18 of 20 resistant clinical isolates from one study. The two remaining resistant isolates overexpressed *SNQ2* alone. The susceptible dose dependent isolates overexpressed the ABC transporters to a lesser extent than the resistant isolates (130). Another group showed 10 of 12 resistant clinical isolates and 6 of 7 laboratory generated resistant mutants exhibited increased expression of *CDR1* or both *CDR1* and *PDH1* (119). A third study of resistant clinical isolates found *CDR1* or *PDH1* overexpression in the resistant isolate of 12 of 14 matched clinical isolates (51). A study in which expression of *CDR1*, *PDH1* and *PDR1* were measured in a panel of clinical isolates for the purpose of developing a qPCR based assay for determination of resistance in *C. glabrata* found that *CDR1* expression alone could be used to predict resistance with 100% sensitivity and 95% specificity. The same was not true for *PDH1* expression or *PDR1* expression (205).

Our experiments show that the three ABC transporters previously implicated in Pdr1 mediated azole resistance in *C. glabrata* are not able to fully explain the decrease in susceptibility in the absence of Pdr1. In addition to controlling expression of ABC transporters, Pdr1 also regulates expression of many other genes both directly and indirectly. We predict that there likely are genes among this group that make small contributions to azole resistance that in combination may explain the phenotypic difference between the *PDR1* deletion strain and the triple ABC transporter deletion strain.

Among the list of genes whose promotors were found to be directly bound by Pdr1 are a major facilitator superfamily (MFS) transporter, *QDR2*, and two additional ABC transporters, *YBT1* and *YOR1* (126). Deletion of *QDR2* in *C. glabrata* resulted in increased susceptibility to the imidazoles, clotrimazole, ketoconazole, miconazole, but had no effect on fluconazole or itraconazole susceptibility (169). YOR1 and YBT1 are frequently found among genes with altered expression in relation to azole susceptibility, but not direct relationship has been described. The effects of *QDR2*, *YOR1* and *YBT1* on fluconazole susceptibility could potentially be masked by the presence of the more dominant transporters *CDR1*, P*DH1* and *SNQ2* and therefore cannot be ruled out as contributing to azole resistance, albeit likely a minor contribution.

Other genes of interest shown previously to be upregulated in clinical isolates (122, 124) and laboratory derived strains (168) of *C. glabrata* with activating mutations in *PDR1* are *RSB1* and *RTA1*. Rsb1 is a putative sphingolipid flippase. The homolog for Rta1 in *S. cerevisiae* is a member of the fungal lipid-translocating exporter family of proteins. The promoter regions of both *RSB1* and *RTA1* possess a PDRE that is bound directly by Pdr1 (125). Recent work in *C. albicans* has implicated the putative lipid translocase encoded by *RTA3* and the sphingolipid flippase encoded by *RTA2* in azole resistance (**Appendix A**, **Figures A-1** to **A-4** and **Tables A-1** to **A-3**) (206, 207). Rsb1 and Rta1 may make similar contributions to azole resistance in *C. glabrata*.

CHAPTER 4. *UPC2A* IS REQUIRED FOR HIGH-LEVEL AZOLE ANTIFUNGAL RESISTANCE IN *CANDIDA GLABRATA**

INTRODUCTION

Fungal infections caused by opportunistic organisms have continued to increase in recent decades and have become an important medical concern (208-210). *Candida glabrata* in particular has emerged over the past two decades as the predominant cause of yeast infections in diabetics (54%) and the elderly (51%) and is second to *Candida albicans* in most other patient populations (13, 17, 211, 212). Candidemia mortality rates continue to rise with rates for *C. glabrata* reported as high as 50% (151, 213, 214). The emergence of *C. glabrata* as a common pathogen is complicated by, and likely related to, its intrinsically low susceptibility to azole antifungals and its ability to rapidly develop high-level azole resistance during treatment (119, 134, 199, 205).

Ergosterol is an essential component of the fungal cell membrane and is an important signaling molecule in the cell. It helps maintain membrane integrity and fluidity, which facilitates several membrane-bound enzymatic reactions. Ergosterol is not synthesized by the host, so the ergosterol biosynthesis pathway has long been a target for antifungal agents (**Figure 4-1**). Compounds that inhibit this pathway are broadly categorized as sterol biosynthesis inhibitors (SBIs). The azole class of antifungals specifically targets lanosterol 14-alpha-demethylase (Erg11), which catalyzes the C-14 demethylation of lanosterol (215-217). Statins, such as lovastatin, inhibit the gene products of *HMG1* and *HMG2*, which convert 3-hydroxy-3-methyl-glutaryl (HMG)-CoA to mevalonate, resulting in a reduction in the synthesis of cholesterol in mammals and the synthesis of ergosterol in yeasts (**Figure 4-1**).

As has been observed in *Saccharomyces cerevisiae* and *C. albicans*, exposure to azoles also results in upregulation of genes from the ergosterol biosynthesis pathway (including *ERG11*) in *C. glabrata* (119, 215-217). The predominant mechanism of azole resistance in *C. glabrata* is the constitutive over-expression of ATP-binding cassette (ABC) transporter genes, *CDR1, PDH1* and *SNQ2*, which are under the transcriptional regulation of a hyperactive form of the transcription factor Pdr1. *ERG* gene expression and regulation could also be important in acquired azole resistance, as is the case in *C. albicans*, or may potentially contribute to the intrinsic reduced azole susceptibility in *C. glabrata* (71-73, 119, 124, 178, 218-220).

Resistant isolates of *S. cerevisiae* often have increased expression of *ERG11*, as well as other ergosterol biosynthesis genes, which are under the control of the

---

*Reprinted with permission. **Whaley SG, Caudle KE, Vermitsky JP, Chadwick SG, Toner G, Barker KS, Gygax SE, Rogers PD.** 2014. *UPC2A* is required for high-level azole antifungal resistance in *Candida glabrata*. Antimicrob Agents Chemother **58:**4543-4554.

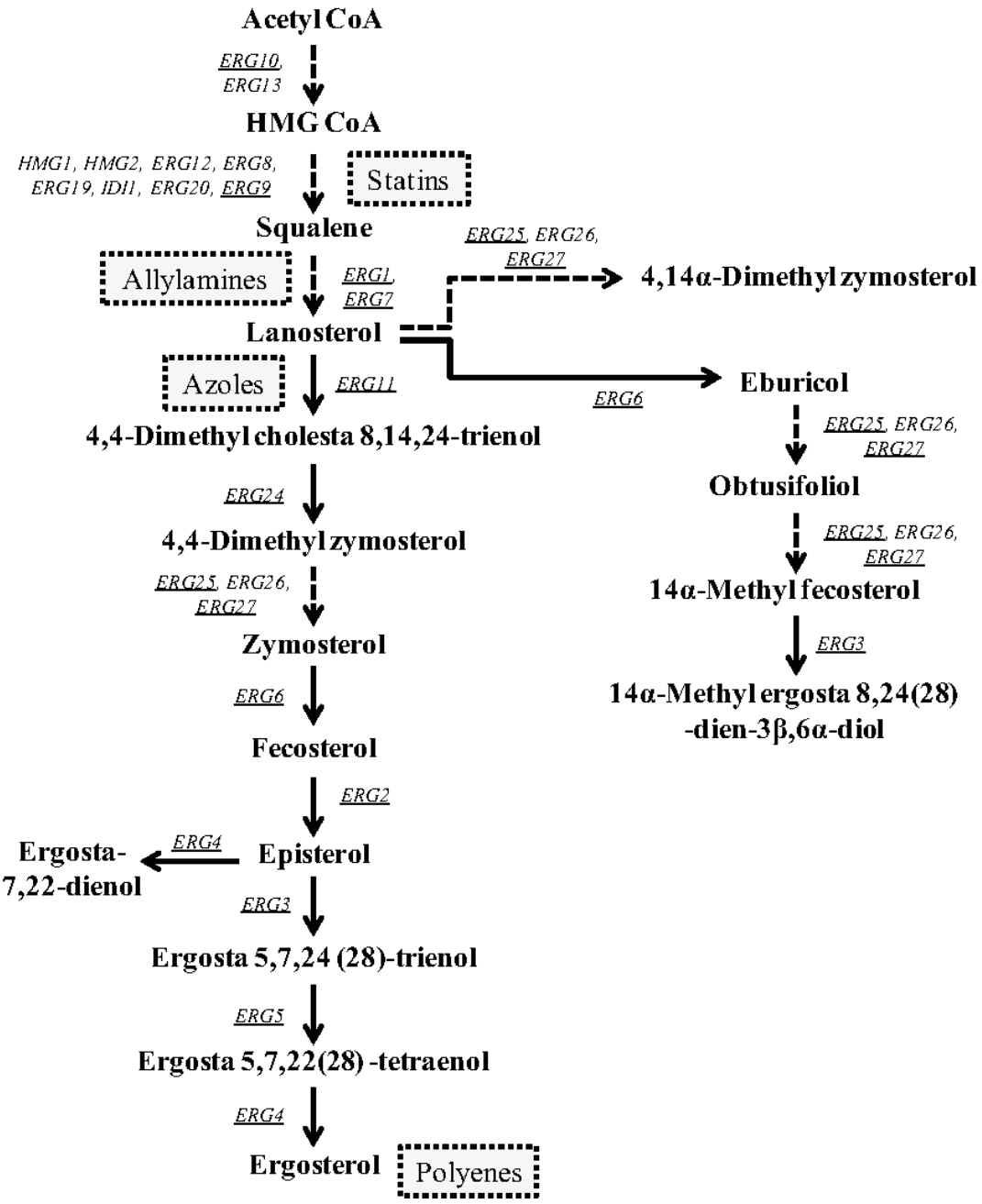

Figure 4-1. Representation of the ergosterol biosynthesis pathway in *Candida glabrata*.

Genes (in italics) whose expression was monitored in this study are underlined. Site of action for specific drug classes indicated by dashed box. CoA, coenzyme A.

transcriptional regulators Upc2 and Ecm22 (221, 222). In *C. albicans*, a single homolog, Upc2, has been identified and found to be involved in *ERG* gene regulation (70, 217, 220, 223, 224). These transcriptional regulators are members of the well-characterized fungal-specific Zn(2)-Cys(6) family of transcriptional activators (218). *ERG11* is not an essential gene in *C. glabrata*. Disruption of this gene or pharmacologic inhibition of its product prevents ergosterol production, which causes accumulation of alternate sterols including lanosterol, obtusifoliol, and 4, 14α-dimethyl zymosterol leading to decreased susceptibility to fluconazole, itraconazole, and amphotericin B (55, 225). Biosynthesis of these alternate sterols does not require *ERG11*, but does require other genes in the ergosterol biosynthesis pathway.

Nagi *et al*. recently described two Upc2 homologs in *C. glabrata*, Upc2A and Upc2B. Upc2A was shown to play a major role in the regulation of *ERG2* and *ERG3* in the ergosterol biosynthesis pathway (178). A strain disrupted for *UPC2A* also exhibited a 4-fold and 16-fold increase in fluconazole and lovastatin (a member of the statin class of cholesterol lowering agents) susceptibility, respectively (178). Given the global role of Upc2 in regulation of sterol biosynthesis, we reasoned that disruption of *UPC2A* might enhance the activity of fluconazole in azole-resistant as well as -SDD clinical isolates.

MATERIALS AND METHODS

Strains and growth media

The matched fluconazole-SDD and -resistant clinical isolate set used in this study has been described previously (124, 199). All isolates/strains (**Table 4-1**) were maintained in YPD (1% yeast extract, 2% peptone, and 2% dextrose) broth at 30°C and stored as 40% glycerol stocks at −80°C. One Shot *Escherichia coli* TOP10 chemically competent cells (Invitrogen, Carlsbad, CA) were used as the host for plasmid construction and propagation. These strains were grown at 37°C in Luria-Bertani (LB) broth or on LB plates supplemented with 100 μg/ml ampicillin (Sigma, St. Louis, MO) or 50 μg/ml kanamycin (Fisher BioReagents, Fair Lawn, NJ).

Gene disruption

Mutant strains (**Table 4-1**) were generated by the *SAT1*-flipper gene disruption method (200). Briefly, approximately 900 bp of sequence immediately upstream of target gene plus the first 50 bp of the open reading frame (ORF), referred to as the 5'flanking region, was cloned upstream of the *SAT1*-flipper cassette in pSFS2A and the final 50 bp of the target gene ORF plus approximately 900 bp of sequence immediately downstream of the target gene, referred to as the 3' flanking region, was cloned downstream of the *SAT1*-flipper cassette. The disruption cassettes consisting of the *SAT1*-flipper and 5' and 3' flanking sequences of the either the *UPC2A* or *UPC2B* genes were excised from the final plasmid construct and gel purified. Primers used to construct the cassettes are listed

Table 4-1. Strains used in the *UPC2* study.

Strain	Parent	Genotype or description	Reference
SM1		Azole-SDD clinical isolate	(199)
SM1Δ*upc2A*	SM1	*upc2A*Δ::*FRT*	This study
SM1Δ*upc2B*	SM1	*upc2B*Δ::*FRT*	This study
SM1Δ*upc2A*Δ*upc2B*	SM1	*upc2A*Δ::*FRT*/*upc2B*Δ::*FRT*	This study
SM1Δ*upc2A*/*UPC2A*	SM1	*upc2A*Δ::*FRT*-*UPC2A*	This study
SM1Δ*upc2A*Δ*upc2B*/*UPC2A*	SM1	*upc2A*Δ::*FRT*-*UPC2A*/*upc2B*Δ::*FRT*	This study
SM3		Azole-resistant clinical isolate	(199)
SM3Δ*upc2A*	SM3	*upc2A*Δ::*FRT*	This study
SM3Δ*upc2B*	SM3	*upc2B*Δ::*FRT*	This study
SM3Δ*upc2A*Δ*upc2B*	SM3	*upc2A*Δ::*FRT*/*upc2B*Δ::*FRT*	This study
SM3Δ*upc2A*/*UPC2A*	SM3	*upc2A*Δ::*FRT*-*UPC2A*	This study
SM3Δ*upc2A*Δ*upc2B*/*UPC2A*	SM3	*upc2A*Δ::*FRT*-*UPC2A*/*upc2B*Δ::*FRT*	This study

in **Table 4-2**. *C. glabrata* cells were transformed by the lithium acetate method using approximately 1 μg of DNA. The transformed cells were allowed to recover 6 h in YPD at 30ºC before being plated on YPD-agar plates containing 200 μg/ml nourseothricin (Jena Biochemical, Germany) and incubated at 30ºC. Positive transformants were selected within 24 h and successful insertion of the disruption cassette at the target gene locus was confirmed by Southern hybridization. Subsequently, induction of the flipper recombinase gene in the disruption cassette was performed by overnight growth of the positive transformant clones in YPD at 30ºC with shaking (under no selective pressure). Selection of cassette excision was then performed by plating a series of dilutions of this culture on YPD-agar plates containing 25 μg/ml nourseothricin and incubating for up to 24 h at 30ºC. Clones were selected due to size differences (slower growing colonies usually indicated successful cassette excision) and confirmed by Southern hybridization (**Figure 4-2**).

Likewise, reintroduction of the *UPC2A* gene into the *UPC2A* locus was accomplished as above with a *SAT1*-flipper cassette in which the 5' flanking sequence cloned upstream of the flipper cassette was replaced with a DNA fragment consisting of the 5'flanking sequence and full-length ORF of *UPC2A*. Isolate-specific constructs were prepared to reintroduce the native *UPC2A* alleles back into their original locus. This cassette was excised, gel purified, and used for cell transformation as above. Screening for positive clones was accomplished as described above (**Figure 4-2**).

Isolation of genomic DNA and Southern hybridization

Genomic DNA from *C. glabrata* was isolated as described previously (201). For confirmation by Southern hybridization, approximately 10 μg of genomic DNA was digested with the appropriate restriction enzymes, separated on a 1% agarose gel containing ethidium bromide, transferred by vacuum blotting onto a nylon membrane and fixed by UV-crosslinking. Hybridization was performed with the Amersham ECL Direct Nucleic Acid Labeling and Detection System (GE Healthcare, Pittsburg, PA) as per manufacturer's instructions.

Susceptibility testing

Susceptibility testing was performed by microbroth dilution assay according to the CLSI guidelines outlined in M27-A3 with a few modifications (202). Antifungal agents were obtained from the following sources: fluconazole (LKT Laboratories, St. Paul, MN), miconazole (MP Biomedicals, Inc., Solon, OH), anidulafungin and voriconazole (Pfizer, New York, N.Y.), ketoconazole, amphotericin B, lovastatin and terbinafine (Sigma, St. Louis, MO). All drugs were dissolved in dimethyl sulfoxide (DMSO) and diluted to give a final DMSO concentration of $\leq 0.5\%$ in all experiments. Growth of *C. glabrata* was not affected at this concentration of DMSO (data not shown). Cultures were diluted to 2.5×10^3 cells/ml in RPMI 1640 (Sigma, St. Louis, MO) with 2% glucose, MOPS, pH 7.0. Plates were incubated at 35°C for 24, 48 and 72 h. Absorbance

Table 4-2. Primers used in the *UPC2* study (grouped by application).

Primer name and function	Primer sequence[1]
Cassettes for constructing mutants	
CgUPC2A-A	5'-GTTAAAACGGGCCCATGATCGTCGTATCC-3'
CgUPC2A-B	5'-AATAGCTTTGGCTCGGTATCCTCTATGT-3'
CgUPC2A-C	5'-CTAGAGATGCGGCCGCTTATAGTGGTGGT-3'
CgUPC2A-D	5'-TATCGATTTAACCGCGGTGATATTCTTCCA-3'
CgUPC2A-E	5'-GTACCTAGTGGGCCCACCTTGATCTGT-3'
CgUPC2A-F	5'-AATAAAGGAAGTAAATTGCATATTTCAGAG-3'
CgUPC2B-A	5'-TGAGTTCAGTTTTATGGGCCCTTAGAAAG-3'
CgUPC2B-B	5'-AGTTGTACTAACCTTCTTACCTCGAGTATCTA-3'
CgUPC2B-C	5'-TAAGATATTGCCGCGGTTTACTAACGATGT-3'
CgUPC2B-D	5'-CAAAACTATAGGAGCTCGAAGGAATATGTG-3'
qRT-PCR	
ACT1F	5'-CGCTTTGGACTTCGAACAAGAA-3'
ACT1R	5'-GTTACCGATGGTGATGACTTGAC-3'
ERG1F	5'-GGTAAGAAGGTGCTGATTG-3'
ERG1R	5'-GATGTTGTTGATGGACTGG-3'
ERG2F	5'-AATCTGCTATTGCTGGTTGCC-3'
ERG2R	5'-CGCTGCCGTTGTGTTTGG-3'
ERG3F	5'-AAGCGTGTGAACAAGGAC-3'
ERG3R	5'-TACAATAGCAGACCGAAGAC-3'
ERG4F	5'-GCTGTACGCTAACGCTTGTG-3'
ERG4R	5'-CAGTGGCAGTATGTGTATGGAAC-3'
ERG5F	5'-CCCAGCCCTACACGACCCAGAAG-3'
ERG5R	5'-GGACCACAGCCGAAGACCAACC-3'
ERG6F	5'-TCCTCTTTCCACTTCTCCCGTTTC-3'
ERG6R	5'-GCCACCGACACCGCAACC-3'
ERG7F	5'-ATGCCTGATGGTGGTTGG-3'
ERG7R	5'-TCTTCATTTGGACACTTAGCC-3'
ERG9F	5'-CAGCACCAATGACACCAG-3'
ERG9R	5'-CCTCAGAATCAGATAGAAGACC-3'
ERG10F	5'-GTTATCGCTGGTGGTTGTG-3'
ERG10R	5'-CATTGGTTGGTGGTCGTAAG-3'
ERG11F	5'-TACCAAGCCATACGAGTTC-3'
ERG11R	5'-GGTCAAGTGGGAGTAAGC-3'
ERG24F	5'-ACTCGCTGGACTACTACTTC-3'
ERG24R	5'-CAACTTAGTGCCGTCTCTTAG-3'
ERG25F	5'-ATGTGTATGGATTACCTTGAGAC-3'
ERG25R	5'-GTAGTTACCGATGAAGTAGTGG-3'

Table 4-2. (Continued).

Primer name and function	Primer sequence[1]
qRT-PCR (continued)	
ERG27F	5’-CCAGGAAAGTAGCCGTTATCAC-3’
18SF	5’-TCGGCACCTTACGAGAAATCA-3’
18SR	5’-CGACCATACTCCCCCCAGA-3’
PDR1F	5’-TTTGACTCTGTTATGAGCGATTACG-3’
PDR1R	5’-TTCGGATTTTTCTGTGACAATGG-3’
CDR1F	5’-CATACAAGAAACACCAAAGTCGGT-3’
CDR1R	5’-GAGACACGCTTACGTTCACCAC-3’
SNQ2F	5’-CGTCCTATGTCTTCCTTACACCATT-3’
SNQ2R	5’-TTTGAACCGCTTTTGTCTCTGA-3’
PDH1F	5’-ACGAGGAGGAAGACGACTACGA-3’
PDH1R	5’-CTTTACTGGAGAACTCATCGCTGGT-3’

[1] Underlined bases indicate introduction of restriction enzyme cloning sites to allow directional cloning into the *SAT1*-flipper cassette.

Figure 4-2. Construction of *upc2a*Δ and *upc2b*Δ mutants and complemented strains.

Construction of *upc2a*Δ and *upc2b*Δ mutants and complemented strains. A. Structure of the deletion cassette from plasmid pCgUPC2A (top), which was used to delete the *UPC2A* ORF in strains SM1 and SM3 and genomic structure of the *UPC2A* locus in the parental strains (bottom). The *UPC2A* coding region is represented by the white arrow and the upstream and downstream regions (5'UPC2A and 3'UPC2A) by the solid lines. The *SAT1* flipper cassette (*SAT1*-FLIP), in which the *caFLP* gene is expressed from the inducible *SAP2* promoter (33), is represented by the grey rectangle bordered by *FRT* sites (black arrows). The 34 bp *FRT* sites are not drawn to scale. The probes used for Southern hybridization analysis of the mutants are indicated by the black bars. B. Structure of the deletion cassette from plasmid pCgUPC2B which was used to delete the *UPC2B* ORF in strains SM1 and SM3 and the genomic structure of the *UPC2B* locus in the parental strains. See A for further explanation. C. Structure of the DNA fragment from plasmid pCgUPC2Apb (top), which was used for reintegration of an intact *UPC2A* copy into the disrupted *UPC2A* locus in the *upc2a*Δ single and *upc2a*Δ*upc2b*Δ double mutants (bottom) Only relevant restriction sites are given in panels A, B and C, as follows: A, ApaI; H, HindIII; N, NotI; S, ScaI; ScI, SacI; ScII, SacII; X, XhoI. D. Southern hybridization of ScaI-digested (top) or HindIII-digested (bottom) genomic DNA of SM1, SM3, *upc2a*Δ and *upc2b*Δ mutants, and complemented strains with the *UPC2A*-specific probe 2 (top) or *UPC2B*-specific probe 2 (bottom). The sizes of the hybridizing fragments (in kb) are given on the left side of the blot and their identities are indicated on the right. The genotype of the strains is given above the respective lanes. Only one of the two independently constructed series of strains is shown.

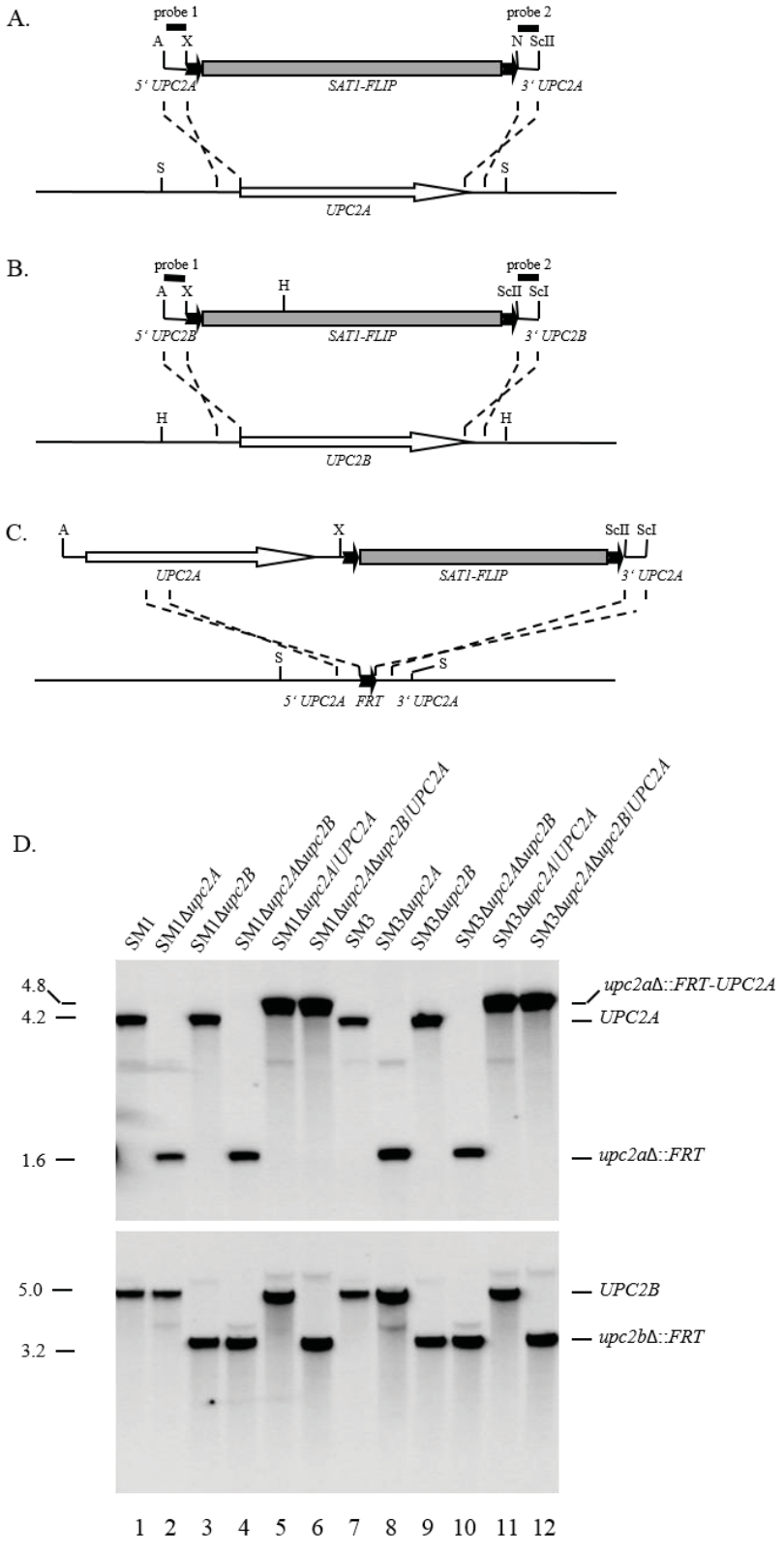
A.
probe 1
probe 2
A X
N ScII
5' UPC2A
SAT1-FLIP
3' UPC2A
S
S
UPC2A
B.
probe 1
probe 2
A X
H
ScII ScI
5' UPC2B
SAT1-FLIP
3' UPC2B
H
H
UPC2B
C.
A
X
ScII ScI
UPC2A
SAT1-FLIP
3' UPC2A
S
S
5' UPC2A FRT 3' UPC2A
D.
SM1
SM1Δupc2A
SM1Δupc2B
SM1Δupc2AΔupc2B
SM1Δupc2A/UPC2A
SM1Δupc2AΔupc2B/UPC2A
SM3
SM3Δupc2A
SM3Δupc2B
SM3Δupc2AΔupc2B
SM3Δupc2A/UPC2A
SM3Δupc2AΔupc2B/UPC2A
4.8
4.2
1.6
upc2aΔ::FRT-UPC2A
UPC2A
upc2aΔ::FRT
5.0
3.2
UPC2B
upc2bΔ::FRT
1 2 3 4 5 6 7 8 9 10 11 12

at 620 nm was read with a microplate reader (Beckman Coulter, Inc., Fullerton, CA); background due to medium was subtracted from all readings. The minimum inhibitory concentration (MIC) was defined as the lowest concentration inhibiting growth by at least 80% (or no visible growth for amphotericin B) relative to the drug-free control after incubation with drug for 24 h. While CSI guidelines indicate an endpoint of 50% inhibition of growth, we chose to use a more stringent endpoint of 80% inhibition of growth in order to detect a more pronounced effect. Absorbance measured at 72 h was used to assess regrowth of the cultures (226). The minimum fungicidal concentration (MFC) was determined by spotting 5 µl from each well of the 48 h MIC plate onto YPD solid media and incubating at 30°C for an additional 24 h. The MFC was defined as the lowest concentration that exhibited complete inhibition of growth (227, 228).

Spot assays

Colonies from cultures grown on Sabouraud dextrose (BD Biosciences, San Jose, CA) solid media for 24 h were diluted in sterile water to an optical density at 600 nm of 0.1. Cultures were serially diluted one to four in sterile water. Two microliters of each dilution were spotted on each of three solid media: YPD, YPD with 5 µg/ml fluconazole, and YPD with 10 µg/ml fluconazole. The serial dilutions were incubated at 30°C for 24 and 72 h. Plates were imaged at each time point and growth inhibition compared (71, 127, 226).

Time kill analysis

Time kill experiments were adapted from the methods described by Klepser et al. (229). Briefly, isolates started from freezer stocks were subcultured twice on potato dextrose agar (BD Biosciences, San Jose, CA). Colonies were picked from the plates into sterile water and the densities adjusted to that of a 0.5 McFarland standard. The suspensions were then diluted 1:10 in RPMI 1640 to a final volume of 3 ml with or without 10 µg/ml fluconazole. Cultures were incubated with agitation at 35°C. One hundred microliter samples were removed from each culture at 0, 6, 12, and 24 h time points, serially diluted in sterile water, and 50 µl aliquots were spread on potato dextrose agar. Plates were incubated at 35°C and colonies counted at 24 and 48 h. Each experiment was performed in triplicate.

Ergosterol quantification analysis

Ergosterol was extracted and quantified as described by Arthington-Skaggs et al., 1999 (230). Briefly a single colony of *C. glabrata* from a fresh YPD plate was used to inoculate 50 ml of RPMI-1640 (Sigma, St. Louis, MO) and incubated for 16 h shaking at 35°C. Stationary-phase cells were collected by centrifugation for 5 minutes at 2700 rpm and washed twice with sterile distilled water. The net weight of the pellet was determined. To each pellet, 3 ml of 25% alcoholic potassium hydroxide solution (25 g of

KOH, 35 ml of sterile distilled water brought up to 100 ml with 100% ethanol) was added, then vortexed for 1 min. Cell suspensions were transferred to a sterile borosilicate glass screw cap tube and incubated at 85ºC for 1 h. Sterols were then extracted from cool tubes by the addition of the mixture of 3 ml *n*-heptane and 1 ml sterile distilled water followed by vortexing for 3 min. The heptane layer was transferred to a clean sterile borosilicate glass tube and stored at -20˚C for up to 24 h. 100 µl of sterol/heptane mixture was scanned spectrophotometrically between 240 nm and 300 nm with a DU530 Life Sciences UV spectrophotometer (Beckman Coulter, Brea, CA). The presence of ergosterol in the extracted sample results in a characteristic four-peaked curve with peaks located at approximately 262, 270, 281, and 290 nm. The absence of detectible ergosterol was indicated by a flat line. All samples were blanked to *n*-heptane. A decrease in the height of the absorbance peaks correlates to a decrease in ergosterol content. Statistical significance was determined by using Student's *t* test ($P < 0.05$).

RNA isolation

For RNA analysis, log phase cultures grown in YPD medium at 30˚C were adjusted to an optical density of 0.2 measured at 600 nm. Indicated concentrations of drug or DMSO control were added and the cultures were incubated an additional 3 h to mid-log phase. RNA was extracted by the hot phenol method (231), as previously described (232). RNA was treated with RQ1 DNAse (Promega, Madison, WI). Quantity and purity were determined by spectrophotometer (NanoDrop Technologies, Inc., Wilmington, DE).

Quantitative RT-PCR analysis

Quantitative RT-PCR was conducted as described previously (232). Single strand cDNA was synthesized from 2 µg of total RNA using the SuperScript First Strand Synthesis System for RT-PCR (Invitrogen, Carlsbad, CA) according to the manufacturer's instructions. Relative quantitative real-time PCR reactions were performed in triplicate using the 7000 Sequence Detection System (Applied Biosystems, Foster City, CA). Independent PCRs were performed using the primers listed in Table 2 for both the genes of interest and either 18s ribosomal RNA or *ACT1* using SYBR Green PCR Master Mix (Applied Biosystems). Relative gene expression was calculated by the comparative C_T Method ($\Delta\Delta C_T$ Method). For expression of *PDR1*, *CDR1*, *SNQ2* and *PDH1* samples were normalized first to *18S* expression and then to the untreated SM1 sample. For expression of genes in the ergosterol biosynthesis pathway, samples were first normalized to *ACT1* and then to the untreated parent sample, SM1 or SM3.

RESULTS

Disruption of *CgUPC2A* results in increased susceptibility to azole antifungals and other sterol biosynthesis inhibitors in *C. glabrata*

Using the *C. glabrata* genome database (www.genolevures.org/cagl.html), BLASTP analysis was performed to search for homologs of either ScUpc2 or ScEcm22. Two potential homologs were identified, CAGL0C01199g and CAGL0F07865g, which were recently reported by Nagi *et al*. as *UPC2A* and *UPC2B*, respectively (178). *UPC2A* (CAGL0C01199g) alone, *UPC2B* (CAGL0F07865g) alone, and both genes together were disrupted in fluconazole-SDD clinical isolate, SM1, and first tested against fluconazole (**Table 4-3**). As observed by Nagi et al., the disruption of *UPC2A*, alone or in combination with disruption of *UPC2B,* showed a marked increase in susceptibility to fluconazole, whereas the disruption of *UPC2B* alone did not. Complementation of *UPC2A* back into its native locus restored wild type susceptibility. In addition to fluconazole, strains were tested against a panel of azoles, non-azole SBIs (terbinafine and lovastatin), and antifungal agents not involved in sterol biosynthesis (amphotericin B and anidulafungin) (**Table 4-3**). The additional azoles tested exhibited similar susceptibility patterns as was observed with fluconazole. Terbinafine inhibits squalene epoxidase and lovastatin inhibits HMG-CoA reductase, both early enzymes in the ergosterol biosynthesis pathway (**Figure 4-1**). As was observed with the azole antifungals, strains disrupted for *UPC2A* exhibited increased susceptibility to both of these agents (**Table 4-3**). As reported previously for *C. albicans* (223), disruption of either *UPC2A* or *UPC2B* had no effect on susceptibility to amphotericin B, which binds ergosterol in the fungal cell membrane. Likewise, disruption of *UPC2* had no effect on susceptibility to the echinocandin, anidulafungin, which affects cell wall stability by targeting β-1,3-glucan synthase. (**Table 4-3**) Finally, reintroduction of *UPC2A* was able to restore wild-type susceptibilities. These results demonstrate that *UPC2A* influences the susceptibility of *C. glabrata* to a range of clinically used azoles as well as other SBIs.

Disruption of *UPC2A* results in enhanced activity of fluconazole against *C. glabrata*

Fluconazole remains the most widely used antifungal agent prescribed for the treatment of *Candida* infections (5). We therefore wished to further investigate the extent to which *UPC2A* influences fluconazole susceptibility in *C. glabrata*. In isolate SM1, disruption of *UPC2A* alone or in combination with disruption of *UPC2B* resulted not only in a reduction in fluconazole MIC (**Table 4-3**), but also in fluconazole MFC, whereas disruption of *UPC2B* had no effect on either of these parameters (**Figure 4-3A**). This phenotype reverted to that of the parent, SM1, when *UPC2A* was reintroduced. We used a 72 h endpoint for a broth microdilution assay in RPMI medium as a way to assess the ability of the organism to resume growth in the presence of fluconazole. The *UPC2A* mutant was unable to resume growth at this extended timepoint, whereas isolate SM1 was able to resume growth in concentrations up to 8 μg/ml (**Figure 4-3B**). Serial dilutions of the strains disrupted for *UPC2A* spotted on YPD solid medium containing 5 μg/ml or 10

Table 4-3. Broth microdilution susceptibility testing of the susceptible-dose dependent clinical parent isolate SM1, mutant strains disrupted for *UPC2*, and revertant.

	MICs (µg/ml)								
Strain	**FLC[1]**	**ITC**	**VRC**	**KTC**	**MC**	**AMB**	**LOVA**	**TRB**	**ANID**
SM1	8	2	2	2	0.5	2	200	512	0.016
SM1Δ*upc2A*	0.5	0.0078	0.125	0.0625	0.01563	2	25	32	0.016
SM1Δ*upc2B*	8	1	1	0.5	0.25	2	256	512	0.016
SM1Δ*upc2A*Δ*upc2B*	0.5	0.0078	0.125	0.01563	0.01563	2	16	8	0.016
SM1Δ*upc2A*/*UPC2A*	8	2	2	2	0.5	2	200	512	0.016

[1]Fluconazole (FLC), Itraconazole (ITC), Voriconazole (VRC), Ketoconazole (KTC), Miconazole (MC), Amphotericin B (AMB), Lovastatin (LOVA), Terbinafine (TRB), Anidulafungin (ANID)

Figure 4-3. Enhanced activity of fluconazole in a SDD clinical isolate, SM1, disrupted for *UPC2A*.

(A) Minimum fungicidal concentrations (MFC) were determined by spotting cultures on solid media after 48 h of growth in liquid RPMI. The MFC is the lowest concentration of fluconazole that inhibited growth completely when transferred to solid medium. (B) Broth microdilution assays were conducted according to CLSI guidelines. As a measure of the ability of the strains to regrow the plates were allowed to incubate for 72 h prior to measuring optical density at 600 nm. (C) Serial dilutions of indicated strains were incubated for 24 or 72 h on YPD solid media containing 0, 5 or 10 μg/ml fluconazole. (D) Time kill curves for *UPC2A* disruptants and revertants in a susceptible clinical isolate, SM1, treated with 10 μg/ml fluconazole (open symbols) or DMSO control (closed symbols). Cultures were grown in RPMI media with aliquots removed at the indicated time points and plated on potato dextrose agar for colony counts.

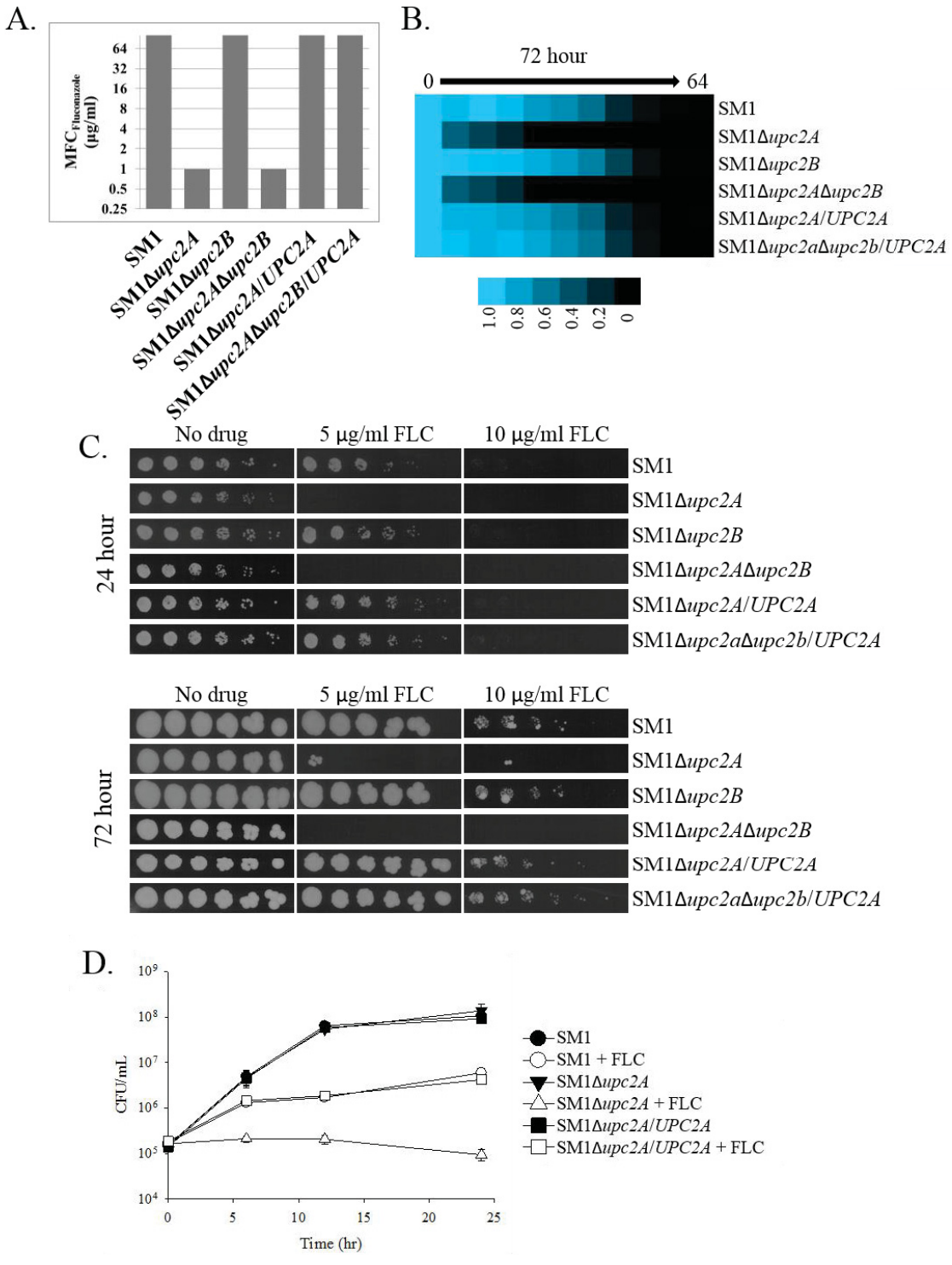
A.
MFC Fluconazole (μg/ml)
64
32
16
8
4
2
1
0.5
0.25
SM1
SM1Δupc2A
SM1Δupc2B
SM1Δupc2AΔupc2B
SM1Δupc2A/UPC2A
SM1Δupc2B/UPC2A
B.
72 hour
0
64
SM1
SM1Δupc2A
SM1Δupc2B
SM1Δupc2AΔupc2B
SM1Δupc2A/UPC2A
SM1Δupc2aΔupc2b/UPC2A
1.0
0.8
0.6
0.4
0.2
0
C.
No drug
5 μg/ml FLC
10 μg/ml FLC
24 hour
SM1
SM1Δupc2A
SM1Δupc2B
SM1Δupc2AΔupc2B
SM1Δupc2A/UPC2A
SM1Δupc2aΔupc2b/UPC2A
No drug
5 μg/ml FLC
10 μg/ml FLC
72 hour
SM1
SM1Δupc2A
SM1Δupc2B
SM1Δupc2AΔupc2B
SM1Δupc2A/UPC2A
SM1Δupc2aΔupc2b/UPC2A
D.
CFU/mL
Time (hr)
SM1
SM1 + FLC
SM1Δupc2A
SM1Δupc2A + FLC
SM1Δupc2A/UPC2A
SM1Δupc2A/UPC2A + FLC

μg/ml of fluconazole exhibited reduced growth, while SM1Δ*upc2B* and the *UPC2A* revertants were no different than the parent, SM1. Moreover, the cultures were unable to recover after incubation for 72 h. (**Figure 4-3C**) Likewise, by time-kill analysis, disruption of *UPC2A* in isolate SM1 resulted in greater inhibition by 10 μg/ml fluconazole compared to the wild type isolate (**Figure 4-3D**). These results demonstrate that disruption of *UPC2A* greatly influences the ability of *C. glabrata* to grow in the presence of fluconazole.

UPC2A is essential for resistance to sterol biosynthesis inhibitors in an azole-resistant clinical isolate of *C. glabrata*

In order to determine if *UPC2A* or *UPC2B* influence resistance to SBIs, we disrupted these genes in a clinical isolate that exhibits high level azole resistance due to overexpression of the *CDR1*, *PDH1*, and *SNQ2* transporter genes, as a result of an activating mutation in the transcription factor gene, *PDR1*. This isolate, SM3, was collected from the same patient as isolate SM1 after azole treatment failure and is described in detail elsewhere (124, 199). SM3 exhibited elevated MICs compared to SM1 for fluconazole, itraconazole, voriconazole, ketoconazole, and miconazole, as well as lovastatin and terbinafine. As was observed in isolate SM1, disruption of *UPC2A* alone or in combination with *UPC2B* resulted in increased susceptibility to all azoles and sterol biosynthesis inhibitors tested (**Table 4-4**). Indeed, disruption of *UPC2A* reduced the susceptibility of fluconazole to that observed in the wild-type isolate SM1, 8 μg/ml. Fluconazole MFCs of the strains lacking *UPC2A* decreased to 16 μg/ml as compared to >256 μg/ml for isolate SM3 and the revertants (**Figure 4-4A**). After 72 h in RPMI medium, growth of this strain was unable to resume at a fluconazole concentration of ≥ 16 μg/ml (**Figure 4-4B**). When serial dilutions of *UPC2A* disruptant strains were spotted on solid YPD medium containing 10 μg/ml fluconazole, growth was inhibited (**Figure 4-4C**). The growth inhibition was maintained after incubation for 72 h. By time-kill analysis, fluconazole concentrations of 10 μg/ml had no effect on isolate SM3 after 24 h, whereas disruption of *UPC2A* resulted in approximately a log-fold reduction in growth after 24 h of fluconazole treatment (**Figure 4-4D**). This was roughly equivalent to the effect of fluconazole on isolate SM1. These results demonstrate that *UPC2A* is essential for high-level fluconazole resistance in *C. glabrata*.

Disruption of *UPC2A* does not affect expression of *PDR1*, *CDR1*, *SNQ2*, and *PDH1* in an azole-resistant clinical isolate of *C. glabrata*

We observed that disruption of *UPC2A* not only increased susceptibility to fluconazole in clinical isolate SM1, but also in matched azole-resistant isolate SM3, which carries an activating mutation in *PDR1* and overexpresses *CDR1* and *PDH1*, as well as *PDR1* itself. Recently CaUpc2 was shown to bind *in vivo* to the promoter of *CDR1* suggesting that *C. glabrata* Cdr1 may also be a direct target of CgUpc2A (233, 234). These authors found that CaUpc2 is involved in maintaining baseline expression of

Table 4-4. Broth microdilution susceptibility testing of the resistant clinical isolate SM3, mutant strains disrupted for *UPC2*, and revertant.

	MICs (µg/ml)								
Strain	**FLC[1]**	**ITC**	**VRC**	**KTC**	**MC**	**AMB**	**LOVA**	**TRB**	**ANID**
SM1	256	8	8	8	2	2	200	512	0.016
SM1Δ*upc2A*	8	0.125	0.25	0.25	0.062	2	25	32	0.016
SM1Δ*upc2B*	256	16	4	8	2	2	256	512	0.016
SM1Δ*upc2A*Δ*upc2B*	8	0.25	0.25	0.25	0.062	2	64	16	0.016
SM1Δ*upc2A*/*UPC2A*	256	8	8	8	2	2	200	512	0.016

[1]Fluconazole (FLC), Itraconazole (ITC), Voriconazole (VRC), Ketoconazole (KTC), Miconazole (MC), Amphotericin B (AMB), Lovastatin (LOVA), Terbinafine (TRB), Anidulafungin (ANID)

Figure 4-4. Enhanced activity of fluconazole in a resistant clinical isolate, SM3, disrupted for *UPC2A*.

(A) Minimum fungicidal concentrations (MFC) were determined by spotting cultures on solid media after 48 h of growth in liquid RPMI. The MFC is the lowest concentration of fluconazole that inhibited growth completely when transferred to solid medium. (B) Broth microdilution assays conducted according to CLSI guidelines. As a measure of the ability of the strains to regrow the plates were allowed to incubate for 72 h prior to measuring optical density at 600 nm. (C) Serial dilutions of indicated strains were incubated for 24 or 72 h on YPD solid media containing 0, 5 or 10 μg/ml fluconazole. (D) Time kill curves for UPC2A disruptants and revertants in a resistant clinical isolate, SM3, treated with 10 μg/ml fluconazole (open symbols) or DMSO control (closed symbols). Cultures were grown in RPMI media with aliquots removed at the indicated time points and plated on potato dextrose agar for colony counts.

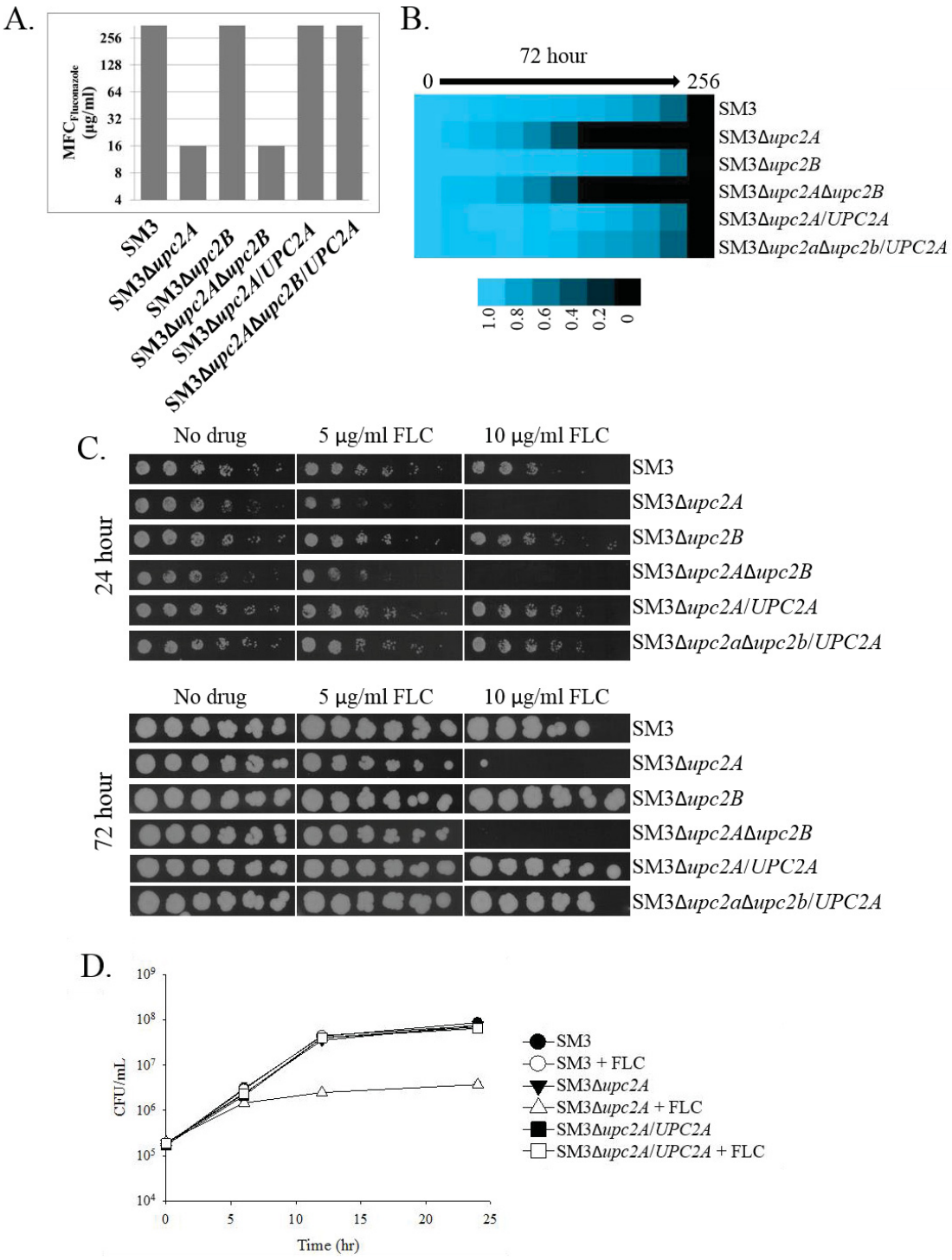
A.
MFC fluconazole (μg/ml)
256
128
64
32
16
8
4
SM3
SM3Δupc2A
SM3Δupc2B
SM3Δupc2AΔupc2B
SM3Δupc2A/UPC2A
SM3Δupc2B/UPC2A
B.
72 hour
0
256
SM3
SM3Δupc2A
SM3Δupc2B
SM3Δupc2AΔupc2B
SM3Δupc2A/UPC2A
SM3Δupc2aΔupc2b/UPC2A
1.0
0.8
0.6
0.4
0.2
0
C.
No drug
5 μg/ml FLC
10 μg/ml FLC
24 hour
SM3
SM3Δupc2A
SM3Δupc2B
SM3Δupc2AΔupc2B
SM3Δupc2A/UPC2A
SM3Δupc2aΔupc2b/UPC2A
No drug
5 μg/ml FLC
10 μg/ml FLC
72 hour
SM3
SM3Δupc2A
SM3Δupc2B
SM3Δupc2AΔupc2B
SM3Δupc2A/UPC2A
SM3Δupc2aΔupc2b/UPC2A
D.
CFU/mL
Time (hr)
SM3
SM3 + FLC
SM3Δupc2A
SM3Δupc2A + FLC
SM3Δupc2A/UPC2A
SM3Δupc2A/UPC2A + FLC

CDR1 in *C. albicans* and observed a slight decrease in *CDR1* expression in the absence of *UPC2*.

To determine what role, if any, the deletion of *UPC2A* in *C. glabrata* has on the expression of the efflux pump genes *CDR1*, *PDH1*, *SNQ2*, as well as *PDR1*, we examined the expression of these genes by qRT-PCR in strains SM1 and SM3, as well as their respective mutants disrupted for *UPC2A* and the revertants grown for 3 h with or without 32 μg/ml fluconazole. Disruption of *UPC2A* had no effect on the expression of these genes in the absence of fluconazole (**Figure 4-5**). However, in fluconazole-treated cells, we did observe a reduction in the upregulation of all of the genes tested in the SM1Δ*upc2A* mutant strain as compared to wild-type (**Figure 4-5**). Moreover, disruption of *UPC2A* in isolate SM3 had no effect on the constitutive overexpression of *CDR1*, *PDH1*, or *SNQ2*, suggesting that the reduced azole resistance observed in SM3 upon disruption of *UPC2A* is independent of these transporters.

Disruption of *UPC2A* results in a reduction in ergosterol levels in azole-SDD and -resistant *C. glabrata* isolates

Upc2 has previously been shown to be involved in the regulation of sterol biosynthesis and uptake in both *S. cerevisiae* and *C. albicans* (217, 222). To determine whether the observed decrease in susceptibility to SBIs corresponds to a decrease in ergosterol biosynthesis, we determined the effect of disruption of *UPC2A* and *UPC2B* on total ergosterol content in clinical isolates SM1 and SM3. Sterols were extracted from the mutant and parent strains and measured at an absorption spectra between 240 and 300 nm as described previously by Arthington-Skaggs et al., who demonstrated a direct correlation between ergosterol content and azole susceptibility in *S. cerevisiae* (230). As shown in **Figure 4-6**, disruption of *UPC2A* alone or in combination with *UPC2B* resulted in a reduction in ergosterol levels in both azole-SDD isolate, SM1, as well as azole-resistant isolate, SM3. These results suggest that ergosterol biosynthesis is impaired in both SDD and resistant isolates of *C. glabrata* in the absence of *UPC2A*.

***UPC2* is essential for both baseline and sterol biosynthesis inhibitor-induced expression of ergosterol biosynthesis genes**

Disruption of *UPC2A* resulted in increased susceptibility to SBIs and a significant decrease in total ergosterol content. In order to determine if disruption of *UPC2A* influences baseline expression of genes involved in sterol biosynthesis, thirteen *ERG* genes were examined by qRT-PCR. Disruption of *UPC2A* in both SM1 and SM3 resulted in ≥ 2-fold downregulation of all *ERG* genes examined. Reintroduction of *UPC2A* into its native locus partially or completely restored expression of most *ERG* genes (**Figure 4-7**). There was no significant difference between SM1 and SM3 in expression of any of the *ERG* genes tested.

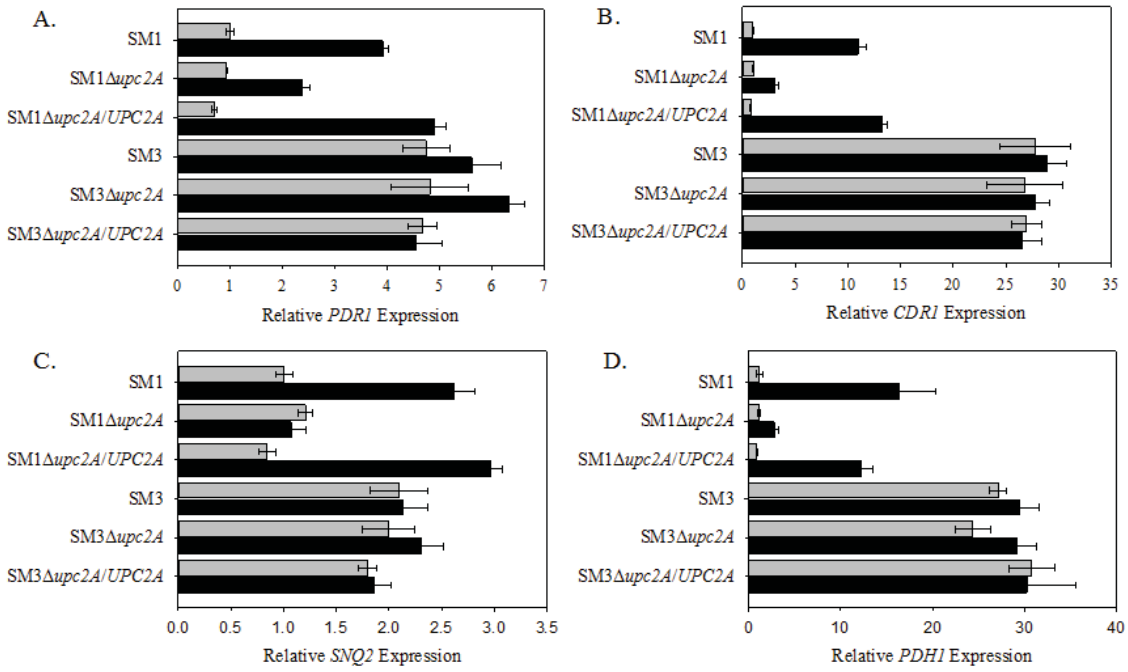

Figure 4-5. Effect of *UPC2A* disruption on constitutive and fluconazole-induced gene expression.

RNA was isolated from mid-log cultures in parent clinical isolates, Δ*upc2A* mutants, and revertants and qRT-PCR analysis of relative gene expression was performed. Light bars represent untreated controls and dark bars represent treatment with 32 µg/ml fluconazole for 3 h. (A) *PDR1* (B) *CDR1* (C) *SNQ2* and (D) *PDH1* Data are shown as the mean ± SE (n=3).

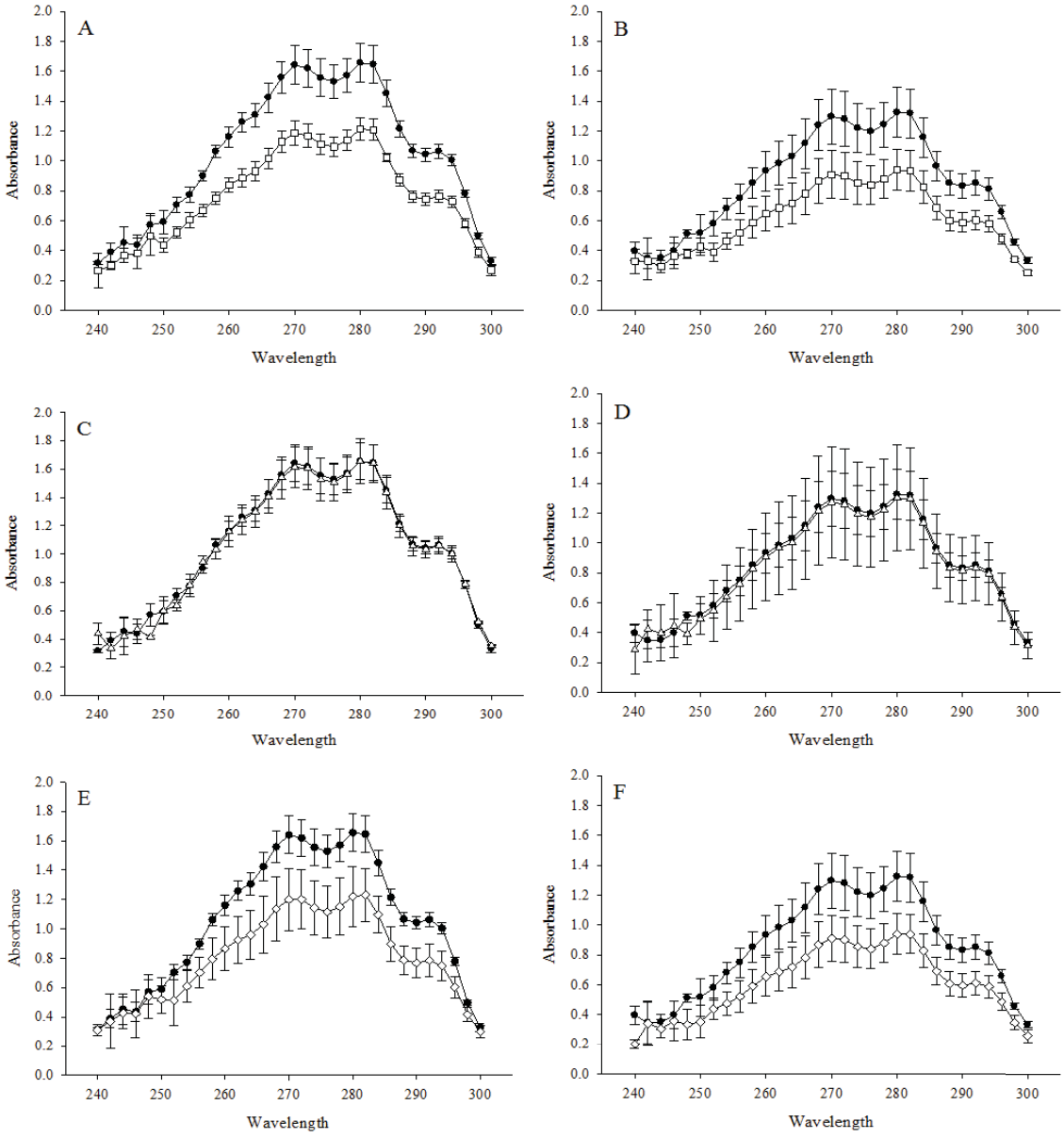

Figure 4-6. Ergosterol quantification for *UPC2A* disruptants in a SDD clinical isolate, SM1 and matched resistant isolate SM3.

Wild-type *UPC2A* allele (solid circles), Δ*upc2a* (open squares) (A,B), Δ*upc2b* (open triangles) (C,D) and Δ*upc2a*Δ*upc2b* (open diamonds) (E,F). The results for the *UPC2A* disruptants shown in panels A, B, E, and F showed statistically significant lower ergosterol content than were found in the wild type ($P < 0.05$). Knockout strains with the wild type allele complemented back in showed no difference in ergosterol content compared to the wild type isolates (data not shown). Strains were grown in CSM medium for 48 h, followed by a heptane extraction and spectrophotometric scan between 240 – 300 nm (41). Each isolate was extracted and analyzed in three independent experiments.

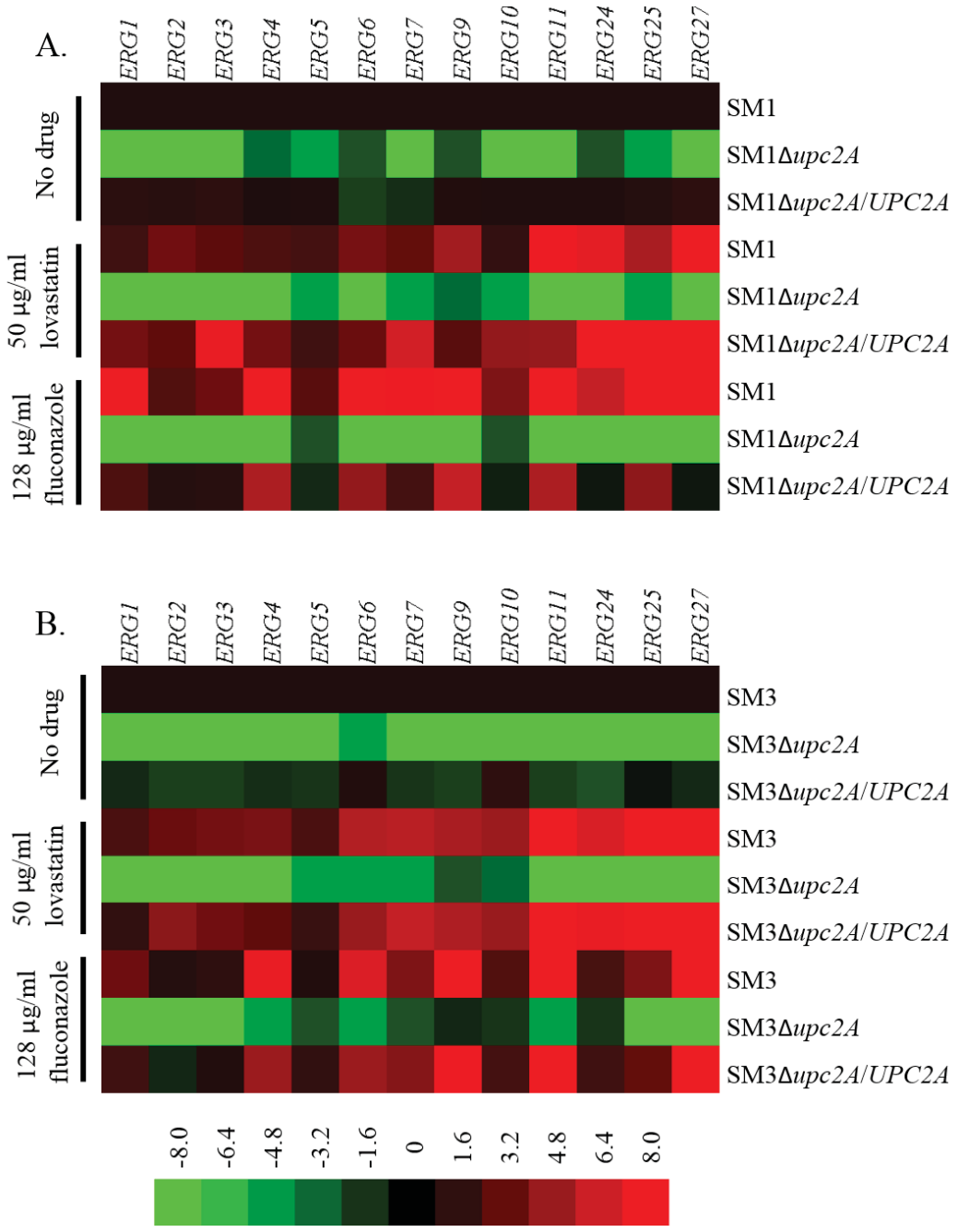

Figure 4-7. Effect of *UPC2A* disruption on both baseline and sterol biosynthesis inhibitor-induced expression of ergosterol biosynthesis genes.

RNA was isolated from mid-log cultures in parent clinical isolates, Δ*upc2A* mutants, and revertants. qRT-PCR analysis of relative gene expression was performed. A. SM1, Δ*upc2A* mutant, and revertant gene expression. Gene expression was normalized to the untreated SM1 sample for each ergosterol biosynthesis gene. B. SM3, Δ*upc2A* mutant, and revertant gene expression. Gene expression was normalized to the untreated SM3 sample for each ergosterol biosynthesis gene.

Multiple fungal pathogens, including *C. glabrata*, upregulate ergosterol biosynthesis genes in response to treatment with SBIs, which likely contributes to the decreased susceptibility observed with these agents (178, 235). We used qRT-PCR to determine the effects of SBI treatment on strains disrupted for *UPC2A*. Gene expression of *ERG* genes was measured for SM1 and SM3, as well as their respective *UPC2A* mutants and revertants, grown for 2 h in the presence or absence of 50 μg/ml lovastatin or 128 μg/ml fluconazole.

Similar to *S. cerevisiae* (236), treatment of isolates SM1 and SM3 with lovastatin resulted in ≥ 2-fold upregulation of twelve of the thirteen *ERG* genes examined in SM1 and all of the *ERG* genes examined in SM3. Treatment with fluconazole resulted in upregulation of all of these genes in SM1 and ten of the thirteen *ERG* genes examined in SM3. In the absence of *UPC2A*, lovastatin and fluconazole were unable to induce the expression of any of these *ERG* genes. Moreover, the majority of the thirteen *ERG* genes were downregulated ≥ 2-fold even in the presence of drug treatment. In most cases, reintroduction of *UPC2A* into its native locus in both SM1 and SM3 restored the ability of SBI treatment to induce *ERG* gene expression. (**Figure 4-7**) These data demonstrate that *UPC2A* is required for both baseline and SBI induction of *ERG* gene expression in *C. glabrata*.

DISCUSSION

Despite the more recent development of the lipid-based formulations of amphotericin B and the echinocandins, fluconazole remains the most prescribed antifungal agent for the treatment of *Candida* infections. It is inexpensive, available as both intravenous and oral formulations and is associated with minimal adverse effects. Although its use is complicated by many drug-drug interactions, these are well understood and somewhat predictable. Indeed fluconazole maintains excellent activity against many common and clinically important *Candida* species such as *C. albicans*, *C. parapsilosis*, and *C. tropicalis* (38). Of particular concern however is *C. glabrata* which has emerged as the second-leading cause of candidiasis in the U.S. and which exhibits intrinsically low susceptibility to the azole antifungals (157, 160, 210, 237-240).

Furthermore, the development of high-level resistance to the azoles is common in *C. glabrata* and has been well documented in isolates from head and neck radiation patients, stem cell transplant patients, human immunodeficiency virus (HIV) patients, and in vulvovaginal candidiasis (12, 51, 127, 134, 205). The development of azole resistance has also been implicated in the fluconazole treatment failure and death of a patient suffering from *C. glabrata* candidemia (199). Such resistance appears to be almost exclusively due to activating mutations in the gene encoding the transcription factor Pdr1 leading to overexpression of multidrug resistance transporters Cdr1, Pdh1, and Snq2 (121, 123, 168). Strategies to preserve this antifungal class for use against *C. glabrata* by both enhancing activity and overcoming resistance are needed.

The azoles exert their antifungal action by binding to and inhibiting the activity of the cytochrome P450 enzyme, lanosterol demethylase, which is a key enzyme in the ergosterol biosynthesis pathway that is encoded by *ERG11*. In both *S. cerevisiae* and *C. albicans*, the zinc cluster transcription factor Upc2 has been shown to be a central regulator of not only *ERG11*, but additional genes in the ergosterol biosynthesis pathway, as well. When lansosterol demethylase is inhibited genetically or pharmacologically in *C. glabrata*, alternate sterols and toxic sterol precursors such as lanosterol, 4,14α-dimethyl zymosterol, and 14α-methyl ergosta 8,24(28)-dien-3β,6α-diol are produced leading to reduced growth (55, 225) (**Figure 4-1**). In *S. cerevisiae*, *C. albicans*, and *C. glabrata*, Upc2 has been shown to be a central regulator of baseline and inducible expression of the genes encoding enzymes of the ergosterol biosynthesis pathway (178, 215, 222, 223, 241). Moreover, disruption of *UPC2* has been shown to increase the susceptibility of these organisms to the azole antifungals (178, 241, 242).

Given its global influence on sterol biosynthesis, we hypothesized that disruption of Upc2 might enhance the activity of the azole antifungals against azole-resistant, as well as, -SDD clinical isolates of *C. glabrata*. We have recently characterized a matched pair of azole-SDD and -resistant *C. glabrata* clinical isolates in which high-level azole resistance developed during fluconazole treatment (124). The resistant isolate in the pair carries an activating mutation in *PDR1* leading to the overexpression of *CDR1*, *PDH1*, and *SNQ2* and an increase in fluconazole MIC from 8 μg/ml to 256 μg/ml. Interestingly, disruption of *UPC2A* not only led to a reduction in fluconazole MIC from 8 μg/ml to 0.5 μg/ml, but also a reduction in fluconazole MFC from >64 μg/ml to 1 μg/ml in the SDD isolate. Similar reductions in MIC were observed for other azoles and the SBIs, terbinafine and lovastatin, but not for amphotericin B or the echinocandin, anidulafungin, which act directly on ergosterol in the cell membrane or on the cell wall, respectively. Despite the reduction in ergosterol content we expected no change in amphotericin B susceptibility based on previous findings in *C. albicans* and *C. glabrata* (74, 178, 223). We agree with the hypotheisis of Silver et al. that this could potentially be due to the amount of remaining ergosterol being above the threshold necessary for amphotericin B to cause cell death (223).

As fluconazole is the most commonly prescribed azole antifungal, we examined its activity against these strains more closely. We used a 72 h endpoint in a broth microdilution assay to assess the ability of the organism to resume growth in the presence of fluconazole. Disruption of *UPC2A* greatly impeded the ability of isolate SM1 to resume growth in even relatively low concentrations of the drug. Likewise, when spotted on YPD plates containing either 5 or 10 μg/ml of fluconazole, isolate SM1 was unable to grow when *UPC2A* was disrupted. Similar results were observed by time-kill analysis in RPMI medium where isolate SM1 exhibited modest growth at 24 h in the presence of 10 μg/ml fluconazole, whereas growth was inhibited in the absence of *UPC2A*. These results further demonstrate that *UPC2A* is required for optimal azole activity against *C. glabrata*.

We then examined the azole-resistant clinical isolate SM3 under the same conditions and observed remarkably similar results. Disruption of *UPC2A* led to increased susceptibility to fluconazole resulting in an MIC equal to that of SDD isolate

SM1. Moreover, the MFC for fluconazole was reduced from >256 μg/ml to 16 μg/ml. Disruption of *UPC2A* resulted in similar effects on susceptibility to other azoles and sterol biosynthesis inhibitors. Growth in the presence of fluconazole was likewise greatly reduced when measured at 72 h in liquid RPMI medium, on YPD plates containing 10 μg/ml fluconazole and by time kill analysis at 24 h in 10 μg/ml fluconazole. These results demonstrate that *UPC2A* is required for high-level azole resistance in *C. glabrata*.

One possible explanation for the increased fluconazole susceptibility observed in these isolates is a change in expression of the genes encoding the multidrug resistant transporters Cdr1, Pdh1, and Snq2. Indeed, it has been shown that in *C. albicans*, Upc2 binds the promoter of *CDR1* suggesting it may contribute to its regulation (224). Interestingly, the sterol response element recognized by Upc2, as defined by Znaidi et al., is present in the promoter region of *CDR1* in *C. glabrata*, as well (224). It has also been shown that fluconazole treatment activates the transcription factor Pdr1 and induces the expression of its targets, multidrug transporter genes (170). We therefore examined the influence of *UPC2A* on both baseline and inducible expression of *PDR1*, *CDR1*, *PDH1*, *SNQ2* in isolates SM1 and SM3. Disruption of *UPC2A* had no effect on baseline expression of these genes in isolate SM1 or on their constitutive overexpression in isolate SM3. Interestingly, disruption of *UPC2A* reduced the inducible expression of all four genes in response to fluconazole. This suggests that Upc2A is required for optimal activation of the Pdr1 transcriptional pathway. The diminished capacity of isolate SM1 to respond to fluconazole stress by up-regulating these transporter genes may contribute to its increased susceptibility to the azoles and other sterol biosynthesis inhibitors.

Another possible explanation for the increased fluconazole susceptibility observed in these isolates is a change in the expression of genes involved in ergosterol biosynthesis that are regulated by *UPC2A*. Both SM1 and SM3 exhibited reduced cellular ergosterol when *UPC2A* was disrupted. Likewise, baseline expression as well as inducible expression by fluconazole or lovastatin of all ergosterol biosynthesis genes analyzed was reduced in the absence of *UPC2A*. Importantly, the azole target, *ERG11*, is included in this group of ergosterol biosynthesis genes, which would result in a reduced amount of target that would need to be inhibited in order to effectively inhibit ergosterol biosynthesis. These data suggest that the global impact on sterol biosynthesis in the absence of *UPC2A* greatly increases the vulnerability of *C. glabrata* to fluconazole, even in the setting of Pdr1 activation and overexpression of *CDR1*, *PDH1*, and *SNQ2*.

Additionally, the incorporation of alternate sterols into the cell membrane affects fluidity of the membrane and may compromise the ability of the efflux pumps to function properly. Krishnamurthy and Prasad demonstrated altered accumulation of various compounds when tested against a panel of *S. cerevisiae ERG* mutants expressing *C. albicans* Cdr1 (243). Altered membrane fluidity and asymmetry has also been associated with increased resistance to fluconazole in *C. albicans* independent of efflux pump function (244). Taken together, our findings suggest that Upc2A and the transcriptional activation pathway it regulates represents a potential target for overcoming azole antifungal resistance in *C. glabrata*.

CHAPTER 5. JJJ1 IS A NEGATIVE REGULATOR OF PDR1-MEDIATED FLUCONAZOLE RESISTANCE IN *CANDIDA GLABRATA*

INTRODUCTION

Candida glabrata is the second most common cause of human fungal infection (44). Fluconazole has long been among frontline therapies for the treatment of invasive candidiasis. However, *C. glabrata* exhibits intrinsic reduced susceptibility to fluconazole and often develops high-level resistance during fluconazole therapy (50, 161). As such, the most recent clinical guidelines for treatment of candidiasis now recommend empiric therapy with an echinocandin rather than fluconazole in large part due to the problem of fluconazole resistance in this *Candida* species (39).

In *C. glabrata*, resistance to fluconazole is almost exclusively due to activating mutations in the gene encoding the zinc cluster transcription factor Pdr1. Pdr1 is the homolog of Pdr1 and Pdr3 in *Saccharomyces cerevisiae*, which regulates genes involved in the pleiotropic drug resistance phenotype. In *C. glabrata*, Pdr1 activates the expression of the genes encoding the ABC transporters Cdr1, Pdh1, and Snq2. It has been proposed that fluconazole can activate Pdr1 by binding directly to its xenobiotic binding domain (170). Moreover, Pdr1 can be activated by mitochondrial loss as is observed in "petite" mutants (121). While activation of Pdr1 in the presence of xenobiotics is dependent on binding of the activation domain of Pdr1 to the KIX domain of the Mediator complex component Gal11a, our understanding of how Pdr1 is regulated in *C. glabrata* is incomplete (170).

In an effort to better understand this process, we screened a collection of 217 single gene deletion strains of *C. glabrata* for increased resistance to fluconazole (245). Deletion of the putative J protein CAGL0J07370g resulted in fluconazole resistance. This gene shares greatest homology with the *Saccharomyces cerevisiae* gene *JJJ1*. We show here that disruption of *JJJ1* in a wild-type *C. glabrata* clinical isolate results in increased resistance to fluconazole through a Pdr1-dependent increased expression of the ABC transporter gene *CDR1*.

MATERIALS AND METHODS

Strains and growth conditions

Strains used in this study are listed in **Table 5-1**. The parent clinical isolate and the *PDR1* deletion strain have been described previously (124, 199). All strains were stored as frozen stocks at -80°C in 40% glycerol. Strains were routinely grown in yeast extract peptone dextrose (YPD; 1% yeast extract, 2% peptone, and 2% dextrose) broth at 30°C in a shaking incubator except as indicated for specific experimental conditions.

Table 5-1. Strains used in the *JJJ1* study.

Strain	Parent	Genotype or description	Reference
SM1		Azole-susceptible clinical isolate	(199)
SM1Δ*jjj1*	SM1	*jjj1*Δ::*FRT*	This study
SM1Δ*jjj1*::*JJJ1*	SM1Δ*jjj1*	*jjj1*Δ::*JJJ1-FRT*	This study
SM1Δ*cdr1*	SM1	*cdr1*Δ::*FRT*	This study
SM1Δ*pdr1*	SM1	*pdr1*Δ::*FRT*	(124)
SM1Δ*jjj1*Δ*cdr1*	SM1Δ*jjj1*	*jjj1*Δ::*FRT/cdr1*Δ::*FRT*	This study
SM1Δ*jjj1*Δ*pdr1*	SM1Δ*pdr1*	*jjj1*Δ::*FRT/pdr1*Δ::*FRT*	This study

One Shot *Escherichia coli* TOP10 chemically competent cells (Invitrogen, Carlsbad, CA) were used as the host for plasmid construction and propagation. These strains were grown at 37°C in LB broth or on LB plates supplemented with 100 μg/ml ampicillin (Sigma, St. Louis, MO) or 50 μg/ml kanamycin (Fisher BioReagents, Fair Lawn, NJ).

Deletion library screen

We obtained 217 *C. glabrata* single gene deletion strains from a previously published collection (245). These included genes encoding putative transcription factors and DNA binding proteins. The mutant strains were generated in a histidine auxotrophic mutant of *C. glabrata* strain ATCC 2001 (CBS138). Fluconazole MICs were determined for each deletion strain according to the CLSI reference method with minor modifications as described below (202, 246). Strains were tested at concentrations ranging from 64 mg/L to 0.125 mg/L fluconazole in duplicate.

Plasmid construction

For deletion of *JJJ1* and *CDR1* we modified plasmid pSFS2 (200). Upstream homology regions approximately 800 - 1000 bp long were amplified using primer pairs CgJJJ1-A/CgJJJ1-B or CgCDR1-A/CgCDR1-B and digested with ApaI and XhoI for insertion into their respective plasmids. Downstream homology regions approximately 900 - 1000 bp long were amplified using primer pairs CgJJJ1-C/CgJJJ1-D or CgCDR1-C/CgCDR1-D and digested with SacI and SacII for insertion into their respective plasmids. The disruption cassettes consisting of the *SAT1* flipper cassette and upstream and downstream flanking sequences of either *JJJ1* or *CDR1* were excised from the final plasmids pCgJJJ1 or pCgCDR1 and gel purified. Primers used to construct the cassettes are listed in **Table 5-2**.

For reintegration of *JJJ1* into Δ*jjj1* mutants we modified plasmid pCgJJJ1. The open reading frame in addition to some upstream and downstream sequence was amplified using primer pair CgJJJ1-A/CgJJJ1-E and digested with ApaI and XhoI. This replaced the upstream homology region from plasmid pCgJJJ1, such that upon transformation and homologous recombination *JJJ1* would be reintegrated into its original locus. The resulting plasmid is called pCgJJJ1pb.

Strain construction

C. glabrata cells were transformed by the lithium acetate method using approximately 1 μg of DNA. The ApaI/SacI fragments from pCgJJJ1, pCgCDR1, and pCgJJJ1pb were excised and gel purified prior to transformation. The transformed cells were allowed to recover 6 h in YPD at 30°C before being plated on YPD-agar plates containing 200 μg/ml nourseothricin (Jena Biochemical, Germany) and incubated at

Table 5-2. Primers used in the *JJJ1* study (grouped by application).

Primer name and function	Primer sequence[1]
Cassettes for constructing mutants	
CgJJJ1-A	5'- AATTACAAAGGGCCCTATTTGAGTTACAGC -3'
CgJJJ1-B	5'- ATTATCTGGATTCTCGAGAGGATGATAC -3'
CgJJJ1-C	5'- AAGTAGGAATCCGCGGTTTAGTCATATACA -3'
CgJJJ1-D	5'- TATTTATGCTACGAGCTCTATTGACGTTAT -3'
CgJJJ1-E	5'- GTTTCCAAGCAACTCGAGATGATTAGT -3'
CgCDR1-A	5'- CATAGATCAGGGCCCATTACATTAGCACAG -3'
CgCDR1-B	5'- CTCAGTGTTGCTCGAGATAGGGTTGATAC -3'
CgCDR1-C	5'- GTTCTGTTAGTTCCGCGGACTCTCGTAGAT -3'
CgCDR1-D	5'- GTGAATACAAACAAGAGCTCCACAATAATA -3'
qRT-PCR	
18SF	5'-TCGGCACCTTACGAGAAATCA-3'
18SR	5'-CGACCATACTCCCCCCAGA-3'
PDR1F	5'-TTTGACTCTGTTATGAGCGATTACG-3'
PDR1R	5'-TTCGGATTTTTCTGTGACAATGG-3'
CDR1F	5'-CATACAAGAAACACCAAAGTCGGT-3'
CDR1R	5'-GAGACACGCTTACGTTCACCAC-3'
SNQ2F	5'-CGTCCTATGTCTTCCTTACACCATT-3'
SNQ2R	5'-TTTGAACCGCTTTTGTCTCTGA-3'
PDH1F	5'-ACGAGGAGGAAGACGACTACGA-3'
PDH1R	5'-CTTTACTGGAGAACTCATCGCTGGT-3'

[1]Underlined bases indicate introduction of restriction enzyme cloning sites to allow directional cloning into the *SAT1*-flipper cassette.

30ºC. Positive transformants were selected within 24 h and successful insertion of the disruption cassette at the target gene locus was confirmed by Southern hybridization using gene specific probes. Subsequently, induction of the flipper recombinase gene in the disruption cassette was performed by overnight growth of the positive transformant clones in YPD at 30ºC with shaking (under no selective pressure). Selection for excision of the *SAT1* flipper cassette was then performed by plating on YPD-agar plates and incubating for up to 24 h at 30ºC. Clones were selected and confirmed by Southern hybridization using gene specific probes.

Genomic DNA isolation and Southern analysis

Genomic DNA from *C. glabrata* was isolated as described previously (201). For confirmation by Southern hybridization, approximately 10 μg of genomic DNA was digested with the appropriate restriction enzymes, separated on a 1% agarose gel containing ethidium bromide, transferred by vacuum blotting onto a nylon membrane and fixed by UV-crosslinking. Hybridization was performed with the Amersham ECL Direct Nucleic Acid Labeling and Detection System (GE Healthcare, Pittsburg, PA) as per manufacturer's instructions.

Susceptibility testing

Susceptibility testing was performed by microbroth dilution assay according to the CLSI guidelines outlined in M27-A3 with a few modifications (202, 246). Fluconazole (MP Biomedicals, Salon, OH) stock solution was prepared by reconstitution in water to 5 mg/mL. Cultures were diluted to $2.5x10^3$ cells/ml in RPMI 1640 (Sigma, St. Louis, MO) with 2% glucose, MOPS, pH 7.0. Plates were incubated at 35°C for 48 h. Absorbance at 600 nm was read with a BioTek Synergy 2 microplate reader (BioTek, Winooski, VT); background due to medium was subtracted from all readings. The MIC was defined as the lowest concentration inhibiting growth by at least 50% relative to the drug-free control after incubation with drug for 48 h.

RNA isolation

RNA isolation procedure was the same for both quantitative real time PCR and RNA-Seq experiments. Log phase cultures grown in YPD medium at 30°C were adjusted to an OD of 0.2 measured at 600 nm and the cultures were incubated an additional 3 h to mid-log phase. RNA was extracted by the hot phenol method (231), as previously described (232). RNA was treated with RQ1 DNAse (Promega, Madison, WI). Quantity and purity were determined by spectrophotometer (NanoDrop Technologies, Inc., Wilmington, DE) and verified using a Bioanalyzer 2100 (Agilent Technologies, Santa Clara, CA).

Quantitative real time PCR

Quantitative RT-PCR was conducted as described previously (232). Single strand cDNA was synthesized from 2 μg of total RNA using the SuperScript First Strand Synthesis System for RT-PCR (Invitrogen, Carlsbad, CA) according to the manufacturer's instructions. Relative quantitative real-time PCR reactions were performed in triplicate using the 7000 Sequence Detection System (Applied Biosystems, Foster City, CA). Independent PCRs were performed using the primers listed in **Table 5-2** for both the genes of interest and 18s ribosomal RNA using SYBR Green PCR Master Mix (Applied Biosystems). Relative gene expression was calculated by the comparative C_T Method ($\Delta\Delta C_T$ Method). For expression of *PDR1*, *CDR1*, *SNQ2* and *PDH1* samples were normalized first to *18S* expression and then to the parent strain SM1.

Protein isolation and Western analysis

Log-phase cells grown in YPD at 30°C were diluted to an OD of 0.2 measured at 600nm and were grown in YPD for an additional 3 hours. Three OD_{600} units of culture were harvested per sample and two colonies of each strain were analyzed. Protein extracts were prepared as previously described (247). Protein pellets were resuspended in urea sample buffer (8 M urea, 1% 2-mercaptoethanol, 40 mM Tris-HCl pH 8.0, 5% SDS, bromophenol blue) and boiled at 90˚C for 10 min. An aliquot from each sample was resolved on a precast ExpressPlus™ 4-15% gradient gel (GenScript) following the manufacturer's SDS-PAGE protocol. Proteins were electroblotted onto a nitrocellulose membrane, blocked with 5% nonfat dry milk, and then probed with anti-Pdr1 antibody (126) diluted 1:1500. All membranes were probed for tubulin as the loading control with 12G10 anti-alpha-tubulin monoclonal antibody (Developmental Studies Hybridoma Bank at the University of Iowa) for 30 min at room temperature. The membrane was probed with secondary LI-COR antibodies IRDye 680LT goat anti-rabbit diluted 1:20,000 and IRDye 800CW goat anti-mouse diluted 1:10,000. Western blot signal was detected using the Li-Cor Odyssey infrared imaging system, application software version 3.0.

RNA sequencing

Barcoded libraries were prepared using the Lexogen mRNA Sense kit for Ion Torrent according to manufacturer's standard protocol. Libraries were sequenced on the Ion Torrent Proton sequencer. Individual sample fragments were concatenated to form the whole sample fastq file. Files were then run through FASTQC to check data quality. Any reads with a phred score <20 were trimmed. After trimming reads were aligned to the *C. glabrata* CBS138 reference transcriptome using RNA-Star long method. After alignment transcriptome alignment counts were gathered. The read counts for each sample were normalized using transcripts per kilobase million (TPM) method.

Accession number

The RNA sequencing data was submitted to the Gene Expression Omnibus (GEO) database (https://www.ncbi.nlm.nih.gov/geo/). The accession number is GSE104476.

RESULTS

Deletion of *JJJ1* results in fluconazole resistance in a laboratory strain of *C. glabrata*

We screened 217 strains from a previously published collection of mutants deleted for genes encoding putative transcription factors and DNA binding proteins for increased resistance to fluconazole (245). Three strains exhibited fluconazole MICs that were greater than one dilution higher than that of the parent strain (**Table 5-3**). Two mutants, those deleted for CAGL0K05797g (*EMI1*) and CAGL0C00297g (*ScSET2*), exhibited a four-fold increase in fluconazole MIC. One strain, deleted for CAGL0J07370g, exhibited a sixteen-fold increase in fluconazole MIC. CAGL0J07370g has sequence homology to the gene encoding the type III J protein Jjj1 in *S. cerevisiae.*

Deletion of *JJJ1* in a susceptible-dose dependent clinical isolate of *C. glabrata* confers resistance to fluconazole

To confirm the phenotype of the *JJJ1* mutant strain, we generated an additional *JJJ1* deletion strain in clinical isolate SM1 using the *SAT1* flipper method (200). Isolate SM1 was originally recovered from an antifungal naïve patient undergoing cancer chemotherapy (199). Deletion of *JJJ1* in this susceptible-dose dependent clinical isolate resulted in a sixteen-fold increase in MIC to fluconazole from 4 mg/L to 64 mg/L (**Table 5-4**, **Figure 5-1**). This increase was identical to that observed in the *JJJ1* mutant strain from the deletion collection. We then constructed a complemented derivative strain using the *SAT1* flipper method. The MIC of fluconazole upon reintroduction of *JJJ1* was restored to that of parent, clinical isolate SM1.

Jjj1-mediated fluconazole resistance is dependent upon Cdr1

In clinical isolates of *C. glabrata* fluconazole resistance is mediated by the ABC transporters Cdr1, Pdh1, and Snq2 (127-130). To determine if increased fluconazole resistance observed when *JJJ1* is deleted is also mediated by these transporters, we first measured the expression levels of their respective genes using qRT-PCR. Deletion of *JJJ1* in clinical isolate SM1 resulted in *CDR1* expression over twenty-fold and *PDH1* expression over four-fold that observed in the parent strain (**Figure 5-2A**). There was no significant change in expression of *SNQ2*.

Table 5-3. Fluconazole MICs for single gene deletion mutant strains.

C. glabrata designation	*C. glabrata* gene name	*S. cerevisiae* ortholog	MIC50 (mg/L)
Parent			4
CAGL0K05797g	*EMI1*	*EMI1*	16
CAGL0C00297g		*SET2*	16
CAGL0J07370g	*JJJ1*	*JJJ1*	64

Table 5-4. Fluconazole MICs for indicated strains.

Strain	MIC50 (mg/L)
SM1	4
SM1Δ*jjj1*	64
SM1Δ*jjj1*::*JJJ1*	4
SM1Δ*cdr1*	1
SM1Δ*pdr1*	1
SM1Δ*jjj1*Δ*cdr1*	2
SM1Δ*jjj1*Δ*pdr1*	2

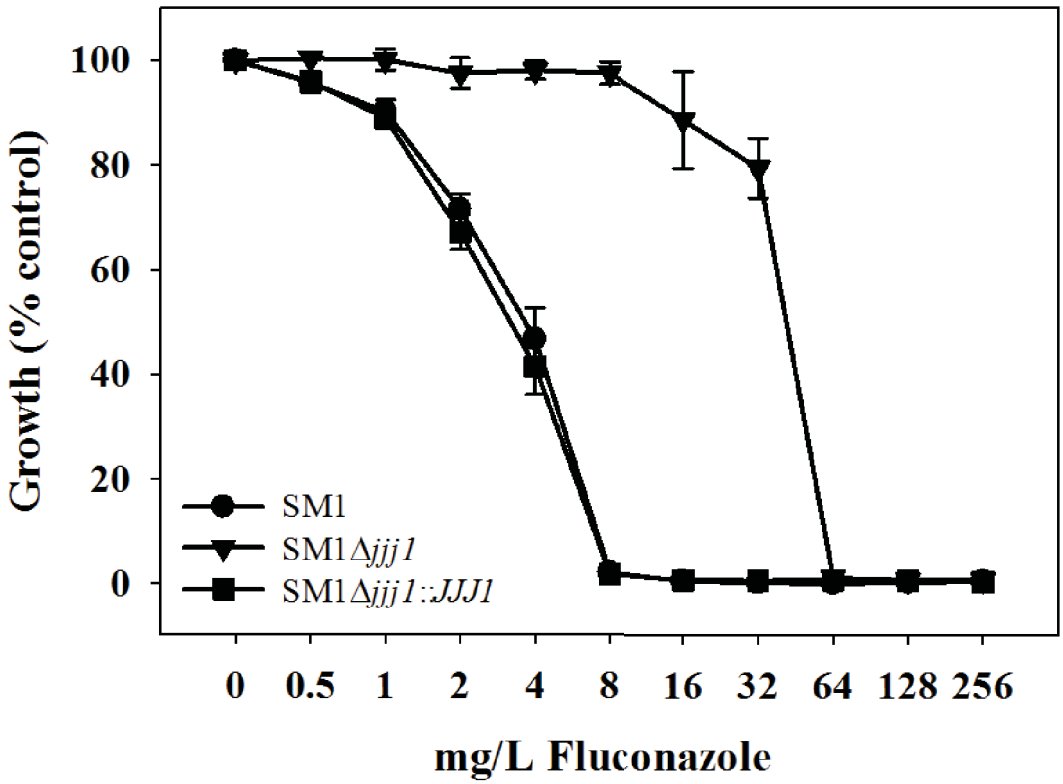

Figure 5-1. Deletion of *JJJ1* in the susceptible dose dependent clinical isolate SM1 results in decreased fluconazole susceptibility.

Reintegration of *JJJ1* to its original locus restored the susceptible dose dependent phenotype. Strains were grown in 96 well plates according to standard CLSI methods with minor modifications and optical density at 600nm was measured after 48 hours.

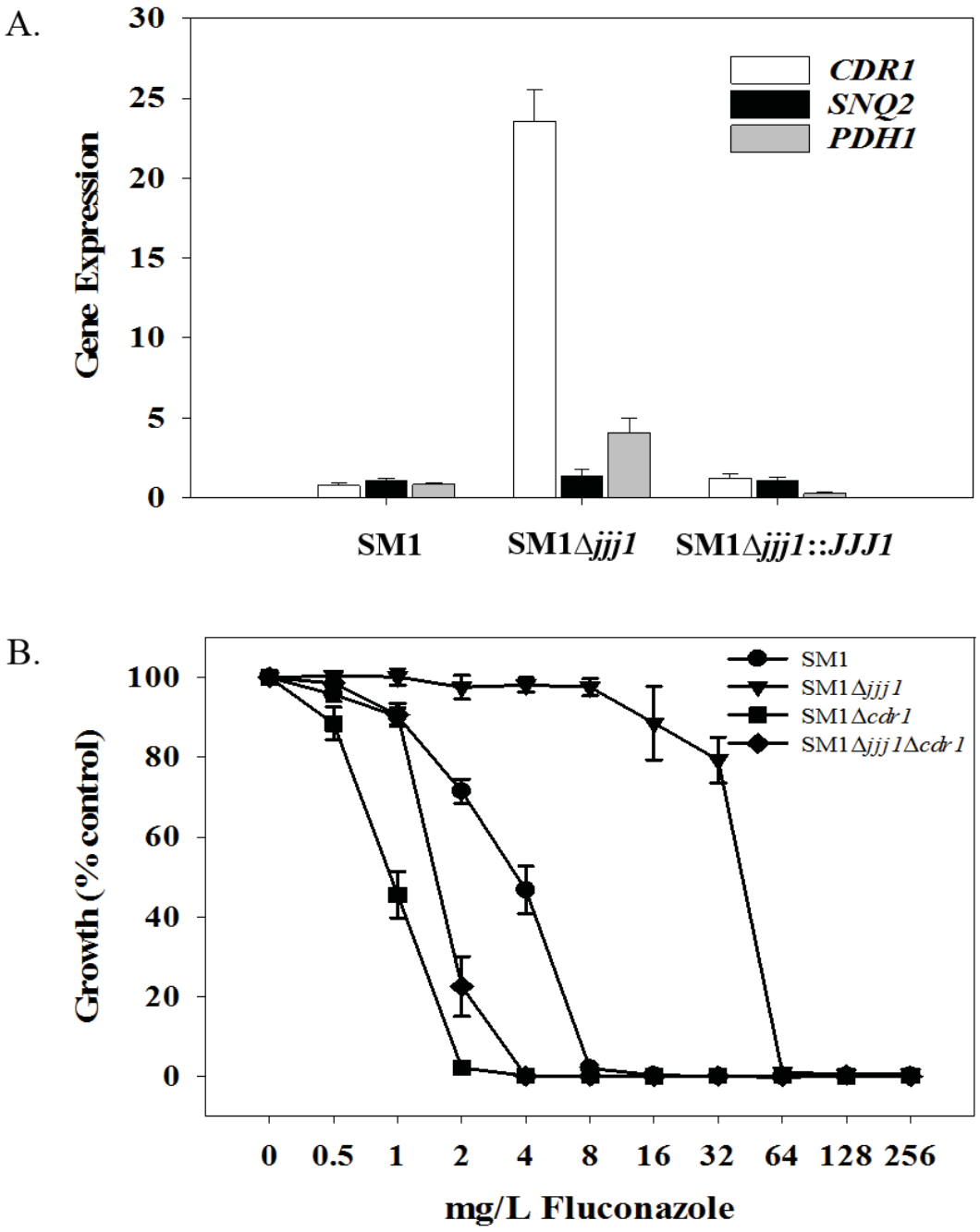

Figure 5-2. *JJJ1* influences fluconazole susceptibility in a *CDR1* dependent manner.

(A) The effect of *JJJ1* deletion on expression of the ABC transporters *CDR1*, *SNQ2*, and *PDH1* was measured by qRT-PCR. Expression was normalized to 18S expression in the parent isolate SM1. (B) Strains were grown in 96 well plates according to standard CLSI methods with minor modifications and optical density at 600nm was measured after 48 hours.

We then deleted *CDR1* in the *JJJ1* deletion mutant. Deletion of *CDR1* resulted in greater susceptibility to fluconazole than the wild-type parent isolate SM1 (**Figure 5-2B**). However, this mutant was not as susceptible as a *CDR1* deletion mutant in the SM1 background. These observations suggest that the increased fluconazole resistance observed upon deletion of *JJJ1* is due in large part to *CDR1*, but that other determinants, possibly *PDH1*, contribute modestly to this phenotype as well.

Jjj1-mediated fluconazole resistance and *CDR1* expression is dependent on Pdr1

CDR1 is a direct target of the zinc cluster transcription factor Pdr1. The expression of *CDR1* in response to fluconazole requires activation of Pdr1, and overexpression of *CDR1* in fluconazole resistant clinical isolates is due to activating mutations in *PDR1* (119, 121, 127). Of note, *PDR1* is autoregulated (121, 125), so we predicted that deletion of *JJJ1* would result in upregulation of *PDR1* gene expression and concomitant increased Pdr1 protein expression. *PDR1* expression increased 2.7-fold in the *JJJ1* knockout compared to the parent strain (**Figure 5-3A**). As expected there is no *PDR1* expression in the strain with *PDR1* deleted alone or in the strain with *JJJ1* and *PDR1* deleted. Pdr1 protein levels followed the same pattern (**Figure 5-3B**).

To determine if the effects on *CDR1* expression and fluconazole susceptibility observed upon deletion of *JJJ1* is dependent upon activation of Pdr1, we deleted *PDR1* in the *JJJ1* deletion mutant and measured expression of *CDR1* and susceptibility to fluconazole. Deletion of *PDR1* reduced expression of *CDR1* in the absence of *JJJ1* to levels observed in the wild-type parent strain (**Figure 5-4A**). Deletion of *PDR1* in the *JJJ1* deletion mutant increased fluconazole susceptibility beyond what was observed in the wild-type parent strain (**Figure 5-4B**), but not to the extent of that observed in the *PDR1* deletion mutant. This suggests that while most of the effect of deleting *JJJ1* on fluconazole susceptibility is dependent upon Pdr1, some of the effects of Pdr1 on fluconazole susceptibility are not affected by Jjj1.

Deletion of *JJJ1* activates genes of the Pdr1 regulon

In order to determine what genes in addition to *CDR1*, *PDH1*, and *PDR1* are differentially expressed when *JJJ1* is deleted, we used RNA-seq to compare the transcriptional profiles of both the *JJJ1* deletion mutant and the *JJJ1*/*PDR1* deletion mutant to that of parent isolate SM1. In the *JJJ1* deletion mutant as compared to the parent strain, 204 genes were up-regulated and 224 genes were down-regulated by 1.5-fold or greater (**Appendix B**, **Table B-1** and **B-2**). Up-regulation and down-regulation of 119 and 149 of these, respectively, required *PDR1* (**Table B-1** and **B-2**, bolded genes). As expected, we observed *CDR1*, *PDH1*, and *PDR1* to be among those genes whose up-regulation upon deletion of *JJJ1* required *PDR1*. Of the twenty-five targets of Pdr1 that have been previously confirmed by ChIP-seq (126), seven were found to be up-regulated when *JJJ1* was deleted. These were *CDR1*, *YBT1*, *YOR1*, *RSB1*, *RTA1*, *PDH1*, and *NCE103*. One of these, *NCE103*, remained up-regulated in the absence of both *JJJ1* and

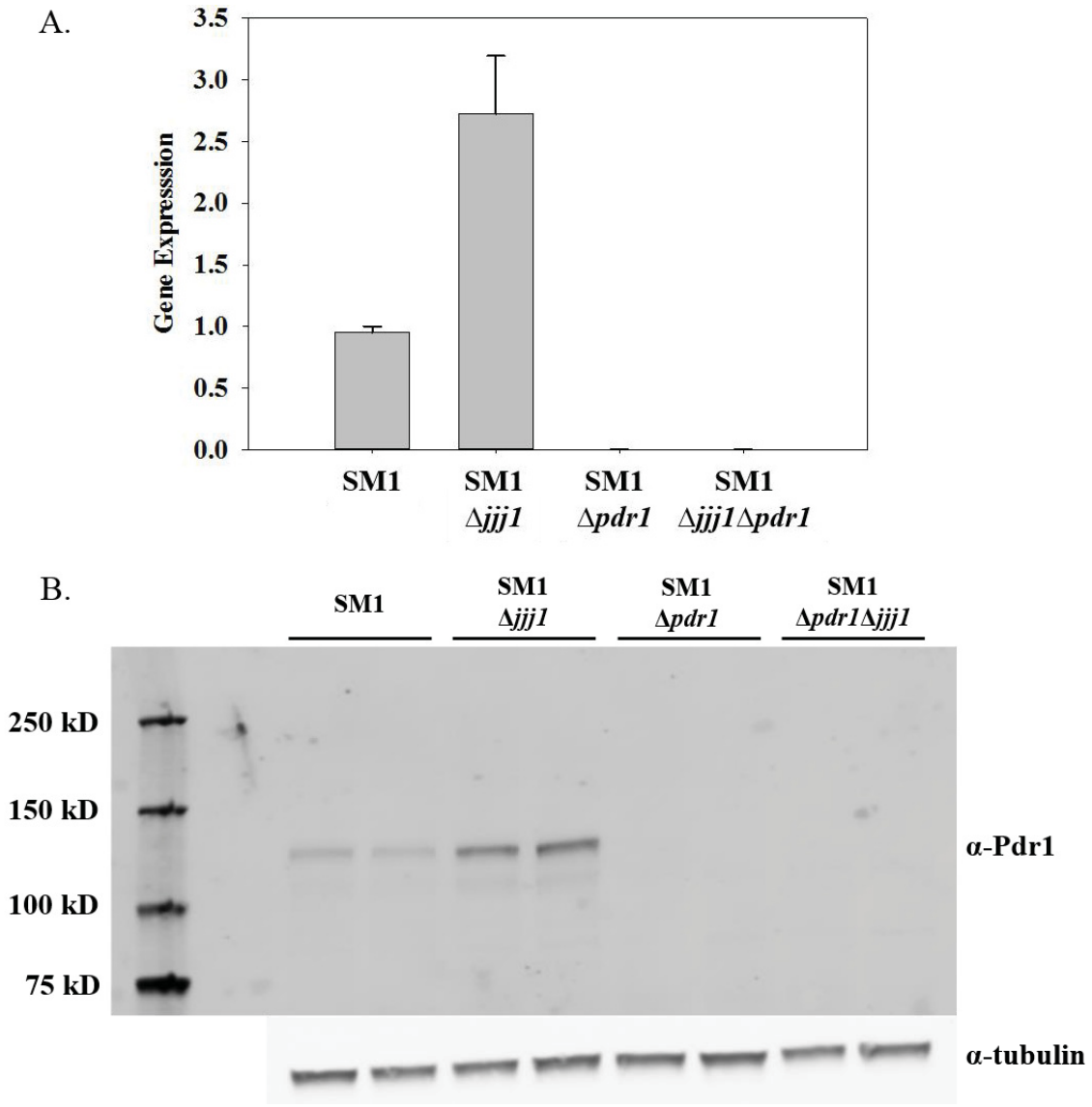

Figure 5-3. *JJJ1* deletion results in altered expression of *PDR1* at both transcript and protein levels.

(A) The effect of *JJJ1* and *PDR1* deletion alone and in combination on expression of the transcription factor *PDR1* was measured by qRT-PCR. Expression was normalized to 18S expression in the parent isolate SM1. (B) The effect of *JJJ1* and *PDR1* deletion alone and in combination on protein levels of the transcription factor Pdr1 was assessed by Western analysis. (Panel B contributed by W. Scott Moye-Rowley and Lucia Simonicova)

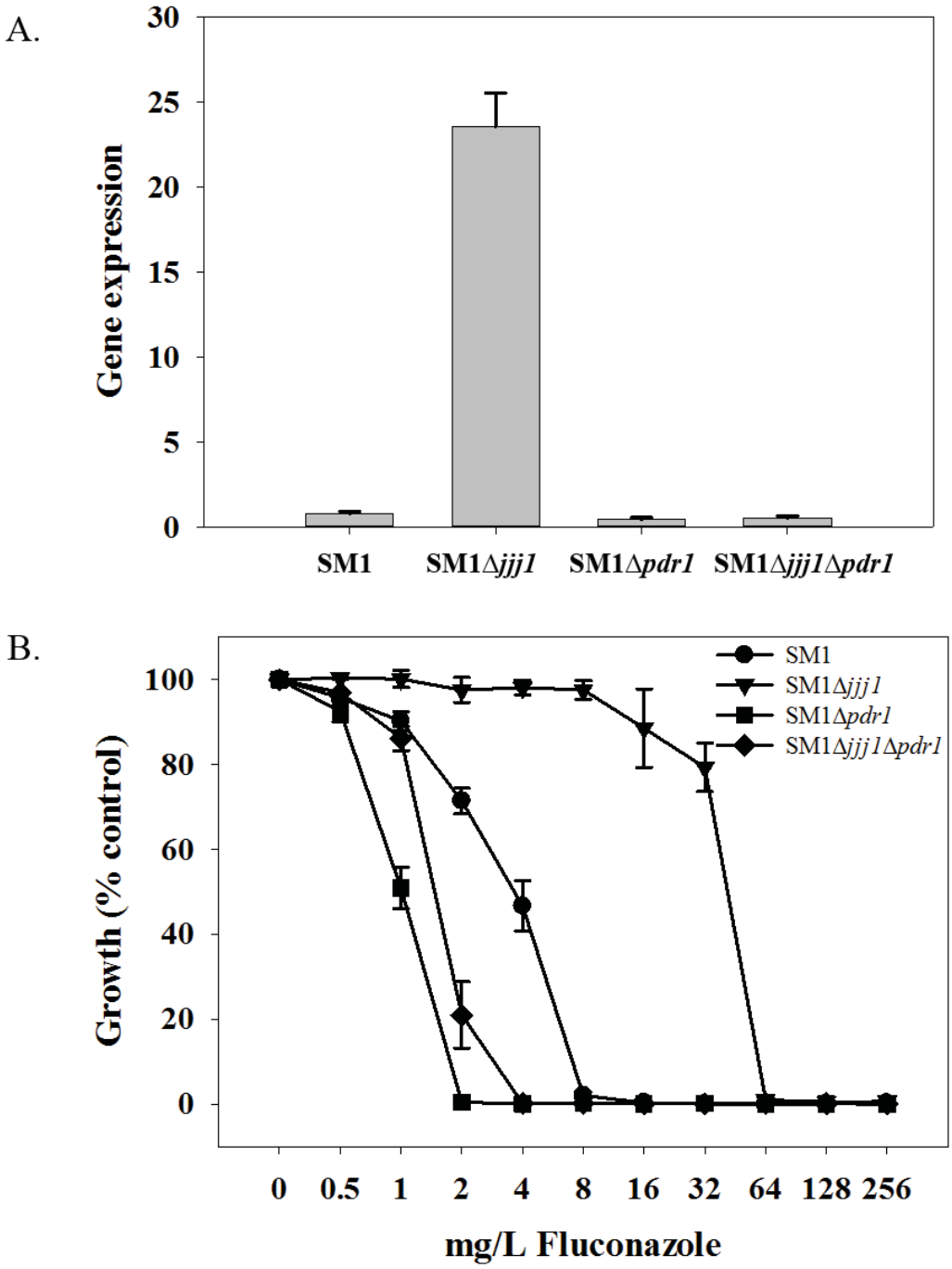

Figure 5-4. *JJJ1* influences fluconazole susceptibility in a *PDR1* dependent manner.

(A) The effect of *JJJ1* and *PDR1* deletion alone and in combination on expression of the ABC transporter *CDR1* was measured by qRT-PCR. Expression was normalized to 18S expression in the parent isolate SM1. (B) Strains were grown in 96 well plates according to standard CLSI methods with minor modifications and optical density at 600nm was measured after 48 hours.

PDR1. Of the eighty-five genes up-regulated in the absence of both *JJJ1* and *PDR1*, seven are involved in methionine biosynthesis (*MET6*, *MUP1*, *MET8*, *MET13*, *ScMET2*, *ScMXR1*, and *MET15*). Seventeen genes predicted to have a role in adhesion were observed to be up-regulated in the absence of *JJJ1*, four of which required *PDR1* (**Table B-3**).

DISCUSSION

Unlike other species of *Candida*, azole resistance in clinical isolates of *C. glabrata* is almost exclusively due to activating mutations in the gene encoding the transcription factor Pdr1 that lead to increased expression of the genes encoding the ATP binding cassette (ABC) transporters *CDR1*, *PDH1*, and *SNQ2*. Single amino acid substitutions in Pdr1 can result in its activation and the effects on expression of downstream target genes vary depending on the mutation (123, 124, 185). This lends itself to a hypothesis that Pdr1 is negatively regulated and that single amino acid changes interfere with the negative regulation resulting in altered gene expression. The varied patterns of gene expression seen with the different activating Pdr1 mutations would indicate there may exist more than one negative regulatory mechanism.

Regulation of Pdr1 in *C. glabrata* is not fully understood, but recent work in this area provides some insight. The transcription factor Stb5 has been shown to be a negative regulator of Pdr1. Deletion of *STB5* in a wild type background resulted in minimal decreased susceptibility, however in a Δ*pdr1* mutant strain deletion of *STB5* resulted in marked decreased susceptibility to the azoles. Overexpression of *STB5* increased azole susceptibility. In addition, the expression profile of the *STB5* deletion strain overlaps with that of a mutant strain overexpressing *PDR1* (175). In the closely related nonpathogenic yeast *Saccharomyces cerevisiae*, Stb5 forms a heterodimer with the transcription factor Pdr1 and binds the promoter of the ABC transporter *PDR5* directly (174). However, susceptibility to ketoconazole was not shown to be affected in an *S. cerevisiae STB5* deletion strain (248).

Pdr1 is also regulated at the level of transcription through the mediator complex. Deletion of *GAL11A*, which codes for a member of the mediator complex, results in decreased expression of the ABC transporter *PDH1* and increased azole sensitivity. A direct interaction between the Gal11a KIX domain and Pdr1 has been demonstrated (170). Pdr1 was shown to act as a xenobiotic receptor and bind ketoconazole directly. Gal11a is important for drug induced Pdr1 activation, however it is dispensable for Pdr1 activation in petite mutants (125). Pdr1 is also autoregulated through binding of the PDRE located in its promotor region (125, 126).

In *S. cerevisiae* two zinc finger transcription factors, Pdr1 and Pdr3, are responsible for regulation of the pleiotropic drug response. Understanding how this regulation occurs is informative for forming a model for regulation in *C. glabrata*, which has not been studied as thoroughly to date. Pdr1 and Pdr3 regulation occurs through similar, yet distinct pathways.

Pdr1 function in *S. cerevisiae* is regulated by the Hsp70/Hsp40 co chaperone pair Ssz1/Zuo1. Ssz1 and Zuo1 are part of a ribosome associated complex that is involved in folding of newly synthesized proteins (249), however this activity is distinct from that involved in regulation of Pdr1 and the multidrug resistant phenotype (250, 251). Ssz1 and Zuo1 are both able to activate Pdr1 independently of one another indicating that they are not acting as chaperones in this case (250). A region at the C terminus of Zuo1 has been shown to bind directly to Pdr1 similar to xenobiotic direct binding of Pdr1 (251). Overexpression of Ssz1 leads to an increase in Pdr1 target genes, and increases tolerance to cyclohexamide and oligomycin indicating that it acts as a positive regulator (252).

Pdr3 in *S. cerevisiae* is also regulated by an Hsp70, however in this case it appears to be a negative regulation. Overexpression of the Hsp70 gene, *SSA1* leads to increased sensitivity to cyclohexamide and decreased Pdr1 target gene expression (253). Previous work had shown Pdr3 is activated in mitochondrial deficient mutants (187). There is less Ssa1 associated with Pdr3 in these mutants indicating this regulatory pathway is involved in the altered drug susceptibility associated with mitochondrial insufficiency. Deletion of the nucleotide exchange factor Fes1, which is thought to inhibit Ssa1 activity also increased sensitivity to cyclohexamide, but no Hsp40 working in conjunction with the Hsp70, Ssa1 has been described (253).

The *C. glabrata* ORF CAGL0J07370g identified in our screen to affect fluconazole susceptibility has the characteristic J domain present in members of the Hsp40 class of proteins. The primary role for Hsp40 proteins attributed to the J domain is stimulation of adenosine triphosphate (ATP) hydrolysis through interaction of Hsp70 ATPase domains (254, 255). The closest homolog to CAGL0J07370g is *ScJJJ1* from *S. cerevisiae*, which shares 66.2% amino acid similarity and 51.2% identity as calculated with EMBOSS Needle (256). *ScJJJ1* and *ScZUO1* have the J domain in common, as well as another region thought to bind the ribosome, which is unique to these two genes among all Hsp40s in *S. cerevisiae* (257, 258). Importantly, deletion of *ScJJJ1* results in increased sensitivity to the azoles, which is the opposite effect from that observed upon deletion of CAGL0J07370g in *C. glabrata* (259).

The experiments described here demonstrate a role for *JJJ1* in fluconazole susceptibility in *C. glabrata*. Deletion of *JJJ1* in a susceptible dose dependent isolate results in fluconazole resistance. This altered susceptibility is primarily a result of *PDR1* dependent activation of *CDR1*. Based on what is known in the closely related species *S. cerevisiae* as well as what is known in *C. glabrata* we propose a model for the role of the Hsp40 Jjj1 in Pdr1 regulation. Post transcriptionally Pdr1 is negatively regulated by Jjj1 and may involve an Hsp70 a nucleotide exchange factor or both. When the Jjj1/Pdr1 interaction is disrupted Pdr1 is activated and able to upregulate a distinct set of target genes.

Our transcriptional profiling data supports this proposed mechanism. Chromatin immunoprecipitation combined with sequencing has been used to determine the direct binding targets of Pdr1 (126). Eight genes whose altered expression in the *JJJ1* mutant is

dependent on *PDR1* are direct Pdr1 targets six exhibited upregulation (*CDR1*, *YBT1*, *YOR1*, *RSB1*, *RTA1*, and *PDH1*) and two were downregulated (*ATF2* and *ScBAG7*). Only one known direct Pdr1 target, *NCE103*, showed altered expression that was independent of *PDR1* expression. Additional indirect Pdr1 targets identified by previously published microarray data are also among the genes upregulated in the *JJJ1* deletion strain in a *PDR1* dependent manner (*ScGPP1*, *ScCIS1*, *ScLAC1*, *ScMCP1*, *ScGUT2*, *ScPBI2*, *ScGSF2*, *GLK1*, and *ILV5*) (122, 124, 168, 185).

While the Pdr1 pathway appears to be primarily responsible for the altered gene expression in the *JJJ1* deletion strain there is a consistent one dilution change in MIC when *JJJ1* is deleted in strains lacking *CDR1* or *PDR1*. This finding allows for the possibility that there may be Pdr1 independent effects as well.

Among the genes upregulated in the *JJJ1* deletion strain that were independent of *PDR1* expression were many adhesion related genes. Five members of the *EPA* family were in this group. Three of these, *EPA1*, *EPA2*, and *EPA3* are part of a cluster of genes whose transcription is controlled by subtelomeric silencing (260, 261). Adhesins are known to be upregulated when nicotinic acid is limited (262), however, that does not appear to be happening in this experiment. None of the genes known to exhibit increased expression under nicotinic acid limited conditions, for example *TNA1*, *TNR1*, and *TNR2*, have increased expression. Of particular interest among the adhesin genes found to be upregulated, *EPA1* has a role in increased adhesion to epithelial cells in strains of *C. glabrata* with activating mutations in *PDR1* (184). *EPA1* has the putative PDRE site in its promoter (184), however Pdr1 does not bind tightly (126). *EPA1* along with many other adhesins were still upregulated in the mutant strain lacking *JJJ1* and *PDR1*. In addition to the *EPA* genes were *PWP1* and *PWP3*, which belong to adhesin cluster II. In total there are 17 genes predicted to have a role in adhesion among the upregulated genes in the *JJJ1* deletion strain, for 13 of these genes the increased expression is independent of Pdr1.

The experiments described here provide further insight into regulation of Pdr1 in the important fungal pathogen *C. glabrata*. Our data suggest that the J protein Jjj1 acts as a negative regulator of fluconazole resistance primarily through transcription factor Pdr1 and its target ABC transporter Cdr1.

CHAPTER 6. CONCLUSION

In the field of infectious disease fungal pathogens are often overlooked in discussions of difficult to treat infections. However, due to the increasing rates of patients with serious systemic fungal infections due to advances in medicine that have resulted in an increased population of immunocompromised patients and the increasing rates of resistance to available antifungals this is likely to change in the coming years. The current state of antifungal drug development, like all antibiotic drug development is worrisome. Emergence of multidrug resistant infecting fungal pathogens including multiple species of *Candida* is alarming when considering the lack of new drugs in development. The increasing threat of resistance has simply evolved more quickly than new drugs are being discovered and brought to market. One strategy to combat resistance in the race we are losing is to overcome resistance to current antifungals in order to reestablish their utility. In order to do that, we must first develop a thorough understanding of the mechanisms of resistance to current antifungals and then use that information to propose strategies to circumvent the resistance mechanisms. The focus of the work described here is resistance to the azole class of antifungals. While they are fungistatic, their side effect profile, dosage form options and affordability make them a desirable choice for treatment in most patient populations. The increasing rates of resistance to the azoles put them in danger of becoming obsolete.

While multiple mechanisms of azole resistance in *C. albicans* have been described, additional as yet unidentified contributors cannot be ruled out, as exhibited by the novel contributor to azole resistance described here. Admittedly the impact on resistance is minor, however *RTA3* represents one of likely multiple genes in the Tac1 regulon that contribute to resistance. Further characterization of these additional factors will better inform development of drug targeting strategies.

In *C. glabrata* clinical resistance to the azoles revolves around the transcription factor Pdr1 and the ABC transporters which it regulates. We were able to delineate the contributions of the relevant ABC transporters that had previously been shown to influence azole susceptibility. When all three are overexpressed the one that is most influential is *CDR1*, followed by *PDH1* and then *SNQ2*, both of which have a much smaller impact compared to *CDR1*. This establishes *CDR1* as the key to clinical azole resistance, which potentially simplifies the drug development strategy for overcoming resistance. If a small molecule could be targeted to block azole uptake by the pump coded for by *CDR1* alone or perhaps *CDR1* and *PDH1*, we would predict that majority of the clinical isolates of *C. glabrata* would again succumb to azole therapy. While this does strategy would be ineffective against isolates that do not overexpress *CDR1*, the literature reveals this would be a small percentage of the isolates currently recovered from patients and an assay to identify which susceptible isolates using a simple PCR based assay would be relatively easily developed an implemented.

Future directions for this work would include further characterization of the ABC transporters. The activating mutation in Pdr1 described here upregulates *CDR1*, *PDH1*,

and *SNQ2*. However, we know that there are many activating mutations and they do not all show the same patterns of expression for these three efflux pumps. Further characterization of representative mutations that result in alternative expression patterns, perhaps a mutation that only upregulates *SNQ2* or *PDH1* would provide important insight. In addition further characterization of what might be contributing to azole resistance other than the ABC transporters is necessary. Identification of alternative potential contributors, however minor they may be, will give us insight into strategies *C. glabrata* might utilize if we were able to prevent increased efflux.

Knowing that Pdr1 plays such a crucial role in azole resistance, it's regulation is another potential source for discovering small molecule targets that would allow for continued use of the azoles. We describe here a novel negative regulator of Pdr1, the J protein encoded by *JJJ1*. Deletion of *JJJ1* in *C. glabrata* results in decreased susceptibility to the azoles. While we can speculate on how Jjj1 is impacting susceptibility based on what is known about Pdr1 regulation in *S. cerevisiae*, we do not have a definitive answer. We do not know if Jjj1 interacts with Pdr1 directly or indirectly. The next steps would be to determine the exact mechanism involved, with the ultimate goal being to use that information to inform potential drug targeting. Our transcriptional profiling data also warrants a closer examination for additional genes affected by deletion of *JJJ1* that are contributing to altered azole susceptibility. Another important area of investigation is whether or not overexpression of *JJJ1* in a resistant isolate has any impact on azole susceptibility. In theory since deletion of *JJJ1* results in decreased susceptibility, depending on the mechanisms at play, overexpression could potentially enhance azole susceptibility.

While Pdr1 is the main player in clinical azole resistance, exploration of the Upc2A pathway for additional potential druggable targets shows promise. Previous work had identified Upc2A in *C. glabrata* as vital for sterol homeostasis. Upc2A is the transcriptional regulator that controls expression of multiple genes in the ergosterol biosynthesis pathway, which includes the drug target for the azoles. Deletion of *UPC2A* had previously been shown to result in enhanced azole activity in susceptible isolates of *C. glabrata*. In the work described here deletion of *UPC2A* in an azole-resistant clinical isolate was shown to decrease susceptibility to that of the parent clinical isolate.

In order to best exploit the Upc2 regulatory pathway we need to better understand which genes are important for the effect on azole resistance. We know that many genes in the ergosterol biosynthesis pathway are upregulated in response to treatment with azoles, but we do not know what other genes may be involved. Further exploration of how the alterations in the sterol biosynthesis pathway are affecting the fungistatic versus fungicidal property of the azoles is also of interest. When the Upc2 pathway is altered the sterol composition of the cell is altered and the enzymes necessary for cell survival change. Understanding these compensatory changes will allow targeting strategies that could force the production of toxic sterols instead of the altered sterol profile that produces the fungistatic effect.

Many questions remain unanswered with regard to *C. glabrata*. We do not fully understand why *C. glabrata*, which is so closely related to the benign yeast *S. cerevisiae* is pathogenic. The presence of adhesion genes that increase virulence has been implicated, but this remains largely a mystery. We also don't have a good understanding of why *C. glabrata* has high intrinsic resistance to the azoles. One could speculate this could be related to the structure of the drug target, which has not been characterized. The evolved mechanism of resistance to the azoles itself provides unanswered questions as well. One would predict the necessity for multiple resistance mechanisms, as seen in *C. albicans*, however the reality is that clinical resistance is very simply attributable to activating mutations in *PDR1*. All of these questions warrant further thought and investigation.

LIST OF REFERENCES

1. **Cleveland AA, Harrison LH, Farley MM, Hollick R, Stein B, Chiller TM, Lockhart SR, Park BJ.** 2015. Declining incidence of candidemia and the shifting epidemiology of Candida resistance in two US metropolitan areas, 2008-2013: results from population-based surveillance. PLoS One **10:**e0120452.
2. **Klingspor L, Tortorano AM, Peman J, Willinger B, Hamal P, Sendid B, Velegraki A, Kibbler C, Meis JF, Sabino R, Ruhnke M, Arikan-Akdagli S, Salonen J, Doczi I.** 2015. Invasive Candida infections in surgical patients in intensive care units: a prospective, multicentre survey initiated by the European Confederation of Medical Mycology (ECMM) (2006-2008). Clin Microbiol Infect **21:**87 e81-87 e10.
3. **Sharifzadeh A, Khosravi AR, Shokri H, Asadi Jamnani F, Hajiabdolbaghi M, Ashrafi Tamami I.** 2013. Oral microflora and their relation to risk factors in HIV+ patients with oropharyngeal candidiasis. J Mycol Med **23:**105-112.
4. **Sobel JD.** 2010. Changing trends in the epidemiology of Candida blood stream infections: a matter for concern? Crit Care Med **38:**990-992.
5. **Azie N, Neofytos D, Pfaller M, Meier-Kriesche HU, Quan SP, Horn D.** 2012. The PATH (Prospective Antifungal Therapy) Alliance(R) registry and invasive fungal infections: update 2012. Diagn Microbiol Infect Dis **73:**293-300.
6. **Pfaller MA, Jones RN, Castanheira M.** 2014. Regional data analysis of Candida non-albicans strains collected in United States medical sites over a 6-year period, 2006-2011. Mycoses **57:**602-611.
7. **Lortholary O, Renaudat C, Sitbon K, Madec Y, Denoeud-Ndam L, Wolff M, Fontanet A, Bretagne S, Dromer F, French Mycosis Study G.** 2014. Worrisome trends in incidence and mortality of candidemia in intensive care units (Paris area, 2002-2010). Intensive Care Med **40:**1303-1312.
8. **Milazzo L, Peri AM, Mazzali C, Grande R, Cazzani C, Ricaboni D, Castelli A, Raimondi F, Magni C, Galli M, Antinori S.** 2014. Candidaemia observed at a university hospital in Milan (northern Italy) and review of published studies from 2010 to 2014. Mycopathologia **178:**227-241.
9. **Pfaller MA, Diekema DJ, Gibbs DL, Newell VA, Ellis D, Tullio V, Rodloff A, Fu W, Ling TA, Global Antifungal Surveillance G.** 2010. Results from the ARTEMIS DISK Global Antifungal Surveillance Study, 1997 to 2007: a 10.5-year analysis of susceptibilities of Candida Species to fluconazole and voriconazole as determined by CLSI standardized disk diffusion. J Clin Microbiol **48:**1366-1377.
10. **Corsello S, Spinillo A, Osnengo G, Penna C, Guaschino S, Beltrame A, Blasi N, Festa A.** 2003. An epidemiological survey of vulvovaginal candidiasis in Italy. Eur J Obstet Gynecol Reprod Biol **110:**66-72.
11. **Holland J, Young ML, Lee O, S CAC.** 2003. Vulvovaginal carriage of yeasts other than Candida albicans. Sex Transm Infect **79:**249-250.
12. **Richter SS, Galask RP, Messer SA, Hollis RJ, Diekema DJ, Pfaller MA.** 2005. Antifungal susceptibilities of Candida species causing vulvovaginitis and epidemiology of recurrent cases. J Clin Microbiol **43:**2155-2162.

13. **Vermitsky JP, Self MJ, Chadwick SG, Trama JP, Adelson ME, Mordechai E, Gygax SE.** 2008. Survey of vaginal-flora Candida species isolates from women of different age groups by use of species-specific PCR detection. J Clin Microbiol **46:**1501-1503.
14. **Mahmoudi Rad M, Zafarghandi A, Amel Zabihi M, Tavallaee M, Mirdamadi Y.** 2012. Identification of Candida species associated with vulvovaginal candidiasis by multiplex PCR. Infect Dis Obstet Gynecol **2012:**872169.
15. **Sobel JD, Kauffman CA, McKinsey D, Zervos M, Vazquez JA, Karchmer AW, Lee J, Thomas C, Panzer H, Dismukes WE.** 2000. Candiduria: a randomized, double-blind study of treatment with fluconazole and placebo. The National Institute of Allergy and Infectious Diseases (NIAID) Mycoses Study Group. Clin Infect Dis **30:**19-24.
16. **Kauffman CA.** 2005. Candiduria. Clin Infect Dis **41 Suppl 6:**S371-376.
17. **Goswami D, Goswami R, Banerjee U, Dadhwal V, Miglani S, Lattif AA, Kochupillai N.** 2006. Pattern of Candida species isolated from patients with diabetes mellitus and vulvovaginal candidiasis and their response to single dose oral fluconazole therapy. J Infect **52:**111-117.
18. **Ray D, Goswami R, Banerjee U, Dadhwal V, Goswami D, Mandal P, Sreenivas V, Kochupillai N.** 2007. Prevalence of Candida glabrata and its response to boric acid vaginal suppositories in comparison with oral fluconazole in patients with diabetes and vulvovaginal candidiasis. Diabetes Care **30:**312-317.
19. **Hachem R, Hanna H, Kontoyiannis D, Jiang Y, Raad I.** 2008. The changing epidemiology of invasive candidiasis: Candida glabrata and Candida krusei as the leading causes of candidemia in hematologic malignancy. Cancer **112:**2493-2499.
20. **Abi-Said D, Anaissie E, Uzun O, Raad I, Pinzcowski H, Vartivarian S.** 1997. The epidemiology of hematogenous candidiasis caused by different Candida species. Clin Infect Dis **24:**1122-1128.
21. **Krcmery V, Jr., Mrazova M, Kunova A, Grey E, Mardiak J, Jurga L, Sabo A, Sufliarsky J, Sevcikova L, Sorkovska D, West D, Trupl J, Novotny J, Mateicka F.** 1999. Nosocomial candidaemias due to species other than Candida albicans in cancer patients. Aetiology, risk factors, and outcome of 45 episodes within 10 years in a single cancer institution. Support Care Cancer **7:**428-431.
22. **Weems JJ, Jr.** 1992. Candida parapsilosis: epidemiology, pathogenicity, clinical manifestations, and antimicrobial susceptibility. Clin Infect Dis **14:**756-766.
23. **Garzoni C, Nobre VA, Garbino J.** 2007. Candida parapsilosis endocarditis: a comparative review of the literature. Eur J Clin Microbiol Infect Dis **26:**915-926.
24. **Kothari A, Sagar V.** 2009. Epidemiology of candida bloodstream infections in a tertiary care institute in India. Indian J Med Microbiol **27:**171-172.
25. **Weinberger M, Leibovici L, Perez S, Samra Z, Ostfeld I, Levi I, Bash E, Turner D, Goldschmied-Reouven A, Regev-Yochay G, Pitlik SD, Keller N.** 2005. Characteristics of candidaemia with Candida-albicans compared with non-albicans Candida species and predictors of mortality. J Hosp Infect **61:**146-154.
26. **Nucci M, Colombo AL.** 2007. Candidemia due to Candida tropicalis: clinical, epidemiologic, and microbiologic characteristics of 188 episodes occurring in tertiary care hospitals. Diagn Microbiol Infect Dis **58:**77-82.

27. **Tang HJ, Liu WL, Lin HL, Lai CC.** 2014. Epidemiology and prognostic factors of candidemia in cancer patients. PLoS One **9:**e99103.
28. **Tang JL, Kung HC, Lei WC, Yao M, Wu UI, Hsu SC, Lin CT, Li CC, Wu SJ, Hou HA, Chou WC, Huang SY, Tsay W, Chen YC, Chen YC, Chang SC, Ko BS, Tien HF.** 2015. High Incidences of Invasive Fungal Infections in Acute Myeloid Leukemia Patients Receiving Induction Chemotherapy without Systemic Antifungal Prophylaxis: A Prospective Observational Study in Taiwan. PLoS One **10:**e0128410.
29. **Cornely OA, Gachot B, Akan H, Bassetti M, Uzun O, Kibbler C, Marchetti O, de Burghgraeve P, Ramadan S, Pylkkanen L, Ameye L, Paesmans M, Donnelly JP, Group EID.** 2015. Epidemiology and outcome of fungemia in a cancer Cohort of the Infectious Diseases Group (IDG) of the European Organization for Research and Treatment of Cancer (EORTC 65031). Clin Infect Dis **61:**324-331.
30. **Morii D, Seki M, Binongo JN, Ban R, Kobayashi A, Sata M, Hashimoto S, Shimizu J, Morita S, Tomono K.** 2014. Distribution of Candida species isolated from blood cultures in hospitals in Osaka, Japan. J Infect Chemother **20:**558-562.
31. **Wang E, Farmakiotis D, Yang D, McCue DA, Kantarjian HM, Kontoyiannis DP, Mathisen MS.** 2015. The ever-evolving landscape of candidaemia in patients with acute leukaemia: non-susceptibility to caspofungin and multidrug resistance are associated with increased mortality. J Antimicrob Chemother **70:**2362-2368.
32. **Pfaller MA, Andes DR, Diekema DJ, Horn DL, Reboli AC, Rotstein C, Franks B, Azie NE.** 2014. Epidemiology and outcomes of invasive candidiasis due to non-albicans species of Candida in 2,496 patients: data from the Prospective Antifungal Therapy (PATH) registry 2004-2008. PLoS One **9:**e101510.
33. **Merz WG, Karp JE, Schron D, Saral R.** 1986. Increased incidence of fungemia caused by Candida krusei. J Clin Microbiol **24:**581-584.
34. **Wingard JR, Merz WG, Rinaldi MG, Johnson TR, Karp JE, Saral R.** 1991. Increase in Candida krusei infection among patients with bone marrow transplantation and neutropenia treated prophylactically with fluconazole. N Engl J Med **325:**1274-1277.
35. **Pfaller MA, Diekema DJ, Gibbs DL, Newell VA, Nagy E, Dobiasova S, Rinaldi M, Barton R, Veselov A, Global Antifungal Surveillance G.** 2008. Candida krusei, a multidrug-resistant opportunistic fungal pathogen: geographic and temporal trends from the ARTEMIS DISK Antifungal Surveillance Program, 2001 to 2005. J Clin Microbiol **46:**515-521.
36. **Whaley SG, Berkow EL, Rybak JM, Nishimoto AT, Barker KS, Rogers PD.** 2016. Azole Antifungal Resistance in Candida albicans and Emerging Non-albicans Candida Species. Front Microbiol **7:**2173.
37. **Pfaller MA, Diekema DJ.** 2012. Progress in antifungal susceptibility testing of Candida spp. by use of Clinical and Laboratory Standards Institute broth microdilution methods, 2010 to 2012. J Clin Microbiol **50:**2846-2856.
38. **Pfaller MA, Messer SA, Woosley LN, Jones RN, Castanheira M.** 2013. Echinocandin and Triazole Antifungal Susceptibility Profiles for Clinical Opportunistic Yeast and Mold Isolates Collected from 2010 to 2011: Application

of New CLSI Clinical Breakpoints and Epidemiological Cutoff Values for Characterization of Geographic and Temporal Trends of Antifungal Resistance. J Clin Microbiol **51:**2571-2581.

39. **Pappas PG, Kauffman CA, Andes DR, Clancy CJ, Marr KA, Ostrosky-Zeichner L, Reboli AC, Schuster MG, Vazquez JA, Walsh TJ, Zaoutis TE, Sobel JD.** 2016. Clinical Practice Guideline for the Management of Candidiasis: 2016 Update by the Infectious Diseases Society of America. Clin Infect Dis **62:**e1-e50.
40. **Oxman DA, Chow JK, Frendl G, Hadley S, Hershkovitz S, Ireland P, McDermott LA, Tsai K, Marty FM, Kontoyiannis DP, Golan Y.** 2010. Candidaemia associated with decreased in vitro fluconazole susceptibility: is Candida speciation predictive of the susceptibility pattern? J Antimicrob Chemother **65:**1460-1465.
41. **Lortholary O, Desnos-Ollivier M, Sitbon K, Fontanet A, Bretagne S, Dromer F, French Mycosis Study G.** 2011. Recent exposure to caspofungin or fluconazole influences the epidemiology of candidemia: a prospective multicenter study involving 2,441 patients. Antimicrob Agents Chemother **55:**532-538.
42. **Fothergill AW, Sutton DA, McCarthy DI, Wiederhold NP.** 2014. Impact of new antifungal breakpoints on antifungal resistance in Candida species. J Clin Microbiol **52:**994-997.
43. **Diekema D, Arbefeville S, Boyken L, Kroeger J, Pfaller M.** 2012. The changing epidemiology of healthcare-associated candidemia over three decades. Diagn Microbiol Infect Dis **73:**45-48.
44. **Pfaller MA, Rhomberg PR, Messer SA, Jones RN, Castanheira M.** 2015. Isavuconazole, micafungin, and 8 comparator antifungal agents' susceptibility profiles for common and uncommon opportunistic fungi collected in 2013: temporal analysis of antifungal drug resistance using CLSI species-specific clinical breakpoints and proposed epidemiological cutoff values. Diagn Microbiol Infect Dis **82:**303-313.
45. **Ying Y, Zhang J, Huang SB, Liu FD, Liu JH, Zhang J, Hu XF, Zhang ZQ, Liu X, Huang XT.** 2015. Fluconazole susceptibility of 3,056 clinical isolates of Candida species from 2005 to 2009 in a tertiary-care hospital. Indian J Med Microbiol **33:**413-415.
46. **Enwuru CA, Ogunledun A, Idika N, Enwuru NV, Ogbonna F, Aniedobe M, Adeiga A.** 2008. Fluconazole resistant opportunistic oro-pharyngeal Candida and non-Candida yeast-like isolates from HIV infected patients attending ARV clinics in Lagos, Nigeria. Afr Health Sci **8:**142-148.
47. **Berberi A, Noujeim Z, Aoun G.** 2015. Epidemiology of Oropharyngeal Candidiasis in Human Immunodeficiency Virus/Acquired Immune Deficiency Syndrome Patients and CD4+ Counts. J Int Oral Health **7:**20-23.
48. **Castanheira M, Messer SA, Rhomberg PR, Dietrich RR, Jones RN, Pfaller MA.** 2014. Isavuconazole and nine comparator antifungal susceptibility profiles for common and uncommon Candida species collected in 2012: application of new CLSI clinical breakpoints and epidemiological cutoff values. Mycopathologia **178:**1-9.

49. **Fidel PL, Jr., Vazquez JA, Sobel JD.** 1999. Candida glabrata: review of epidemiology, pathogenesis, and clinical disease with comparison to C. albicans. Clin Microbiol Rev **12:**80-96.
50. **Lee I, Fishman NO, Zaoutis TE, Morales KH, Weiner MG, Synnestvedt M, Nachamkin I, Lautenbach E.** 2009. Risk factors for fluconazole-resistant Candida glabrata bloodstream infections. Arch Intern Med **169:**379-383.
51. **Bennett JE, Izumikawa K, Marr KA.** 2004. Mechanism of increased fluconazole resistance in Candida glabrata during prophylaxis. Antimicrob Agents Chemother **48:**1773-1777.
52. **Imhof A, Balajee SA, Fredricks DN, Englund JA, Marr KA.** 2004. Breakthrough fungal infections in stem cell transplant recipients receiving voriconazole. Clin Infect Dis **39:**743-746.
53. **Manzano-Gayosso P, Hernandez-Hernandez F, Mendez-Tovar LJ, Gonzalez-Monroy J, Lopez-Martinez R.** 2003. Fungal peritonitis in 15 patients on continuous ambulatory peritoneal dialysis (CAPD). Mycoses **46:**425-429.
54. **Chapeland-Leclerc F, Hennequin C, Papon N, Noel T, Girard A, Socie G, Ribaud P, Lacroix C.** 2010. Acquisition of flucytosine, azole, and caspofungin resistance in Candida glabrata bloodstream isolates serially obtained from a hematopoietic stem cell transplant recipient. Antimicrob Agents Chemother **54:**1360-1362.
55. **Hull CM, Parker JE, Bader O, Weig M, Gross U, Warrilow AG, Kelly DE, Kelly SL.** 2012. Facultative sterol uptake in an ergosterol-deficient clinical isolate of Candida glabrata harboring a missense mutation in ERG11 and exhibiting cross-resistance to azoles and amphotericin B. Antimicrob Agents Chemother **56:**4223-4232.
56. **Pfaller MA, Castanheira M, Lockhart SR, Ahlquist AM, Messer SA, Jones RN.** 2012. Frequency of decreased susceptibility and resistance to echinocandins among fluconazole-resistant bloodstream isolates of Candida glabrata. J Clin Microbiol **50:**1199-1203.
57. **Cho EJ, Shin JH, Kim SH, Kim HK, Park JS, Sung H, Kim MN, Im HJ.** 2015. Emergence of multiple resistance profiles involving azoles, echinocandins and amphotericin B in Candida glabrata isolates from a neutropenia patient with prolonged fungaemia. J Antimicrob Chemother **70:**1268-1270.
58. **Yang YL, Ho YA, Cheng HH, Ho M, Lo HJ.** 2004. Susceptibilities of Candida species to amphotericin B and fluconazole: the emergence of fluconazole resistance in Candida tropicalis. Infect Control Hosp Epidemiol **25:**60-64.
59. **Yang YL, Wang AH, Wang CW, Cheng WT, Li SY, Lo HJ, Hospitals T.** 2008. Susceptibilities to amphotericin B and fluconazole of Candida species in Taiwan Surveillance of Antimicrobial Resistance of Yeasts 2006. Diagn Microbiol Infect Dis **61:**175-180.
60. **Yoo JI, Choi CW, Lee KM, Kim YK, Kim TU, Kim EC, Joo SI, Yun SH, Lee YS, Kim BS.** 2009. National surveillance of antifungal susceptibility of Candida species in South Korean hospitals. Med Mycol **47:**554-558.
61. **Chen KH, Chang CT, Yu CC, Huang JY, Yang CW, Hung CC.** 2006. Candida parapsilosis peritonitis has more complications than other Candida peritonitis in peritoneal dialysis patients. Ren Fail **28:**241-246.

62. **Marti-Carrizosa M, Sanchez-Reus F, March F, Coll P.** 2014. Fungemia in a Spanish hospital: the role of Candida parapsilosis over a 15-year period. Scand J Infect Dis **46:**454-461.
63. **Hope W, Morton A, Eisen DP.** 2002. Increase in prevalence of nosocomial non-Candida albicans candidaemia and the association of Candida krusei with fluconazole use. J Hosp Infect **50:**56-65.
64. **Lin MY, Carmeli Y, Zumsteg J, Flores EL, Tolentino J, Sreeramoju P, Weber SG.** 2005. Prior antimicrobial therapy and risk for hospital-acquired Candida glabrata and Candida krusei fungemia: a case-case-control study. Antimicrob Agents Chemother **49:**4555-4560.
65. **Blot S, Janssens R, Claeys G, Hoste E, Buyle F, De Waele JJ, Peleman R, Vogelaers D, Vandewoude K.** 2006. Effect of fluconazole consumption on long-term trends in candidal ecology. J Antimicrob Chemother **58:**474-477.
66. **Gong X, Luan T, Wu X, Li G, Qiu H, Kang Y, Qin B, Fang Q, Cui W, Qin Y, Li J, Zang B.** 2016. Invasive candidiasis in intensive care units in China: Risk factors and prognoses of Candida albicans and non-albicans Candida infections. Am J Infect Control **44:**e59-63.
67. **Marichal P, Koymans L, Willemsens S, Bellens D, Verhasselt P, Luyten W, Borgers M, Ramaekers FC, Odds FC, Bossche HV.** 1999. Contribution of mutations in the cytochrome P450 14alpha-demethylase (Erg11p, Cyp51p) to azole resistance in Candida albicans. Microbiology **145 (Pt 10):**2701-2713.
68. **Flowers SA, Colon B, Whaley SG, Schuler MA, Rogers PD.** 2015. Contribution of clinically derived mutations in ERG11 to azole resistance in Candida albicans. Antimicrob Agents Chemother **59:**450-460.
69. **Xiang MJ, Liu JY, Ni PH, Wang S, Shi C, Wei B, Ni YX, Ge HL.** 2013. Erg11 mutations associated with azole resistance in clinical isolates of Candida albicans. FEMS Yeast Res **13:**386-393.
70. **MacPherson S, Akache B, Weber S, De Deken X, Raymond M, Turcotte B.** 2005. Candida albicans zinc cluster protein Upc2p confers resistance to antifungal drugs and is an activator of ergosterol biosynthetic genes. Antimicrob Agents Chemother **49:**1745-1752.
71. **Dunkel N, Liu TT, Barker KS, Homayouni R, Morschhauser J, Rogers PD.** 2008. A gain-of-function mutation in the transcription factor Upc2p causes upregulation of ergosterol biosynthesis genes and increased fluconazole resistance in a clinical Candida albicans isolate. Eukaryot Cell **7:**1180-1190.
72. **Heilmann CJ, Schneider S, Barker KS, Rogers PD, Morschhauser J.** 2010. An A643T mutation in the transcription factor Upc2p causes constitutive ERG11 upregulation and increased fluconazole resistance in Candida albicans. Antimicrob Agents Chemother **54:**353-359.
73. **Hoot SJ, Smith AR, Brown RP, White TC.** 2011. An A643V amino acid substitution in Upc2p contributes to azole resistance in well-characterized clinical isolates of Candida albicans. Antimicrob Agents Chemother **55:**940-942.
74. **Flowers SA, Barker KS, Berkow EL, Toner G, Chadwick SG, Gygax SE, Morschhauser J, Rogers PD.** 2012. Gain-of-function mutations in UPC2 are a frequent cause of ERG11 upregulation in azole-resistant clinical isolates of Candida albicans. Eukaryot Cell **11:**1289-1299.

75. **Coste AT, Karababa M, Ischer F, Bille J, Sanglard D.** 2004. TAC1, transcriptional activator of CDR genes, is a new transcription factor involved in the regulation of Candida albicans ABC transporters CDR1 and CDR2. Eukaryot Cell **3:**1639-1652.
76. **Liu TT, Znaidi S, Barker KS, Xu L, Homayouni R, Saidane S, Morschhauser J, Nantel A, Raymond M, Rogers PD.** 2007. Genome-wide expression and location analyses of the Candida albicans Tac1p regulon. Eukaryot Cell **6:**2122-2138.
77. **Coste A, Selmecki A, Forche A, Diogo D, Bougnoux ME, d'Enfert C, Berman J, Sanglard D.** 2007. Genotypic evolution of azole resistance mechanisms in sequential Candida albicans isolates. Eukaryot Cell **6:**1889-1904.
78. **Coste A, Turner V, Ischer F, Morschhauser J, Forche A, Selmecki A, Berman J, Bille J, Sanglard D.** 2006. A mutation in Tac1p, a transcription factor regulating CDR1 and CDR2, is coupled with loss of heterozygosity at chromosome 5 to mediate antifungal resistance in Candida albicans. Genetics **172:**2139-2156.
79. **Selmecki A, Gerami-Nejad M, Paulson C, Forche A, Berman J.** 2008. An isochromosome confers drug resistance in vivo by amplification of two genes, ERG11 and TAC1. Mol Microbiol **68:**624-641.
80. **Alarco AM, Raymond M.** 1999. The bZip transcription factor Cap1p is involved in multidrug resistance and oxidative stress response in Candida albicans. J Bacteriol **181:**700-708.
81. **Morschhauser J, Barker KS, Liu TT, Bla BWJ, Homayouni R, Rogers PD.** 2007. The transcription factor Mrr1p controls expression of the MDR1 efflux pump and mediates multidrug resistance in Candida albicans. PLoS Pathog **3:**e164.
82. **Dunkel N, Blass J, Rogers PD, Morschhauser J.** 2008. Mutations in the multi-drug resistance regulator MRR1, followed by loss of heterozygosity, are the main cause of MDR1 overexpression in fluconazole-resistant Candida albicans strains. Mol Microbiol **69:**827-840.
83. **Kelly SL, Lamb DC, Kelly DE.** 1997. Sterol 22-desaturase, cytochrome P45061, possesses activity in xenobiotic metabolism. FEBS Lett **412:**233-235.
84. **Nolte FS, Parkinson T, Falconer DJ, Dix S, Williams J, Gilmore C, Geller R, Wingard JR.** 1997. Isolation and characterization of fluconazole- and amphotericin B-resistant Candida albicans from blood of two patients with leukemia. Antimicrob Agents Chemother **41:**196-199.
85. **Miyazaki Y, Geber A, Miyazaki H, Falconer D, Parkinson T, Hitchcock C, Grimberg B, Nyswaner K, Bennett JE.** 1999. Cloning, sequencing, expression and allelic sequence diversity of ERG3 (C-5 sterol desaturase gene) in Candida albicans. Gene **236:**43-51.
86. **Chau AS, Gurnani M, Hawkinson R, Laverdiere M, Cacciapuoti A, McNicholas PM.** 2005. Inactivation of sterol Delta5,6-desaturase attenuates virulence in Candida albicans. Antimicrob Agents Chemother **49:**3646-3651.
87. **Martel CM, Parker JE, Bader O, Weig M, Gross U, Warrilow AG, Rolley N, Kelly DE, Kelly SL.** 2010. Identification and characterization of four azole-

resistant erg3 mutants of Candida albicans. Antimicrob Agents Chemother **54:**4527-4533.

88. **Morio F, Pagniez F, Lacroix C, Miegeville M, Le Pape P.** 2012. Amino acid substitutions in the Candida albicans sterol Delta5,6-desaturase (Erg3p) confer azole resistance: characterization of two novel mutants with impaired virulence. J Antimicrob Chemother **67:**2131-2138.
89. **Selmecki A, Forche A, Berman J.** 2006. Aneuploidy and isochromosome formation in drug-resistant Candida albicans. Science **313:**367-370.
90. **Zhang L, Xiao M, Watts MR, Wang H, Fan X, Kong F, Xu YC.** 2015. Development of fluconazole resistance in a series of Candida parapsilosis isolates from a persistent candidemia patient with prolonged antifungal therapy. BMC Infect Dis **15:**340.
91. **Souza AC, Fuchs BB, Pinhati HM, Siqueira RA, Hagen F, Meis JF, Mylonakis E, Colombo AL.** 2015. Candida parapsilosis Resistance to Fluconazole: Molecular Mechanisms and In Vivo Impact in Infected Galleria mellonella Larvae. Antimicrob Agents Chemother **59:**6581-6587.
92. **Grossman NT, Pham CD, Cleveland AA, Lockhart SR.** 2015. Molecular mechanisms of fluconazole resistance in Candida parapsilosis isolates from a U.S. surveillance system. Antimicrob Agents Chemother **59:**1030-1037.
93. **Silva AP, Miranda IM, Guida A, Synnott J, Rocha R, Silva R, Amorim A, Pina-Vaz C, Butler G, Rodrigues AG.** 2011. Transcriptional profiling of azole-resistant Candida parapsilosis strains. Antimicrob Agents Chemother **55:**3546-3556.
94. **Branco J, Silva AP, Silva RM, Silva-Dias A, Pina-Vaz C, Butler G, Rodrigues AG, Miranda IM.** 2015. Fluconazole and Voriconazole Resistance in Candida parapsilosis Is Conferred by Gain-of-Function Mutations in MRR1 Transcription Factor Gene. Antimicrob Agents Chemother **59:**6629-6633.
95. **Berkow EL, Manigaba K, Parker JE, Barker KS, Kelly SL, Rogers PD.** 2015. Multidrug Transporters and Alterations in Sterol Biosynthesis Contribute to Azole Antifungal Resistance in Candida parapsilosis. Antimicrob Agents Chemother **59:**5942-5950.
96. **Jiang C, Dong D, Yu B, Cai G, Wang X, Ji Y, Peng Y.** 2013. Mechanisms of azole resistance in 52 clinical isolates of Candida tropicalis in China. J Antimicrob Chemother **68:**778-785.
97. **Choi MJ, Won EJ, Shin JH, Kim SH, Lee WG, Kim MN, Lee K, Shin MG, Suh SP, Ryang DW, Im YJ.** 2016. Resistance Mechanisms and Clinical Features of Fluconazole-Nonsusceptible Candida tropicalis Isolates Compared with Fluconazole-Less-Susceptible Isolates. Antimicrob Agents Chemother **60:**3653-3661.
98. **Vandeputte P, Larcher G, Berges T, Renier G, Chabasse D, Bouchara JP.** 2005. Mechanisms of azole resistance in a clinical isolate of Candida tropicalis. Antimicrob Agents Chemother **49:**4608-4615.
99. **Eddouzi J, Parker JE, Vale-Silva LA, Coste A, Ischer F, Kelly S, Manai M, Sanglard D.** 2013. Molecular mechanisms of drug resistance in clinical Candida species isolated from Tunisian hospitals. Antimicrob Agents Chemother **57:**3182-3193.

100. **Tan J, Zhang J, Chen W, Sun Y, Wan Z, Li R, Liu W.** 2015. The A395T mutation in ERG11 gene confers fluconazole resistance in Candida tropicalis causing candidemia. Mycopathologia **179:**213-218.
101. **Barchiesi F, Calabrese D, Sanglard D, Falconi Di Francesco L, Caselli F, Giannini D, Giacometti A, Gavaudan S, Scalise G.** 2000. Experimental induction of fluconazole resistance in Candida tropicalis ATCC 750. Antimicrob Agents Chemother **44:**1578-1584.
102. **Marichal P, Gorrens J, Coene MC, Le Jeune L, Vanden Bossche H.** 1995. Origin of differences in susceptibility of Candida krusei to azole antifungal agents. Mycoses **38:**111-117.
103. **Katiyar SK, Edlind TD.** 2001. Identification and expression of multidrug resistance-related ABC transporter genes in Candida krusei. Med Mycol **39:**109-116.
104. **Lamping E, Ranchod A, Nakamura K, Tyndall JD, Niimi K, Holmes AR, Niimi M, Cannon RD.** 2009. Abc1p is a multidrug efflux transporter that tips the balance in favor of innate azole resistance in Candida krusei. Antimicrob Agents Chemother **53:**354-369.
105. **Venkateswarlu K, Denning DW, Kelly SL.** 1997. Inhibition and interaction of cytochrome P450 of Candida krusei with azole antifungal drugs. J Med Vet Mycol **35:**19-25.
106. **Orozco AS, Higginbotham LM, Hitchcock CA, Parkinson T, Falconer D, Ibrahim AS, Ghannoum MA, Filler SG.** 1998. Mechanism of fluconazole resistance in Candida krusei. Antimicrob Agents Chemother **42:**2645-2649.
107. **Guinea J, Sanchez-Somolinos M, Cuevas O, Pelaez T, Bouza E.** 2006. Fluconazole resistance mechanisms in Candida krusei: the contribution of efflux-pumps. Med Mycol **44:**575-578.
108. **Mansfield BE, Oltean HN, Oliver BG, Hoot SJ, Leyde SE, Hedstrom L, White TC.** 2010. Azole drugs are imported by facilitated diffusion in Candida albicans and other pathogenic fungi. PLoS Pathog **6:**e1001126.
109. **Kolaczkowska A, Kolaczkowski M.** 2016. Drug resistance mechanisms and their regulation in non-albicans Candida species. J Antimicrob Chemother **71:**1438-1450.
110. **Venkateswarlu K, Denning DW, Manning NJ, Kelly SL.** 1996. Reduced accumulation of drug in Candida krusei accounts for itraconazole resistance. Antimicrob Agents Chemother **40:**2443-2446.
111. **Tavakoli M, Zaini F, Kordbacheh M, Safara M, Raoofian R, Heidari M.** 2010. Upregulation of the ERG11 gene in Candida krusei by azoles. Daru **18:**276-280.
112. **He X, Zhao M, Chen J, Wu R, Zhang J, Cui R, Jiang Y, Chen J, Cao X, Xing Y, Zhang Y, Meng J, Deng Q, Sui T.** 2015. Overexpression of Both ERG11 and ABC2 Genes Might Be Responsible for Itraconazole Resistance in Clinical Isolates of Candida krusei. PLoS One **10:**e0136185.
113. **Rubio MC, de Ocariz IR, Gil J, Benito R, Rezusta A.** 2005. Potential fungicidal effect of voriconazole against Candida spp. Int J Antimicrob Agents **25:**264-267.

114. **Ricardo E, Miranda IM, Faria-Ramos I, Silva RM, Rodrigues AG, Pina-Vaz C.** 2014. In vivo and in vitro acquisition of resistance to voriconazole by Candida krusei. Antimicrob Agents Chemother **58:**4604-4611.
115. **Silva DB, Rodrigues LM, Almeida AA, Oliveira KM, Grisolia AB.** 2016. Novel point mutations in the ERG11 gene in clinical isolates of azole resistant Candida species. Mem Inst Oswaldo Cruz **111:**192-199.
116. **Lee JK, Peters D, Obias AA, Noskin GA, Peterson LR.** 2000. Activity of voriconazole against Candida albicans and Candida krusei isolated since 1984. Int J Antimicrob Agents **16:**205-209.
117. **Rybak JM, Marx KR, Nishimoto AT, Rogers PD.** 2015. Isavuconazole: Pharmacology, Pharmacodynamics, and Current Clinical Experience with a New Triazole Antifungal Agent. Pharmacotherapy **35:**1037-1051.
118. **Espinel-Ingroff A, Pfaller MA, Bustamante B, Canton E, Fothergill A, Fuller J, Gonzalez GM, Lass-Florl C, Lockhart SR, Martin-Mazuelos E, Meis JF, Melhem MS, Ostrosky-Zeichner L, Pelaez T, Szeszs MW, St-Germain G, Bonfietti LX, Guarro J, Turnidge J.** 2014. Multilaboratory study of epidemiological cutoff values for detection of resistance in eight Candida species to fluconazole, posaconazole, and voriconazole. Antimicrob Agents Chemother **58:**2006-2012.
119. **Vermitsky JP, Edlind TD.** 2004. Azole resistance in Candida glabrata: coordinate upregulation of multidrug transporters and evidence for a Pdr1-like transcription factor. Antimicrob Agents Chemother **48:**3773-3781.
120. **Healey KR, Zhao Y, Perez WB, Lockhart SR, Sobel JD, Farmakiotis D, Kontoyiannis DP, Sanglard D, Taj-Aldeen SJ, Alexander BD, Jimenez-Ortigosa C, Shor E, Perlin DS.** 2016. Prevalent mutator genotype identified in fungal pathogen Candida glabrata promotes multi-drug resistance. Nat Commun **7:**11128.
121. **Tsai HF, Krol AA, Sarti KE, Bennett JE.** 2006. Candida glabrata PDR1, a transcriptional regulator of a pleiotropic drug resistance network, mediates azole resistance in clinical isolates and petite mutants. Antimicrob Agents Chemother **50:**1384-1392.
122. **Tsai HF, Sammons LR, Zhang X, Suffis SD, Su Q, Myers TG, Marr KA, Bennett JE.** 2010. Microarray and molecular analyses of the azole resistance mechanism in Candida glabrata oropharyngeal isolates. Antimicrob Agents Chemother **54:**3308-3317.
123. **Ferrari S, Ischer F, Calabrese D, Posteraro B, Sanguinetti M, Fadda G, Rohde B, Bauser C, Bader O, Sanglard D.** 2009. Gain of function mutations in CgPDR1 of Candida glabrata not only mediate antifungal resistance but also enhance virulence. PLoS Pathog **5:**e1000268.
124. **Caudle KE, Barker KS, Wiederhold NP, Xu L, Homayouni R, Rogers PD.** 2011. Genomewide expression profile analysis of the Candida glabrata Pdr1 regulon. Eukaryot Cell **10:**373-383.
125. **Paul S, Schmidt JA, Moye-Rowley WS.** 2011. Regulation of the CgPdr1 transcription factor from the pathogen Candida glabrata. Eukaryot Cell **10:**187-197.

126. **Paul S, Bair TB, Moye-Rowley WS.** 2014. Identification of genomic binding sites for Candida glabrata Pdr1 transcription factor in wild-type and rho0 cells. Antimicrob Agents Chemother **58:**6904-6912.
127. **Sanglard D, Ischer F, Calabrese D, Majcherczyk PA, Bille J.** 1999. The ATP binding cassette transporter gene CgCDR1 from Candida glabrata is involved in the resistance of clinical isolates to azole antifungal agents. Antimicrob Agents Chemother **43:**2753-2765.
128. **Miyazaki H, Miyazaki Y, Geber A, Parkinson T, Hitchcock C, Falconer DJ, Ward DJ, Marsden K, Bennett JE.** 1998. Fluconazole resistance associated with drug efflux and increased transcription of a drug transporter gene, PDH1, in Candida glabrata. Antimicrob Agents Chemother **42:**1695-1701.
129. **Sanglard D, Ischer F, Bille J.** 2001. Role of ATP-binding-cassette transporter genes in high-frequency acquisition of resistance to azole antifungals in Candida glabrata. Antimicrob Agents Chemother **45:**1174-1183.
130. **Sanguinetti M, Posteraro B, Fiori B, Ranno S, Torelli R, Fadda G.** 2005. Mechanisms of azole resistance in clinical isolates of Candida glabrata collected during a hospital survey of antifungal resistance. Antimicrob Agents Chemother **49:**668-679.
131. **Torelli R, Posteraro B, Ferrari S, La Sorda M, Fadda G, Sanglard D, Sanguinetti M.** 2008. The ATP-binding cassette transporter-encoding gene CgSNQ2 is contributing to the CgPDR1-dependent azole resistance of Candida glabrata. Mol Microbiol **68:**186-201.
132. **Costa C, Ribeiro J, Miranda IM, Silva-Dias A, Cavalheiro M, Costa-de-Oliveira S, Rodrigues AG, Teixeira MC.** 2016. Clotrimazole Drug Resistance in Candida glabrata Clinical Isolates Correlates with Increased Expression of the Drug:H(+) Antiporters CgAqr1, CgTpo1_1, CgTpo3, and CgQdr2. Front Microbiol **7:**526.
133. **vanden Bossche H, Marichal P, Odds FC, Le Jeune L, Coene MC.** 1992. Characterization of an azole-resistant Candida glabrata isolate. Antimicrob Agents Chemother **36:**2602-2610.
134. **Redding SW, Kirkpatrick WR, Saville S, Coco BJ, White W, Fothergill A, Rinaldi M, Eng T, Patterson TF, Lopez-Ribot J.** 2003. Multiple patterns of resistance to fluconazole in Candida glabrata isolates from a patient with oropharyngeal candidiasis receiving head and neck radiation. J Clin Microbiol **41:**619-622.
135. **Marichal P, Vanden Bossche H, Odds FC, Nobels G, Warnock DW, Timmerman V, Van Broeckhoven C, Fay S, Mose-Larsen P.** 1997. Molecular biological characterization of an azole-resistant Candida glabrata isolate. Antimicrob Agents Chemother **41:**2229-2237.
136. **Nakayama H, Izuta M, Nakayama N, Arisawa M, Aoki Y.** 2000. Depletion of the squalene synthase (ERG9) gene does not impair growth of Candida glabrata in mice. Antimicrob Agents Chemother **44:**2411-2418.
137. **Tsai HF, Bard M, Izumikawa K, Krol AA, Sturm AM, Culbertson NT, Pierson CA, Bennett JE.** 2004. Candida glabrata erg1 mutant with increased sensitivity to azoles and to low oxygen tension. Antimicrob Agents Chemother **48:**2483-2489.

138. **Bard M, Sturm AM, Pierson CA, Brown S, Rogers KM, Nabinger S, Eckstein J, Barbuch R, Lees ND, Howell SA, Hazen KC.** 2005. Sterol uptake in Candida glabrata: rescue of sterol auxotrophic strains. Diagn Microbiol Infect Dis **52:**285-293.
139. **Nakayama H, Tanabe K, Bard M, Hodgson W, Wu S, Takemori D, Aoyama T, Kumaraswami NS, Metzler L, Takano Y, Chibana H, Niimi M.** 2007. The Candida glabrata putative sterol transporter gene CgAUS1 protects cells against azoles in the presence of serum. J Antimicrob Chemother **60:**1264-1272.
140. **Zavrel M, Hoot SJ, White TC.** 2013. Comparison of sterol import under aerobic and anaerobic conditions in three fungal species, Candida albicans, Candida glabrata, and Saccharomyces cerevisiae. Eukaryot Cell **12:**725-738.
141. **Defontaine A, Bouchara JP, Declerk P, Planchenault C, Chabasse D, Hallet JN.** 1999. In-vitro resistance to azoles associated with mitochondrial DNA deficiency in Candida glabrata. J Med Microbiol **48:**663-670.
142. **Brun S, Aubry C, Lima O, Filmon R, Berges T, Chabasse D, Bouchara JP.** 2003. Relationships between respiration and susceptibility to azole antifungals in Candida glabrata. Antimicrob Agents Chemother **47:**847-853.
143. **Bouchara JP, Zouhair R, Le Boudouil S, Renier G, Filmon R, Chabasse D, Hallet JN, Defontaine A.** 2000. In-vivo selection of an azole-resistant petite mutant of Candida glabrata. J Med Microbiol **49:**977-984.
144. **Ferrari S, Sanguinetti M, De Bernardis F, Torelli R, Posteraro B, Vandeputte P, Sanglard D.** 2011. Loss of mitochondrial functions associated with azole resistance in Candida glabrata results in enhanced virulence in mice. Antimicrob Agents Chemother **55:**1852-1860.
145. **Brun S, Berges T, Poupard P, Vauzelle-Moreau C, Renier G, Chabasse D, Bouchara JP.** 2004. Mechanisms of azole resistance in petite mutants of Candida glabrata. Antimicrob Agents Chemother **48:**1788-1796.
146. **Pfaller MA, Diekema DJ.** 2010. Epidemiology of invasive mycoses in North America. Crit Rev Microbiol **36:**1-53.
147. **Wisplinghoff H, Bischoff T, Tallent SM, Seifert H, Wenzel RP, Edmond MB.** 2004. Nosocomial bloodstream infections in US hospitals: analysis of 24,179 cases from a prospective nationwide surveillance study. Clin Infect Dis **39:**309-317.
148. **Edmond MB, Wallace SE, McClish DK, Pfaller MA, Jones RN, Wenzel RP.** 1999. Nosocomial bloodstream infections in United States hospitals: a three-year analysis. Clin Infect Dis **29:**239-244.
149. **Pappas PG, Rex JH, Lee J, Hamill RJ, Larsen RA, Powderly W, Kauffman CA, Hyslop N, Mangino JE, Chapman S, Horowitz HW, Edwards JE, Dismukes WE, Group NMS.** 2003. A prospective observational study of candidemia: epidemiology, therapy, and influences on mortality in hospitalized adult and pediatric patients. Clin Infect Dis **37:**634-643.
150. **Falagas ME, Apostolou KE, Pappas VD.** 2006. Attributable mortality of candidemia: a systematic review of matched cohort and case-control studies. Eur J Clin Microbiol Infect Dis **25:**419-425.
151. **Andes DR, Safdar N, Baddley JW, Playford G, Reboli AC, Rex JH, Sobel JD, Pappas PG, Kullberg BJ, Mycoses Study G.** 2012. Impact of treatment strategy

on outcomes in patients with candidemia and other forms of invasive candidiasis: a patient-level quantitative review of randomized trials. Clin Infect Dis **54:**1110-1122.

152. **Khatib R, Johnson LB, Fakih MG, Riederer K, Briski L.** 2016. Current trends in candidemia and species distribution among adults: Candida glabrata surpasses C. albicans in diabetic patients and abdominal sources. Mycoses doi:10.1111/myc.12531.
153. **Lockhart SR, Iqbal N, Cleveland AA, Farley MM, Harrison LH, Bolden CB, Baughman W, Stein B, Hollick R, Park BJ, Chiller T.** 2012. Species identification and antifungal susceptibility testing of Candida bloodstream isolates from population-based surveillance studies in two U.S. cities from 2008 to 2011. J Clin Microbiol **50:**3435-3442.
154. **Borg-von Zepelin M, Kunz L, Ruchel R, Reichard U, Weig M, Gross U.** 2007. Epidemiology and antifungal susceptibilities of Candida spp. to six antifungal agents: results from a surveillance study on fungaemia in Germany from July 2004 to August 2005. J Antimicrob Chemother **60:**424-428.
155. **Matsumoto E, Boyken L, Tendolkar S, McDanel J, Castanheira M, Pfaller M, Diekema D.** 2014. Candidemia surveillance in Iowa: emergence of echinocandin resistance. Diagn Microbiol Infect Dis **79:**205-208.
156. **Tortorano AM, Kibbler C, Peman J, Bernhardt H, Klingspor L, Grillot R.** 2006. Candidaemia in Europe: epidemiology and resistance. Int J Antimicrob Agents **27:**359-366.
157. **Trick WE, Fridkin SK, Edwards JR, Hajjeh RA, Gaynes RP, National Nosocomial Infections Surveillance System H.** 2002. Secular trend of hospital-acquired candidemia among intensive care unit patients in the United States during 1989-1999. Clin Infect Dis **35:**627-630.
158. **Chow JK, Golan Y, Ruthazer R, Karchmer AW, Carmeli Y, Lichtenberg D, Chawla V, Young J, Hadley S.** 2008. Factors associated with candidemia caused by non-albicans Candida species versus Candida albicans in the intensive care unit. Clin Infect Dis **46:**1206-1213.
159. **Segireddy M, Johnson LB, Szpunar SM, Khatib R.** 2011. Differences in patient risk factors and source of candidaemia caused by Candida albicans and Candida glabrata. Mycoses **54:**e39-43.
160. **Bodey GP, Mardani M, Hanna HA, Boktour M, Abbas J, Girgawy E, Hachem RY, Kontoyiannis DP, Raad, II.** 2002. The epidemiology of Candida glabrata and Candida albicans fungemia in immunocompromised patients with cancer. Am J Med **112:**380-385.
161. **Kontoyiannis DP, Reddy BT, Hanna H, Bodey GP, Tarrand J, Raad, II.** 2002. Breakthrough candidemia in patients with cancer differs from de novo candidemia in host factors and Candida species but not intensity. Infect Control Hosp Epidemiol **23:**542-545.
162. **Khan ZU, Ahmad S, Al-Obaid I, Al-Sweih NA, Joseph L, Farhat D.** 2008. Emergence of resistance to amphotericin B and triazoles in Candida glabrata vaginal isolates in a case of recurrent vaginitis. J Chemother **20:**488-491.
163. **Farmakiotis D, Tarrand JJ, Kontoyiannis DP.** 2014. Drug-resistant Candida glabrata infection in cancer patients. Emerg Infect Dis **20:**1833-1840.

164. **Garnaud C, Botterel F, Sertour N, Bougnoux ME, Dannaoui E, Larrat S, Hennequin C, Guinea J, Cornet M, Maubon D.** 2015. Next-generation sequencing offers new insights into the resistance of Candida spp. to echinocandins and azoles. J Antimicrob Chemother **70:**2556-2565.
165. **Izumikawa K, Kakeya H, Tsai HF, Grimberg B, Bennett JE.** 2003. Function of Candida glabrata ABC transporter gene, PDH1. Yeast **20:**249-261.
166. **Sanglard D, Kuchler K, Ischer F, Pagani JL, Monod M, Bille J.** 1995. Mechanisms of resistance to azole antifungal agents in Candida albicans isolates from AIDS patients involve specific multidrug transporters. Antimicrob Agents Chemother **39:**2378-2386.
167. **Sanglard D, Ischer F, Monod M, Bille J.** 1996. Susceptibilities of Candida albicans multidrug transporter mutants to various antifungal agents and other metabolic inhibitors. Antimicrob Agents Chemother **40:**2300-2305.
168. **Vermitsky JP, Earhart KD, Smith WL, Homayouni R, Edlind TD, Rogers PD.** 2006. Pdr1 regulates multidrug resistance in Candida glabrata: gene disruption and genome-wide expression studies. Mol Microbiol **61:**704-722.
169. **Costa C, Pires C, Cabrito TR, Renaudin A, Ohno M, Chibana H, Sa-Correia I, Teixeira MC.** 2013. Candida glabrata drug:H+ antiporter CgQdr2 confers imidazole drug resistance, being activated by transcription factor CgPdr1. Antimicrob Agents Chemother **57:**3159-3167.
170. **Thakur JK, Arthanari H, Yang F, Pan SJ, Fan X, Breger J, Frueh DP, Gulshan K, Li DK, Mylonakis E, Struhl K, Moye-Rowley WS, Cormack BP, Wagner G, Naar AM.** 2008. A nuclear receptor-like pathway regulating multidrug resistance in fungi. Nature **452:**604-609.
171. **Nishikawa JL, Boeszoermenyi A, Vale-Silva LA, Torelli R, Posteraro B, Sohn YJ, Ji F, Gelev V, Sanglard D, Sanguinetti M, Sadreyev RI, Mukherjee G, Bhyravabhotla J, Buhrlage SJ, Gray NS, Wagner G, Naar AM, Arthanari H.** 2016. Inhibiting fungal multidrug resistance by disrupting an activator-Mediator interaction. Nature **530:**485-489.
172. **Borah S, Shivarathri R, Kaur R.** 2011. The Rho1 GTPase-activating protein CgBem2 is required for survival of azole stress in Candida glabrata. J Biol Chem **286:**34311-34324.
173. **Borah S, Shivarathri R, Srivastava VK, Ferrari S, Sanglard D, Kaur R.** 2014. Pivotal role for a tail subunit of the RNA polymerase II mediator complex CgMed2 in azole tolerance and adherence in Candida glabrata. Antimicrob Agents Chemother **58:**5976-5986.
174. **Akache B, MacPherson S, Sylvain MA, Turcotte B.** 2004. Complex interplay among regulators of drug resistance genes in Saccharomyces cerevisiae. J Biol Chem **279:**27855-27860.
175. **Noble JA, Tsai HF, Suffis SD, Su Q, Myers TG, Bennett JE.** 2013. STB5 is a negative regulator of azole resistance in Candida glabrata. Antimicrob Agents Chemother **57:**959-967.
176. **Ma B, Pan SJ, Domergue R, Rigby T, Whiteway M, Johnson D, Cormack BP.** 2009. High-affinity transporters for NAD+ precursors in Candida glabrata are regulated by Hst1 and induced in response to niacin limitation. Mol Cell Biol **29:**4067-4079.

177. **Orta-Zavalza E, Guerrero-Serrano G, Gutierrez-Escobedo G, Canas-Villamar I, Juarez-Cepeda J, Castano I, De Las Penas A.** 2013. Local silencing controls the oxidative stress response and the multidrug resistance in Candida glabrata. Mol Microbiol **88:**1135-1148.
178. **Nagi M, Nakayama H, Tanabe K, Bard M, Aoyama T, Okano M, Higashi S, Ueno K, Chibana H, Niimi M, Yamagoe S, Umeyama T, Kajiwara S, Ohno H, Miyazaki Y.** 2011. Transcription factors CgUPC2A and CgUPC2B regulate ergosterol biosynthetic genes in Candida glabrata. Genes Cells **16:**80-89.
179. **Whaley SG, Caudle KE, Vermitsky JP, Chadwick SG, Toner G, Barker KS, Gygax SE, Rogers PD.** 2014. UPC2A is required for high-level azole antifungal resistance in Candida glabrata. Antimicrob Agents Chemother **58:**4543-4554.
180. **Hazen KC, Stei J, Darracott C, Breathnach A, May J, Howell SA.** 2005. Isolation of cholesterol-dependent Candida glabrata from clinical specimens. Diagn Microbiol Infect Dis **52:**35-37.
181. **Nagi M, Tanabe K, Ueno K, Nakayama H, Aoyama T, Chibana H, Yamagoe S, Umeyama T, Oura T, Ohno H, Kajiwara S, Miyazaki Y.** 2013. The Candida glabrata sterol scavenging mechanism, mediated by the ATP-binding cassette transporter Aus1p, is regulated by iron limitation. Mol Microbiol **88:**371-381.
182. **Sasse C, Dunkel N, Schafer T, Schneider S, Dierolf F, Ohlsen K, Morschhauser J.** 2012. The stepwise acquisition of fluconazole resistance mutations causes a gradual loss of fitness in Candida albicans. Mol Microbiol **86:**539-556.
183. **Vale-Silva L, Ischer F, Leibundgut-Landmann S, Sanglard D.** 2013. Gain-of-function mutations in PDR1, a regulator of antifungal drug resistance in Candida glabrata, control adherence to host cells. Infect Immun **81:**1709-1720.
184. **Vale-Silva LA, Moeckli B, Torelli R, Posteraro B, Sanguinetti M, Sanglard D.** 2016. Upregulation of the Adhesin Gene EPA1 Mediated by PDR1 in Candida glabrata Leads to Enhanced Host Colonization. mSphere **1**.
185. **Ferrari S, Sanguinetti M, Torelli R, Posteraro B, Sanglard D.** 2011. Contribution of CgPDR1-regulated genes in enhanced virulence of azole-resistant Candida glabrata. PLoS One **6:**e17589.
186. **Devaux F, Carvajal E, Moye-Rowley S, Jacq C.** 2002. Genome-wide studies on the nuclear PDR3-controlled response to mitochondrial dysfunction in yeast. FEBS Lett **515:**25-28.
187. **Hallstrom TC, Moye-Rowley WS.** 2000. Multiple signals from dysfunctional mitochondria activate the pleiotropic drug resistance pathway in Saccharomyces cerevisiae. J Biol Chem **275:**37347-37356.
188. **Brun S, Dalle F, Saulnier P, Renier G, Bonnin A, Chabasse D, Bouchara JP.** 2005. Biological consequences of petite mutations in Candida glabrata. J Antimicrob Chemother **56:**307-314.
189. **Peng Y, Dong D, Jiang C, Yu B, Wang X, Ji Y.** 2012. Relationship between respiration deficiency and azole resistance in clinical Candida glabrata. FEMS Yeast Res **12:**719-727.
190. **Shin JH, Chae MJ, Song JW, Jung SI, Cho D, Kee SJ, Kim SH, Shin MG, Suh SP, Ryang DW.** 2007. Changes in karyotype and azole susceptibility of

sequential bloodstream isolates from patients with Candida glabrata candidemia. J Clin Microbiol **45:**2385-2391.
191. **Klempp-Selb B, Rimek D, Kappe R.** 2000. Karyotyping of Candida albicans and Candida glabrata from patients with Candida sepsis. Mycoses **43:**159-163.
192. **Polakova S, Blume C, Zarate JA, Mentel M, Jorck-Ramberg D, Stenderup J, Piskur J.** 2009. Formation of new chromosomes as a virulence mechanism in yeast Candida glabrata. Proc Natl Acad Sci U S A **106:**2688-2693.
193. **Ahmad KM, Ishchuk OP, Hellborg L, Jorgensen G, Skvarc M, Stenderup J, Jorck-Ramberg D, Polakova S, Piskur J.** 2013. Small chromosomes among Danish Candida glabrata isolates originated through different mechanisms. Antonie Van Leeuwenhoek **104:**111-122.
194. **El-Halfawy OM, Valvano MA.** 2015. Antimicrobial heteroresistance: an emerging field in need of clarity. Clin Microbiol Rev **28:**191-207.
195. **Ben-Ami R, Zimmerman O, Finn T, Amit S, Novikov A, Wertheimer N, Lurie-Weinberger M, Berman J.** 2016. Heteroresistance to Fluconazole Is a Continuously Distributed Phenotype among Candida glabrata Clinical Strains Associated with In Vivo Persistence. MBio **7**.
196. **Prasad R, Khandelwal NK, Banerjee A.** 2016. Yeast ABC transporters in lipid trafficking. Fungal Genet Biol **93:**25-34.
197. **MacCallum DM, Coste A, Ischer F, Jacobsen MD, Odds FC, Sanglard D.** 2010. Genetic dissection of azole resistance mechanisms in Candida albicans and their validation in a mouse model of disseminated infection. Antimicrob Agents Chemother **54:**1476-1483.
198. **Tsao S, Rahkhoodaee F, Raymond M.** 2009. Relative contributions of the Candida albicans ABC transporters Cdr1p and Cdr2p to clinical azole resistance. Antimicrob Agents Chemother **53:**1344-1352.
199. **Magill SS, Shields C, Sears CL, Choti M, Merz WG.** 2006. Triazole cross-resistance among Candida spp.: case report, occurrence among bloodstream isolates, and implications for antifungal therapy. J Clin Microbiol **44:**529-535.
200. **Reuss O, Vik A, Kolter R, Morschhauser J.** 2004. The SAT1 flipper, an optimized tool for gene disruption in Candida albicans. Gene **341:**119-127.
201. **Amberg DC, Burke DJ, Strathern JN.** 2006. Isolation of yeast genomic DNA for southern blot analysis. CSH Protoc **2006**.
202. **CLSI.** 2008. Reference method for broth dilution antifungal susceptibility testing of yeasts. Approved standard M27-A3, 3rd ed. Clinical and Laboratory Standards Institute, Wayne, PA.
203. **Katzmann DJ, Hallstrom TC, Mahe Y, Moye-Rowley WS.** 1996. Multiple Pdr1p/Pdr3p binding sites are essential for normal expression of the ATP binding cassette transporter protein-encoding gene PDR5. J Biol Chem **271:**23049-23054.
204. **Gohar AA, Badali H, Shokohi T, Nabili M, Amirrajab N, Moazeni M.** 2017. Expression Patterns of ABC Transporter Genes in Fluconazole-Resistant Candida glabrata. Mycopathologia **182:**273-284.
205. **Gygax SE, Vermitsky JP, Chadwick SG, Self MJ, Zimmerman JA, Mordechai E, Adelson ME, Trama JP.** 2008. Antifungal resistance of Candida glabrata vaginal isolates and development of a quantitative reverse transcription-

PCR-based azole susceptibility assay. Antimicrob Agents Chemother **52:**3424-3426.

206. **Whaley SG, Tsao S, Weber S, Zhang Q, Barker KS, Raymond M, Rogers PD.** 2016. The RTA3 Gene, Encoding a Putative Lipid Translocase, Influences the Susceptibility of Candida albicans to Fluconazole. Antimicrob Agents Chemother **60:**6060-6066.
207. **Jia XM, Ma ZP, Jia Y, Gao PH, Zhang JD, Wang Y, Xu YG, Wang L, Cao YY, Cao YB, Zhang LX, Jiang YY.** 2008. RTA2, a novel gene involved in azole resistance in Candida albicans. Biochem Biophys Res Commun **373:**631-636.
208. **Odds FC.** 1988. *Candida* and candidosis: a review and bibliography, 2nd ed. Bailliere Tindall, London.
209. **Ostrosky-Zeichner L, Rex JH, Pappas PG, Hamill RJ, Larsen RA, Horowitz HW, Powderly WG, Hyslop N, Kauffman CA, Cleary J, Mangino JE, Lee J.** 2003. Antifungal susceptibility survey of 2,000 bloodstream Candida isolates in the United States. Antimicrob Agents Chemother **47:**3149-3154.
210. **Pfaller MA, Messer SA, Hollis RJ, Jones RN, Doern GV, Brandt ME, Hajjeh RA.** 1999. Trends in species distribution and susceptibility to fluconazole among blood stream isolates of Candida species in the United States. Diagn Microbiol Infect Dis **33:**217-222.
211. **Bader MS, Lai SM, Kumar V, Hinthorn D.** 2004. Candidemia in patients with diabetes mellitus: epidemiology and predictors of mortality. Scand J Infect Dis **36:**860-864.
212. **Dan M, Segal R, Marder V, Leibovitz A.** 2006. Candida colonization of the vagina in elderly residents of a long-term-care hospital. Eur J Clin Microbiol Infect Dis **25:**394-396.
213. **Almirante B, Rodriguez D, Park BJ, Cuenca-Estrella M, Planes AM, Almela M, Mensa J, Sanchez F, Ayats J, Gimenez M, Saballs P, Fridkin SK, Morgan J, Rodriguez-Tudela JL, Warnock DW, Pahissa A, Barcelona Candidemia Project Study G.** 2005. Epidemiology and predictors of mortality in cases of Candida bloodstream infection: results from population-based surveillance, barcelona, Spain, from 2002 to 2003. J Clin Microbiol **43:**1829-1835.
214. **Gudlaugsson O, Gillespie S, Lee K, Vande Berg J, Hu J, Messer S, Herwaldt L, Pfaller M, Diekema D.** 2003. Attributable mortality of nosocomial candidemia, revisited. Clin Infect Dis **37:**1172-1177.
215. **Davies BS, Wang HS, Rine J.** 2005. Dual activators of the sterol biosynthetic pathway of Saccharomyces cerevisiae: similar activation/regulatory domains but different response mechanisms. Mol Cell Biol **25:**7375-7385.
216. **Song JL, Harry JB, Eastman RT, Oliver BG, White TC.** 2004. The Candida albicans lanosterol 14-alpha-demethylase (ERG11) gene promoter is maximally induced after prolonged growth with antifungal drugs. Antimicrob Agents Chemother **48:**1136-1144.
217. **White TC, Silver PM.** 2005. Regulation of sterol metabolism in Candida albicans by the UPC2 gene. Biochem Soc Trans **33:**1215-1218.
218. **Akache B, Wu K, Turcotte B.** 2001. Phenotypic analysis of genes encoding yeast zinc cluster proteins. Nucleic Acids Res **29:**2181-2190.

219. **Hoehamer CF, Cummings ED, Hilliard GM, Morschhauser J, David Rogers P.** 2009. Upc2p-associated differential protein expression in Candida albicans. Proteomics **9:**4726-4730.
220. **White TC, Marr KA, Bowden RA.** 1998. Clinical, cellular, and molecular factors that contribute to antifungal drug resistance. Clin Microbiol Rev **11:**382-402.
221. **Shianna KV, Dotson WD, Tove S, Parks LW.** 2001. Identification of a UPC2 homolog in Saccharomyces cerevisiae and its involvement in aerobic sterol uptake. J Bacteriol **183:**830-834.
222. **Vik A, Rine J.** 2001. Upc2p and Ecm22p, dual regulators of sterol biosynthesis in Saccharomyces cerevisiae. Mol Cell Biol **21:**6395-6405.
223. **Silver PM, Oliver BG, White TC.** 2004. Role of Candida albicans transcription factor Upc2p in drug resistance and sterol metabolism. Eukaryot Cell **3:**1391-1397.
224. **Znaidi S, Weber S, Al-Abdin OZ, Bomme P, Saidane S, Drouin S, Lemieux S, De Deken X, Robert F, Raymond M.** 2008. Genomewide location analysis of Candida albicans Upc2p, a regulator of sterol metabolism and azole drug resistance. Eukaryot Cell **7:**836-847.
225. **Geber A, Hitchcock CA, Swartz JE, Pullen FS, Marsden KE, Kwon-Chung KJ, Bennett JE.** 1995. Deletion of the Candida glabrata ERG3 and ERG11 genes: effect on cell viability, cell growth, sterol composition, and antifungal susceptibility. Antimicrob Agents Chemother **39:**2708-2717.
226. **Epp E, Vanier G, Harcus D, Lee AY, Jansen G, Hallett M, Sheppard DC, Thomas DY, Munro CA, Mullick A, Whiteway M.** 2010. Reverse genetics in Candida albicans predicts ARF cycling is essential for drug resistance and virulence. PLoS Pathog **6:**e1000753.
227. **Onyewu C, Blankenship JR, Del Poeta M, Heitman J.** 2003. Ergosterol biosynthesis inhibitors become fungicidal when combined with calcineurin inhibitors against Candida albicans, Candida glabrata, and Candida krusei. Antimicrob Agents Chemother **47:**956-964.
228. **Espinel-Ingroff A.** 1998. Comparison of In vitro activities of the new triazole SCH56592 and the echinocandins MK-0991 (L-743,872) and LY303366 against opportunistic filamentous and dimorphic fungi and yeasts. J Clin Microbiol **36:**2950-2956.
229. **Klepser ME, Ernst EJ, Lewis RE, Ernst ME, Pfaller MA.** 1998. Influence of test conditions on antifungal time-kill curve results: proposal for standardized methods. Antimicrob Agents Chemother **42:**1207-1212.
230. **Arthington-Skaggs BA, Jradi H, Desai T, Morrison CJ.** 1999. Quantitation of ergosterol content: novel method for determination of fluconazole susceptibility of Candida albicans. J Clin Microbiol **37:**3332-3337.
231. **Schmitt ME, Brown TA, Trumpower BL.** 1990. A rapid and simple method for preparation of RNA from Saccharomyces cerevisiae. Nucleic Acids Res **18:**3091-3092.
232. **Liu TT, Lee RE, Barker KS, Lee RE, Wei L, Homayouni R, Rogers PD.** 2005. Genome-wide expression profiling of the response to azole, polyene,

echinocandin, and pyrimidine antifungal agents in Candida albicans. Antimicrob Agents Chemother **49:**2226-2236.
233. **Hoot SJ, Brown RP, Oliver BG, White TC.** 2010. The UPC2 promoter in Candida albicans contains two cis-acting elements that bind directly to Upc2p, resulting in transcriptional autoregulation. Eukaryot Cell **9:**1354-1362.
234. **Oliver BG, Song JL, Choiniere JH, White TC.** 2007. cis-Acting elements within the Candida albicans ERG11 promoter mediate the azole response through transcription factor Upc2p. Eukaryot Cell **6:**2231-2239.
235. **Henry KW, Nickels JT, Edlind TD.** 2000. Upregulation of ERG genes in Candida species by azoles and other sterol biosynthesis inhibitors. Antimicrob Agents Chemother **44:**2693-2700.
236. **Smith SJ, Crowley JH, Parks LW.** 1996. Transcriptional regulation by ergosterol in the yeast Saccharomyces cerevisiae. Mol Cell Biol **16:**5427-5432.
237. **Ghannoum MA, Rice LB.** 1999. Antifungal agents: mode of action, mechanisms of resistance, and correlation of these mechanisms with bacterial resistance. Clin Microbiol Rev **12:**501-517.
238. **Pfaller MA, Jones RN, Doern GV, Sader HS, Hollis RJ, Messer SA.** 1998. International surveillance of bloodstream infections due to Candida species: frequency of occurrence and antifungal susceptibilities of isolates collected in 1997 in the United States, Canada, and South America for the SENTRY Program. The SENTRY Participant Group. J Clin Microbiol **36:**1886-1889.
239. **Schuman P, Sobel JD, Ohmit SE, Mayer KH, Carpenter CC, Rompalo A, Duerr A, Smith DK, Warren D, Klein RS.** 1998. Mucosal candidal colonization and candidiasis in women with or at risk for human immunodeficiency virus infection. HIV Epidemiology Research Study (HERS) Group. Clin Infect Dis **27:**1161-1167.
240. **Vazquez JA, Sobel JD, Peng G, Steele-Moore L, Schuman P, Holloway W, Neaton JD.** 1999. Evolution of vaginal Candida species recovered from human immunodeficiency virus-infected women receiving fluconazole prophylaxis: the emergence of Candida glabrata? Terry Beirn Community Programs for Clinical Research in AIDS (CPCRA). Clin Infect Dis **28:**1025-1031.
241. **Hoot SJ, Oliver BG, White TC.** 2008. Candida albicans UPC2 is transcriptionally induced in response to antifungal drugs and anaerobicity through Upc2p-dependent and -independent mechanisms. Microbiology **154:**2748-2756.
242. **Barker KS, Pearson MM, Rogers PD.** 2003. Identification of genes differentially expressed in association with reduced azole susceptibility in Saccharomyces cerevisiae. J Antimicrob Chemother **51:**1131-1140.
243. **Krishnamurthy SS, Prasad R.** 1999. Membrane fluidity affects functions of Cdr1p, a multidrug ABC transporter of Candida albicans. FEMS Microbiol Lett **173:**475-481.
244. **Kohli A, Smriti, Mukhopadhyay K, Rattan A, Prasad R.** 2002. In vitro low-level resistance to azoles in Candida albicans is associated with changes in membrane lipid fluidity and asymmetry. Antimicrob Agents Chemother **46:**1046-1052.
245. **Schwarzmuller T, Ma B, Hiller E, Istel F, Tscherner M, Brunke S, Ames L, Firon A, Green B, Cabral V, Marcet-Houben M, Jacobsen ID, Quintin J,**

Seider K, Frohner I, Glaser W, Jungwirth H, Bachellier-Bassi S, Chauvel M, Zeidler U, Ferrandon D, Gabaldon T, Hube B, d'Enfert C, Rupp S, Cormack B, Haynes K, Kuchler K. 2014. Systematic phenotyping of a large-scale Candida glabrata deletion collection reveals novel antifungal tolerance genes. PLoS Pathog **10:**e1004211.

246. **CLSI.** 2012. Reference Method for Broth Dilution Antifungal Susceptibility Testing of Yeasts; Fourth Informational Supplement, 4th ed. Clinical Laboratory Standards Institute, Wayne, PA.
247. **Shahi P, Gulshan K, Naar AM, Moye-Rowley WS.** 2010. Differential roles of transcriptional mediator subunits in regulation of multidrug resistance gene expression in Saccharomyces cerevisiae. Mol Biol Cell **21:**2469-2482.
248. **Akache B, Turcotte B.** 2002. New regulators of drug sensitivity in the family of yeast zinc cluster proteins. J Biol Chem **277:**21254-21260.
249. **Gautschi M, Mun A, Ross S, Rospert S.** 2002. A functional chaperone triad on the yeast ribosome. Proc Natl Acad Sci U S A **99:**4209-4214.
250. **Eisenman HC, Craig EA.** 2004. Activation of pleiotropic drug resistance by the J-protein and Hsp70-related proteins, Zuo1 and Ssz1. Mol Microbiol **53:**335-344.
251. **Ducett JK, Peterson FC, Hoover LA, Prunuske AJ, Volkman BF, Craig EA.** 2013. Unfolding of the C-terminal domain of the J-protein Zuo1 releases autoinhibition and activates Pdr1-dependent transcription. J Mol Biol **425:**19-31.
252. **Hallstrom TC, Katzmann DJ, Torres RJ, Sharp WJ, Moye-Rowley WS.** 1998. Regulation of transcription factor Pdr1p function by an Hsp70 protein in Saccharomyces cerevisiae. Mol Cell Biol **18:**1147-1155.
253. **Shahi P, Gulshan K, Moye-Rowley WS.** 2007. Negative transcriptional regulation of multidrug resistance gene expression by an Hsp70 protein. J Biol Chem **282:**26822-26831.
254. **Wall D, Zylicz M, Georgopoulos C.** 1994. The NH2-terminal 108 amino acids of the Escherichia coli DnaJ protein stimulate the ATPase activity of DnaK and are sufficient for lambda replication. J Biol Chem **269:**5446-5451.
255. **Greene MK, Maskos K, Landry SJ.** 1998. Role of the J-domain in the cooperation of Hsp40 with Hsp70. Proc Natl Acad Sci U S A **95:**6108-6113.
256. **Rice P, Longden I, Bleasby A.** 2000. EMBOSS: the European Molecular Biology Open Software Suite. Trends Genet **16:**276-277.
257. **Meyer AE, Hung NJ, Yang P, Johnson AW, Craig EA.** 2007. The specialized cytosolic J-protein, Jjj1, functions in 60S ribosomal subunit biogenesis. Proc Natl Acad Sci U S A **104:**1558-1563.
258. **Kaschner LA, Sharma R, Shrestha OK, Meyer AE, Craig EA.** 2015. A conserved domain important for association of eukaryotic J-protein co-chaperones Jjj1 and Zuo1 with the ribosome. Biochim Biophys Acta **1853:**1035-1045.
259. **Gillies AT, Taylor R, Gestwicki JE.** 2012. Synthetic lethal interactions in yeast reveal functional roles of J protein co-chaperones. Mol Biosyst **8:**2901-2908.
260. **De Las Penas A, Pan SJ, Castano I, Alder J, Cregg R, Cormack BP.** 2003. Virulence-related surface glycoproteins in the yeast pathogen Candida glabrata are encoded in subtelomeric clusters and subject to RAP1- and SIR-dependent transcriptional silencing. Genes Dev **17:**2245-2258.

261. **Gallegos-Garcia V, Pan SJ, Juarez-Cepeda J, Ramirez-Zavaleta CY, Martin-del-Campo MB, Martinez-Jimenez V, Castano I, Cormack B, De Las Penas A.** 2012. A novel downstream regulatory element cooperates with the silencing machinery to repress EPA1 expression in Candida glabrata. Genetics **190:**1285-1297.
262. **Domergue R, Castano I, De Las Penas A, Zupancic M, Lockatell V, Hebel JR, Johnson D, Cormack BP.** 2005. Nicotinic acid limitation regulates silencing of Candida adhesins during UTI. Science **308:**866-870.
263. **Brown GD, Denning DW, Gow NA, Levitz SM, Netea MG, White TC.** 2012. Hidden killers: human fungal infections. Sci Transl Med **4:**165rv113.
264. **Magill SS, Edwards JR, Bamberg W, Beldavs ZG, Dumyati G, Kainer MA, Lynfield R, Maloney M, McAllister-Hollod L, Nadle J, Ray SM, Thompson DL, Wilson LE, Fridkin SK, Emerging Infections Program Healthcare-Associated I, Antimicrobial Use Prevalence Survey T.** 2014. Multistate point-prevalence survey of health care-associated infections. N Engl J Med **370:**1198-1208.
265. **Pfaller MA, Moet GJ, Messer SA, Jones RN, Castanheira M.** 2011. Geographic variations in species distribution and echinocandin and azole antifungal resistance rates among Candida bloodstream infection isolates: report from the SENTRY Antimicrobial Surveillance Program (2008 to 2009). J Clin Microbiol **49:**396-399.
266. **CDC.** 2013. Antibiotic Resistance Threats in the United States, 2013.
267. **White TC, Holleman S, Dy F, Mirels LF, Stevens DA.** 2002. Resistance mechanisms in clinical isolates of Candida albicans. Antimicrob Agents Chemother **46:**1704-1713.
268. **Smriti, Krishnamurthy S, Dixit BL, Gupta CM, Milewski S, Prasad R.** 2002. ABC transporters Cdr1p, Cdr2p and Cdr3p of a human pathogen Candida albicans are general phospholipid translocators. Yeast **19:**303-318.
269. **Jiang L, Xu D, Chen Z, Cao Y, Gao H, Jiang Y.** 2016. The putative ABC transporter encoded by the orf19.4531 plays a role in the sensitivity of Candida albicans cells to azole antifungal drugs. FEMS Yeast Res doi:10.1093/femsyr/fow024.
270. **Saidane S, Weber S, De Deken X, St-Germain G, Raymond M.** 2006. PDR16-mediated azole resistance in Candida albicans. Mol Microbiol **60:**1546-1562.
271. **Jia XM, Wang Y, Jia Y, Gao PH, Xu YG, Wang L, Cao YY, Cao YB, Zhang LX, Jiang YY.** 2009. RTA2 is involved in calcineurin-mediated azole resistance and sphingoid long-chain base release in Candida albicans. Cell Mol Life Sci **66:**122-134.
272. **Park YN, Morschhauser J.** 2005. Tetracycline-inducible gene expression and gene deletion in Candida albicans. Eukaryot Cell **4:**1328-1342.
273. **Znaidi S, De Deken X, Weber S, Rigby T, Nantel A, Raymond M.** 2007. The zinc cluster transcription factor Tac1p regulates PDR16 expression in Candida albicans. Mol Microbiol **66:**440-452.
274. **Gillum AM, Tsay EY, Kirsch DR.** 1984. Isolation of the Candida albicans gene for orotidine-5'-phosphate decarboxylase by complementation of S. cerevisiae ura3 and E. coli pyrF mutations. Mol Gen Genet **198:**179-182.

275. **Kohler GA, White TC, Agabian N.** 1997. Overexpression of a cloned IMP dehydrogenase gene of Candida albicans confers resistance to the specific inhibitor mycophenolic acid. J Bacteriol **179:**2331-2338.
276. **Holstege FC, Jennings EG, Wyrick JJ, Lee TI, Hengartner CJ, Green MR, Golub TR, Lander ES, Young RA.** 1998. Dissecting the regulatory circuitry of a eukaryotic genome. Cell **95:**717-728.
277. **Schneider CA, Rasband WS, Eliceiri KW.** 2012. NIH Image to ImageJ: 25 years of image analysis. Nat Methods **9:**671-675.
278. **Bruno VM, Wang Z, Marjani SL, Euskirchen GM, Martin J, Sherlock G, Snyder M.** 2010. Comprehensive annotation of the transcriptome of the human fungal pathogen Candida albicans using RNA-seq. Genome Res **20:**1451-1458.
279. **Marr KA, Rustad TR, Rex JH, White TC.** 1999. The trailing end point phenotype in antifungal susceptibility testing is pH dependent. Antimicrob Agents Chemother **43:**1383-1386.
280. **Pasrija R, Panwar SL, Prasad R.** 2008. Multidrug transporters CaCdr1p and CaMdr1p of Candida albicans display different lipid specificities: both ergosterol and sphingolipids are essential for targeting of CaCdr1p to membrane rafts. Antimicrob Agents Chemother **52:**694-704.
281. **Panwar SL, Moye-Rowley WS.** 2006. Long chain base tolerance in Saccharomyces cerevisiae is induced by retrograde signals from the mitochondria. J Biol Chem **281:**6376-6384.
282. **Kolaczkowska A, Manente M, Kolaczkowski M, Laba J, Ghislain M, Wawrzycka D.** 2012. The regulatory inputs controlling pleiotropic drug resistance and hypoxic response in yeast converge at the promoter of the aminocholesterol resistance gene RTA1. FEMS Yeast Res **12:**279-292.
283. **Manente M, Ghislain M.** 2009. The lipid-translocating exporter family and membrane phospholipid homeostasis in yeast. FEMS Yeast Res **9:**673-687.
284. **Kihara A, Igarashi Y.** 2002. Identification and characterization of a Saccharomyces cerevisiae gene, RSB1, involved in sphingoid long-chain base release. J Biol Chem **277:**30048-30054.
285. **Kihara A, Igarashi Y.** 2004. Cross talk between sphingolipids and glycerophospholipids in the establishment of plasma membrane asymmetry. Mol Biol Cell **15:**4949-4959.
286. **Soustre I, Letourneux Y, Karst F.** 1996. Characterization of the Saccharomyces cerevisiae RTA1 gene involved in 7-aminocholesterol resistance. Curr Genet **30:**121-125.

APPENDIX A. THE *RTA3* GENE, ENCODING A PUTATIVE LIPID TRANSLOCASE, INFLUENCES THE SUSCEPTIBILITY OF *CANDIDA ALBICANS* TO FLUCONAZOLE*

INTRODUCTION

Invasive fungal infections are an increasing problem worldwide (263). Among fungal infections, those caused by *Candida* species are by far the most common (5). A recent study of health care associated infections in the U.S. found *Candida* species to be the 7th most common pathogen overall and the most common pathogen isolated from bloodstream infections in the population studied (264). Among *Candida* infections, *Candida albicans* is the most prevalent species and was responsible for 44.4% of all *Candida* infections in the U.S. between 2006-2011 (6).

Along with the increasing rates of *Candida* infection, there has also been an increase in resistance to fluconazole, which is the most commonly prescribed antifungal agent (5, 265). The Centers for Disease Control and Prevention (CDC) reports roughly 3,400 cases of fluconazole resistant *Candida* infections with 220 associated deaths annually (266). *Candida* has evolved multiple mechanisms of resistance to fluconazole. One common mechanism of resistance found in clinical isolates is the overexpression of the *CDR1* and *CDR2* genes, encoding two homologous ATP-binding cassette (ABC) transporters functioning as multidrug efflux pumps and phospholipid translocases (267, 268). Overexpression of *CDR1* and *CDR2* has been shown to be the result of activating mutations in the gene encoding the zinc cluster transcription factor Tac1p (75, 78). Our previous characterization of the Tac1p regulon by microarray RNA profiling revealed that azole-resistant clinical isolates carrying an activated Tac1p protein overexpress many genes in addition to *CDR1* and *CDR2*, including *PDR16* (a phospholipid transferase), *LCB4* (a sphingolipid long chain base kinase) and *RTA3* (a putative lipid translocase), suggesting a function for Tac1p in regulating lipid/phospholipid homeostasis (76). (75)Recently the ABC transporter gene *ROA1*, a known Tac1p target (76), was also shown to contribute to azole resistance (269). Genetic dissection of the roles of *CDR1*, *CDR2, PDR16,* and *ROA1* showed that they all participate in the azole-resistant phenotype in *C. albicans*, although to different extents (198, 269, 270). *RTA2* has been shown to be involved in calcineurin-mediated azole resistance and sphingolipid LCB release in *C. albicans* (271). Given the overexpression of *RTA3* in azole-resistant clinical isolates carrying Tac1p activating mutations and its sequence homology to *RTA2*, we investigated its contribution to azole resistance.

---

* Reprinted with permission. **Whaley SG, Tsao S, Weber S, Zhang Q, Barker KS, Raymond M, Rogers PD.** 2016. The *RTA3* Gene, Encoding a Putative Lipid Translocase, Influences the Susceptibility of *Candida albicans* to Fluconazole. Antimicrob Agents Chemother **60:**6060-6066.

MATERIALS AND METHODS

Strains and growth media

The *C. albicans* strains used in this study are listed in (**Table A-1**). All strains were routinely maintained in YPD (1% yeast extract, 2% peptone, and 2% dextrose) broth at 30°C (unless otherwise stated) and stored as 40% glycerol stocks at -80°C. One Shot *Escherichia coli* TOP10 chemically competent cells (Invitrogen, Carlsbad, CA) were used as the host for plasmid construction and propagation. These strains were grown at 37°C in Luria-Bertani (LB) broth or on LB plates supplemented with 100 μg/mL ampicillin (Sigma, St. Louis, MO) or 50 μg/mL kanamycin (Fisher BioReagents, Fair Lawn, NJ).

Strain construction

***RTA3* disruptants and revertant.** The *SAT1*-flipper cassette was used to construct mutants as previously described (200). Fragments of the *RTA3* sequence containing the 5' region -453 to +96 relative to the start codon and the 3' region +1260 to +1816 were amplified by PCR and cloned on each side of the *SAT1*-flipper cassette. Two rounds of transformation and induction of the flippase resulted in replacement of the region +96 to +1260 relative to the *RTA3* start codon in both alleles with an *FRT* site. Primers are listed in **Table A-2**. For reintegration, the 5' fragment in the disruption cassette was replaced with a fragment containing the *RTA3* open reading frame (-453 to +2392). After one round of transformation and induction of the flippase, the resulting revertant strain has one allele of *RTA3* reintroduced into the original locus with a downstream *FRT* site. The second allele remains disrupted for *RTA3*.

***RTA3* overexpression.** The *RTA3* open reading frame (primers RTA3-5' and RTA3-3'), *ADH1* promoter region (primers ADH1 and ADH2) and 3' fragment of *ADH1* (primers ADH8 and ADH11) were PCR amplified from SC5314. The *ACT1* termination sequence and *SAT1* selection marker were PCR amplified from vector pBSS2 (primers ACT16 and SAT2), which contains the *SAT1* flipper construct in the pBluescript backbone. All primers used are listed in **Table A-2**. The assembled cassette was designed to replace one allele of *ADH1* with the *RTA3* open reading frame followed by the *ACT1* termination sequence and the *SAT1* selection marker, which allowed expression of *RTA3* from the *ADH1* promoter.

***GFP* tagged *RTA3*.** A 3 kb fragment was amplified by PCR from the pNIM vector (272) using the primers listed in **Table A-2**. The final DNA product contained 95 bp of homology to the 3' end of *RTA3* (just before the stop codon) followed by a fragment of the pNIM cassette (*GFP*, *ACT1* termination sequence, *ACT1* promoter, *SAT1*, *URA3* termination sequence) and a 116-bp region homologous to the 3' UTR immediately following the *RTA3* ORF. This construct was transformed into the 5674

Table A-1. *C. albicans* strains used in the *RTA3* study.

Strain	Parent	Genotype	Reference
5457		Azole-susceptible clinical isolate	(270)
5674	5457	Azole-resistant clinical isolate; $Tac1p^{N972D}$	(270), (273)
SZY31	5674	*tac1*Δ*::FRT*/*tac1*Δ*::FRT*	(273)
5674RTA3M4A	5674	*rta3*Δ*::FRT*/*rta3*Δ*::FRT*	This study
5674RTA3M4B	5674	*rta3*Δ*::FRT*/*rta3*Δ*::FRT*	This study
5674RTA3R2A	5674RTA3M4A	*rta3*Δ*::FRT*/*RTA3-FRT*	This study
5674RTA3R2B	5674RTA3M4A	*rta3*Δ*::FRT*/*RTA3-FRT*	This study
5674RTA3G2A	5674RTA3R2B	*rta3*Δ*::FRT/RTA3-GFP-caSAT1*	This study
5674-GFP	5674	*ADH1/adh1*::P_{tet}-*caGFP*	This study
SC5314		Azole-susceptible clinical isolate	(274)
SCRTA3M4A	SC5314	*rta3*Δ*::FRT*/*rta3*Δ*::FRT*	This study
SCRTA3OE1G	SC5314	*ADH1/adh1::*P_{ADH1}*-RTA3-caSAT1*	This study

Table A-2. Primers used in the *RTA3* study.

Primer	Sequence (5' – 3')[1]
Northern blot	
RTA3 probe Forward	ATGAATACTATGGATCTTGCGGTAATTAC
RTA3 probe Reverse	CGACCCAAATATCCGAGAAATTCTAATG
***RTA3* disruption and reintegration**	
RTA3A	AATTGGATTTCCTGGTGGTGGGCCCAAGATTA
RTA3B	TGGGGCATAAGTTGCAGCAATCTCGAGTAGAG
RTA3C	AACAAAGACCAAGCGGCCGCGGACAAAAGT
RTA3D	CTTTTAAACTATAAAAGTTTATGCCGCGGGTC
RTA3E	AAGGGTGGGAATCTCGAGGTACACCAAG
GFP-tagged *RTA3*	
RTA3gfpA	TTGTTAGGGGTGATCCTATTCAAGAGAATAAG GAAGGTGCTGGAGCTGGAGCTATGAGTAAGGG AGAAGAACTTTTCACT
RTA3gfpB	AAAAAACTAATAATGATATTGTTAGTGACAAT GAAGAATCGACGTTGCAAGGTCAAAATATTGT TAGGGGTGATCCTATT
RTA3gfpC	TTTCACTTGCATTTAAGTTGCTAGGAATCATAC CACCCCTTAGTTAACATTCAAATCTGCAGGACC ACCTTTGATTGTAA
RTA3gfpD	ACAAAAGCAAGTACAATTAATAAGCAAACATC TATAAACATCTAATAACATAGCCACCTTTTTCA CTTGCATTTAAGTTG
***RTA3* overexpression**	
ADH1	TGTCAAAGGATTGGTACCTTGAGATGGAG
ADH2	TTTGTGGGCCCCATAATTGTTTTTGTATTTGTTG
RTA3-5'	GAAAATCTAGAAGGCTCATGAATACTATGG
RTA3-3'	CTTAGTTAAAGATCTAATTCATTCCTTATTC
ACT16	TTCTAAGATCTAAATTCTGGAAATCTGG
SAT2	CTAGTGATTTCTGCAGGACCACCTTTG
ADH8	GGTGCTGAACCAAACTGCAGTGAAGCTGAC
ADH11	GAACCTTTGATTTCCGCGGATTTGACAACAGC

[1]Underlined bases indicate introduction of restriction enzyme cloning sites to allow directional cloning.

RTA3 revertant strain to allow expression of the Rta3p-GFP fusion protein from the endogenous *RTA3* promoter.

***GFP* expression in 5674.** The empty pNIM plasmid was digested with *Kpn*I and *Sac*II to release the *GFP* cassette and used to transform 5674, generating a strain in which *GFP* expression can be induced in the presence of doxycycline following integration at the *ADH1* locus (272).

C. albicans transformation

C. albicans transformations were performed either using a standard lithium acetate protocol (273) or as described previously (275), with minor modifications. Overnight cultures were diluted to an optical density at 600 nm (OD_{600}) of 0.1 in 50 mL of fresh YPD and allowed to grow to an OD_{600} of approximately 2. The cells were harvested and resuspended in a 10 mL solution containing 100mM lithium acetate (LiAc), 10mM Tris-HCl, 1mM EDTA and then incubated with shaking for one hour at 30°C. Next, 250 µL of 1M dithiothreitol was added and the cells were incubated for an additional 30 minutes with shaking. Cells were diluted with 40 mL H_2O, centrifuged and washed with 25 mL H_2O, then with 5 mL 1M sorbitol and resuspended in 50 µL 1M sorbitol. Plasmids were digested, separated by gel electrophoresis and purified using the Geneclean II kit (MP Biomedicals, Solon, OH). Then 5 µL of purified DNA or H_2O control were added to 40 µL of electrocompetent cells. Electroporation was performed in a CelljecT Pro (Thermo Fisher, Waltham, MA) at 1.5 kV in a 2mm cuvette. Cells were immediately resuspended in 1 mL of 1 M sorbitol and transferred to a microcentrifuge tube. Transformed cells were allowed to recover in YPD at 30°C with shaking for 4-6 hours then plated on YPD agar plates containing 200 µg/mL nourseothricin (Jena Biochemical, Germany). Transformants were selected after 24-48 hour growth and confirmed by Southern blot analysis.

gDNA preparation and Southern blot analysis

Genomic DNA was isolated as described previously (201). For confirmation by Southern hybridization, approximately 10 µg of genomic DNA was digested with the appropriate restriction enzymes, separated on a 1% agarose gel containing ethidium bromide, transferred by vacuum blotting onto a nylon membrane and fixed by UV-crosslinking. Hybridization was performed with the Amersham ECL Direct Nucleic Acid Labeling and Detection System (GE Healthcare, Pittsburg, PA) as per manufacturer's instructions.

RNA preparation and Northern blot analysis

C. albicans strains (50 mL cultures) were grown in YPD medium at 30˚C to an OD_{600} of 1.0. Total RNA was extracted using a hot phenol method (276). Northern

blotting was performed as previously described (270). The *RTA3* probe used for membrane hybridization was obtained by PCR amplification from SC5314 genomic DNA using primers corresponding to a region from +1 to +500 with respect to the *RTA3* start codon (**Table A-2**). After washing, the membrane was exposed to a Fujifilm imaging plate and the results were visualized using Multi Gauge software version 3.0 (Fujifilm).

Fluconazole susceptibility assays

Liquid microtiter plate assays were performed as described previously (198). Fluconazole (FLC; Sigma, St. Louis, MO) concentrations tested in the deletion strains were 1.5, 3, 9, 25, 37.5, 50, 62.5, 75, 87.5, 100 and 200 μg/mL; each strain was tested as four biological replicates, each with technical duplicates. FLC concentrations tested in the overexpression strain were 0.2, 0.4, 0.8, 1.6, 3.1, 6.3, 12.5, 25, 50, 100 and 200 μg/mL; each strain was tested in triplicate. Cell growth was measured spectrophotometrically at OD_{620} after 48 hours of incubation at 30˚C in YPD. Data was plotted using GraphPad Prism (GraphPad Software, Inc., La Jolla, CA) as a dose-response curve where the X values are the logarithms of FLC concentrations and Y values are percent cell growth in the presence of FLC relative to cell growth in the absence of FLC. The data was fitted using non-linear regression allowing the determination of the IC_{50} for each strain in response to FLC treatment.

Spot assay

Colonies from cultures grown on YPD solid media for 24 hours were diluted in YPD to OD_{600} of 1.0. Cultures were serially diluted one to five in YPD. Approximately 2 μL of each dilution were applied to solid YPD containing the indicated concentrations of fluconazole using a handheld pin transfer tool. The serial dilutions were incubated at 30°C for 24, 48, and 72 hours. Plates were imaged using an Epson Perfection V700 Photo scanner at each time point and growth inhibition was compared.

Fluorescence microscopy

Cells were grown in synthetic complete medium (2% glucose, 0.67% Yeast Nitrogen base without amino acids (Difco, Sparks, MD), 0.2% amino acids). The 5674/pNIM strain (5674-GFP) was treated with 50 μg/mL doxycycline (Sigma, St. Louis, MO) to induce expression of *GFP* as described (272). Cells were harvested at an OD_{600} of 0.4, washed with 0.1 M potassium phosphate buffer pH 6.4 and resuspended in 0.1 M potassium phosphate buffer pH 7.4. The cells were then placed on a 15-well microscope slide pre-treated with poly-L-lysine (Sigma, St. Louis, MO). Non-adhering cells were aspirated and 0.05 μg/mL DAPI (Sigma, St. Louis, MO) was added to each well. Images were acquired using a Zeiss LSM 700 inverted confocal laser scanning microscope equipped with a 63x oil immersion objective (1.4 NA, DIC) at a 2x zoom. GFP images

were captured using a 488 nm diode laser for excitation and a beam splitter set to capture emission above 505 nm. All images were acquired using the same laser strength, detector gain value and pixel dwell time to enable subsequent comparative analyses using ImageJ software (http://imagej.net; version 2.0.0-rc-29/1.49s) (277). Quantification of the autofluorescence intensity was achieved by analyzing 15 individual cells (one transverse line per cell), which determined the threshold value of 25 arbitrary units for background subtraction.

RESULTS

Increased *RTA3* expression in an azole-resistant clinical isolate of *C. albicans* is Tac1p dependent

The *SAT1* flipper method was used to delete both copies of *RTA3* in a well-characterized fluconazole-resistant clinical isolate 5674. This strain and its azole-susceptible parental strain 5457 were isolated from the same patient 58 days apart (270). Compared to strain 5457, strain 5674 is resistant to several azole derivatives and overexpresses *CDR1*, *CDR2* and many other genes, including *RTA3*, due to a strong gain-of-function mutation (N972D) in Tac1p (76, 273).

Northern blot analysis was performed on all strains, using an *RTA3*-derived probe. The RNA detected was approximately 1.7 kb, consistent with the size of the *RTA3* transcript (**Figure A-1**) (278). As predicted from the microarray studies, *RTA3* transcripts were strongly induced in strain 5674 as compared to strain 5457, in a Tac1p-dependent manner (76). *RTA3* transcripts were undetectable in the 5674 *rta3*Δ/Δ strain, confirming the *RTA3* deletion in this strain. Reintegration of one copy of *RTA3* into its original locus in the 5674 *rta3*Δ/Δ strain gave rise to intermediate levels of *RTA3* RNA **(Figure A-1**).

Deletion of *RTA3* in an azole-resistant clinical isolate of *C. albicans* results in increased susceptibility to fluconazole

The fluconazole sensitivity of clinical isolates 5457 and 5674 and the mutant strains was determined by microtiter plate assay. Cell growth was assessed by measuring optical density at 620 nm and normalized to the no fluconazole controls. This experiment showed that the deletion of *RTA3* in isolate 5674 decreased the fluconazole resistance of the cells by 2-fold, an effect that was partially suppressed in the *RTA3* revertant (**Figure A-2A** and **Table A-3**). A fluconazole resistance assay was also carried out on solid media, yielding similar results (**Figure A-2B**). These results demonstrate that *RTA3* contributes to the overall azole resistance of the 5674 clinical isolate. This contribution, although minor as compared to that of *CDR1* in strain 5674 (6-fold), is similar in extent to that of *CDR2* (1.5-fold) (198) and *PDR16* (2-fold) (270). Taken together, these data demonstrate that the high level of azole resistance in clinical isolate 5674 is achieved through the combined action of multiple Tac1p targets.

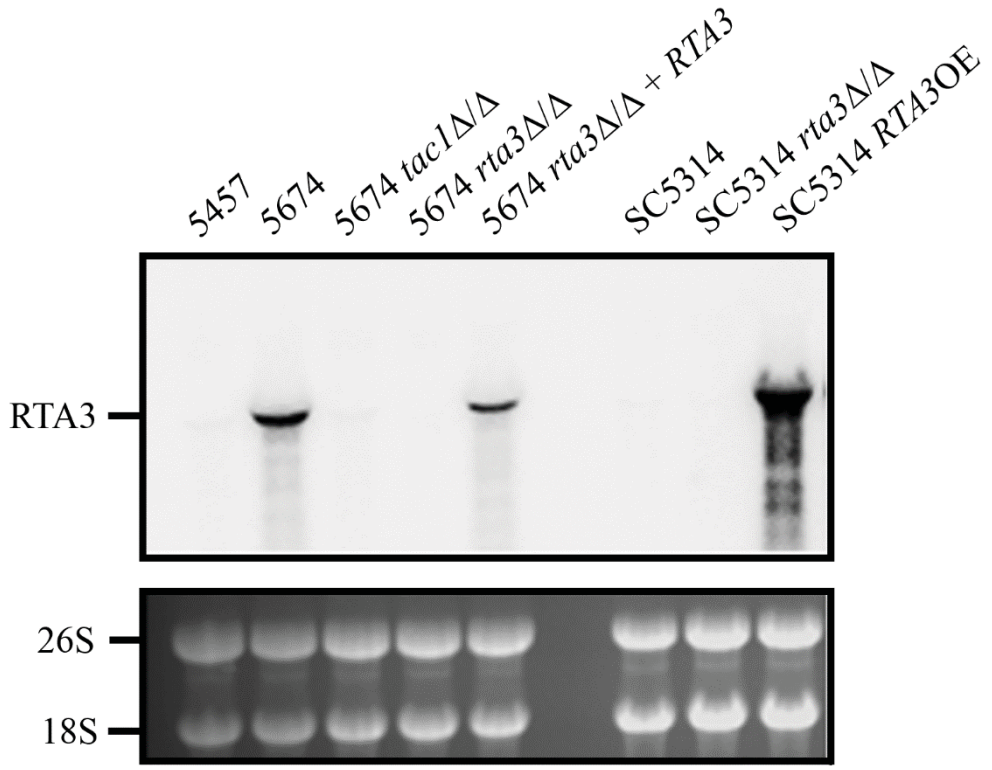

Figure A-1. Northern blot analysis of *RTA3* expression.

Total RNA was prepared from the indicated strains and analyzed by Northern blotting with an *RTA3*-specific probe. rRNAs are shown as loading controls (bottom) and the position of the 26S and 18S rRNAs is indicated on the left.

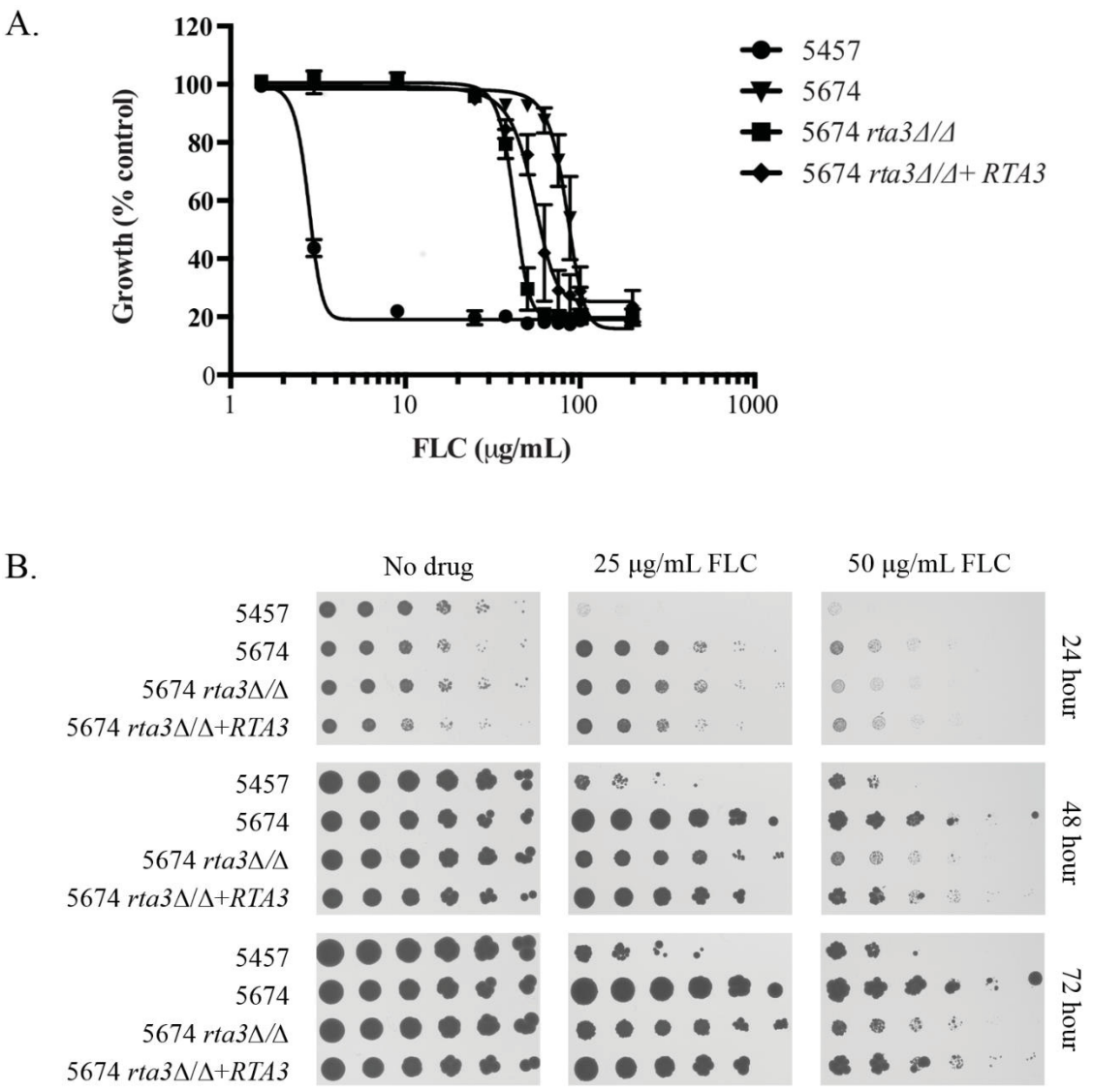

Figure A-2. Deletion of *RTA3* in the azole-resistant clinical isolate 5674 results in decreased fluconazole resistance.

(A) Strains were grown for 48 hours in YPD at the fluconazole concentrations tested and OD_{620} readings were measured and normalized to the no drug control wells. n=4. (B) Serial dilutions of the strains were incubated for 24, 48, or 72 hours on YPD solid media containing 0, 25, or 50 μg/mL fluconazole.

Table A-3. Fluconazole susceptibility of strains tested in the *RTA3* study.

Strain	IC_{50}[a]	Fold change[b]
5457	2.79 (±0.08)	0.03
5674	83.68 (±1.05)	1.00
5674 *rta3*Δ/Δ	41.79 (±0.30)	0.50
5674 *rta3*Δ/Δ+*RTA3*	53.70 (±1.05)	0.64

[a] IC_{50} of each strain to FLC (μg/mL)
[b] Relative to 5674

The same strategy was used to delete *RTA3* in the azole-susceptible clinical isolate SC5314. Assessment of the fluconazole sensitivity of the resulting strain by microtiter plate and spot assays revealed that it was identical to that of SC5314 (data not shown). This was consistent with the finding that *RTA3* is not expressed in the azole-susceptible strains SC5314 and 5457 (**Figure A-1**).

Overexpression of *RTA3* in an azole-susceptible *C. albicans* strain results in increased tolerance to fluconazole

We used an overexpression strategy to further test the role for *RTA3* in azole resistance. One allele of the highly expressed *ADH1* gene was replaced with *RTA3* in the SC5314 background such that *RTA3* expression was under the control of the strong *ADH1* promoter. This resulted in high levels of *RTA3* expression as determined by Northern blot analysis (**Figure A-1**). A liquid microtiter plate assay with the resulting strains showed that, in the presence of fluconazole, the strain overexpressing *RTA3* exhibited enhanced growth as compared to the parental strain, accompanied by growth trailing (**Figure A-3A**) (279); this trailing effect was also seen after 24 hours of growth and with another independently constructed *RTA3*-overexpressing strain (data not shown). Interestingly, the *RTA3*-overexpressing strain clearly demonstrated enhanced growth compared to SC5314 on solid YPD medium containing 5, 25, or 50 μg/mL fluconazole incubated for 24, 48, and 72 hours (**Figure A-3B**). These results indicate that an increased dosage of *RTA3* expression can confer fluconazole tolerance in the absence of additional molecular alterations – i.e. activation of additional Tac1p targets.

Rta3p localizes to the plasma membrane

Subcellular localization of Rta3p was assessed by tagging the protein with the green fluorescent protein (GFP) and analyzing the fluorescence of the resulting cells by confocal microscopy. Rta3p-GFP expressing cells exhibited a faint rim staining pattern consistent with plasma membrane localization, although intracellular staining was found to be strong, as shown in the GFP intensity plot (**Figure A-4A**). Interestingly, Rta3p-GFP also displayed a punctate distribution pattern, suggesting an association with lipid rafts, as previously shown for Cdr1p (280). Parental 5674 cells analyzed similarly to determine their level and pattern of autofluorescence exhibited a faint, diffuse signal that appeared mostly intracellular (**Figure A-4B**). Quantification of the autofluorescence intensity across individual cells allowed the autofluorescence threshold value to be set at 25 arbitrary units (**Figure A-4B**, right panel). Subtracting autofluorescence from the Rta3p-GFP signal decreased the intracellular staining and enhanced punctate staining at the cell periphery (**Figure A-4A**). Results obtained with the Rta3p-GFP cells were different from those obtained with cells expressing untagged GFP, which displayed primarily intracellular staining. Upon induction with doxycycline, cells expressing GFP were found to be very bright (**Figure A-4C**). The GFP intensity plot for these cells before and after autofluorescence correction showed similar bell-shaped distribution curves corresponding to an intracellular localization of GFP, confirming that the rim-like staining pattern

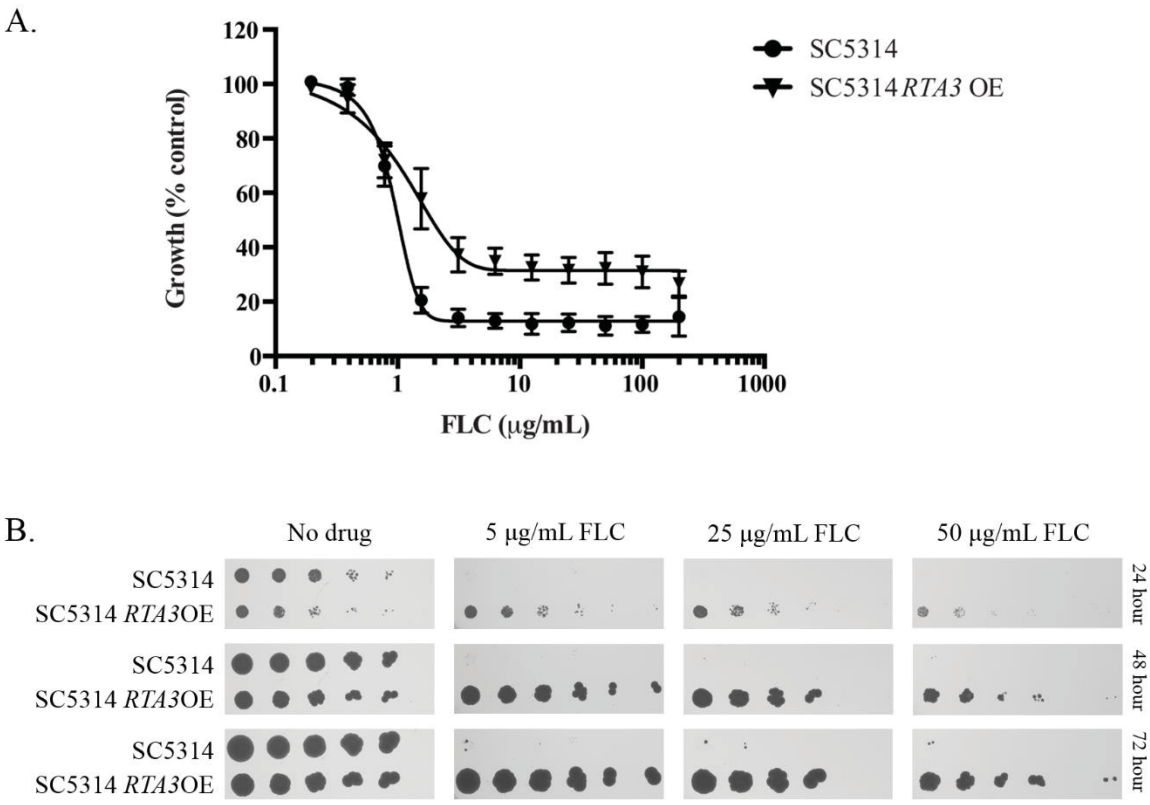

Figure A-3. Overexpression of *RTA3* in the azole-susceptible clinical isolate SC5314 results in enhanced fluconazole tolerance.

(A) Strains were incubated for 48 hours in YPD at the concentrations tested and OD_{620} readings were measured and normalized to the no drug control wells. N = 3, in duplicate. (B) Serial dilutions of the strains were incubated for 24, 48, or 72 hours on YPD solid media containing 0, 5, 25, or 50 μg/mL fluconazole.

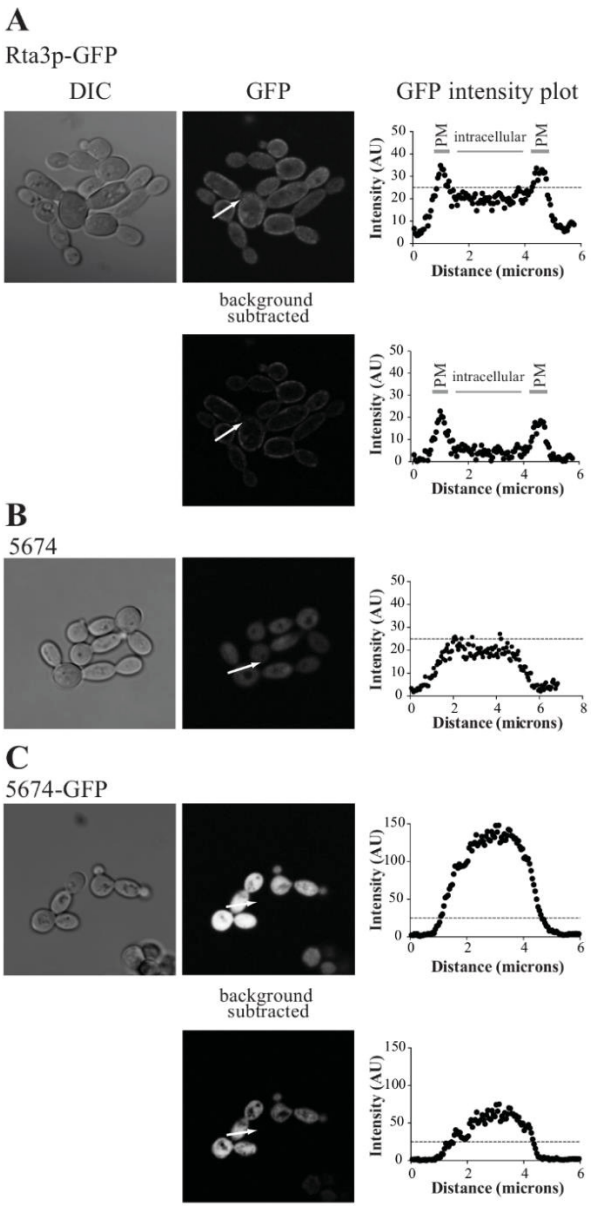

Figure A-4. Analysis of Rta3p-GFP sub-cellular localization.

(A) Confocal microscope image of strain 5674 expressing Rta3p-GFP grown to log phase in synthetic complete medium. The DIC and corresponding fluorescence (GFP) images are shown. The fluorescence intensity of the selected transversal section of the cell (arrow line) was quantified using ImageJ software (GFP intensity plot, where the length and direction are expressed as increased distance on the x-axis). The threshold for autofluorescence signal (25 arbitrary units, AU) determined from 5674 cells is indicated as a dashed line in the intensity plots. An autofluorescence subtraction image and its corresponding intensity plot are also shown. Two peaks in the intensity plot corresponding to plasma membrane (PM) fluorescence are indicated. (B) 5674 cells were analyzed as described in panel A. (C) 5674-GFP cells were analyzed as described in panel A.

observed with Rta3p-GFP is not due to the GFP moiety of the fusion protein. Taken together, these results demonstrate that Rta3p-GFP localizes predominantly to the plasma membrane, similar to *S. cerevisiae* Rsb1p and Rta1p (281, 282).

DISCUSSION

Here we show that *RTA3* participates along with *CDR1*, *CDR2*, and *PDR16* in Tac1p-mediated azole resistance in *C. albicans*. Disruption of *RTA3* in a resistant clinical isolate carrying a *TAC1* activating mutation resulted in a modest increase in susceptibility. Such an effect is not surprising as this isolate still overexpresses *CDR1*, *CDR2*, and *PDR16*. Overexpression of *RTA3* alone in the susceptible isolate SC5314 resulted in an increase in fluconazole tolerance and in its ability to grow on solid medium in the presence of fluconazole. While this Tac1p target gene clearly contributes to this phenotype, the mechanism by which it does so remains unclear.

The function of *C. albicans RTA3* remains uncharacterized. The closest homologs to this gene in the yeast *Saccharomyces cerevisiae* are *RSB1* and *RTA1*, both of which are members of the lipid-translocating exporter family (283). *RSB1* encodes a translocase that moves sphingolipid long chain bases (LCB) from the cytoplasmic side of the plasma membrane to the external side and glycerophospholipids inward toward the cytoplasm, thus conferring plasma membrane lipid asymmetry (284, 285). *RTA1* encodes a similar protein that is involved in 7-aminocholesterol resistance by a yet unknown mechanism (286). The *C. albicans* genome contains four genes encoding proteins belonging to this family: *RTA2*, *RTA3*, *RTA4* and orf19.6224. While the other members of the *C. albicans* family are not yet functionally characterized, *RTA2* has been shown to be involved in calcineurin-mediated azole resistance and sphingolipid LCB release in *C. albicans* (271).

In addition to *CDR1* and *CDR2*, other target genes of Tac1p have been implicated in the azole resistance mediated by activating mutations in this transcription factor. Disruption of the phospholipid transferase gene *PDR16* in an azole- resistant clinical isolate resulted in increased susceptibility to fluconazole, whereas overexpression of *PDR16* increased resistance (270). Interestingly, the Tac1p target gene *ROA1*, which encodes a putative ABC transporter, was recently shown to influence azole susceptibility in *C. albicans* (269). Disruption of *ROA1* increased tolerance to a panel of azoles. It is therefore tempting to speculate that other Tac1p target genes, in addition to *PDR16*, *RTA3*, and *ROA1* may play a supporting role in this process.

Based on the plasma membrane localization of Rta3p and its homology to proteins involved in maintaining optimal membrane lipid asymmetry, its overexpression (ectopic or Tac1p-mediated) could attenuate plasma membrane alterations caused by azoles, as shown for Rta2p (271). Alternatively, it could also alter plasma membrane permeability and/or the activity of plasma membrane-associated azole transporters like Cdr1p. The determination of Rta3p molecular and cellular function(s) should help to answer these questions.

APPENDIX B. SUPPLEMENTAL DATA

Table B-1. Genes up-regulated by at least 1.5-fold in SM1Δ*jjj1* versus SM1.

C. glabrata designation	*C. glabrata* gene names	*S. cerevisiae* orthologs	SM1Δ*jjj1* vs SM1		SM1Δ*jjj1*Δ*pdr1* vs SM1		Description
			Exp. 1	Exp. 2	Exp. 1	Exp. 2	
CAGL0M01760g	***CDR1***	***PDR5***	**9.22**	**11.59**	**-4.81**	**-6.65**	**Multidrug transporter of ATP-binding cassette (ABC) superfamily, involved in resistance to azoles; expression regulated by Pdr1p; increased abundance in azole-resistant strains; expression increased by loss of the mitochondrial genome**
CAGL0K00170g	*EPA22*		7.06	2.98	13.57	4.81	Putative adhesin-like protein; belongs to adhesin cluster I
CAGL0L05434g	*SUN4*	*UTH1*	6.01	4.74	5.00	5.53	Ortholog(s) have role in fungal-type cell wall biogenesis, fungal-type cell wall organization, mitochondrion degradation
CAGL0E06688g	*EPA3*		5.21	3.96	6.76	3.76	Epithelial adhesion protein; belongs to adhesin cluster I; GPI-anchored
CAGL0C03289g	***YBT1***	***YBT1***	**4.74**	**8.73**	**1.35**	**-1.41**	**Putative ABC transporter involved in bile acid transport; gene is upregulated in azole-resistant strain**
CAGL0E06666g	*EPA2*		4.35	3.22	6.57	4.38	Epithelial adhesion protein; predicted GPI-anchor; belongs to adhesin cluster I
CAGL0G05544g		*HBT1*	4.20	6.02	4.21	40.23	Ortholog(s) have role in cell morphogenesis involved in conjugation with cellular fusion and cell surface, fungal-type cell wall, mating projection, plasma membrane localization
CAGL0F00649g		*RCK2*	4.03	1.54	3.04	2.55	Ortholog(s) have protein serine/threonine kinase activity
CAGL0I10147g	*PWP1*		3.83	5.07	4.13	6.44	Protein with 32 tandem repeats; putative adhesin-like protein; belongs to adhesin cluster II
CAGL0H02563g		***DDR2***	**3.80**	**7.00**	**2.30**	**1.42**	**Predicted GPI-linked protein**
CAGL0F07777g		*ALD3*	3.26	3.59	2.15	14.73	Putative aldehyde dehydrogenase; expression upregulated in biofilm vs planktonic cell culture
CAGL0J04202g	*HSP12*	*HSP12*	3.18	8.68	3.40	13.54	Heat shock protein; gene is upregulated in azole-resistant strain; expression upregulated in biofilm vs planktonic cell culture
CAGL0K07854g		*DIB1*	2.97	2.14	3.06	2.81	Ortholog(s) have role in mRNA splicing, via spliceosome and U4/U6 x U5 tri-snRNP complex, U5 snRNP localization
CAGL0M11660g			**2.97**	**6.44**	**2.75**	**-7.64**	**Has domain(s) with predicted hydrolase activity**
CAGL0J05159g			**2.96**	**1.79**	**2.70**	**1.49**	**Putative adhesin-like protein**
CAGL0G02739g		*XBP1*	2.95	4.82	3.92	9.05	Ortholog(s) have sequence-specific DNA binding, sequence-specific DNA binding RNA polymerase II transcription factor activity

Table B-1. (Continued).

C. glabrata designation	*C. glabrata* gene names	*S. cerevisiae* orthologs	SM1Δ*jjj1* vs SM1		SM1Δ*jjj1*Δ*pdr1* vs SM1		Description
			Exp. 1	Exp. 2	Exp. 1	Exp. 2	
CAGL0E06644g	*EPA1*		2.90	4.56	2.46	2.59	Sub-telomerically encoded adhesin with a role in cell adhesion; GPI-anchored cell wall protein; N-terminal ligand binding domain binds to ligands containing a terminal galactose residue; belongs to adhesin cluster I
CAGL0K04785g		*MRX7*	2.88	3.40	2.04	2.85	Ortholog(s) have mitochondrion localization
CAGL0L07832g		***YCR016W***	**2.82**	**1.58**	**1.65**	**-1.18**	**Ortholog(s) have nucleolus localization**
CAGL0M07766g			2.80	2.29	2.40	2.71	Putative protein; gene is upregulated in azole-resistant strain
CAGL0L00157g			2.73	6.48	2.82	3.72	Putative adhesin-like protein; multiple tandem repeats; predicted GPI-anchor; belongs to adhesin cluster III
CAGL0J07502g		***YNL234W***	**2.63**	**3.46**	**1.73**	**-1.67**	**Putative protein similar to globins with a heme-binding domain; gene is upregulated in azole-resistant strain**
CAGL0I10224g			**2.60**	**1.86**	**-1.67**	**1.86**	**Unknown**
CAGL0G01540g	*NCE103*	*NCE103*	2.57	2.81	2.27	6.29	Beta carbonic anhydrase with a predicted role in non-classical protein export; upregulated in azole-resistant strain; enzyme activity increased by amines and amino acids; protein abundance decreased in ace2 cells
CAGL0H00418g			2.54	1.56	1.96	2.84	Protein of unknown function
CAGL0J01727g			2.53	2.27	2.21	1.89	Putative adhesion protein; predicted GPI-anchor; belongs to adhesin cluster VI
CAGL0L00583g		*USV1*	2.48	1.90	2.08	2.43	Ortholog(s) have sequence-specific DNA binding, sequence-specific DNA binding transcription factor activity
CAGL0K07007g			**2.46**	**3.45**	**1.75**	**-1.28**	**Protein of unknown function**
CAGL0D02640g			2.44	2.01	2.06	3.30	Has domain(s) with predicted substrate-specific transmembrane transporter activity, transmembrane transporter activity, role in transmembrane transport and integral component of membrane, membrane localization
CAGL0D02662g			2.44	2.01	2.06	3.30	Has domain(s) with predicted substrate-specific transmembrane transporter activity, transmembrane transporter activity, role in transmembrane transport and integral component of membrane, membrane localization
CAGL0J01774g			2.41	2.18	2.80	2.62	Putative adhesin-like protein; has glycine and serine rich repeats; belongs to adhesin cluster VI
CAGL0I04994g	*MET6*	*MET6*	2.36	3.56	2.99	8.43	5-methyltetrahydropteroyltriglutamate homocysteine methyltransferase; protein abundance increased in ace2 mutant cells

Table B-1. (Continued).

C. glabrata designation	*C. glabrata* gene names	*S. cerevisiae* orthologs	SM1Δ*jjj1* vs SM1		SM1Δ*jjj1*Δ*pdr1* vs SM1		Description
			Exp. 1	Exp. 2	Exp. 1	Exp. 2	
CAGL0K04367g			2.34	8.67	1.85	1.63	Has domain(s) with predicted amino acid transmembrane transporter activity, role in amino acid transmembrane transport and membrane localization
CAGL0G00242g	***YOR1***	***YOR1***	**2.34**	**2.74**	**-1.79**	**1.03**	**Putative ABC transporter involved in multidrug efflux; gene is upregulated in azole-resistant strain**
CAGL0M01716g		*TEC1*	2.31	2.35	1.95	1.51	Ortholog(s) have RNA polymerase II core promoter proximal region sequence-specific DNA binding, more
CAGL0K12254g		*VID24*	2.30	2.19	1.87	1.55	Ortholog(s) have role in negative regulation of gluconeogenesis, proteasome-mediated ubiquitin-dependent protein catabolic process, protein catabolic process in the vacuole, protein targeting to vacuole
CAGL0L06666g	*YHB1*	*YHB1*	2.25	2.93	1.66	1.63	Putative flavohemoglobin, involved in nitric oxide detoxification
CAGL0I09724g			**2.24**	**2.32**	**2.43**	**-2.09**	**Has domain(s) with predicted role in transmembrane transport and integral component of membrane localization**
CAGL0E01155g		***RPA14***	**2.24**	**3.00**	**-1.31**	**1.73**	**Ortholog(s) have RNA polymerase I activity, role in regulation of cell size, transcription of nuclear large rRNA transcript from RNA polymerase I promoter and DNA-directed RNA polymerase I complex localization**
CAGL0M06699g		***SDS3***	**2.24**	**1.67**	**3.29**	**1.33**	**Ortholog(s) have histone deacetylase activity**
CAGL0G01738g		*PIL1*	2.23	3.43	1.67	7.37	Ortholog(s) have lipid binding activity and role in eisosome assembly, endocytosis, negative regulation of protein kinase activity, protein localization, response to heat
CAGL0H06853g	*ADH6*		2.21	3.72	1.83	1.55	Putative NADP-dependent alcohol dehydrogenase VI; protein abundance increased in ace2 mutant cells
CAGL0L01287g	*UTR4*	*UTR4*	2.18	1.96	1.52	3.69	Haloacid dehalogenase-like hydrolase
CAGL0G01122g		***CIS1***	**2.17**	**3.08**	**-1.30**	**1.22**	**Putative protein; gene is upregulated in azole-resistant strain**
CAGL0D06666g			**2.17**	**1.78**	**2.67**	**1.44**	**Protein of unknown function**
CAGL0M10219g		***LAC1***	**2.14**	**2.40**	**1.40**	**-1.50**	**Putative ceramide synthase component; gene is upregulated in azole-resistant strain**

Table B-1. (Continued).

C. glabrata designation	*C. glabrata* gene names	*S. cerevisiae* orthologs	SM1Δ*jjj1* vs SM1		SM1Δ*jjj1*Δ*pdr1* vs SM1		Description
			Exp. 1	Exp. 2	Exp. 1	Exp. 2	
CAGL0M04587g		***RMP1***	**2.11**	**1.58**	**1.47**	**-1.14**	**Ortholog(s) have rRNA primary transcript binding activity, role in mRNA cleavage, maturation of 5.8S rRNA from tricistronic rRNA transcript (SSU-rRNA, 5.8S rRNA, LSU-rRNA) and cytoplasm, nucleolus, ribonuclease MRP complex localization**
CAGL0I00286g			**2.10**	**3.37**	**1.47**	**1.17**	**Has domain(s) with predicted substrate-specific transmembrane transporter activity, transmembrane transporter activity, role in transmembrane transport and integral component of membrane, membrane localization**
CAGL0M14047g		*ADH6*	2.10	6.39	1.98	3.28	Putative NADPH-dependent cinnamyl alcohol dehydrogenase; gene is upregulated in azole-resistant strain
CAGL0E00110g			2.09	2.98	3.01	2.30	Putative adhesin-like protein; ORF appears artificially broken into fragments due to sequencing errors; belongs to adhesin cluster III; predicted GPI anchor
CAGL0J00275g		*RRP45*	2.06	2.11	2.30	3.72	Ortholog(s) have role in U1 snRNA 3'-end processing, U4 snRNA 3'-end processing and U5 snRNA 3'-end processing, more
CAGL0B02838g	*MUP1*	*MUP1*	2.05	6.16	2.10	3.95	Ortholog(s) have L-methionine secondary active transmembrane transporter activity and role in cysteine transport, methionine import
CAGL0H04851g		*PPZ1*	2.05	1.92	2.15	12.37	Ortholog(s) have protein serine/threonine phosphatase activity, role in cellular protein localization, cellular sodium ion homeostasis, protein dephosphorylation and cytoplasm, extrinsic component of plasma membrane, nucleus localization
CAGL0G03179g			2.03	2.55	1.81	4.26	Has domain(s) with predicted phospholipid binding activity
CAGL0E00116g			2.00	3.84	2.77	2.08	Protein of unknown function
CAGL0K06677g	*MET8*	*MET8*	2.00	2.07	1.63	6.71	Putative bifunctional dehydrogenase and ferrochelatase; gene is upregulated in azole-resistant strain
CAGL0B00528g		*HLR1*	1.99	1.65	1.81	1.65	Ortholog(s) have role in fungal-type cell wall organization and cytoplasm localization
CAGL0E01529g		*PFK27*	1.98	1.76	1.63	1.56	Ortholog(s) have role in fructose 2,6-bisphosphate metabolic process, regulation of glycolytic process

Table B-1. (Continued).

C. glabrata designation	*C. glabrata* gene names	*S. cerevisiae* orthologs	SM1Δ*jjj1* vs SM1		SM1Δ*jjj1*Δ*pdr1* vs SM1		Description
			Exp. 1	Exp. 2	Exp. 1	Exp. 2	
CAGL0J04884g		***UBX6***	**1.98**	**1.83**	**1.31**	**3.94**	**Ortholog(s) have role in sporulation resulting in formation of a cellular spore, ubiquitin-dependent protein catabolic process and nucleus localization**
CAGL0A01804g	***HXT1***	***HXT1***	**1.98**	**1.86**	**1.49**	**-3.43**	**Ortholog(s) have fructose transmembrane transporter activity, pentose transmembrane transporter activity, role in glucose transport, mannose transport and plasma membrane localization**
CAGL0K04675g			**1.94**	**1.59**	**1.94**	**1.26**	**Protein of unknown function**
CAGL0L06094g	*STR3*	*STR3*	1.94	8.16	3.11	11.32	Putative cystathionine beta-lyase; gene is upregulated in azole-resistant strain
CAGL0E05522g		***YOR342C***	**1.94**	**2.81**	**1.75**	**-1.07**	**Ortholog(s) have cytoplasm, nucleus localization**
CAGL0M01914g			1.92	1.92	1.61	2.21	Protein of unknown function
CAGL0F07029g	*MET13*	*MET13*	1.92	2.36	2.17	5.70	Ortholog(s) have methylenetetrahydrofolate reductase (NAD(P)H) activity, role in methionine biosynthetic process, one-carbon metabolic process and cytosol, mitochondrion, nucleus localization
CAGL0D04048g		*VMA7*	1.92	1.67	1.59	1.99	Ortholog(s) have role in cellular metal ion homeostasis, cellular response to biotic stimulus and cellular response to starvation, more
CAGL0H05137g		*ALD6*	1.92	1.71	1.58	2.06	Ortholog(s) have aldehyde dehydrogenase [NAD(P)+] activity, role in NADPH regeneration, acetate biosynthetic process, response to salt stress and cytosol, mitochondrion localization
CAGL0H03619g		*YNL011C*	1.91	2.09	1.56	8.14	Ortholog of S. cerevisiae : YNL011C, C. albicans SC5314 : C7_01230C_A, C. dubliniensis CD36 : Cd36_71090, C. parapsilosis CDC317 : CPAR2_300420 and Candida tenuis NRRL Y-1498 : CANTEDRAFT_111980
CAGL0J11550g			1.90	5.38	2.00	31.09	Protein of unknown function
CAGL0M07293g		***PDR12***	**1.90**	**2.14**	**1.67**	**-3.52**	**Putative ABC transporter of weak organic acids; gene is downregulated in azole-resistant strain**
CAGL0M04257g		***DCN1***	**1.88**	**2.62**	**1.21**	**1.02**	**Ortholog(s) have NEDD8 transferase activity, cullin family protein binding, protein binding, bridging, ubiquitin binding, ubiquitin conjugating enzyme binding activity**
CAGL0L05786g		***CMR3***	**1.87**	**1.60**	**1.97**	**1.08**	**Ortholog(s) have sequence-specific DNA binding activity**

Table B-1. (Continued).

C. glabrata designation	*C. glabrata* gene names	*S. cerevisiae* orthologs	SM1Δ*jjj1* vs SM1		SM1Δ*jjj1*Δ*pdr1* vs SM1		Description
			Exp. 1	Exp. 2	Exp. 1	Exp. 2	
CAGL0M00154g	*CYN1*		1.87	3.46	1.64	1.78	Plasma membrane high affinity cystine specific transporter; present only in pathogenic yeasts; confers the ability to utilize cystine as a sulfur source
CAGL0I01144g		*YPT35*	1.87	1.64	1.81	3.16	Ortholog(s) have phosphatidylinositol-3-phosphate binding activity and endosome localization
CAGL0K12518g		*AGX1*	1.86	2.77	1.52	7.48	Ortholog(s) have alanine-glyoxylate transaminase activity, role in glycine biosynthetic process, by transamination of glyoxylate and mitochondrion localization
CAGL0C05461g		***OST4***	**1.86**	**1.85**	**2.43**	**-1.63**	**Ortholog(s) have dolichyl-diphosphooligosaccharide-protein glycotransferase activity, protein binding, bridging activity, role in protein N-linked glycosylation and oligosaccharyltransferase complex localization**
CAGL0J04004g		***MCP1***	**1.86**	**1.60**	**1.46**	**10.41**	**Ortholog(s) have role in lipid homeostasis, mitochondrion organization and integral component of mitochondrial membrane, mitochondrial outer membrane localization**
CAGL0B02860g			1.85	2.08	2.24	6.67	Protein of unknown function
CAGL0L10318g		*LPL1*	1.82	3.32	1.57	3.16	Putative protein; gene is upregulated in azole-resistant strain
CAGL0J03762g	***MET7***	***MET7***	**1.80**	**3.69**	**2.01**	**1.43**	**Ortholog(s) have tetrahydrofolylpolyglutamate synthase activity, role in one-carbon metabolic process, regulation of DNA methylation and cytosol, mitochondrion, nucleus localization**
CAGL0I02178g		***MPC2***	**1.80**	**1.84**	**1.42**	**1.88**	**Ortholog(s) have pyruvate transmembrane transporter activity, role in mitochondrial pyruvate transport and integral component of mitochondrial inner membrane localization**
CAGL0L10142g	***RSB1***	***RSB1***	**1.79**	**1.87**	**1.22**	**-3.35**	**Putative sphingolipid flippase; gene is upregulated in azole-resistant strain**
CAGL0I04928g		***AIM11***	**1.79**	**2.84**	**-1.17**	**1.52**	**Ortholog of S. cerevisiae : AIM11, C. albicans SC5314 : C3_00840C_A, C. dubliniensis CD36 : Cd36_80770, C. parapsilosis CDC317 : CPAR2_102260 and Candida tenuis NRRL Y-1498 : CANTEDRAFT_114262**
CAGL0A01694g		***YGL036W***	**1.78**	**2.47**	**1.45**	**2.63**	**Ortholog(s) have cytoplasm localization**

Table B-1. (Continued).

C. glabrata designation	*C. glabrata* gene names	*S. cerevisiae* orthologs	SM1Δ*jjj1* vs SM1		SM1Δ*jjj1*Δ*pdr1* vs SM1		Description
			Exp. 1	Exp. 2	Exp. 1	Exp. 2	
CAGL0B03465g		*SYM1*	1.78	1.70	1.58	2.09	Ortholog(s) have role in ethanol metabolic process and mitochondrial inner membrane localization
CAGL0L13299g	*EPA11*		1.78	1.91	1.98	1.81	Putative adhesin; belongs to adhesin cluster I
CAGL0K00715g	***RTA1***	***YLR046C***	**1.77**	**2.45**	**-1.20**	**-1.27**	**Putative protein involved in 7-aminocholesterol resistance; gene is upregulated in azole-resistant strain**
CAGL0J05544g		***END3***	**1.77**	**1.61**	**1.45**	**2.65**	**Ortholog(s) have protein binding, bridging activity, role in ascospore wall assembly, endocytosis and mating projection tip localization**
CAGL0A02728g		***SEM1***	**1.77**	**2.07**	**1.05**	**1.45**	**Ortholog(s) have role in SAGA complex localization to transcription regulatory region, exocytosis, filamentous growth, histone deubiquitination and mRNA export from nucleus, more**
CAGL0F03025g		***ARO80***	**1.76**	**2.84**	**1.47**	**2.19**	**Ortholog(s) have sequence-specific DNA binding, sequence-specific DNA binding RNA polymerase II transcription factor activity**
CAGL0D03894g	***PRO1***	***YHR033W***	**1.76**	**2.04**	**1.44**	**2.44**	**Putative gamma-glutamyl phosphate reductase**
CAGL0J05632g		***RHO2***	**1.76**	**1.55**	**1.18**	**1.83**	**Ortholog(s) have GTPase activity and role in establishment or maintenance of actin cytoskeleton polarity, establishment or maintenance of cell polarity regulating cell shape, regulation of alpha-glucan biosynthetic process**
CAGL0L01067g		*PAR32*	1.76	1.80	1.56	1.90	Ortholog(s) have cytoplasm localization
CAGL0L04664g	*HEM15*	*HEM15*	1.76	2.03	1.91	2.72	Ortholog(s) have ferrochelatase activity, role in heme biosynthetic process and cytosol, mitochondrial inner membrane, nucleus localization
CAGL0J03190g		*TDA2*	1.76	2.04	1.50	2.52	Ortholog(s) have cytoplasm, mating projection tip localization
CAGL0G08844g		***ASG1***	**1.74**	**1.91**	**1.28**	**1.37**	**Ortholog(s) have sequence-specific DNA binding activity**
CAGL0J05984g		***AAH1***	**1.74**	**2.08**	**1.56**	**-1.76**	**Ortholog(s) have adenine deaminase activity, role in adenine catabolic process, cell-abiotic substrate adhesion, hypoxanthine salvage and cytosol, nucleus localization**
CAGL0H07337g			**1.73**	**2.07**	**2.13**	**1.08**	**Protein of unknown function**
CAGL0L03846g		***DBP2***	**1.73**	**3.18**	**1.41**	**-1.41**	**Ortholog(s) have ATP-dependent RNA helicase activity**
CAGL0A02772g		***CDC40***	**1.73**	**1.53**	**1.13**	**-1.18**	**Ortholog(s) have second spliceosomal transesterification activity**

Table B-1. (Continued).

C. glabrata designation	*C. glabrata* gene names	*S. cerevisiae* orthologs	SM1Δ*jjj1* vs SM1		SM1Δ*jjj1*Δ*pdr1* vs SM1		Description
			Exp. 1	Exp. 2	Exp. 1	Exp. 2	
CAGL0J10846g		*PCL5*	1.73	3.79	1.58	2.40	Ortholog(s) have cyclin-dependent protein serine/threonine kinase regulator activity
CAGL0K01947g		***YER137C***	**1.73**	**1.74**	**-1.47**	**1.22**	**Has domain(s) with predicted nucleic acid binding, zinc ion binding activity**
CAGL0H06699g		***GUT2***	**1.72**	**2.34**	**1.40**	**3.22**	**Ortholog(s) have glycerol-3-phosphate dehydrogenase activity, role in NADH oxidation, glycerol metabolic process, replicative cell aging and integral component of mitochondrial outer membrane, plasma membrane localization**
CAGL0L09911g		***CSS1***	**1.72**	**1.75**	**1.65**	**1.41**	**Putative adhesin-like cell wall protein; 5 tandem repeats; predicted GPI-anchor**
CAGL0F01419g	***AUS1***	***AUS1***	**1.72**	**1.90**	**1.76**	**1.18**	**ATP-binding cassette transporter involved in sterol uptake**
CAGL0H02387g			1.72	1.56	1.81	7.46	Putative trehalose-6-phosphate synthase/phosphatase subunit; gene is upregulated in azole-resistant strain
CAGL0I05874g			**1.71**	**3.92**	**1.32**	**3.54**	**Haloacid dehalogenase-like hydrolase**
CAGL0K04697g		***STP3***	**1.71**	**1.63**	**1.20**	**1.48**	**Ortholog(s) have sequence-specific DNA binding activity, role in filamentous growth and nucleus localization**
CAGL0D06512g		*CDC25*	1.70	2.01	1.69	3.70	Putative membrane bound guanine nucleotide exchange factor; gene is upregulated in azole-resistant strain
CAGL0J08316g		*MET2*	1.70	2.86	1.68	4.52	Ortholog(s) have homoserine O-acetyltransferase activity, role in homoserine metabolic process, methionine biosynthetic process, regulation of DNA methylation and cytosol localization
CAGL0K09680g		***FYV6***	**1.69**	**1.55**	**1.77**	**1.14**	**Ortholog(s) have role in double-strand break repair via nonhomologous end joining and nucleus localization**
CAGL0F06897g		***YIR035C***	**1.69**	**1.67**	**1.56**	**1.05**	**Putative protein with alcohol dehydrogenase domain; gene is downregulated in azole-resistant strain**
CAGL0M05665g		***PBI2***	**1.69**	**1.94**	**1.10**	**3.43**	**Ortholog(s) have endopeptidase inhibitor activity, role in regulation of proteolysis, vacuole fusion, non-autophagic and fungal-type vacuole, nucleus localization**

Table B-1. (Continued).

C. glabrata designation	*C. glabrata* gene names	*S. cerevisiae* orthologs	SM1Δ*jjj1* vs SM1		SM1Δ*jjj1*Δ*pdr1* vs SM1		Description
			Exp. 1	Exp. 2	Exp. 1	Exp. 2	
CAGL0D04246g		***VPS20***	**1.69**	**2.43**	**1.43**	**1.90**	**Ortholog(s) have role in cellular response to lithium ion, cellular response to pH, filamentous growth of a population of unicellular organisms in response to neutral pH and intralumenal vesicle formation, more**
CAGL0L02453g			**1.69**	**1.52**	**1.26**	**1.67**	**Protein of unknown function**
CAGL0M02343g		*ATG5*	1.68	2.37	1.69	1.83	Ortholog(s) have Atg8 ligase activity, enzyme activator activity
CAGL0E03762g		*RIM101*	1.68	2.11	1.83	2.24	Ortholog(s) have RNA polymerase II core promoter proximal region sequence-specific DNA binding transcription factor activity involved in negative regulation of transcription, sequence-specific DNA binding activity
CAGL0H10384g		***RRP42***	**1.68**	**1.58**	**1.64**	**1.05**	**Ortholog(s) have role in exonucleolytic trimming to generate mature 3'-end of 5.8S rRNA from tricistronic rRNA transcript (SSU-rRNA, 5.8S rRNA, LSU-rRNA), nuclear polyadenylation-dependent tRNA catabolic process, rRNA catabolic process**
CAGL0J00429g	***COX6***	***COX6***	**1.68**	**2.34**	**1.38**	**2.82**	**Cytochrome c oxidase subunit VI**
CAGL0F03047g		*SIP1*	1.68	2.61	1.52	3.12	Ortholog(s) have AMP-activated protein kinase activity, receptor signaling complex scaffold activity
CAGL0C02623g		*COX8*	1.68	3.17	2.79	3.13	Ortholog(s) have cytochrome-c oxidase activity, role in mitochondrial electron transport, cytochrome c to oxygen and mitochondrial respiratory chain complex IV, plasma membrane localization
CAGL0A00451g	***PDR1***	***PDR1***	**1.68**	**2.66**	**-10.23**	**-5.16**	**Zinc finger transcription factor, activator of drug resistance genes via pleiotropic drug response elements (PDRE); regulates drug efflux pumps and controls multi-drug resistance; gene upregulated and/or mutated in azole-resistant strains**
CAGL0L07238g		***RPN6***	**1.67**	**2.21**	**1.23**	**1.68**	**Ortholog(s) have structural molecule activity, role in proteasome assembly, ubiquitin-dependent protein catabolic process and nucleus, proteasome regulatory particle, lid subcomplex, proteasome storage granule localization**
CAGL0G02717g		*SGA1*	1.67	1.75	1.60	2.72	Ortholog(s) have glucan 1,4-alpha-glucosidase activity, role in glycogen catabolic process and Golgi apparatus, endoplasmic reticulum, fungal-type vacuole, prospore membrane localization

Table B-1. (Continued).

C. glabrata designation	*C. glabrata* gene names	*S. cerevisiae* orthologs	SM1Δ*jjj1* vs SM1		SM1Δ*jjj1*Δ*pdr1* vs SM1		Description
			Exp. 1	Exp. 2	Exp. 1	Exp. 2	
CAGL0D01837g			**1.67**	**3.00**	**-1.50**	**2.50**	**Unknown**
CAGL0J06088g		***YNL162W-A***	**1.67**	**2.20**	**1.44**	**2.60**	**Ortholog(s) have cytoplasm, nucleus localization**
CAGL0E04004g		***MUP3***	**1.66**	**2.17**	**1.41**	**3.03**	**Ortholog(s) have L-methionine transmembrane transporter activity and role in methionine import**
CAGL0J08184g		***CAN1***	**1.66**	**1.67**	**1.28**	**2.51**	**Ortholog(s) have arginine transmembrane transporter activity, role in arginine transport, transmembrane transport and membrane raft, mitochondrion, plasma membrane localization**
CAGL0D05082g		***UBI4***	**1.65**	**1.82**	**1.24**	**8.37**	**Ortholog(s) have protein tag activity and role in cell morphogenesis, cellular response to heat, filamentous growth of a population of unicellular organisms, pathogenesis, phenotypic switching, protein ubiquitination**
CAGL0G01969g		***VHS3***	**1.65**	**1.63**	**1.38**	**-1.85**	**Ortholog(s) have phosphopantothenoylcysteine decarboxylase activity, protein phosphatase inhibitor activity and role in cellular monovalent inorganic cation homeostasis**
CAGL0I03366g		***FAP7***	**1.65**	**1.93**	**1.78**	**-1.50**	**Ortholog(s) have ATP binding, nucleoside-triphosphatase activity**
CAGL0D02420g		***SRN2***	**1.65**	**1.68**	**1.38**	**2.44**	**Ortholog(s) have role in protein targeting to membrane, protein targeting to vacuole and ESCRT I complex localization**
CAGL0I00110g			1.64	1.56	1.65	2.31	Putative adhesin-like with multiple tandem repeats; ORF appears artificially broken into fragments due to sequencing errors; belongs to adhesin cluster III; predicted GPI-anchor
CAGL0H02343g		*SAP30*	1.64	2.09	1.73	2.05	Ortholog(s) have histone deacetylase activity
CAGL0L10186g		*TMC1*	1.64	3.33	1.82	6.54	Putative stress-induced protein; gene is upregulated in azole-resistant strain
CAGL0L00935g	***APQ12***	***APQ12***	**1.64**	**1.86**	**1.48**	**1.61**	**Ortholog(s) have role in cellular lipid metabolic process, mRNA export from nucleus, nuclear envelope organization and endoplasmic reticulum, nuclear envelope localization**
CAGL0A02233g	***HXT4/6/7***		**1.64**	**3.14**	**1.12**	**3.04**	**Has domain(s) with predicted substrate-specific transmembrane transporter activity, transmembrane transporter activity, role in transmembrane transport and integral component of membrane, membrane localization**

Table B-1. (Continued).

C. glabrata designation	*C. glabrata* gene names	*S. cerevisiae* orthologs	SM1Δ*jjj1* vs SM1		SM1Δ*jjj1*Δ*pdr1* vs SM1		Description
			Exp. 1	Exp. 2	Exp. 1	Exp. 2	
CAGL0K04257g		*RME1|VMA9*	1.63	2.55	1.83	4.43	Ortholog(s) have ATPase activity, coupled to transmembrane movement of ions, RNA polymerase II core promoter proximal region sequence-specific DNA binding, sequence-specific DNA binding RNA polymerase II transcription factor activity
CAGL0A02211g	***HXT6/7***		**1.62**	**2.42**	**1.02**	**2.87**	**Has domain(s) with predicted substrate-specific transmembrane transporter activity, transmembrane transporter activity, role in transmembrane transport and integral component of membrane, membrane localization**
CAGL0H09328g		***QCR9***	**1.62**	**2.36**	**-1.03**	**3.02**	**Ortholog(s) have ubiquinol-cytochrome-c reductase activity and role in aerobic respiration, iron-sulfur cluster assembly, mitochondrial electron transport, ubiquinol to cytochrome c**
CAGL0E05456g			**1.62**	**1.90**	**1.77**	**-3.60**	**Has domain(s) with predicted DNA binding activity**
CAGL0J09306g		***VCX1***	**1.62**	**1.68**	**1.33**	**2.78**	**Ortholog(s) have calcium:proton antiporter activity, potassium:proton antiporter activity and role in calcium ion transport, cellular calcium ion homeostasis, transmembrane transport**
CAGL0G03531g		***SPR6***	**1.62**	**1.61**	**1.32**	**-1.01**	**Ortholog(s) have mitochondrion localization**
CAGL0L09086g		***CIT3***	**1.61**	**1.76**	**1.13**	**1.50**	**Ortholog(s) have 2-methylcitrate synthase activity, citrate (Si)-synthase activity, role in propionate catabolic process, 2-methylcitrate cycle, tricarboxylic acid cycle and mitochondrion localization**
CAGL0L09185g		***YFR006W***	**1.61**	**2.15**	**1.15**	**1.66**	**Ortholog(s) have cytoplasm localization**
CAGL0D05522g		***EMC6***	**1.60**	**1.96**	**1.06**	**1.30**	**Ortholog(s) have role in protein folding in endoplasmic reticulum and ER membrane protein complex localization**
CAGL0L01485g		***GSF2***	**1.60**	**2.52**	**1.19**	**2.54**	**Putative protein of the ER membrane involved in hexose transporter secretion; gene is upregulated in azole-resistant strain**
CAGL0H00286g		***YPR172W***	**1.60**	**2.28**	**1.10**	**1.29**	**Ortholog(s) have cytoplasm, nucleus localization**
CAGL0K10604g		***CMK2***	**1.60**	**2.03**	**1.25**	**2.00**	**Ortholog(s) have calmodulin-dependent protein kinase activity, role in cellular response to oxidative stress, fungal-type cell wall organization, protein phosphorylation and cytoplasm localization**

Table B-1. (Continued).

C. glabrata designation	*C. glabrata* gene names	*S. cerevisiae* orthologs	SM1Δ*jjj1* vs SM1		SM1Δ*jjj1*Δ*pdr1* vs SM1		Description
			Exp. 1	Exp. 2	Exp. 1	Exp. 2	
CAGL0C02233g		*MXR1*	1.60	3.51	1.84	3.86	Ortholog(s) have L-methionine-(S)-S-oxide reductase activity, peptide-methionine (S)-S-oxide reductase activity and role in L-methionine biosynthetic process from methionine sulphoxide, cellular response to hydrogen peroxide
CAGL0F03135g		*RPN9*	1.60	2.26	1.52	2.33	Ortholog(s) have structural molecule activity, role in proteasome assembly, ubiquitin-dependent protein catabolic process and nucleus, proteasome regulatory particle, lid subcomplex, proteasome storage granule localization
CAGL0M11473g			**1.60**	**2.22**	**1.40**	**-2.25**	**Unknown**
CAGL0M08404g		***TPK3***	**1.60**	**2.02**	**1.46**	**-1.18**	**Ortholog(s) have cAMP-dependent protein kinase activity and role in Ras protein signal transduction, mitochondrion organization, protein kinase A signaling, protein phosphorylation**
CAGL0G05467g		***GCR2***	**1.59**	**1.79**	**1.14**	**2.87**	**Ortholog(s) have RNA polymerase II activating transcription factor binding, RNA polymerase II transcription factor binding transcription factor activity**
CAGL0A04829g			**1.59**	**3.18**	**1.20**	**5.49**	**Putative hexokinase isoenzyme 2; protein differentially expressed in azole-resistant strain**
CAGL0G04807g		***VAM3***	**1.58**	**1.68**	**1.17**	**2.11**	**Ortholog(s) have SNAP receptor activity**
CAGL0L06204g		***COX13***	**1.58**	**1.90**	**1.18**	**2.36**	**Ortholog(s) have cytochrome-c oxidase activity, enzyme regulator activity, role in aerobic respiration, mitochondrial respiratory chain supercomplex assembly and mitochondrial respiratory chain complex IV, plasma membrane localization**
CAGL0H08844g		*DDR48*	1.58	1.66	1.60	15.23	Putative adhesin-like protein
CAGL0F04477g		***PRE7***	**1.58**	**2.17**	**1.49**	**2.21**	**Ortholog(s) have role in proteasomal ubiquitin-independent protein catabolic process, proteasome-mediated ubiquitin-dependent protein catabolic process and cytosol, nucleus, proteasome core complex, beta-subunit complex localization**
CAGL0C05489g		***GYP7***	**1.57**	**1.75**	**1.29**	**2.36**	**Ortholog(s) have GTPase activator activity, role in regulation of vacuole fusion, non-autophagic, vesicle-mediated transport and cytosol, nucleus localization**
CAGL0C03916g			**1.57**	**1.65**	**1.31**	**2.13**	**Has domain(s) with predicted role in protein glycosylation**

Table B-1. (Continued).

C. glabrata designation	*C. glabrata* gene names	*S. cerevisiae* orthologs	SM1Δ*jjj1* vs SM1		SM1Δ*jjj1*Δ*pdr1* vs SM1		Description
			Exp. 1	Exp. 2	Exp. 1	Exp. 2	
CAGL0H07997g	***KNH1***	***KNH1***	**1.57**	**1.83**	**1.50**	**1.42**	**Protein involved in cell wall beta 1,6-glucan synthesis, similar to Kre9p**
CAGL0B00858g		*STE50*	1.57	3.01	1.54	3.77	Ortholog(s) have SAM domain binding, protein kinase regulator activity
CAGL0J07216g		***RAD17***	**1.57**	**2.11**	**1.25**	**1.75**	**Ortholog(s) have double-stranded DNA binding activity and role in double-strand break repair, intra-S DNA damage checkpoint, mitotic DNA replication checkpoint, mitotic G2 DNA damage checkpoint, reciprocal meiotic recombination**
CAGL0G04543g		*VPS60*	1.57	1.93	1.70	1.78	Ortholog(s) have role in cellular response to drug, filamentous growth, late endosome to vacuole transport via multivesicular body sorting pathway and fungal-type vacuole membrane localization
CAGL0L06754g		***SUP45***	**1.56**	**1.72**	**1.39**	**-1.25**	**Ortholog(s) have translation release factor activity, codon specific activity and role in DNA-templated transcription, termination, asexual sporulation resulting in formation of a cellular spore, cytoplasmic translational termination**
CAGL0D06688g	***ALD4***	***ALD4***	**1.56**	**2.12**	**1.27**	**3.89**	**Ortholog(s) have aldehyde dehydrogenase (NAD) activity, aldehyde dehydrogenase [NAD(P)+] activity and role in NADPH regeneration, acetate biosynthetic process, ethanol metabolic process, pyruvate metabolic process**
CAGL0I00836g			**1.56**	**1.59**	**1.29**	**3.38**	**Ortholog(s) have Golgi apparatus, endoplasmic reticulum, fungal-type vacuole membrane localization**
CAGL0G02893g		*POS5*	1.55	1.69	1.55	1.95	Ortholog(s) have NADH kinase activity, role in NADP biosynthetic process, cellular response to oxidative stress and mitochondrial matrix localization
CAGL0D06402g	*MET15*	*MET17*	1.55	2.23	1.81	6.58	O-acetyl homoserine sulfhydrylase (OAHSH), ortholog of S. cerevisiae MET17; required for utilization of inorganic sulfate as sulfur source; able to utilize cystine as a sulfur source while S. cerevisiae met15 mutants are unable to do so
CAGL0F06941g	*PYC1*		1.55	2.89	1.60	4.48	Putative pyruvate carboxylase isoform; gene is upregulated in azole-resistant strain

Table B-1. (Continued).

C. glabrata designation	*C. glabrata* gene names	*S. cerevisiae* orthologs	SM1Δ*jjj1* vs SM1		SM1Δ*jjj1*Δ*pdr1* vs SM1		Description
			Exp. 1	Exp. 2	Exp. 1	Exp. 2	
CAGL0K04103g		***CAX4***	**1.55**	**1.70**	**1.17**	**1.27**	**Ortholog(s) have dolichyldiphosphatase activity, role in lipid biosynthetic process, protein N-linked glycosylation and integral component of endoplasmic reticulum membrane localization**
CAGL0I09702g		***MCH5***	**1.55**	**1.76**	**1.70**	**1.14**	**Ortholog(s) have riboflavin transporter activity, role in riboflavin transport and plasma membrane localization**
CAGL0L03289g			**1.55**	**1.87**	**1.37**	**-1.15**	**Protein of unknown function**
CAGL0K10868g	*CTA1*	*CTA1*	1.54	1.64	1.97	4.66	Putative catalase A; gene is downregulated in azole-resistant strain; regulated by oxidative stress and glucose starvation; protein abundance increased in ace2 mutant cells
CAGL0E01881g	*YPS11*		1.54	1.97	1.50	3.48	Putative aspartic protease; member of a YPS gene cluster that is required for virulence in mice; induced in response to low pH and high temperature
CAGL0F01243g		***MDM38***	**1.53**	**2.05**	**1.24**	**2.67**	**Ortholog(s) have ribosome binding activity**
CAGL0M05445g		***COS111***	**1.53**	**1.59**	**1.30**	**2.99**	**Ortholog(s) have role in signal transduction and mitochondrion localization**
CAGL0H05379g		***GCR1***	**1.53**	**1.82**	**1.10**	**-1.46**	**Ortholog(s) have RNA polymerase II core promoter proximal region sequence-specific DNA binding, more**
CAGL0B03443g		***MCP2***	**1.53**	**1.68**	**1.35**	**3.50**	**Ortholog(s) have role in lipid homeostasis, mitochondrion organization and integral component of mitochondrial membrane, mitochondrial inner membrane localization**
CAGL0D02156g		***GNA1***	**1.53**	**1.92**	**1.20**	**2.24**	**Ortholog(s) have glucosamine 6-phosphate N-acetyltransferase activity, role in UDP-N-acetylglucosamine biosynthetic process, pathogenesis and cytosol, nucleus localization**
CAGL0J02530g			1.53	2.27	1.92	4.41	Putative adhesion protein; predicted GPI-anchor; belongs to adhesin cluster VI
CAGL0F00605g	***GLK1***	***EMI2***	**1.53**	**2.89**	**1.16**	**7.91**	**Aldohexose specific glucokinase**
CAGL0J04048g			**1.53**	**1.67**	**1.47**	**1.83**	**Has domain(s) with predicted iron ion binding, iron-sulfur cluster binding activity and role in iron-sulfur cluster assembly**
CAGL0L08932g	***LSP1***	***LSP1***	**1.53**	**1.89**	**1.29**	**2.90**	**Long chain base-responsive inhibitor of protein kinases; protein abundance decreased in ace2 mutant cells**
CAGL0L04378g		***PNS1***	**1.53**	**1.50**	**1.36**	**2.09**	**Ortholog(s) have plasma membrane localization**

Table B-1. (Continued).

C. glabrata designation	*C. glabrata* gene names	*S. cerevisiae* orthologs	SM1Δ*jjj1* vs SM1		SM1Δ*jjj1*Δ*pdr1* vs SM1		Description
			Exp. 1	Exp. 2	Exp. 1	Exp. 2	
CAGL0K06985g		***ERT1***	**1.53**	**2.17**	**1.58**	**1.09**	**Ortholog(s) have RNA polymerase II core promoter proximal region sequence-specific DNA binding transcription factor activity involved in negative regulation of transcription, more**
CAGL0J04554g			1.53	4.11	1.77	5.72	Has domain(s) with predicted catalytic activity, pyridoxal phosphate binding, transaminase activity and role in biosynthetic process, cellular amino acid metabolic process
CAGL0F04741g			**1.53**	**1.67**	**1.32**	**3.32**	**Ortholog(s) have calmodulin binding, calmodulin-dependent protein kinase activity**
CAGL0K10824g		***YLR149C***	**1.52**	**1.52**	**1.11**	**2.58**	**Ortholog of S. cerevisiae : YLR149C, C. albicans SC5314 : C7_03280C_A, C. dubliniensis CD36 : Cd36_72930, C. parapsilosis CDC317 : CPAR2_704080 and Candida tenuis NRRL Y-1498 : CANTEDRAFT_112372**
CAGL0H09768g		***FMP52***	**1.52**	**2.79**	**1.13**	**1.73**	**Ortholog(s) have endoplasmic reticulum, mitochondrial outer membrane localization**
CAGL0F02717g	***PDH1***	***PDR15***	**1.51**	**2.15**	**-1.17**	**5.10**	**Multidrug transporter, predicted plasma membrane ATP-binding cassette (ABC) transporter; regulated by Pdr1p; involved in fluconazole resistance**
CAGL0M12837g		*SER33*	1.51	1.77	1.58	2.09	Ortholog(s) have phosphoglycerate dehydrogenase activity, role in serine family amino acid biosynthetic process and cytosol localization
CAGL0D00198g		***BDH1***	**1.51**	**2.46**	**1.08**	**4.59**	**Ortholog(s) have (R,R)-butanediol dehydrogenase activity, role in butanediol biosynthetic process and cytoplasm localization**
CAGL0G01672g		***RPN7***	**1.51**	**1.56**	**1.35**	**1.95**	**Ortholog(s) have structural molecule activity, role in positive regulation of mitotic metaphase/anaphase transition and cytosol, nucleus, proteasome regulatory particle, lid subcomplex localization**
CAGL0L05390g		***ARC19***	**1.51**	**1.77**	**1.46**	**2.43**	**Ortholog(s) have structural molecule activity and role in Arp2/3 complex-mediated actin nucleation, actin cortical patch assembly, cellular response to drug, spore germination**
CAGL0E00231g			**1.51**	**2.26**	**1.60**	**-1.06**	**Putative adhesin-like protein; contains tandem repeats and a predicted GPI-anchor; belongs to adhesin cluster III**
CAGL0D03234g			**1.50**	**1.97**	**1.15**	**2.50**	**Has domain(s) with predicted phosphatase activity**

Table B-1. (Continued).

C. glabrata designation	*C. glabrata* gene names	*S. cerevisiae* orthologs	SM1Δ*jjj1* vs SM1		SM1Δ*jjj1*Δ*pdr1* vs SM1		Description
			Exp. 1	Exp. 2	Exp. 1	Exp. 2	
CAGL0B03047g	***ILV5***	***ILV5***	**1.50**	**1.76**	**1.44**	**3.06**	**Ketol-acid reducto-isomerase; mass spectrometry data indicates this gene is likely to be protein-coding**
CAGL0I10200g	***PWP3***		**1.50**	**1.93**	**1.33**	**2.58**	**Protein with tandem repeats; putative adhesin-like protein; belongs to adhesin cluster II**
CAGL0K06380g			1.50	3.08	1.64	5.25	Unknown
CAGL0E02937g		*CGR1*	1.50	2.75	1.92	1.75	Ortholog(s) have role in cellular response to drug, rRNA processing and nucleolus, preribosome, large subunit precursor localization
CAGL0B00374g		***ADF1***	**1.50**	**2.67**	**1.50**	**1.17**	**Ortholog(s) have RNA polymerase II regulatory region DNA binding activity**
CAGL0I05434g		***TOA2***	**1.50**	**2.41**	**-1.56**	**-1.55**	**Ortholog(s) have TBP-class protein binding, TBP-class protein binding RNA polymerase II transcription factor activity involved in preinitiation complex assembly activity**

Notes: Fold change is defined as the ratio of gene expression in SM1Δ*jjj1* compared to SM1 in two independent RNA-seq experiments. Bolded rows indicate genes whose up-regulation is dependent on *PDR1* expression.

Table B-2. Genes down-regulated by at least 1.5-fold in SM1Δ*jjj1* versus SM1.

C. glabrata designation	*C. glabrata* gene names	*S. cerevisiae* orthologs	SM1Δ*jjj1* vs SM1		SM1Δ*jjj1*Δ*pdr1* vs SM1		Description
			Exp. 1	Exp. 2	Exp. 1	Exp. 2	
CAGL0J07370g		*JJJ1*	-19.95	-12.84	-12.67	-11.37	Ortholog(s) have ATPase activator activity and role in endocytosis, rRNA processing, regulation of cell size, ribosomal large subunit biogenesis, ribosomal large subunit export from nucleus
CAGL0B02651g		*MET31*	-10.00	-1.57	-3.33	-1.83	Ortholog(s) have core promoter proximal region sequence-specific DNA binding, sequence-specific transcription regulatory region DNA binding RNA polymerase II transcription factor recruiting transcription factor activity
CAGL0L01023g			**-8.00**	**-2.33**	**-2.00**	**1.29**	**Protein of unknown function**
CAGL0B02475g	***PHO84***	***PHO84***	**-7.70**	**-3.75**	**-2.99**	**-1.12**	**Ortholog(s) have inorganic phosphate transmembrane transporter activity, manganese ion transmembrane transporter activity, phosphate:proton symporter activity, selenite:proton symporter activity**
CAGL0M07359g		***LEE1***	**-7.00**	**-1.71**	**1.14**	**1.08**	**Has domain(s) with predicted nucleic acid binding, zinc ion binding activity**
CAGL0F00116g			-6.00	-1.80	-2.00	-2.25	Protein of unknown function
CAGL0L11990g		***GRX4***	**-5.46**	**-2.90**	**-2.37**	**2.36**	**Ortholog(s) have RNA polymerase II activating transcription factor binding, disulfide oxidoreductase activity**
CAGL0M10912g		***HUB1***	**-5.00**	**-1.50**	**-1.67**	**1.17**	**Ortholog(s) have protein tag activity, role in cell morphogenesis involved in conjugation with cellular fusion, cellular protein modification process, mRNA cis splicing, via spliceosome and cytosol, mating projection, nucleus localization**
CAGL0I01936g		***SPO16***	**-4.67**	**-4.67**	**-1.75**	**-1.40**	**Ortholog(s) have role in ascospore formation, positive regulation of protein sumoylation, regulation of reciprocal meiotic recombination, synaptonemal complex assembly and condensed nuclear chromosome localization**
CAGL0J00451g			**-4.61**	**-2.04**	**-2.64**	**1.81**	**Putative glyceraldehyde-3-phosphate dehydrogenase; protein differentially expressed in azole-resistant strain; expression downregulated in biofilm vs planktonic cell culture**
CAGL0K01529g		*SLM3*	-4.41	-2.62	-2.27	-1.74	Ortholog(s) have tRNA (5-methylaminomethyl-2-thiouridylate)-methyltransferase activity, role in mitochondrial tRNA thio-modification and mitochondrion localization

Table B-2. (Continued).

C. glabrata designation	*C. glabrata* gene names	*S. cerevisiae* orthologs	SM1Δ*jjj1* vs SM1		SM1Δ*jjj1*Δ*pdr1* vs SM1		Description
			Exp. 1	Exp. 2	Exp. 1	Exp. 2	
CAGL0G00105g			**-4.33**	**-1.50**	**-1.30**	**-3.75**	**Protein of unknown function**
CAGL0G08734g		*RPL9B*	-4.27	-4.10	-4.02	-3.89	Ortholog(s) have structural constituent of ribosome activity, role in cytoplasmic translation and cytosolic large ribosomal subunit, nucleus localization
CAGL0A03102g	*ARO10*	*ARO10*	-4.17	-3.41	-2.15	-3.11	Ortholog(s) have phenylpyruvate decarboxylase activity
CAGL0M00308g			**-4.00**	**-6.00**	**-2.00**	**1.00**	**Protein of unknown function**
CAGL0D00105g			**-4.00**	**-2.00**	**-1.71**	**-1.14**	**Protein of unknown function**
CAGL0D00869g			**-4.00**	**-1.75**	**1.00**	**-3.50**	**Unknown**
CAGL0F09141g			**-4.00**	**-1.67**	**-4.00**	**1.40**	**Protein of unknown function**
CAGL0G06050g			**-3.95**	**-3.59**	**-1.79**	**3.97**	**Protein of unknown function**
CAGL0L13431g			-3.92	-2.38	-2.32	-7.13	Unknown
CAGL0H06809g		***VPS51***	**-3.75**	**-2.14**	**1.07**	**1.33**	**Putative component of Golgi-associated retrograde protein complex; gene is upregulated in azole-resistant strain**
CAGL0M00792g			-3.71	-1.90	-1.86	-2.11	Protein of unknown function
CAGL0J09174g		***YDL186W***	**-3.50**	**-2.00**	**-1.75**	**-1.33**	**Ortholog of S. cerevisiae : YDL186W and Saccharomyces cerevisiae S288C : YDL186W**
CAGL0A00627g		*ERP6*	-3.42	-2.69	-2.93	-2.06	Ortholog(s) have role in ER to Golgi vesicle-mediated transport and mitochondrion localization
CAGL0G00946g		***ERV1***	**-3.30**	**-9.75**	**-1.43**	**-3.90**	**Ortholog(s) have flavin-linked sulfhydryl oxidase activity and role in cellular iron ion homeostasis, cellular response to oxidative stress, protein import into mitochondrial intermembrane space**
CAGL0C00110g	***EPA6***		**-3.08**	**-1.55**	**-3.35**	**1.11**	**Sub-telomerically encoded adhesin with a role in cell adhesion; binds to ligands containing a terminal galactose residue; expressed during murine urinary tract infection, biofilm-upregulated; belongs to adhesin cluster I**
CAGL0I03520g		***YDL157C***	**-3.00**	**-2.20**	**-1.29**	**1.00**	**Ortholog(s) have mitochondrion localization**
CAGL0I02068g		***REC104***	**-3.00**	**-2.00**	**1.17**	**1.17**	**Ortholog(s) have role in reciprocal meiotic recombination and condensed nuclear chromosome localization**
CAGL0I10010g		***CUR1***	**-2.91**	**-3.70**	**-1.60**	**1.00**	**Ortholog(s) have chaperone binding activity, role in cellular response to heat, intracellular protein transport, protein folding, protein localization to nucleus and nucleus localization**

Table B-2. (Continued).

C. glabrata designation	*C. glabrata* gene names	*S. cerevisiae* orthologs	SM1Δ*jjj1* vs SM1		SM1Δ*jjj1*Δ*pdr1* vs SM1		Description
			Exp. 1	Exp. 2	Exp. 1	Exp. 2	
CAGL0F08767g			-2.88	-1.81	-3.29	-1.71	Protein of unknown function
CAGL0E04092g	*SIT1*	*ARN1*	-2.85	-5.53	-2.11	-2.94	Putative siderophore-iron transporter with 14 transmembrane domains; required for iron-dependent survival in macrophages; mRNA levels elevated under iron deficiency conditions; plasma membrane localized
CAGL0I01914g			**-2.80**	**-3.00**	**-1.40**	**1.13**	**Protein of unknown function**
CAGL0D00116g			**-2.80**	**-2.38**	**-1.40**	**-1.58**	**Protein of unknown function**
CAGL0A04389g		***CMC2***	**-2.78**	**-1.95**	**-1.61**	**1.68**	**Ortholog(s) have role in mitochondrial respiratory chain complex assembly and mitochondrial intermembrane space, nucleus localization**
CAGL0F07755g	***CEP3***	***CEP3***	**-2.72**	**-1.60**	**1.03**	**-1.89**	**Centromere binding factor 3b; inner kinetochore protein**
CAGL0J11979g			**-2.67**	**-2.83**	**1.00**	**-1.89**	**Protein of unknown function**
CAGL0M04620g			**-2.67**	**-2.40**	**-1.14**	**1.25**	**Unknown**
CAGL0L13376g			-2.66	-6.68	-2.69	-2.14	Unknown
CAGL0A01243g	***GIT1***		**-2.65**	**-3.09**	**-2.29**	**1.01**	**Has domain(s) with predicted transmembrane transporter activity, role in transmembrane transport and integral component of membrane localization**
CAGL0I01232g		*ERP5*	-2.60	-5.88	-2.29	-5.88	Has domain(s) with predicted role in transport and integral component of membrane localization
CAGL0L11286g		***SMA2***	**-2.57**	**-1.62**	**-1.29**	**-1.42**	**Ortholog(s) have role in ascospore wall assembly, spore membrane bending pathway and cytoplasm, prospore membrane localization**
CAGL0F00176g			**-2.50**	**-3.00**	**-1.36**	**1.00**	**Unknown**
CAGL0H08624g		***MCM16***	**-2.50**	**-2.67**	**-1.88**	**-1.28**	**Ortholog(s) have role in establishment of mitotic sister chromatid cohesion and condensed nuclear chromosome kinetochore localization**
CAGL0F05709g		*ATC1*	-2.50	-1.78	-2.36	-1.63	Ortholog(s) have role in bipolar cellular bud site selection, cellular cation homeostasis and cytoplasm, nucleus localization
CAGL0C04917g		***CPA2***	**-2.49**	**-2.19**	**-2.18**	**1.07**	**Ortholog(s) have carbamoyl-phosphate synthase (glutamine-hydrolyzing) activity, role in arginine biosynthetic process and carbamoyl-phosphate synthase complex, mitochondrion localization**

Table B-2. (Continued).

C. glabrata designation	*C. glabrata* gene names	*S. cerevisiae* orthologs	SM1Δ*jjj1* vs SM1		SM1Δ*jjj1*Δ*pdr1* vs SM1		Description
			Exp. 1	Exp. 2	Exp. 1	Exp. 2	
CAGL0I09856g		*SFG1*	-2.40	-2.93	-2.73	-2.12	Ortholog(s) have role in mitotic cell cycle, pseudohyphal growth and cytoplasm, nucleus localization
CAGL0F05951g		***IMP2***	**-2.38**	**-1.65**	**-1.29**	**-1.22**	**Ortholog(s) have endopeptidase activity, role in protein processing involved in protein targeting to mitochondrion and mitochondrial inner membrane peptidase complex localization**
CAGL0H07139g		***MCM21***	**-2.36**	**-1.57**	**-1.51**	**1.29**	**Ortholog(s) have role in establishment of mitotic sister chromatid cohesion and COMA complex localization**
CAGL0G02387g		***PXL1***	**-2.36**	**-2.55**	**-1.33**	**-1.88**	**Ortholog(s) have Rho GDP-dissociation inhibitor activity and role in maintenance of cell polarity, regulation of Rho protein signal transduction**
CAGL0A03740g		***POX1***	**-2.36**	**-1.61**	**-1.82**	**1.14**	**Ortholog(s) have role in fatty acid beta-oxidation, long-chain fatty acid catabolic process and peroxisomal matrix localization**
CAGL0F00110g	***AWP10***		**-2.35**	**-1.68**	**-2.30**	**-1.25**	**Putative adhesin-like protein; GPI-anchored; belongs to adhesin cluster V; ORF appears artificially broken into fragments due to sequencing errors but the gene is likely protein-coding based on mass spectrometry data**
CAGL0K08602g		***SLD2***	**-2.33**	**-2.50**	**-1.93**	**-1.25**	**Ortholog(s) have DNA replication origin binding, single-stranded DNA binding activity**
CAGL0F02849g		*RRP17*	-2.33	-2.29	-1.91	-2.00	Ortholog(s) have role in rRNA processing and cytoplasm localization
CAGL0M05533g	***DUR1,2***	***DUR1,2***	**-2.31**	**-1.98**	**-2.43**	**-1.40**	**Ortholog(s) have allophanate hydrolase activity, urea carboxylase activity, role in cellular response to alkaline pH, nitrogen utilization, pathogenesis, urea catabolic process and cytoplasm localization**
CAGL0K00781g		*YGR210C*	-2.29	-2.35	-2.83	-10.80	Ortholog(s) have cytosol, nucleus localization
CAGL0H03025g		***PAN2***	**-2.28**	**-2.25**	**-2.84**	**-1.32**	**Ortholog(s) have poly(A)-specific ribonuclease activity, role in nuclear-transcribed mRNA poly(A) tail shortening, postreplication repair and PAN complex localization**
CAGL0A03828g		***RAX1***	**-2.27**	**-3.09**	**-1.37**	**-1.42**	**Ortholog(s) have role in cellular bud site selection and cellular bud neck, endoplasmic reticulum localization**

Table B-2. (Continued).

C. glabrata designation	*C. glabrata* gene names	*S. cerevisiae* orthologs	SM1Δ*jjj1* vs SM1		SM1Δ*jjj1*Δ*pdr1* vs SM1		Description
			Exp. 1	Exp. 2	Exp. 1	Exp. 2	
CAGL0M06193g		***SWD3***	**-2.26**	**-2.23**	**-1.43**	**-1.98**	**Ortholog(s) have histone methyltransferase activity (H3-K4 specific) activity, role in chromatin silencing at telomere, histone H3-K4 methylation, telomere maintenance and Set1C/COMPASS complex localization**
CAGL0D06336g		***TYW3***	**-2.25**	**-2.15**	**-1.13**	**-1.65**	**Ortholog(s) have tRNA methyltransferase activity, role in tRNA methylation, wybutosine biosynthetic process and cytosol, nucleus localization**
CAGL0K03619g		***SPC24***	**-2.25**	**-2.13**	**-2.25**	**-1.42**	**Ortholog(s) have structural constituent of cytoskeleton activity, role in chromosome segregation, microtubule nucleation and Ndc80 complex, condensed nuclear chromosome kinetochore localization**
CAGL0C02211g	*UTR2*	*UTR2*	-2.22	-3.18	-2.28	-2.27	Putative glycoside hydrolase of the Crh family; predicted GPI-anchor
CAGL0C05115g	***ARG1***	***ARG1***	**-2.19**	**-1.86**	**-2.10**	**-1.08**	**Argininosuccinate synthetase**
CAGL0B04675g		***YCL001W-B***	**-2.19**	**-4.43**	**-3.13**	**1.12**	**Has domain(s) with predicted role in RNA surveillance, nuclear-transcribed mRNA catabolic process, no-go decay, nuclear-transcribed mRNA catabolic process, non-stop decay**
CAGL0K09570g			-2.17	-1.70	-1.67	-2.50	Has domain(s) with predicted phosphotransferase activity, for other substituted phosphate groups activity, role in phospholipid biosynthetic process and membrane localization
CAGL0I08613g	*DUR3*		-2.15	-3.10	-2.17	-5.69	Putative plasma membrane polyamine transporter
CAGL0J06402g			**-2.14**	**-1.77**	**-1.55**	**1.04**	**Has domain(s) with predicted catalytic activity, homocitrate synthase activity and role in lysine biosynthetic process via aminoadipic acid**
CAGL0L12782g		*DIG1*	-2.12	-1.59	-1.85	-5.36	Ortholog(s) have DNA binding, transcription factor binding activity
CAGL0B02717g		*ACS2*	-2.11	-2.52	-1.96	-2.36	Ortholog(s) have acetate-CoA ligase activity, acid-ammonia (or amide) ligase activity and role in acetate catabolic process, acetyl-CoA biosynthetic process, carbon utilization, histone acetylation, replicative cell aging
CAGL0L01243g		*GDA1*	-2.11	-1.92	-2.01	-4.86	Ortholog(s) have guanosine-diphosphatase activity, uridine-diphosphatase activity

Table B-2. (Continued).

C. glabrata designation	*C. glabrata* gene names	*S. cerevisiae* orthologs	SM1Δ*jjj1* vs SM1		SM1Δ*jjj1*Δ*pdr1* vs SM1		Description
			Exp. 1	Exp. 2	Exp. 1	Exp. 2	
CAGL0L10648g		***CLN2***	**-2.10**	**-3.71**	**-1.91**	**-1.39**	**Ortholog(s) have cyclin-dependent protein serine/threonine kinase regulator activity**
CAGL0J00968g			-2.09	-2.69	-1.71	-1.75	Unknown
CAGL0M08602g		***CCC2***	**-2.09**	**-1.63**	**-1.78**	**-1.38**	**Ortholog(s) have cation-transporting ATPase activity, copper ion binding activity and role in cellular iron ion homeostasis, copper ion export, pigment metabolic process involved in developmental pigmentation**
CAGL0F08019g	*PEX21*		-2.06	-2.19	-2.85	-1.67	Protein of unknown function
CAGL0M09383g		***SEA4***	**-2.03**	**-1.91**	**-1.22**	**-1.22**	**Ortholog(s) have Seh1-associated complex, cytosol, extrinsic component of fungal-type vacuolar membrane localization**
CAGL0M03311g		*GTT3*	-2.02	-2.11	-2.26	-2.20	Ortholog(s) have plasma membrane localization
CAGL0L09581g		*DUT1*	-2.01	-1.80	-1.96	-3.79	Ortholog(s) have dITP diphosphatase activity, dUTP diphosphatase activity, role in dITP catabolic process, dUTP catabolic process and cytoplasm, nucleus localization
CAGL0M07854g		***LSM8***	**-2.00**	**-7.00**	**1.00**	**-1.75**	**Ortholog(s) have RNA binding activity, role in mRNA splicing, via spliceosome and U4/U6 x U5 tri-snRNP complex, U6 snRNP, nucleolus localization**
CAGL0L09999g		***BSC2***	**-2.00**	**-3.67**	**-2.00**	**1.27**	**Ortholog(s) have lipid particle localization**
CAGL0M00110g	*AWP11*		-2.00	-2.33	-2.67	-1.75	Putative adhesin-like protein; GPI-anchored; belongs to adhesin cluster V; ORF appears artificially broken into fragments due to sequencing errors but the gene is likely protein-coding based on mass spectrometry data
CAGL0L06050g		*MND1*	-2.00	-2.30	-2.67	-2.56	Ortholog(s) have double-stranded DNA binding activity, role in reciprocal meiotic recombination and condensed nuclear chromosome localization
CAGL0J06006g		***GIM3***	**-2.00**	**-2.00**	**-2.00**	**1.13**	**Ortholog(s) have tubulin binding activity, role in positive regulation of transcription elongation from RNA polymerase II promoter, tubulin complex assembly and cytoplasm, prefoldin complex localization**
CAGL0G03289g	***SSA3***	***SSA4***	**-2.00**	**-1.54**	**-1.69**	**1.66**	**Heat shock protein of the HSP70 family**
CAGL0E01969g		*SMF1*	-2.00	-2.58	-2.09	-1.71	Ortholog(s) have inorganic cation transmembrane transporter activity, solute:proton symporter activity

Table B-2. (Continued).

C. glabrata designation	*C. glabrata* gene names	*S. cerevisiae* orthologs	SM1Δ*jjj1* vs SM1		SM1Δ*jjj1*Δ*pdr1* vs SM1		Description
			Exp. 1	Exp. 2	Exp. 1	Exp. 2	
CAGL0D06314g			**-1.99**	**-1.64**	**-1.53**	**-1.07**	**Has domain(s) with predicted DNA binding, RNA binding activity and role in RNA metabolic process**
CAGL0B02145g		*SKG6*	-1.98	-6.24	-1.67	-3.60	Ortholog(s) have cell cortex, cellular bud neck, cellular bud tip, incipient cellular bud site, integral component of membrane localization
CAGL0J00517g		*RRM3*	-1.98	-2.32	-1.76	-1.73	Ortholog(s) have ATP-dependent DNA helicase activity and role in DNA replication, G-quadruplex DNA unwinding, mitochondrial genome maintenance, replication fork progression beyond termination site
CAGL0I04818g		***CHS2***	**-1.98**	**-1.72**	**-1.71**	**-1.24**	**Ortholog(s) have chitin synthase activity**
CAGL0I10791g		***ARG3***	**-1.98**	**-2.09**	**-1.53**	**1.19**	**Ortholog(s) have ornithine carbamoyltransferase activity, role in arginine biosynthetic process via ornithine, asexual sporulation and cytosol, mitochondrial matrix localization**
CAGL0F04323g		*POL12*	-1.97	-3.26	-1.71	-2.36	Ortholog(s) have DNA-directed DNA polymerase activity, role in DNA replication initiation, telomere capping and alpha DNA polymerase:primase complex, cytosol, nuclear envelope localization
CAGL0B04851g		***BUD3***	**-1.95**	**-2.04**	**-1.94**	**-1.11**	**Ortholog(s) have role in axial cellular bud site selection, cytogamy and cellular bud neck contractile ring localization**
CAGL0M00682g		***YLR446W***	**-1.94**	**-2.53**	**1.03**	**-1.09**	**Has domain(s) with predicted ATP binding, phosphotransferase activity, alcohol group as acceptor activity and role in carbohydrate metabolic process**
CAGL0L01793g		***SPC42***	**-1.94**	**-1.88**	**-1.14**	**-1.69**	**Ortholog(s) have structural constituent of cytoskeleton activity, role in microtubule nucleation, spindle pole body duplication and central plaque of spindle pole body, intermediate layer of spindle pole body localization**
CAGL0L01551g		*SUR7*	-1.93	-2.04	-1.88	-2.60	Ortholog(s) have role in ascospore formation, cellular response to biotic stimulus, cellular response to chemical stimulus, cellular response to glucose starvation and cellular response to neutral pH, more
CAGL0D03256g			-1.92	-1.97	-1.61	-1.50	Has domain(s) with predicted role in lipid metabolic process

Table B-2. (Continued).

C. glabrata designation	*C. glabrata* gene names	*S. cerevisiae* orthologs	SM1Δ*jjj1* vs SM1		SM1Δ*jjj1*Δ*pdr1* vs SM1		Description
			Exp. 1	Exp. 2	Exp. 1	Exp. 2	
CAGL0I03784g		***CRD1***	**-1.92**	**-1.92**	**1.03**	**1.49**	**Ortholog(s) have cardiolipin synthase activity, role in cellular ion homeostasis, lipid biosynthetic process, mitochondrial membrane organization and mitochondrion localization**
CAGL0J05104g		***YHC3***	**-1.92**	**-2.69**	**-1.14**	**1.28**	**Ortholog(s) have role in actin cortical patch localization, arginine transport, cellular protein localization, endocytosis, late endosome to vacuole transport and lysine transport, more**
CAGL0A04081g		*YLR194C*	-1.91	-2.45	-1.81	-1.71	Predicted GPI-linked cell wall protein
CAGL0L08184g	*FEN1*		-1.90	-1.92	-1.75	-4.57	Predicted fatty acid elongase with role in sphingolipid biosynthetic process; mutants show reduced sensitivity to caspofungin and increased sensitivity to micafungin
CAGL0D05918g	***ATF2***	***ATF2***	**-1.90**	**-2.29**	**-1.46**	**-2.89**	**Putative alcohol acetyltransferase involved in steroid detoxification; gene is upregulated in azole-resistant strain**
CAGL0E04818g		*MFB1*	-1.89	-1.53	-1.79	-1.98	Ortholog(s) have role in mitochondrion organization and extrinsic component of mitochondrial outer membrane localization
CAGL0F08591g		*NKP2*	-1.89	-2.78	-1.55	-2.08	Ortholog(s) have role in chromosome segregation and kinetochore, spindle pole body localization
CAGL0F07843g		*GPI10*	-1.87	-1.84	-2.05	-1.98	Ortholog(s) have dolichyl-phosphate-mannose-glycolipid alpha-mannosyltransferase activity, role in GPI anchor biosynthetic process and endoplasmic reticulum localization
CAGL0M11550g		*CDC45*	-1.86	-2.71	-1.77	-2.11	Ortholog(s) have DNA replication origin binding, chromatin binding, single-stranded DNA binding activity
CAGL0K03355g		***SRT1***	**-1.86**	**-2.29**	**1.31**	**1.13**	**Ortholog(s) have dehydrodolichyl diphosphate synthase activity, role in isoprenoid biosynthetic process, protein glycosylation and lipid particle localization**
CAGL0H08712g			-1.85	-3.87	-1.69	-2.54	Has domain(s) with predicted phosphatidylinositol binding activity and role in cell communication
CAGL0G03685g			**-1.85**	**-1.65**	**1.39**	**-1.39**	**Protein of unknown function**
CAGL0M09207g		***STE18***	**-1.85**	**-1.50**	**-2.18**	**1.42**	**Ortholog(s) have signal transducer activity**

Table B-2. (Continued).

C. glabrata designation	*C. glabrata* gene names	*S. cerevisiae* orthologs	SM1Δ*jjj1* vs SM1		SM1Δ*jjj1*Δ*pdr1* vs SM1		Description
			Exp. 1	Exp. 2	Exp. 1	Exp. 2	
CAGL0L07348g		***POL3***	**-1.84**	**-1.77**	**-1.14**	**-3.09**	**Ortholog(s) have 3'-5'-exodeoxyribonuclease activity, DNA-directed DNA polymerase activity and role in DNA replication, removal of RNA primer, DNA-dependent DNA replication maintenance of fidelity, RNA-dependent DNA replication**
CAGL0M06677g		*HHF2*	-1.84	-9.42	-1.89	-3.23	Ortholog(s) have role in histone H3-K79 methylation, sexual sporulation resulting in formation of a cellular spore and nucleus localization
CAGL0D01716g		*POL30*	-1.84	-2.37	-1.57	-2.83	Ortholog(s) have DNA polymerase processivity factor activity
CAGL0D00528g		***FAS1***	**-1.83**	**-1.77**	**-1.83**	**-1.49**	**Ortholog(s) have 3-hydroxyacyl-[acyl-carrier-protein] dehydratase activity, [acyl-carrier-protein] S-acetyltransferase activity and [acyl-carrier-protein] S-malonyltransferase activity, more**
CAGL0F01793g	***ERG3***	***ERG3***	**-1.83**	**-1.64**	**-1.20**	**-4.84**	**Delta 5,6 sterol desaturase; C-5 sterol desaturase; predicted transmembrane domain and endolasmic reticulum (ER) binding motif; gene used for molecular typing of C. glabrata strain isolates**
CAGL0K05599g		*DIA2*	-1.83	-1.53	-1.71	-1.70	Ortholog(s) have DNA replication origin binding, ubiquitin-protein transferase activity
CAGL0F00363g	***OPI3***	***OPI3***	**-1.82**	**-1.61**	**-1.77**	**1.77**	**Ortholog(s) have phosphatidyl-N-dimethylethanolamine N-methyltransferase activity, phosphatidyl-N-methylethanolamine N-methyltransferase activity and role in cleistothecium development, phosphatidylcholine biosynthetic process**
CAGL0K05973g	***HSP60***	***HSP60***	**-1.82**	**-2.32**	**-1.97**	**-1.22**	**Heat shock protein 60, mitochondrial precursor; putative chaperonin**
CAGL0H10054g		***YBR053C***	**-1.80**	**-1.53**	**-1.70**	**1.08**	**Ortholog of S. cerevisiae : YBR053C, C. albicans SC5314 : C4_02760C_A/CGR1, C. dubliniensis CD36 : Cd36_42630, C. parapsilosis CDC317 : CPAR2_400280 and Candida tenuis NRRL Y-1498 : CANTEDRAFT_113139**
CAGL0H09482g			**-1.80**	**-2.67**	**-1.80**	**-1.14**	**Protein of unknown function**
CAGL0J11572g	***NUF2***	***NUF2***	**-1.80**	**-1.81**	**1.00**	**-1.40**	**Putative spindle pole body protein**
CAGL0I02134g	***PEX21B***	***PEX18***	**-1.80**	**-1.70**	**-1.27**	**-1.39**	**Ortholog(s) have role in protein import into peroxisome matrix and cytosol, peroxisome localization**

Table B-2. (Continued).

C. glabrata designation	*C. glabrata* gene names	*S. cerevisiae* orthologs	SM1Δ*jjj1* vs SM1		SM1Δ*jjj1*Δ*pdr1* vs SM1		Description
			Exp. 1	Exp. 2	Exp. 1	Exp. 2	
CAGL0M09086g		*BUD4*	-1.80	-2.29	-1.72	-1.59	Ortholog(s) have GTP binding, cell adhesion molecule binding activity
CAGL0G08668g		*SUN4*	-1.79	-6.64	-1.53	-5.64	Ortholog(s) have glucan endo-1,3-beta-D-glucosidase activity
CAGL0F05533g		***CBS2***	**-1.79**	**-2.00**	**-1.83**	**1.45**	**Ortholog(s) have translation regulator activity and role in mitochondrial respiratory chain complex III biogenesis, positive regulation of mitochondrial translation**
CAGL0M11858g		*SPC25*	-1.79	-2.42	-1.79	-2.23	Ortholog(s) have structural constituent of cytoskeleton activity, role in chromosome segregation, microtubule nucleation and Ndc80 complex, condensed nuclear chromosome kinetochore localization
CAGL0J03740g		***SSP2***	**-1.79**	**-1.71**	**-2.00**	**-1.03**	**Ortholog(s) have role in ascospore wall assembly, positive regulation of protein autophosphorylation and ascospore wall, prospore membrane localization**
CAGL0A04169g		*MMR1*	-1.79	-1.51	-1.60	-1.57	Ortholog(s) have role in mitochondrion inheritance and cellular bud neck, incipient cellular bud site, mitochondrial outer membrane localization
CAGL0E01023g		***CWC15***	**-1.78**	**-1.66**	**-1.05**	**-1.66**	**Ortholog(s) have RNA binding activity, role in mRNA cis splicing, via spliceosome and Prp19 complex, U2-type spliceosomal complex localization**
CAGL0B00242g		***HMLALPHA1***	**-1.78**	**-1.91**	**-1.60**	**-1.31**	**Alpha-domain mating-type protein alpha1p**
CAGL0J11638g		***CDC5***	**-1.78**	**-1.62**	**-1.53**	**-1.07**	**Ortholog(s) have enzyme activator activity, protein kinase activity**
CAGL0F02585g		***URH1***	**-1.78**	**-2.79**	**-2.49**	**-1.07**	**Ortholog(s) have nicotinamide riboside hydrolase activity, nicotinic acid riboside hydrolase activity, uridine nucleosidase activity**
CAGL0G09801g		***DPB2***	**-1.78**	**-3.35**	**-1.12**	**-2.03**	**Ortholog(s) have DNA-directed DNA polymerase activity, double-stranded DNA binding, single-stranded DNA binding activity**
CAGL0K06457g		***RMT2***	**-1.77**	**-1.57**	**1.11**	**-1.60**	**Ortholog(s) have protein-arginine N5-methyltransferase activity, role in peptidyl-arginine methylation and cytosol, nucleus localization**

Table B-2. (Continued).

C. glabrata designation	*C. glabrata* gene names	*S. cerevisiae* orthologs	SM1Δ*jjj1* vs SM1		SM1Δ*jjj1*Δ*pdr1* vs SM1		Description
			Exp. 1	Exp. 2	Exp. 1	Exp. 2	
CAGL0F05731g		***PLP1***	**-1.75**	**-1.67**	**-1.75**	**1.03**	**Ortholog(s) have G-protein beta/gamma-subunit complex binding activity, role in positive regulation of transcription from RNA polymerase II promoter by pheromones, protein folding and cytosol, nucleus localization**
CAGL0K07876g		***MDM36***	**-1.75**	**-2.57**	**-1.00**	**1.31**	**Ortholog(s) have role in mitochondrial fission, mitochondrion inheritance and mitochondrion localization**
CAGL0I05940g		***SFH5***	**-1.75**	**-3.15**	**-1.32**	**-1.68**	**Ortholog(s) have phosphatidylinositol transporter activity**
CAGL0I09328g		*TSC10*	-1.74	-1.96	-1.83	-2.15	Ortholog(s) have 3-dehydrosphinganine reductase activity, role in 3-keto-sphinganine metabolic process, sphingolipid biosynthetic process and endoplasmic reticulum, lipid particle, mitochondrial outer membrane localization
CAGL0E01331g	*SWI5*		-1.74	-2.07	-1.92	-1.69	Transcription factor; mutants display increased fungal burdens in mouse lungs and brain
CAGL0E04268g		***YML037C***	**-1.74**	**-2.13**	**1.06**	**-1.34**	**Ortholog(s) have clathrin-coated vesicle localization**
CAGL0B04873g		*DCC1*	-1.73	-2.38	-2.00	-1.58	Ortholog(s) have role in attachment of spindle microtubules to kinetochore involved in homologous chromosome segregation, cellular response to DNA damage stimulus, maintenance of DNA trinucleotide repeats, mitotic sister chromatid cohesion
CAGL0G04851g	*SUR4*	*ELO3*	-1.72	-1.88	-1.75	-4.01	Predicted fatty acid elongase involved in production of very long chain fatty acids for sphingolipid biosynthesis; mutants show reduced sensitivity to caspofungin and increased sensitivity to micafungin
CAGL0I04422g		***KIN3***	**-1.72**	**-1.86**	**-1.16**	**-1.57**	**Putative protein kinase; gene is upregulated in azole-resistant strain**
CAGL0B01243g	***MATalpha1***	***MATALPHA1***	**-1.72**	**-2.11**	**-1.63**	**-1.19**	**Alpha-domain mating-type protein alpha1p; expressed in all MTLalpha strains and not in MTLa strains**
CAGL0H07161g		*HIM1*	-1.72	-1.62	-1.63	-1.97	Ortholog(s) have role in DNA repair
CAGL0M04499g		***PUT1***	**-1.72**	**-1.79**	**-1.53**	**1.32**	**Ortholog(s) have proline dehydrogenase activity, role in proline catabolic process to glutamate and mitochondrion localization**

Table B-2. (Continued).

C. glabrata designation	*C. glabrata* gene names	*S. cerevisiae* orthologs	SM1Δ*jjj1* vs SM1		SM1Δ*jjj1*Δ*pdr1* vs SM1		Description
			Exp. 1	Exp. 2	Exp. 1	Exp. 2	
CAGL0B04543g		***CRC1***	**-1.71**	**-1.98**	**-1.59**	**-1.12**	**Ortholog(s) have carnitine transmembrane transporter activity, carnitine:acyl carnitine antiporter activity and role in acetate catabolic process, carbon utilization, carnitine transport, fatty acid metabolic process**
CAGL0M13805g	*MP65*	*SCW10*	-1.71	-2.77	-1.51	-2.26	65 kDa mannoprotein
CAGL0I02464g		*SPC97*	-1.71	-1.76	-1.50	-1.73	Putative component of microtubule-nucleating complex; gene is upregulated in azole-resistant strain
CAGL0M06655g		*HHT2*	-1.71	-2.90	-1.75	-3.14	Ortholog(s) have role in DNA methylation, global genome nucleotide-excision repair, mitotic spindle assembly checkpoint, rRNA transcription, regulation of DNA methylation, sexual sporulation resulting in formation of a cellular spore
CAGL0G02409g		***SRP40***	**-1.71**	**-2.83**	**-1.40**	**-3.08**	**Ortholog(s) have nucleolus localization**
CAGL0M05621g			-1.71	-1.60	-1.58	-1.65	Ortholog(s) have role in endocytosed protein transport to vacuole, endocytosis, mannosyl-inositol phosphorylceramide biosynthetic process and cis-Golgi network membrane, trans-Golgi network membrane localization
CAGL0H01683g		***URC2***	**-1.71**	**-4.29**	**-1.05**	**-1.26**	**Ortholog(s) have sequence-specific DNA binding activity and cytoplasm, nucleus localization**
CAGL0C02431g		***FIR1***	**-1.71**	**-3.44**	**-1.47**	**-1.95**	**Ortholog(s) have role in mRNA polyadenylation and cellular bud neck localization**
CAGL0E04906g		***AHA1***	**-1.70**	**-2.04**	**-1.37**	**-1.13**	**Ortholog(s) have ATPase activator activity, chaperone binding activity, role in cellular response to heat, protein folding and cytosol localization**
CAGL0F04092g			**-1.70**	**-1.83**	**1.06**	**1.04**	**Unknown**
CAGL0J08822g		***CLB4***	**-1.70**	**-1.61**	**-1.32**	**-1.82**	**Ortholog(s) have cyclin-dependent protein serine/threonine kinase regulator activity**
CAGL0M06237g		*EEB1*	-1.70	-1.55	-1.56	-1.86	Ortholog(s) have alcohol O-octanoyltransferase activity, short-chain carboxylesterase activity and role in medium-chain fatty acid biosynthetic process, medium-chain fatty acid catabolic process
CAGL0E01243g		***TIS11***	**-1.68**	**-1.75**	**-1.26**	**1.55**	**Ortholog(s) have mRNA binding activity, role in cellular iron ion homeostasis, nuclear-transcribed mRNA catabolic process, regulation of mRNA catabolic process and cytoplasm, nucleus localization**

Table B-2. (Continued).

C. glabrata designation	*C. glabrata* gene names	*S. cerevisiae* orthologs	SM1Δ*jjj1* vs SM1		SM1Δ*jjj1*Δ*pdr1* vs SM1		Description
			Exp. 1	Exp. 2	Exp. 1	Exp. 2	
CAGL0D02948g	*KAR2*	*KAR2*	-1.68	-1.71	-1.75	-1.79	Protein with a predicted role in nuclear fusion
CAGL0G06666g		***POL1***	**-1.68**	**-1.85**	**-1.35**	**-2.32**	**Ortholog(s) have DNA replication origin binding, DNA-directed DNA polymerase activity, chromatin binding, single-stranded DNA binding activity**
CAGL0L01969g		***YKL033W-A***	**-1.68**	**-1.74**	**-2.28**	**-1.33**	**Ortholog(s) have cytosol, nucleus localization**
CAGL0K02387g		***ROK1***	**-1.68**	**-1.87**	**-1.37**	**-2.89**	**Ortholog(s) have ATP-dependent RNA helicase activity**
CAGL0G03795g	*SSA1*	*SSA2*	-1.67	-2.98	-1.78	-3.15	Heat shock protein of the HSP70 family
CAGL0M08096g			**-1.67**	**-3.20**	**-1.15**	**-4.00**	**Protein of unknown function**
CAGL0C01727g		*ALG7*	-1.66	-1.80	-1.83	-1.69	Ortholog(s) have UDP-N-acetylglucosamine-dolichyl-phosphate N-acetylglucosaminephosphotransferase activity and role in N-glycan processing, aerobic respiration, cellular response to drug, dolichyl diphosphate biosynthetic process
CAGL0J11110g		***MRX12***	**-1.66**	**-2.64**	**-1.29**	**-2.07**	**Ortholog(s) have mitochondrion localization**
CAGL0C03135g		***YCS4***	**-1.66**	**-1.60**	**-1.49**	**-1.20**	**Ortholog(s) have chromatin binding activity**
CAGL0I03740g		*YDL144C*	-1.66	-2.12	-1.50	-2.46	Ortholog(s) have cytoplasm, nucleus localization
CAGL0A02431g	*YPS7*	*YPS7*	-1.66	-1.66	-1.79	-2.96	Putative aspartic protease; predicted GPI-anchor; expression induced at high temperature
CAGL0I02508g		***CTR2***	**-1.65**	**-3.81**	**-1.54**	**-1.26**	**Ortholog(s) have copper uptake transmembrane transporter activity and role in cellular copper ion homeostasis, copper ion import, copper ion transmembrane transport, intracellular copper ion transport**
CAGL0J01287g	***AIP1***	***AIP1***	**-1.65**	**-1.91**	**-1.60**	**-1.09**	**Putative actin cytoskeleton component**
CAGL0G08085g			**-1.63**	**-1.80**	**-1.46**	**-1.97**	**Has domain(s) with predicted ATP binding, cation-transporting ATPase activity, magnesium ion binding, metal ion binding, nucleotide binding, phospholipid-translocating ATPase activity and role in cation transport, phospholipid transport**
CAGL0C03575g		***AGA1***	**-1.63**	**-2.29**	**-1.11**	**-1.22**	**Predicted GPI-linked protein; putative adhesin-like protein**
CAGL0K02981g		***NAT4***	**-1.63**	**-2.93**	**-1.20**	**-1.07**	**Ortholog(s) have histone acetyltransferase activity, role in histone acetylation, phenotypic switching, regulation of chromatin silencing at rDNA and cell division site, cytosol, nucleus localization**
CAGL0G04939g		***MDM30***	**-1.63**	**-1.73**	**1.08**	**-1.63**	**Ortholog(s) have ubiquitin-protein transferase activity**

Table B-2. (Continued).

C. glabrata designation	*C. glabrata* gene names	*S. cerevisiae* orthologs	SM1Δ*jjj1* vs SM1		SM1Δ*jjj1*Δ*pdr1* vs SM1		Description
			Exp. 1	Exp. 2	Exp. 1	Exp. 2	
CAGL0I03630g		***RPC53***	**-1.62**	**-2.66**	**-1.32**	**-2.72**	**Ortholog(s) have RNA polymerase III activity, role in tRNA transcription from RNA polymerase III promoter and DNA-directed RNA polymerase III complex, cytosol localization**
CAGL0G07249g		***YOX1***	**-1.61**	**-1.51**	**-1.10**	**-3.10**	**Ortholog(s) have RNA polymerase II regulatory region sequence-specific DNA binding, RNA polymerase II transcription factor binding transcription factor activity involved in negative regulation of transcription activity**
CAGL0L07898g		***MAK32***	**-1.61**	**-1.88**	**-1.45**	**2.67**	**Ortholog(s) have role in interspecies interaction between organisms**
CAGL0L10340g		***SLD7***	**-1.61**	**-3.58**	**1.11**	**-2.15**	**Ortholog(s) have role in regulation of DNA-dependent DNA replication initiation and DNA replication preinitiation complex, chromosome, centromeric region, endoplasmic reticulum, nuclear envelope, spindle pole body localization**
CAGL0G09581g		***TUF1***	**-1.61**	**-1.64**	**-1.68**	**1.17**	**Ortholog(s) have GTPase activity, translation elongation factor activity, role in mitochondrial translational elongation and mitochondrion localization**
CAGL0D05940g	***ERG1***	***ERG1***	**-1.60**	**-1.53**	**-1.39**	**-2.55**	**Squalene epoxidase with a role in ergosterol synthesis; involved in growth under conditions of low oxygen tension**
CAGL0J05236g		*LAS21*	-1.60	-1.65	-1.52	-2.01	Ortholog(s) have mannose-ethanolamine phosphotransferase activity
CAGL0J07480g		***BNI4***	**-1.60**	**-1.68**	**-1.44**	**-1.29**	**Ortholog(s) have role in asymmetric protein localization, barrier septum assembly, cellular response to biotic stimulus, cellular response to starvation and chitin biosynthetic process, more**
CAGL0I01166g	***TRR1***		**-1.60**	**-1.64**	**-1.47**	**-6.19**	**Thioredoxin reductase (NADPH)**
CAGL0M02321g			**-1.59**	**-1.51**	**-1.21**	**-1.77**	**Protein of unknown function**
CAGL0I09746g		*SLY41*	-1.59	-1.95	-1.57	-1.82	Ortholog(s) have phosphoenolpyruvate transmembrane transporter activity, role in ER to Golgi vesicle-mediated transport, phosphoenolpyruvate transmembrane import into Golgi lumen and Golgi apparatus, endoplasmic reticulum localization
CAGL0G00682g			**-1.58**	**-1.66**	**-1.31**	**-1.26**	**Ortholog(s) have Golgi apparatus, endoplasmic reticulum localization**

Table B-2. (Continued).

C. glabrata designation	*C. glabrata* gene names	*S. cerevisiae* orthologs	SM1Δ*jjj1* vs SM1		SM1Δ*jjj1*Δ*pdr1* vs SM1		Description
			Exp. 1	Exp. 2	Exp. 1	Exp. 2	
CAGL0K11418g	***ADK1***	***ADK1***	**-1.58**	**-1.73**	**-1.41**	**-1.45**	**Putative adenylate kinase; protein differentially expressed in azole-resistant strain**
CAGL0L03454g		***SRS2***	**-1.58**	**-1.90**	**-1.35**	**-2.87**	**Ortholog(s) have DNA helicase activity**
CAGL0G06226g		*LTE1*	-1.57	-1.98	-1.60	-1.53	Ortholog(s) have role in vesicle-mediated transport and cellular bud localization
CAGL0F07601g	***CWP1.1***	***CWP2***	**-1.57**	**-1.71**	**-1.23**	**1.06**	**GPI-linked cell wall protein**
CAGL0H09438g		*BIM1*	-1.57	-2.22	-1.61	-2.84	Ortholog(s) have ATPase activator activity, microtubule plus-end binding, protein homodimerization activity, structural constituent of cytoskeleton activity
CAGL0K02739g			**-1.57**	**-2.72**	**-1.46**	**-2.40**	**Ortholog(s) have sphingosine N-acyltransferase activity and role in ceramide biosynthetic process**
CAGL0M05599g		*TOS1*	-1.57	-1.91	-1.51	-2.46	Ortholog(s) have cell surface, endoplasmic reticulum, extracellular region, fungal-type vacuole, hyphal cell wall localization
CAGL0F01287g	***GAS5***	***GAS5***	**-1.57**	**-2.07**	**-1.36**	**-2.04**	**Putative transglycosidase with a predicted role in the elongation of 1,3-beta-glucan**
CAGL0E01727g	*YPS3*		-1.56	-2.69	-1.51	-2.68	Putative aspartic protease; predicted GPI-anchor; member of a YPS gene cluster that is required for virulence in mice
CAGL0D02596g		*PSF3*	-1.56	-1.85	-1.81	-2.28	Ortholog(s) have role in GINS complex assembly, double-strand break repair via break-induced replication, mitotic DNA replication initiation, mitotic DNA replication preinitiation complex assembly
CAGL0J09702g		*ACK1*	-1.56	-1.88	-1.52	-1.65	Ortholog(s) have role in fungal-type cell wall organization, positive regulation of signal transduction and mitochondrion localization
CAGL0I01958g			**-1.56**	**-1.84**	**1.08**	**-1.19**	**Protein of unknown function**
CAGL0M08448g		***MCD4***	**-1.56**	**-2.78**	**-1.47**	**-2.54**	**Ortholog(s) have mannose-ethanolamine phosphotransferase activity and role in ATP transport, GPI anchor biosynthetic process, conidium formation, fungal-type cell wall organization or biogenesis, regulation of growth rate**
CAGL0F01485g	***TIR2***	***TIR4***	**-1.55**	**-1.90**	**-1.30**	**-2.46**	**Putative GPI-linked cell wall mannoprotein of the Srp1p/Tip1p family**

Table B-2. (Continued).

C. glabrata designation	*C. glabrata* gene names	*S. cerevisiae* orthologs	SM1Δ*jjj1* vs SM1		SM1Δ*jjj1*Δ*pdr1* vs SM1		Description
			Exp. 1	Exp. 2	Exp. 1	Exp. 2	
CAGL0H02805g		***SMC3***	**-1.55**	**-1.56**	**-1.28**	**-1.09**	**Ortholog(s) have role in ascospore formation, meiotic sister chromatid cohesion, mitotic sister chromatid cohesion, positive regulation of maintenance of mitotic sister chromatid cohesion and centromeric, more**
CAGL0I07249g		***BAG7***	**-1.54**	**-2.13**	**-1.52**	**1.07**	**Putative GTPase-activating protein involved in cell wall and cytoskeleton homeostasis; gene is upregulated in azole-resistant strain**
CAGL0L05610g		***SPT10***	**-1.54**	**-1.62**	**-1.07**	**-2.11**	**Ortholog(s) have sequence-specific DNA binding activity**
CAGL0K11132g		***SNU56***	**-1.54**	**-1.53**	**-1.12**	**-1.19**	**Ortholog(s) have mRNA binding activity, role in mRNA splicing, via spliceosome and U1 snRNP, U2-type prespliceosome, commitment complex localization**
CAGL0M00330g	*HOM6*	*HOM6*	-1.54	-1.78	-1.81	-1.59	Ortholog(s) have homoserine dehydrogenase activity, role in homoserine biosynthetic process, methionine biosynthetic process, threonine biosynthetic process and cytoplasm, nucleus localization
CAGL0H00759g		***SGS1***	**-1.54**	**-1.58**	**-1.07**	**-1.05**	**Ortholog(s) have ATP-dependent DNA helicase activity**
CAGL0L10714g	*ERG2*	*ERG2*	-1.54	-2.26	-1.68	-2.37	C-8 sterol isomerase
CAGL0K04477g		***ERG25***	**-1.54**	**-3.14**	**-1.06**	**-5.11**	**Ortholog(s) have C-4 methylsterol oxidase activity, role in ergosterol biosynthetic process and endoplasmic reticulum membrane, plasma membrane localization**
CAGL0M08514g	***PIR5***	***PIR3***	**-1.53**	**-2.03**	**-1.26**	**-1.30**	**Pir protein family member, putative cell wall component**
CAGL0G08129g		***MSH6***	**-1.53**	**-3.01**	**-1.35**	**-3.25**	**Ortholog(s) have ATP binding, ATPase activity, four-way junction DNA binding, guanine/thymine mispair binding, single base insertion or deletion binding activity**
CAGL0M13035g		***DEF1***	**-1.52**	**-2.77**	**-1.04**	**-1.66**	**Ortholog(s) have role in protein ubiquitination, telomere maintenance, transcription-coupled nucleotide-excision repair, ubiquitin-dependent protein catabolic process and nucleus localization**
CAGL0A03905g		***HMX1***	**-1.52**	**-1.54**	**-1.01**	**1.40**	**Ortholog(s) have heme oxygenase (decyclizing) activity and role in cellular iron ion homeostasis, heme catabolic process, response to carbon monoxide, response to oxidative stress**
CAGL0M11528g		***APC9***	**-1.52**	**-2.67**	**1.00**	**1.21**	**Ortholog(s) have ubiquitin-protein transferase activity, role in chromatin assembly, protein ubiquitination and anaphase-promoting complex localization**

Table B-2. (Continued).

C. glabrata designation	*C. glabrata* gene names	*S. cerevisiae* orthologs	SM1Δ*jjj1* vs SM1		SM1Δ*jjj1*Δ*pdr1* vs SM1		Description
			Exp. 1	Exp. 2	Exp. 1	Exp. 2	
CAGL0M08228g		***LST4***	**-1.51**	**-1.90**	**-1.56**	**-1.10**	**Ortholog(s) have protein transporter activity, role in Golgi to plasma membrane transport, intracellular protein transport and vesicle coat localization**
CAGL0K11506g		***RAD27***	**-1.51**	**-4.79**	**-1.05**	**-3.29**	**Ortholog(s) have 5'-flap endonuclease activity, single-stranded DNA 5'-3' exodeoxyribonuclease activity**
CAGL0L03333g		***UIP5***	**-1.51**	**-1.77**	**-1.26**	**-2.13**	**Ortholog(s) have nuclear envelope localization**
CAGL0A00561g		***RPN14***	**-1.51**	**-1.56**	**-1.42**	**-1.35**	**Ortholog(s) have role in proteasome regulatory particle assembly, ubiquitin-dependent protein catabolic process and cytosol, nucleus localization**
CAGL0F07557g		*YJU2*	-1.50	-3.60	-1.57	-1.64	Ortholog(s) have first spliceosomal transesterification activity, role in generation of catalytic spliceosome for first transesterification step and U2-type catalytic step 1 spliceosome localization
CAGL0M08580g		***CUE5***	**-1.50**	**-2.92**	**-1.86**	**-1.03**	**Ortholog(s) have protein binding, bridging, ubiquitin binding activity, role in ubiquitin-dependent protein catabolic process and cytoplasm localization**
CAGL0J04334g		***POP8***	**-1.50**	**-2.80**	**1.17**	**-1.75**	**Ortholog(s) have ribonuclease MRP activity, ribonuclease P activity, role in intronic box C/D snoRNA processing, mRNA cleavage, tRNA processing and cytosol, nucleolar ribonuclease P complex, ribonuclease MRP complex localization**
CAGL0L10015g		***TOM6***	**-1.50**	**-1.94**	**-1.38**	**1.09**	**Ortholog(s) have protein channel activity, role in mitochondrial outer membrane translocase complex assembly, protein import into mitochondrial matrix and mitochondrial outer membrane translocase complex localization**
CAGL0F04543g			**-1.50**	**-1.86**	**1.33**	**-1.86**	**Protein of unknown function**
CAGL0I07997g		***MDM20***	**-1.50**	**-1.69**	**-1.05**	**-1.76**	**Ortholog(s) have peptide alpha-N-acetyltransferase activity, role in N-terminal peptidyl-methionine acetylation, cytoskeleton organization, mitochondrion inheritance and NatB complex localization**
CAGL0I09174g		***SHG1***	**-1.50**	**-1.65**	**1.38**	**-2.00**	**Ortholog(s) have histone methyltransferase activity (H3-K4 specific) activity, role in histone H3-K4 methylation and Set1C/COMPASS complex localization**
CAGL0M07744g			**-1.50**	**-1.50**	**1.25**	**1.13**	**Protein of unknown function**

Table B-2. (Continued).

Notes: Fold change is defined as the ratio of gene expression in SM1Δ*jjj1* compared to SM1 in two independent RNA-seq experiments. Bolded rows indicate genes whose down-regulation is dependent on PDR1 expression.

Table B-3. Adhesion related genes up-regulated by at least 1.5-fold in SM1Δ*jjj1* versus SM1.

C. glabrata designation	*C. glabrata* gene names	*S. cerevisiae* orthologs	SM1Δ*jjj1* vs SM1		SM1Δ*jjj1*Δ*pdr1* vs SM1		Description
			Exp. 1	Exp. 2	Exp. 1	Exp. 2	
CAGL0K00170g	*EPA22*		7.06	2.98	13.57	4.81	Putative adhesin-like protein; belongs to adhesin cluster I
CAGL0E06688g	*EPA3*		5.21	3.96	6.76	3.76	Epithelial adhesion protein; belongs to adhesin cluster I; GPI-anchored
CAGL0E06666g	*EPA2*		4.35	3.22	6.57	4.38	Epithelial adhesion protein; predicted GPI-anchor; belongs to adhesin cluster I
CAGL0I10147g	*PWP1*		3.83	5.07	4.13	6.44	Protein with 32 tandem repeats; putative adhesin-like protein; belongs to adhesin cluster II
CAGL0J05159g			**2.96**	**1.79**	**2.70**	**1.49**	**Putative adhesin-like protein**
CAGL0E06644g	*EPA1*		2.90	4.56	2.46	2.59	Sub-telomerically encoded adhesin with a role in cell adhesion; GPI-anchored cell wall protein; N-terminal ligand binding domain binds to ligands containing a terminal galactose residue; belongs to adhesin cluster I
CAGL0L00157g			2.73	6.48	2.82	3.72	Putative adhesin-like protein; multiple tandem repeats; predicted GPI-anchor; belongs to adhesin cluster III
CAGL0J01727g			2.53	2.27	2.21	1.89	Putative adhesion protein; predicted GPI-anchor; belongs to adhesin cluster VI
CAGL0J01774g			2.41	2.18	2.80	2.62	Putative adhesin-like protein; has glycine and serine rich repeats; belongs to adhesin cluster VI
CAGL0E00110g			2.09	2.98	3.01	2.30	Putative adhesin-like protein; ORF appears artificially broken into fragments due to sequencing errors; belongs to adhesin cluster III; predicted GPI anchor
CAGL0L13299g	*EPA11*		1.78	1.91	1.98	1.81	Putative adhesin; belongs to adhesin cluster I
CAGL0L09911g		***CSS1***	**1.72**	**1.75**	**1.65**	**1.41**	**Putative adhesin-like cell wall protein; 5 tandem repeats; predicted GPI-anchor**
CAGL0I00110g			1.64	1.56	1.65	2.31	Putative adhesin-like with multiple tandem repeats; ORF appears artificially broken into fragments due to sequencing errors; belongs to adhesin cluster III; predicted GPI-anchor
CAGL0H08844g		*DDR48*	1.58	1.66	1.60	15.23	Putative adhesin-like protein
CAGL0J02530g			1.53	2.27	1.92	4.41	Putative adhesion protein; predicted GPI-anchor; belongs to adhesin cluster VI

Table B-3. (Continued).

C. glabrata designation	*C. glabrata* gene names	*S. cerevisiae* orthologs	SM1Δ*jjj1* vs SM1		SM1Δ*jjj1*Δ*pdr1* vs SM1		Description
			Exp. 1	Exp. 2	Exp. 1	Exp. 2	
CAGL0E00231g			**1.51**	**2.26**	**1.60**	**-1.06**	**Putative adhesin-like protein; contains tandem repeats and a predicted GPI-anchor; belongs to adhesin cluster III**
CAGL0I10200g	***PWP3***		**1.50**	**1.93**	**1.33**	**2.58**	**Protein with tandem repeats; putative adhesin-like protein; belongs to adhesin cluster II**

Notes: Fold change is defined as the ratio of gene expression in SM1Δ*jjj1* compared to SM1 in two independent RNA-seq experiments. Bolded rows indicate genes whose up-regulation is dependent on *PDR1* expression.

VITA

Sarah Garland Whaley, daughter of D.L. and Martha Whaley, was born in Bristol, Tennessee in 1979. She lived in Piney Flats, Tennessee where she attended Mary Hughes Elementary/ Middle School and graduated from Sullivan East High School in 1997. She attended East Tennessee State University and graduated with a Bachelor of Science in Biology with a Biochemistry concentration in 2001. In 2008 Sarah moved to Memphis to enroll in the Pharm.D./Ph.D. dual degree program at the University of Tennessee Health Science Center. She earned her Doctor of Pharmacy degree in 2012 and anticipates completion of the requirements for her Doctor of Philosophy degree in 2018.